

**Development and Application of ESI-MS Based Techniques for Quantitative
Determination of Protein-Carbohydrate Interactions**

by

Km Shams-Ud-Doha

A thesis submitted in partial fulfillment of the requirements for the degree of

Master of Science

Department of Chemistry

University of Alberta

© Km Shams-Ud-Doha, 2016

Abstract

This thesis describes the development and application of mass spectrometry methods to study protein-ligand interactions *in vitro*. Liquid sample desorption electrospray ionization mass spectrometry (liquid sample DESI-MS) was employed to quantify protein-carbohydrate interactions in aqueous buffer solutions. Protein-carbohydrate interactions were quantified using liquid sample DESI-MS and it was found to be in agreement with values obtained by the direct ESI-MS assay.

A rapid and quantitative method was developed to screen oligosaccharides libraries against lectins by the proxy protein ESI-MS assay. In this present work, the *proxy protein* ESI-MS method combined with direct ESI-MS protein-ligand binding assay and competitive protein binding assay was developed to detect and quantify interactions of protein target e.g. pathogenic protein, with glycan library. When direct detection of target protein by ESI-MS is not possible this method will facilitate the quantification of protein against ligand libraries. This method was applied to screen small oligosaccharide libraries against the N-terminal fragment of the family 51 carbohydrate-binding module, a fucose-binding bacterial lectin from *Ralstonia solanacearum* and the P particle of human norovirus, to demonstrate the reliability and versatility of the assay.

Finally, comparative studies of human milk oligosaccharides (HMOs) specificities of human galectin-1, 3, 9 were described by using direct ESI-MS assay as compared to glycan array method. Human milk oligosaccharides (HMOs) have a variety of biological functions against pathogens and serve as prebiotic. To quantify the interaction between three human galectins and 32 HMOs, electrospray ionization mass spectrometry (ESI-MS) direct binding assay method was used. The data show that

galectins have broad HMO specificity with association constants ranging from 10^3 to 10^5 M^{-1} along with no affinity for several specific HMOs. Binding affinity of galectins was found to be similar to binding affinity to histo-blood type oligosaccharides. Weak or no binding was established for galacto-oligosaccharides (GOS) and fructo-oligosaccharides (FOS). These values were compared to values obtained from glycan array analysis. Significant difference was observed which depicts the reliability of the direct ESI-MS assay for quantifying protein-ligand interaction.

Preface

This dissertation is submitted for the degree of *Master of Science in Chemistry* at the University of Alberta. The research work described herein was conducted under the supervision of John S. Klassen in the Department of Chemistry, University of Alberta, between September 2012 and April 2016.

This research work is to the best of my knowledge new and original. Chapter 2 has been published as: Yao, Y., Shams-Ud-Doha, K., Daneshfar, R., Kitova, E. N., Klassen, J. S., “Quantifying Protein-Carbohydrate Interactions Using Liquid Sample Desorption Electrospray Ionization Mass Spectrometry”, *J. Am. Soc. Mass. Spectrom.*, **2015**, 26, 98-106. Y. Yao and I were responsible for performing experiments and data analysis, as well as preparation of the manuscript. Yuyu did the isothermal titration calorimetry experiments and the binding affinities measurement. I did nonspecific binding corrections. E. Kitova provided input on the manuscript.

Chapter 3 has been submitted as: Shams-Ud-Doha, K. (equal contribution), Han, L. (equal contribution), Kitova, E. N., Klassen, J. S., “Screening Oligosaccharide Libraries against Lectins Using the Proxy Protein ESI-MS assay”, *Anal. Chem.*, (revision requested and resubmitted). L. Han and I equally contributed for performing experiments. I have done the data analysis and E. Kitova provided significant input on the writing of the manuscript. We acknowledge C. Cairo (University of Alberta), A. Boraston (University of Victoria), A. Imberty (CERMAV-CNRS) and M. Tan (Cincinnati Children's Hospital Medical Center) for generously providing proteins and T. Lowary (University of Alberta) for generously providing oligosaccharides used in this study.

Finally, Chapter 4 is under preparation as manuscript. I was responsible for doing all the ESI-MS measurements, analyzing experimental data and writing.

The supervisory author, Prof. J. Klassen, was involved throughout all the projects in concept formation and manuscript composition.

Km Shams-Ud-Doha

June 2016

Acknowledgement

First and foremost, I wish to express my gratitude to my supervisor, Professor John S. Klassen, for his guidance and support. I would like to thank my supervisor and defense committee members, Prof. Alexander Brown, Prof. X. Chris Le and Prof. Mark T. McDermott for their helpful and supportive comments into my research.

I also wish to thank Dr. Elena N. Kitova and Dr. Rambod Daneshfar for their useful advice, technical support and continued encouragement throughout my program. I would like to give my special thanks to previous and present colleagues in the Klassen group, Dr. Amr El-hawiet, Dr. Lan Liu, Dr. Lu Deng, Dr. Aneika C. Leney, Dr. Ling Han, Dr. Michele R. Richards, Dr. Emma-Dune Leriche, Hong Lin, Jingjing Zhang, Sanaz Nikjah, Reza Rezaei Darestani, Xuxin Fan, Yuyu Yao, Jun Li and Yajie Chen for their helpful advice and encouragement.

I wish to thank the valuable technical instruction and support received from Dr. Randy Whittal for mass spectrometry and Chunxia (Cecilia) Zou, R. Blake Zheng for biological work support.

I acknowledge the financial support from Department of Chemistry, University of Alberta.

Finally, I wish to thank my wife and parents for always being by my side.

Table of Contents

List of Tables	x
List of Figures	xi
List of Abbreviations	xxi
Chapter 1 Study of Protein-Carbohydrate Interactions by Electrospray Ionization	
Mass Spectrometry for Development of Mass Spectrometry Methods	1
1.1 Introduction	1
1.1.1 Carbohydrates: Structure and Function	1
1.1.2 Protein-Carbohydrate Interactions	2
1.2 Electrospray Ionization Mass Spectrometry	8
1.2.1 Electrospray Ionization	8
1.2.2 MS Instrumentation	13
1.3 Quantification of Interactions of Non-Covalent Complexes by MS-Based Techniques	22
1.3.1 Desorption Electrospray Ionization Mass Spectrometry (DESI-MS)	22
1.3.2 Direct ESI-MS Binding Assay	27
1.3.3 Indirect ESI-MS Assays	29
1.4 Potential Limitation of the Direct ESI-MS Binding Assay	33
1.4.1 Non-Uniform Response Factors	33
1.4.2 Nonspecific binding	34
1.4.3 In-source dissociation	37
1.5 The Present work	39
1.6 References	42

Table of Contents (*cont'd*)

Chapter 2 Quantifying Protein-Carbohydrate Interactions Using Liquid Sample

Desorption Electrospray Ionization Mass Spectrometry (DESI-MS)	52
2.1 Introduction	52
2.2 Experimental section	54
2.2.1 Materials	54
2.2.2 Mass spectrometry	55
2.2.3 Isothermal titration calorimetry	56
2.2.4 Data analysis	57
2.3 Results and discussion	59
2.3.1 Binding of Lyz to L2 and L3	60
2.3.2 Binding of scFv to L4 and L5	61
2.3.3 Comparison of liquid sample DESI-MS and reactive liquid sample DESI-MS	63
2.4 Conclusions	65
2.5 References	74

Chapter 3 Screening Oligosaccharide Libraries against Lectins Using the Proxy

Protein ESI-MS assay	78
3.1 Introduction	78
3.2 Experimental	81
3.2.1 Proteins	81
3.2.2 Oligosaccharides	82
3.2.3 Mass spectrometry	82
3.2.4 Proxy protein ESI-MS assay	84

Table of Contents (*cont'd*)

3.3 Results and discussion	91
3.4 Conclusions	97
3.5 References	121
Chapter 4 Comparative Studies of Human Milk Oligosaccharide	
Specificities of Human Galectin-1, 3, 9	127
4.1 Introduction	127
4.2 Materials and Methods	130
4.2.1 Oligosaccharides	130
4.2.2 Proteins	131
4.2.3 Mass spectrometry	131
4.2.4 ESI-MS affinity measurements for K_a value determination	132
4.3 Results and discussions	133
4.4 Conclusions	142
4.5 References	179
Chapter 5 Conclusions and Future Work	187
Bibliography	195

List of Tables

Table 2.1. Comparison of association constants (K_a) measured by liquid sample DESI-MS, ESI-MS and ITC for the interactions of **L2** and **L3** with Lyz and **L4** and **L5** with scFv in aqueous ammonium acetate solutions at pH 6.8 and 25 °C.

Table 3.1. Structures of oligosaccharides used in this study (**L1 – L20**).

Table 3.2. Association constants, K_a (units of 10^4 M^{-1}) for binding of HBGA and HMO oligosaccharides ($L_x = \text{L1 – L20}$) to Gal-3C, RSL, huNoV P dimer and CBM measured at 25 °C and pH 6.8 by the direct ESI-MS assay.

Table 3.3. Intrinsic association constants (units of 10^4 M^{-1}) for binding to RSL and the P particle measured at 25 °C and pH 6.8 by the *proxy protein* ESI-MS assay.

Table 4.1. Apparent association constants, $K_{a,app}$ (units of 10^4 M^{-1}) for binding of the HMOs (**L1 – L30**) to Gal3C, Gal1 and Gal9N determined in 20 mM aqueous ammonium acetate at 25 °C and pH 7.2 by the direct ESI-MS assay.

Table 4.2. Association constants ($K_{a,app}$) measured by ESI-MS for the interactions of ligand **L34-L37** with Gal1, Gal-3C and Gal-9N in aqueous ammonium acetate solutions at pH 6.8 and 25 °C.

Table 4.3. Association constants (K_a) measured by ESI-MS for the interactions of ligand **L33** with Gal1, Gal-3C and Gal-9N in aqueous ammonium acetate solutions at pH 6.8 and 25 °C.

Table 4.4. The 7 core structures available in HMOs used in this study

Table 4.5. Structures of HMOs used in this study (**L1 – L32**)

Table 4.6. HMOs structures in HMG 260 microarray V 2.0

Table 4.7. HMOs structures in Defined HMG microarray

Table 4.8. HMOs structures in CFG array V5.0

List of Figures

Figure 1.1. (a) Schematic presentation of a type 1 cross-linked complex. (b) Schematic presentation of a type 2 cross-linked complex

Figure 1.2. Schematic representation of ESI process in positive ion mode, adapted from reference.

Figure 1.3. Proposed ESI models ESI models proposed for the formation of gas-phase ions. (a) IEM: Small ion ejection from a highly charged nanodroplet. (b) CRM: Release of a folded protein into the gas-phase. (c) CEM: Ejection of disordered macromolecule. Figure is taken from reference 70.

Figure 1.4. Schematic diagram of the Bruker Apex Qe 9.4-Tesla FT-ICR mass spectrometer used in this study. Figure is adapted from the Bruker user's manual.

Figure 1.5. Illustration of the cyclotron motion of a positive ion of charge q moving with a velocity (v) in the presence of constant magnetic field (B) directed orthogonal to the motion of the ion. The ion experiences a Lorentz force $F = q (v \times B)$, which directs the ion to move in a counterclockwise orbit.

Figure 1.6. Illustration of excitation, image current detection and the production of mass spectrum by FTICR.

Figure 1.7. Schematic diagrams of (a) Waters Synapt G2 nanoESI-quadrupole -IMS-TOF mass spectrometer and (b) Waters Synapt G2-S nanoESI-quadrupole-IMS-TOF mass spectrometer used in this present study. Figures were adapted from the Waters user's manual.

Figure 1.8. Schematic representation of the quadrupole in Waters Synapt G2 Q-IMS-TOF mass spectrometer.

Figure 1.9. Schematic representation of typical DESI instrument, it is adapted from reference.

Figure 1.10. Schematic representation of the liquid sample DESI used in this study.

Figure 1.11. Schematic representation of the formation of nonspecific protein-ligand interactions (false positive), reproduced from reference 96.

Figure 2.1. Representative liquid sample DESI mass spectra acquired in positive ion mode for aqueous ammonium acetate (20 mM) solutions containing (a) Lyz (10 μ M), and (b) scFv (10 μ M). The ESI spray solution was 50/50 water/acetonitrile.

Figure 2.2. Representative liquid sample DESI mass spectra acquired in positive ion mode for aqueous ammonium acetate (20 mM, pH 6.8 and 25 $^{\circ}$ C) solutions containing Ubq (10 μ M), Lyz (10 μ M) and **L1** at (a) 15 μ M or (b) 40 μ M concentrations. The ESI spray solution was 50/50 water/acetonitrile.

Figure 2.3. ITC data measured for the binding of Lyz (0.087 mM) to **L2** (2.0 mM) in aqueous ammonium acetate (50 mM, pH 6.8 and 25 $^{\circ}$ C) solutions.

Figure 2.4. ITC data measured for the binding of Lyz (0.202 mM) to **L3** (2.0 mM) in aqueous ammonium acetate (50 mM, pH 6.8 and 25 $^{\circ}$ C) solutions.

Figure 2.5. Representative (a), (c) liquid sample DESI and (b), (d) ESI mass spectra acquired in positive ion mode for aqueous ammonium acetate (20 mM, pH 6.8 and 25 $^{\circ}$ C) solutions containing Lyz (10 μ M), **L2** (15 μ M) and Ubq (5 μ M) ((a) and (b)) or Lyz (10 μ M), **L3** (15 μ M) and Ubq (5 μ M) ((c) and (d)). For the liquid sample DESI-MS measurements, the ESI spray solution was 50/50 water/acetonitrile.

Figure 2.6. Representative (a), (c) liquid sample DESI and (b), (d) ESI mass spectra acquired in positive ion mode for aqueous ammonium acetate (20 mM, pH 6.8 and 25 $^{\circ}$ C)

solutions containing scFv (10 μM), **L4** (15 μM) and Lyz (5 μM) ((a) and (b)) or scFv (10 μM), **L5** (40 μM) and Lyz (5 μM) ((c) and (d)). For the liquid sample DESI-MS measurements, the ESI spray solution was 50/50 water/acetonitrile.

Figure 2.7. Representative reactive liquid sample DESI mass spectrum acquired in positive ion mode for an aqueous ammonium acetate (20 mM, pH 6.8 and 25 $^{\circ}\text{C}$) solution containing Lyz (10 μM) and Ubq (5 μM) and an ESI spray solution (50/50 water/acetonitrile) that contained **L2** (50 μM). The flow rates of both the sample and ESI spray solution were 5 $\mu\text{L min}^{-1}$. All other instrumental conditions were identical to those used for the liquid sample DESI measurements.

Figure 3.1. Structures of the oligosaccharides **L1** – **L20**. Monosaccharide key: Glucose (●), galactose (◐), N-acetylgalactosamine (◑), N-acetylglucosamine (■), sialic acid(◆), fucose (▲).

Figure 3.2. ESI mass spectra acquired in positive ion mode for 200 mM aqueous ammonium acetate solutions (pH 6.8 and 25 $^{\circ}\text{C}$) containing Gal-3C (5 μM), P_{ref} (4 μM), and a three-component library (**L1**, **L2** and **L3**, 10 μM each) with (a) 0 μM and (b) 23 μM CBM. (c) Plots of the abundance ratios of **L1**- (■), **L2**- (●) and **L3**-bound Gal-3C (▲) to free Gal-3C (*i.e.*, $R_{\text{proxy},x}$) versus CBM concentration (0 – 23 μM) measured under the same solution conditions as described for (a). Solid curves correspond to the apparent $R_{\text{proxy},x}$ calculated from the average affinity (K_a , Table 3.2). (d) Comparison of the affinities **L1** – **L3** for CBM measured using the *proxy protein* method (■) with those measured using *direct* ESI-MS assay (▨). Errors correspond to one standard deviation.

Figure 3.3. ESI mass spectra acquired in positive ion mode for 200 mM aqueous ammonium acetate solutions (pH 6.8 and 25 $^{\circ}\text{C}$) containing Gal-3C (8 μM), P_{ref} (3 μM),

and a fourteen-component library (L2, L4 – L15, L17, 24 μM each) with (a) 0 μM and (b) 11 μM RSL. (c) Plots of the abundance ratios of L17- (■), L12- (◆), L11- (●), L14- (◇), L2- (■), L5- (▲), L7- (●), L4- (●), L9- (●), L15- (●), L10- (■), L13- (◆), L8- (◇) and L6-bound Gal-3C (■) to free Gal-3C (i.e., $R_{\text{proxy},x}$) versus RSL trimer concentration (0 – 11 μM) measured under the same solution conditions as described for (a). Solid curves correspond to the apparent $R_{\text{proxy},x}$ calculated from the average affinity (K_a , Table 3.2). (d) Comparison of intrinsic affinities of L2, L4 – L15, L17 for RSL measured using the *proxy protein* method (■) with those measured using *direct* ESI-MS assay (▨). Errors correspond to one standard deviation.

Figure 3.4. ESI mass spectra acquired in positive ion mode for 200 mM aqueous ammonium acetate solutions (pH 6.8 and 25 °C) containing Gal-3C (8 μM), P_{ref} (2 μM), and a fourteen-component library (L6 - L15, 24 μM each) with (a) 0 μM and (b) 11 μM RSL. (c) Plots of the abundance ratios of L4- (■), L6- (◆), L9- (●), L10- (▲), L11- (●), L12- (x), L13- (■), L14- (▲) and L15-bound Gal-3C (●) to free Gal-3C (i.e., $R_{\text{proxy},x}$) versus RSL concentration measured under the same solution conditions as described for (a). Solid curves correspond to the apparent $R_{\text{proxy},x}$ calculated from the average affinity (K_a , Table 3.2). (d) Comparison of intrinsic affinities of L6 - L15 for RSL measured using the *proxy protein* method (■) with those measured using *direct* ESI-MS assay (▨). Errors correspond to one standard deviation.

Figure 3.5. ESI mass spectra acquired in positive ion mode for 200 mM aqueous ammonium acetate solutions (pH 6.8 and 25 °C) containing Gal-3C (5 μM), P_{ref} (4 μM) and a ten-component library (L1, L8, L13 and L16, 40 μM each; L2, L3, L5 and L18–L20, 10 μM each) with (a) 0 μM and (b) 7.8 μM P particle. (c) Plots of the

abundance ratios of L1- (■), L2- (■), L3- (◆), L5- (●), L8- (x), L13- (▲), L16- (●), L18- (x) and L19- (■) and L20-bound Gal-3C (▲) to free Gal-3C ($R_{proxy,x}$) versus P particle concentration measured under the same solution conditions as described for (a). Solid curves correspond to the apparent $R_{proxy,x}$ calculated from the average affinity (K_a , Table 3.2). (d) Comparison of intrinsic affinities of L1-L3, L5, L8, L13, L16, L18–L20 for P particle measured using the *proxy protein* method (■) with those measured using *direct* ESI-MS assay for P dimer (▨). Errors correspond to one standard deviation.

Figure 3.6. Calculated plots of R_{proxy} versus $[P_T]_0$. Initial conditions used for the numerical simulations: $[P_{proxy}]_0 = 5 \mu\text{M}$, $[L]_0 = 10 \mu\text{M}$ (a, d, g, j), $20 \mu\text{M}$ (b, e, h, k) and $50 \mu\text{M}$ (c, f, i, l). $K_{a,proxy} = 10^3 \text{ M}^{-1}$ (a-c), 10^4 M^{-1} (d-f), 10^5 M^{-1} (g-i), 10^6 M^{-1} (j-l). $[P_T]_0$ values are shown on the x-axis. $K_{a,PT,x}$ ranged (from top to bottom) from 1×10^3 (blue), 2×10^3 (red), 6×10^3 (green), 1×10^4 (purple), 2×10^4 (light blue), 3×10^4 (orange), 6×10^4 (pale blue), 1×10^5 (pink), 2×10^5 (light green) to 1×10^6 (light purple).

Figure 3.7. Calculated plots of ΔR_{proxy} versus $[P_T]_0$. Initial conditions used for numerical simulations: $[P_{proxy}]_0 = 5 \mu\text{M}$, $[L]_0 = 10 \mu\text{M}$ (a, d, g, j), $20 \mu\text{M}$ (b, e, h, k) and $50 \mu\text{M}$ (c, f, i, l). $K_{a,proxy} = 10^3 \text{ M}^{-1}$ (a-c), 10^4 M^{-1} (d-f), 10^5 M^{-1} (g-i), 10^6 M^{-1} (j-l). $[P_T]_0$ values are shown on the x-axis. $K_{a,PT,x}$ ranged (from top to bottom) from 1×10^3 (blue), 2×10^3 (red), 6×10^3 (green), 1×10^4 (purple), 2×10^4 (light blue), 3×10^4 (orange), 6×10^4 (pale blue), 1×10^5 (pink), 2×10^5 (light green) to 1×10^6 (light purple).

Figure 3.8. ESI mass spectra in positive ion mode for a 30 mM aqueous ammonium acetate solution (pH 6.8, 25 °C) of RSL (P, 1.3 μM) and P_{ref} (1 μM) with (a) 0.8 μM L17 or (b) 2 μM L7. Insets show normalized distribution of free and ligand-bound RSL before (▨) and after (■) correction for nonspecific ligand binding.

Figure 3.9. ESI mass spectra in positive ion mode for a 10 mM aqueous ammonium acetate solution (pH 6.8, 25 °C) of VA387 P dimer (P, 12 μ M) and P_{ref} (10 μ M) with (a) 80 μ M **L8**, or (b) 80 μ M **L13**. Insets show normalized distribution of free and ligand-bound P dimer before (▨) and after (■) correction for nonspecific ligand binding.

Figure 3.10. ESI mass spectra in positive ion mode for a 30 mM aqueous ammonium acetate solution (pH 6.8, 25 °C) of Gal-3C (P, 5 μ M) and P_{ref} (5 μ M) with (a) 40 μ M **L17** or (b) 20 μ M **L7**. Insets show normalized distribution of free and ligand-bound RSL before (▨) and after (■) correction for nonspecific ligand binding.

Figure 4.1. Structures of the oligosaccharides **L1** – **L32**. Monosaccharide key: Glucose (●), galactose (○), N-acetylgalactosamine (◻), N-acetylglucosamine (■), sialic acid (◆), fucose (▲).

Figure 4.2. ESI mass spectra in positive ion mode for a 30 mM aqueous ammonium acetate solution (pH 6.8, 25 °C) of Gal-1 (G1, 3 μ M) and P_{ref} (2 μ M) with (a) 5 μ M **L3** or (b) 10 μ M **L3**. Insets show normalized distribution of free and ligand-bound Gal-1 before (▨) and after (■) correction for nonspecific ligand binding.

Figure 4.3. ESI mass spectra in positive ion mode for a 30 mM aqueous ammonium acetate solution (pH 6.8, 25 °C) of Gal-3C (G3, 8 μ M) and P_{ref} (3 μ M) with (a) 20 μ M **L3** or (b) 40 μ M **L3**. Insets show normalized distribution of free and ligand-bound Gal-3C before (▨) and after (■) correction for nonspecific ligand binding.

Figure 4.4. ESI mass spectra in positive ion mode for a 30 mM aqueous ammonium acetate solution (pH 6.8, 25 °C) of Gal-9N (G9, 10 μ M) and P_{ref} (2 μ M) with (a) 8 μ M **L3** or (b) 15 μ M **L3**. Insets show normalized distribution of free and ligand-bound Gal-9N before (▨) and after (■) correction for nonspecific ligand binding.

Figure 4.5. Summary of the comparison of the ESI-MS ($K_{a,app}$, M^{-1}) and RFU value obtained from HMO microarray for Gal-1. HM-SGM-v2 microarray data compared to ESI-MS ($K_{a,app}$, M^{-1}) are presented at (a) three concentration (2, 20 and 200 $\mu\text{g/ml}$) (b) one highest concentration (200 $\mu\text{g/ml}$) available. Defined HMG microarray compared to ESI-MS ($K_{a,app}$, M^{-1}) are presented at (c) three concentration (2, 20 and 200 $\mu\text{g/ml}$) (d) one highest concentration (200 $\mu\text{g/ml}$) available. Chart ID for HM-SGM-v2 are taken from supplementary data on Table 4.6 and Chart ID for Defined HMG microarray are taken from supplementary data on Table 4.7. Errors correspond to one standard deviation.

Figure 4.6. Summary of the comparison of the ESI-MS ($K_{a,app}$, M^{-1}) and RFU value obtained from HMO microarray for Gal-3C. HM-SGM-v2 microarray data compared to ESI-MS ($K_{a,app}$, M^{-1}) are presented at (a) three concentration (2, 20 and 200 $\mu\text{g/ml}$) (b) one highest concentration (200 $\mu\text{g/ml}$) available. Defined HMG microarray compared to ESI-MS ($K_{a,app}$, M^{-1}) are presented at (c) three concentration (2, 20 and 200 $\mu\text{g/ml}$) (d) one highest concentration (200 $\mu\text{g/ml}$) available. Chart ID for HM-SGM-v2 are taken from supplementary data on Table 4.6 and Chart ID for Defined HMG microarray are taken from supplementary data on Table 4.7. Errors correspond to one standard deviation.

Figure 4.7. Summary of the comparison of the ESI-MS ($K_{a,app}$, M^{-1}) and RFU value obtained from HMO microarray for Gal-9N. HM-SGM-v2 microarray data compared to ESI-MS ($K_{a,app}$, M^{-1}) are presented at (a) two concentration (2 and 20 $\mu\text{g/ml}$) (b) one highest concentration (20 $\mu\text{g/ml}$) available. Defined HMG microarray compared to ESI-MS ($K_{a,app}$, M^{-1}) are presented at (c) one concentration (2 $\mu\text{g/ml}$) (d) one highest concentration (2 $\mu\text{g/ml}$) available. Chart ID for HM-SGM-v2 are taken from

supplementary data on Table 4.6 and Chart ID for Defined HMG microarray are taken from supplementary data on Table 4.7. Errors correspond to one standard deviation.

Figure 4.8. ESI mass spectra in positive ion mode for a 30 mM aqueous ammonium acetate solution (pH 6.8, 25 °C) of Gal-3C (G3, 5 μ M) and P_{ref} (2 μ M) with (a) 0.05 g/L or (b) 0.1 g/L diluted solution of Vivinal GOS 90 powder. Insets show normalized distribution of free and ligand-bound Gal-3C before (■) and after (■) correction for nonspecific ligand binding.

Figure 4.9. ESI mass spectra in positive ion mode for a 30 mM aqueous ammonium acetate solution (pH 6.8, 25 °C) of Gal-3C (G3, 5 μ M) and P_{ref} (2 μ M) with (a) ~ 6000 times or (b) ~ 1200 times diluted solution of Vivinal GOS syrup. Insets show normalized distribution of free and ligand-bound Gal-3C before (■) and after (■) correction for nonspecific ligand binding.

Figure 4.10. ESI mass spectra in positive ion mode for a 30 mM aqueous ammonium acetate solution (pH 6.8, 25 °C) of Gal-3C (G3, 5 μ M) and P_{ref} (3 μ M) with (a) 20 μ M L34 or (b) 40 μ M L34. Insets show normalized distribution of free and ligand-bound Gal-3C before (■) and after (■) correction for nonspecific ligand binding.

Figure 4.11. Structure of the L33 (β -D-Gal-(1 \rightarrow 4)- β -D-GlcNAc).

Figure 4.12. Structure of the of fructo-oligosaccharides; L34 (β -D-Fru-(2 \rightarrow 1)-[β -D-Fru-(2 \rightarrow 1)]₃- α -D-Glc), L35 (β -D-Fru-(2 \rightarrow 1)-[β -D-Fru-(2 \rightarrow 1)]₄- α -D-Glc), L36 (β -D-Fru-(2 \rightarrow 1)-[β -D-Fru-(2 \rightarrow 1)]₅- α -D-Glc), L37 (β -D-Fru-(2 \rightarrow 1)-[β -D-Fru-(2 \rightarrow 1)]₆- α -D-Glc).

Figure 4.13. Structures of galacto-oligosaccharides ($n = 0-6$).

Figure 4.14. ESI mass spectra in positive ion mode for a 30 mM aqueous ammonium acetate solution (pH 6.8, 25 °C) of Gal-1 (G1, 6 μ M) and P_{ref} (1 μ M) with (a) 0.05 g/L or

(b) 0.1 g/L diluted solution of Vivinal GOS 90 powder. Insets show normalized distribution of free and ligand-bound Gal-1 before (■) and after (■) correction for nonspecific ligand binding.

Figure 4.15. ESI mass spectra in positive ion mode for a 30 mM aqueous ammonium acetate solution (pH 6.8, 25 °C) of Gal-1 (G1, 6 μM) and P_{ref} (1 μM) with (a) ~ 6000 times or (b) ~ 2400 times diluted solution of Vivinal GOS syrup. Insets show normalized distribution of free and ligand-bound Gal-1 before (■) and after (■) correction for nonspecific ligand binding.

Figure 4.16. ESI mass spectra in positive ion mode for a 30 mM aqueous ammonium acetate solution (pH 6.8, 25 °C) of Gal-9N (G9, 10 μM) and P_{ref} (0.7 μM) with (a) 0.05 g/L or (b) 0.1 g/L diluted solution of Vivinal GOS 90 powder. Insets show normalized distribution of free and ligand-bound Gal-9N before (■) and after (■) correction for nonspecific ligand binding.

Figure 4.17. ESI mass spectra in positive ion mode for a 30 mM aqueous ammonium acetate solution (pH 6.8, 25 °C) of Gal-9 (G9, 10 μM) and P_{ref} (1 μM) with (a) ~ 2500 times or (b) ~ 2000 times diluted solution of Vivinal GOS syrup. Insets show normalized distribution of free and ligand-bound Gal-9N before (■) and after (■) correction for nonspecific ligand binding

Figure 4.18. ESI mass spectra in positive ion mode for a 30 mM aqueous ammonium acetate solution (pH 6.8, 25 °C) of Gal-1 (G1, 6 μM) and P_{ref} (1 μM) with (a) 30 μM **L34** or (b) 40 μM **L34**. Insets show normalized distribution of free and ligand-bound Gal-1 before (■) and after (■) correction for nonspecific ligand binding.

Figure 4.19. ESI mass spectra in positive ion mode for a 30 mM aqueous ammonium acetate solution (pH 6.8, 25 °C) of Gal-9N (G9, 10 μ M) and P_{ref} (1 μ M) with (a) 40 μ M **L34** or (b) 60 μ M **L34**. Insets show normalized distribution of free and ligand-bound Gal-9N before (■) and after (●) correction for nonspecific ligand binding.

Figure 4.20. Comparison of binding affinity, $K_{a,app}$ (M^{-1}) obtained from direct ESI-MS method to RFU value obtained from CFG glycan microarray data V 5.0 of (a) Gal-1, (b) Gal-3C and (c) Gal-9N. Concentration of each of the 3 galectins is given in the diagram for respective RFU value. Chart ID were taken from glycan microarray data V 5.0 and errors correspond to one standard deviation in the represented data.

List of Abbreviations

<i>Ab</i>	Abundance of gas-phase ions
<i>Ab_{app}</i>	Apparent abundance of gas-phase ions
<i>ACS</i>	Average charge state
BIRD	Blackbody infrared radiative dissociation
CaR	Catch-and-release
CEM	Chain ejection model
CD	Circular dichroism
CID	Collision induced dissociation
CRM	Charge residue model
Da	Dalton
DC	Direct current
DESI	Desorption electrospray ionization
ECD	Electron capture dissociation
ELISA	Enzyme-linked immunosorbent assay
ESI	Electrospray ionization
ESI-MS	Electrospray ionization mass spectrometry
ETD	Electron transfer dissociation
FTICR	Fourier transform ion cyclotron resonance
Fuc	Fucose
Gal	Galactose
Gal-3C	The C-terminal fragment of human galectin-3
GalNAc	N-acetylgalactosamine

Glc	Glucose
GlcNAc	N-acetylglucosamine
H	Hydrogen
H-bond	Hydrogen bond
HEPES	4-(2-hydroxyethyl)-1-piperazineethanesulfonic acid
HMOs	Human milk oligosaccharides
HPLC	High performance liquid chromatography
i.d.	Inner diameter
IEM	Ion evaporation model
IMS	Ion mobility separation
IS	Internal standard
ITC	Isothermal titration calorimetry
K_a	Association constant
$K_{a,app}$	Apparent association constant
L	Ligand
Lyz	Lysozyme
m/z	Mass-to-charge ratio
<i>m</i> -NMA	3-nitrobenzoic acid
MS	Mass spectrometry
MW	Molecular weight
nanoESI	Nanoflow electrospray ionization
N	Nitrogen
Neu	Neuraminic acid

Neu5Ac	N-Acetylneuraminic acid
NMR	Nuclear magnetic resonance
O	Oxygen
o.d.	Outside diameter
P	Protein
PBS	Phosphate buffered saline
PL	Protein-ligand complex
P _{ref}	Reference protein
Pt	Platinum
Q-IMS-TOF	Quadrupole-ion mobility separation time-of-flight
<i>R</i>	Abundance ratio
<i>RF</i>	Response factor
RF	Ratio frequency
S/N	Signal to noise ratio
scFv	Single chain variable fragment
SPR	Surface plasmon resonance spectroscopy
TOF	Time of flight
Tris	Tris(hydroxymethyl) aminomethane
TWIMS	Travelling wave ion mobility spectrometry
Ubq	Ubiquitin
v/v	Volume per volume

Chapter 1

Study of Protein-Carbohydrate Interactions by Electrospray Ionization Mass Spectrometry for Development of Mass Spectrometry Methods

1.1 Introduction

1.1.1 Carbohydrates: Structure and Function

In our living system, proteins, nucleic acids, lipids, and carbohydrates are the major classes of organic molecules. Except carbohydrates, all other molecules caught the attention of the researchers even though carbohydrates underlie a broad area of biological function. This negligence of carbohydrate research might be due to their ubiquitous nature and structural complexity.¹ But recently, carbohydrate research got significant attention with the expansion of the field of glycobiology.^{2,3} Carbohydrates are the most commonly found organic molecules in nature and they are synthesized and metabolized in almost all organisms. They can be used to store energy (glycogen and starch), to form structural components (cellulose and lignin) in plants and do many others housekeeping functions in living system. Carbohydrates are often found as covalently linked to cellular proteins and lipids which are secreted in the cell secretory pathway⁴ and sometime they are found as free oligosaccharides in milk and saliva.⁵ Cell surface carbohydrates, e.g. gangliosides, globosides and histo-blood group antigens (HBGAs) are involved in many physiological functions that include signal transduction and recognition, embryonic growth and development, host pathogen interaction, immune response, metastasis, intracellular trafficking and rigidity of membrane,⁶⁻¹² whereas free carbohydrates in human milk and saliva can act as decoys and inhibit the binding of pathogen lectins to

host cell receptors.¹³ Free human milk oligosaccharides also have prebiotic effects and can promote the growth of *Bifidobacterium bifidum* which is responsible for protecting the gastrointestinal tract from various deleterious effects.⁵ Carbohydrates are mainly present as glycolipids and glycoproteins on the cell surface. Glycolipids form the lipid part of the plasma membrane whereas glycoproteins remain integrated inside the cell membrane proteins. Intriguing features are that they are not encoded by the genome even though they contain enormous amount of biological information.¹⁴ Simple carbohydrates are well known for their chemical and physical properties but complex carbohydrates especially those present on the cell surface are difficult to understand and their role during normal physiological condition and disease condition are yet to be thoroughly studied.^{12,15-22}

1.1.2 Protein-Carbohydrate Interactions

Multivalent binding interactions are common in a large number of biological processes.²³ Among all type of interactions, the bivalent-bivalent interaction got the focus of the scientists because lot of growth factors present in biological system appear to induce receptor dimerization which leads to signal transduction.²⁴ However, other systems involve multivalent interactions, including the multivalent binding between glycoconjugates and carbohydrates with lectins. Cross-linking interactions show that multivalent lectins complexed with glycoconjugates result in the formation of supermolecular assemblies.²⁵

Lectins are one of the common carbohydrate proteins that are widely distributed in nature, including plants, animals and microorganisms. Many animal lectins are well studied and they have known biological functions. For example, lectins are needed for

receptor-mediated endocytosis of glycoproteins; selectins are implicated for cellular recognition and adhesion.²⁶ Galectins have roles in metastasis, cellular growth control, triggering inflammation, and regulation of cell death.²⁷ Structural studies showed that multivalent lectin complexed with carbohydrates by cross linking have different specificities for these types of interactions. Two different types of multivalent complexes are usually observed. Type 1 complexes can be formed by cross linking bivalent lectin and bivalent carbohydrate (Figure 1a) whereas type 2 complexes are formed between lectins and carbohydrates where one of the two molecules possesses a valency of more than 2. An example of tetravalent lectin complexed with divalent carbohydrates is shown in Figure 1b.²⁵

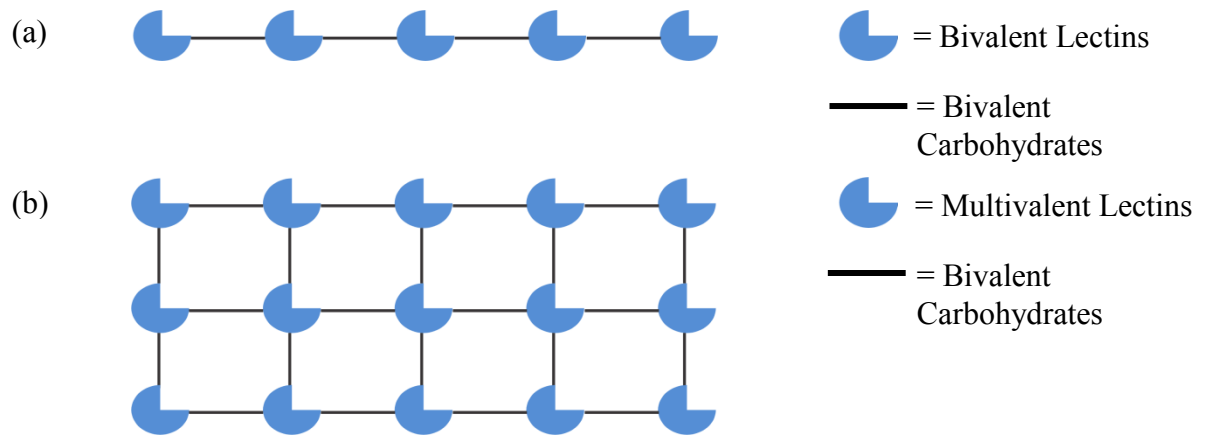


Figure 1.1. (a) Schematic presentation of a type 1 cross-linked complex. (b) Schematic presentation of a type 2 cross-linked complex

Low affinity binding is the common characteristic of protein-carbohydrate interactions. Usually these bindings are weak which is in $10^3 - 10^6 \text{ M}^{-1}$ range. It is known that favorable enthalpy is the key to these types of interactions which is offset by the multiple

contacts that occur during binding. These contact points are driven by van der Waals' interactions, hydrogen bonds and hydrophobic stacking between protein and carbohydrates.²⁸⁻³² Recent studies have shown that polar-polar interactions (hydrogen bonds) in the binding site are responsible for strong affinity in between protein and carbohydrates as it requires charged groups which make the bond distance shorter.^{29,33} It is commonly known, enthalpy-entropy compensations are characteristics of weak interactions and favorable enthalpy is compensated by unfavorable entropy. One of the reasons for this compensation is water molecules which are involved in hydrogen bonding in between themselves as well as with hydrophilic exteriors of proteins and carbohydrates. So, water plays a crucial role in protein-carbohydrate interactions by contributing to the binding affinity with enthalpy-entropy compensations that seems be unique for each protein-ligand involved in interactions.^{32,34-36} So it is clear that, protein-carbohydrate interactions comprise a unique structural-thermodynamic group where enthalpy and entropy changes might be relatively large, however free energy change of binding (ΔG°) between a protein receptor and different ligands is relatively small. Therefore, increasing the protein-carbohydrate binding affinity by increasing free energy (ΔG°) of specific interactions remains a difficult task.

In brief, study of the molecular basis of protein-carbohydrate interaction along with binding specificity and affinity is fundamentally important for drug discovery and disease diagnosis. So, development of suitable analytical methods for in vitro quantification of biologically important protein-carbohydrate interactions is essential. There are two strategies that can be used to study these interactions. Water soluble oligosaccharide

analogues or water insoluble real cellular receptor such as glycolipids can be used to study these interactions.

Various analytical techniques are available for studying protein-carbohydrate interactions. Among them, X-ray crystallography is one of the most powerful techniques. Technology advancement in structure determination by using X-ray crystallography has increased the rapid advancement in three-dimensional protein structure determination. More than 80,000 X-ray structures of protein, protein-ligand and protein-protein complexes are reported in the PDB (PDB; <http://www.pdb.org>). Using X-ray crystallography information about protein-carbohydrate complexes and spatial arrangement can be easily studied. If protein structure and crystallization conditions are already known then routine determination of structure of protein-carbohydrate complexes is possible to investigate.^{37,38} However, strength of the protein-carbohydrate complexes cannot be evaluated by using this costly time-consuming technique. It also does not give idea about the nature of the interaction in solution and in crystal.³⁹

Solid phase chemical tools are gaining popularity day by day. Different approaches are applied to analyze protein carbohydrate interactions using solid-supported strategies. Surface plasmon resonance (SPR), enzyme-linked immunosorbent assay (ELISA), glycan microarray screening are some of the commonly used techniques.

Surface plasmon resonance (SPR) has become an important technique and it is rapidly developing for studying protein-carbohydrate interactions. SPR is applied for binding kinetics determination, affinity of interactions, study of specificities, assay and screening as well as measurement of concentration of the protein and carbohydrates present in the system. Conventionally, SPR technique requires one binding element to be immobilized

on sensor chip. At the same time other binding element in solution is flowed over the surface of the sensor. Thus, protein-carbohydrate interaction is detected by measuring the small changes in refractive index at the sensor surface.⁴⁰⁻⁴³

Enzyme-linked immunosorbent assay (ELISA) is a frequently used biochemical technique for evaluating protein carbohydrate interaction. Here carbohydrates are affixed to a surface and then a specific protein is applied over the surface so that it can bind to the carbohydrate ligands. Sometime proteins are linked to enzyme to convert an added substance to produce a detectable signal.⁴⁴

Glycan microarray is another popular technique which has changed the analysis of protein carbohydrate interactions. It can simultaneously provide enormous amount of protein carbohydrate binding information.⁴⁵⁻⁴⁷ This new technique involves application of a small amount of protein containing buffer to a microarray comprised of carbohydrate library which is then detected by fluorescence signal from a labeled protein or a secondary reagent that binds to protein. This technique allows interpreting result from a single experiment with small reagents. Using other approaches it might require months of work.⁴⁸ However, glycan microarray cannot provide quantitative binding data for protein carbohydrate interactions.

Glycans are most commonly immobilized on glass surface or microtiter plates, gel beads and nitrocellulose membranes are used as solid materials. Both covalent and noncovalent immobilizations have been used for glycan array fabrication and they are modified with functional groups which react to surface of the base.^{49,50} Even though surface based approaches mimic the multivalent presentation of cell surface carbohydrates, their nature of coupling, ligand density and orientation, mobility of the ligands are always in question

and give false negatives.⁵¹ Also, these results are sometime not comparable to the results obtained from solution based methods.

Among all solution based techniques, isothermal titration calorimetry (ITC) is considered as one of the most “clean” binding assay technique which can determine the thermodynamic binding parameters, i.e., affinity of binding (K_a), changes of enthalpy (ΔH), and stoichiometry of binding (n) of protein-carbohydrate interactions. For single analysis it requires large amount of sample (~mg) and long data acquisition time by using conventional ITC instrument.³⁰

Fluorescence polarization (FP) is a technique which provides information on mobility and orientation of a molecule including modulation occurs during protein-ligand interaction. FP utilizes the light emitting capacity of molecules. It measures the amount of light emitted from protein bound fluorescently tagged ligand after excitation by plane polarized light.⁵²

Nuclear magnetic resonance (NMR) spectroscopy is another commonly used technique. It is a solution based method and most commonly used for characterizing small protein structure in solution and for measuring interactions between proteins and ligands.^{53,54}

Saturation transfer difference (STD)-NMR method has been used for identification and characterization of the binding epitopes of ligands. For measuring binding, chemical-shift changes, changes of diffusion constant, relaxation time changes, nuclear overhauser effect changes are some significant parameters that are used for binding affinity measurement.⁵⁵

Electrospray ionization mass spectrometry (ESI-MS) is one of the emerging techniques. It can be used as a reliable tool for quantifying noncovalent protein interactions in

solution phase. The measurements are either direct or indirect. The assay is based on the detection of free and ligand-bound protein ions by ESI-MS following to the determination of the protein – ligand association constant (K_a) from the abundance ratio of the bound and unbound protein ions measured for a known solution of initial concentrations of protein and ligand. Direct ESI-MS assay is simple, doesn't require labeling or immobilization. This method is fast and can be completed in ~1 minute. It gives insight into binding stoichiometry and the ability to measure multiple binding equilibria simultaneously. In addition, sample consumption is minimal while performing nanoflow ESI (nanoESI) which works at solution flow rates in the nL/min range and consume picomoles or less of analyte per analysis. Besides its diverse applications on quantifying noncovalent interactions, ESI-MS has appeared as an important addition to the arsenal of techniques available for reliable measurement of the chemical and biochemical reaction kinetics. Not only that, gas-phase studies of desolvated noncovalent protein complexes by ESI-MS offer an opportunity to study their intrinsic properties, i.e., their structure, kinetic stability and solvent effects. An overview of ESI-MS techniques, starting with instrumentation followed by application is given below.

1.2 Electrospray Ionization Mass Spectrometry

Before explaining the different ESI-MS techniques for studying non-covalent biological complexes, it is important to first explain the basic principles of ESI-MS.

1.2.1 Electrospray Ionization

ESI is a soft ionization method that can be used to introduce biologically important molecules into the gas phase without fragmentation. In 1991, Henion and coworkers discovered a non-covalent biological complex, a protein-ligand complex consisting of a

small hydrophilic immunosuppressive binding protein FKBP, with a specific ligand FK506, by ESI-MS for the very first time.⁵⁶ Later on, ESI-MS has been used to detect a wide variety of non-covalent biological complexes, including enzyme-substrate/inhibitor,⁵⁷ lectin-carbohydrate,⁵⁸ antibody-antigen,⁵⁶ multiprotein⁵⁹ and DNA-ligand complexes.^{60,61}

Shown in Figure 1.2 is a diagram describing the ESI process involved in the formation of gas phase ions. In ESI-MS, analyte solution is placed into an ESI emitter, typically a metal capillary. The mechanism of the ESI process⁶³ involves three separate steps:

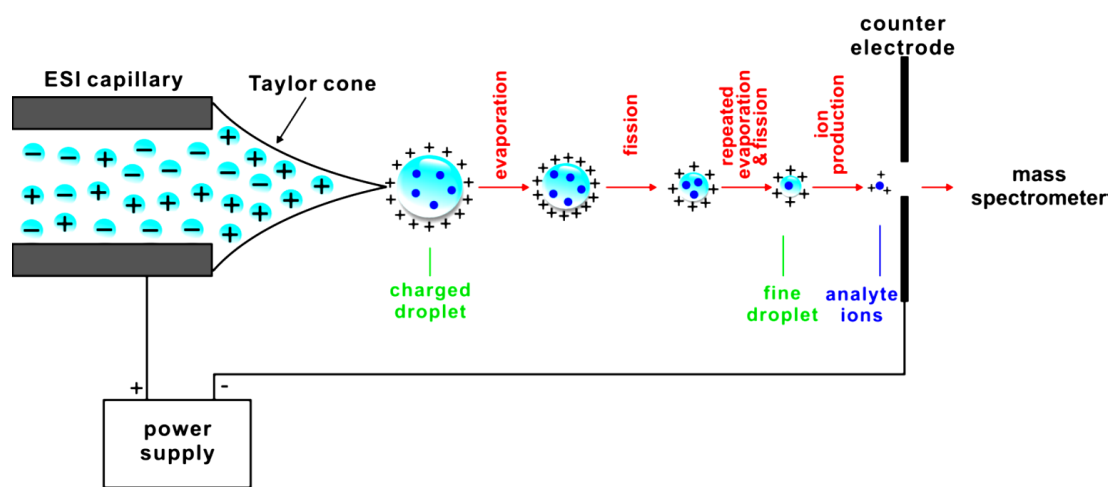


Figure 1.2. Schematic representation of ESI process in positive ion mode, adapted from reference.⁶²

(a) The production of charged droplets.

By applying a high voltage to the ESI emitter, the electric field causes charge separation in the solution, where the charged electrolytes move towards the liquid surface leading to the formation of a liquid cone named as a Taylor cone.⁶⁴ The enhancement of surface

area due to the cone formation is opposed by the surface tension of the liquid. Under adequate high field, the liquid cone becomes unstable and a fine jet emerges from the cone tip. The surface of the jet, which is charged by excess amount of positive ions, will break up into small charged droplets due to the repulsion between the charges.

(b) The shrinkage of the droplets by solvent evaporation followed by droplet fissions.

The charged droplets developed at the spray needle will shrink during solvent evaporation. Electric field is increased and it is normal to the droplet surface and the charge remains constant. As the density of the charges on the surface of the droplet enhances to near the Rayleigh limit, the time when the Columbic repulsion of the surface charges is equal to the surface tension of the droplets, they experience Rayleigh fission, and finally make small highly charged offspring droplets.

(c) The gas phase ions formation.

Three mechanisms have been proposed to account for the formation of gas-phase ions from the small and highly charged droplets:

- I. Ion evaporation model (IEM)
- II. Charge residue model (CRM).
- III. Chain ejection model (CEM)

Ion evaporation model (IEM): Iribarne and Thompson^{65,66} proposed this model. Here it assumes that ions emit from the surface of highly charged droplets at the time when their sizes become small enough to emit from the droplets. Charges are acquired by analyte during evaporation from the droplets. The IEM is considered to operate for small inorganic and organic ions.

Charged residue model (CRM): This model is introduced by Dole and coworkers.⁶⁷ It says that successive fissions of droplets finally produce highly charged nanodroplets which contain a single macromolecule. While the final droplets evaporate to dryness, charges on the droplets surface are transferred to the macromolecules resulting in the production of the gas-phase ions. The consequence of the CRM is the multiple-charged macroions production with a state distribution in a narrow range, and it is believed to be determined by a combination of the accessibility of ionizable residues near the droplet surface and the Rayleigh limit.^{62,68} The CRM is experimentally well-supported for natively folded proteins.⁶⁷⁻⁶⁹

Chain ejection model (CEM): Konermann and coworkers⁷⁰⁻⁷² suggested that the CEM applies to unfolded proteins where the chains of macromolecules are disordered, partially hydrophobic, and they are capable of carrying excess charge. This mechanism assumes that in a highly charged nanodroplet, the unfolded macromolecule chains immediately migrate to the droplet surface to minimize solvent interactions with the hydrophobic regions. When chain reaches the end point they get expelled into the gas-phase. This event is followed by stepwise sequential ejection of the remaining chain resulting in separation from the nanodroplet. In comparison to the ions of the folded protein generated via the CRM, the ions produced by the CEM are multiple-charged, though they usually carry more charges and exhibit a wider charge state distribution.⁷²

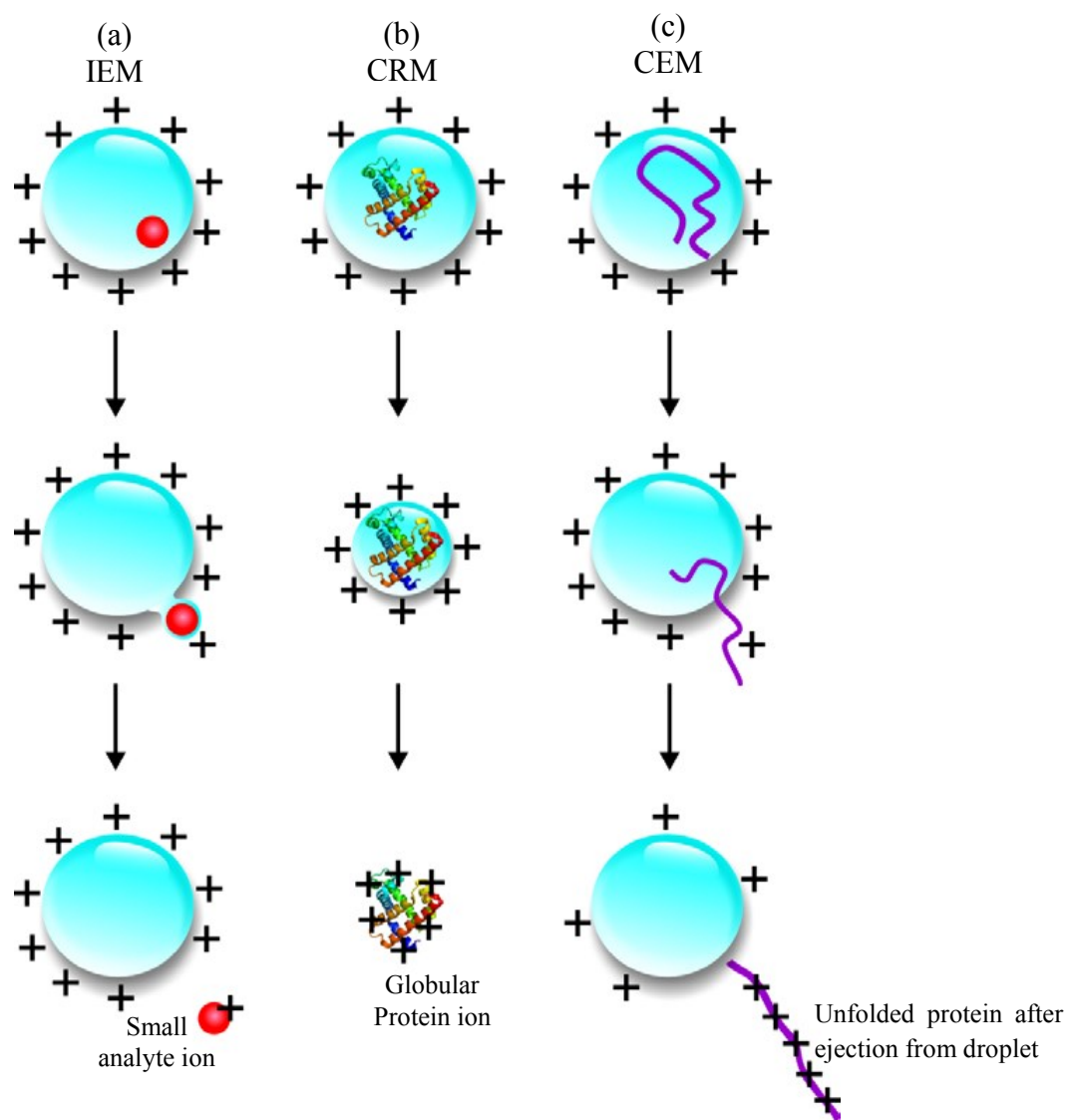


Figure 1.3. ESI models proposed for the formation of gas-phase ions. (a) IEM: Small ion ejection from a highly charged nanodroplet. (b) CRM: Release of a folded protein into the gas-phase. (c) CEM: Ejection of disordered macromolecule. Figure is adapted from reference 70.

1.2.2 MS Instrumentation

Mass analyzers are of different types. They include magnetic sector, quadrupole, ion trap, fourier transform ion cyclotron resonance (FTICR) and time of flight (TOF). In the present study, nanoESI combined with FTICR and hybrid quadrupole-ion mobility separation (IMS)-TOF mass spectrometers were used.

1.2.2.1 Fourier transform ion cyclotron resonance mass spectrometer

Shown in Figure 1.4 is a schematic diagram of the Bruker Apex-Qe nanoESI-FTICR mass spectrometer used in the present work (Chapters 2 and 4). The other mass spectrometer used in this thesis (Chapter 3) is a Synapt G2 and G2S Q-IMS-TOF mass spectrometer (Figure 1.7). The Apex-Qe is a hybrid quadrupole-FTICR mass spectrometer. The quadrupole in mass spectrometer can act as a mass filter to isolate targeted analyte ions for tandem MS (MS/MS) analysis. However, the quadrupole was operated in radio frequency (RF)-only mode and it served as a wide band-pass filter to transmit analyte ions. The operation scheme of the Apex-Qe is very similar to the previous generation Apex-II nanoESI-FTICR, where the ion source represents the main difference between them. The ions generated in the ESI process, with the help of a nebulizer gas and counter-drying gas first enter the vacuum system of the Apex Qe through a metal capillary. Later, these ions enter the transmitting funnels and skimmers orthogonally with the help of a deflector from the capillary exit present in the mass spectrometer. Then the ions are stored electrostatically in the hexapole of the spectrometer followed by further accumulation in the quadrupole. After accumulation, these analyte ions are transferred through ion optics series into the ICR cell for detection.

FTICR mass spectrometers were used in this present study for their good resolving power and mass accuracy. The general operating principles of FTICR are elaborately described in many reviews⁷³⁻⁷⁵ and therefore, only a brief overview is given here. The ICR cell consists of three pairs of plates (trapping, excitation and detection) which are located inside a spatially uniform static superconducting high field magnet and it is cooled by liquid helium and liquid nitrogen. While the ions pass into the magnetic field they are bent into a circular motion in a plane perpendicular to the field (see Fig. 1.5) by the Lorentz force. The cyclotron frequency, ω_c is expressed in eq 1.1:

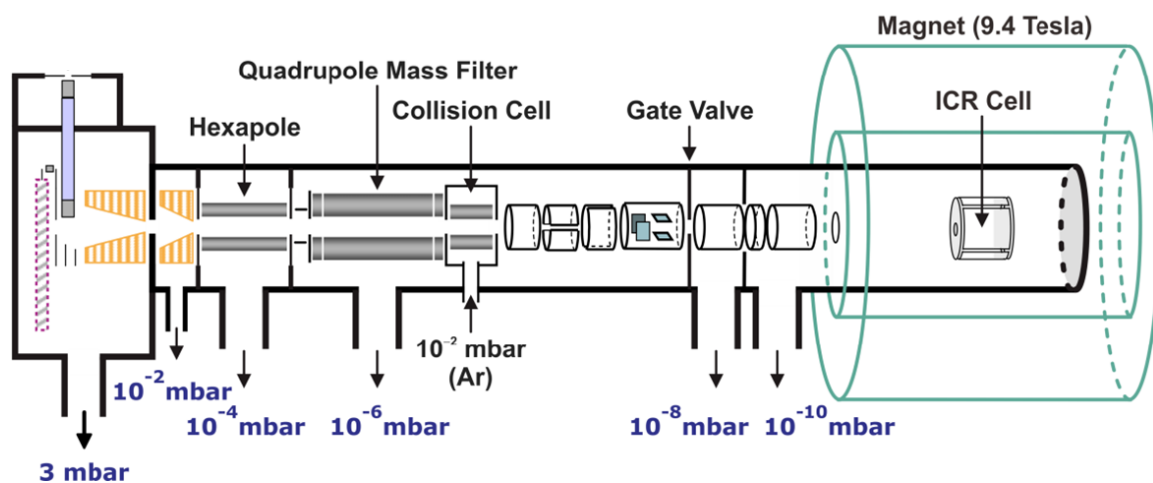


Figure 1.4. Schematic diagram of the Bruker Apex Qe 9.4-Tesla FT-ICR mass spectrometer used in this study. Figure is adapted from the Bruker user's manual.

$$\omega_c = \frac{qB}{m} = \frac{zeB}{m} \quad (1.1)$$

where ω_c is the cyclotron frequency, q is the charge of the ion ($q = ze$, where z and e are the charge and the elementary charge, respectively), B is the magnetic strength and m is

the mass of the ion. An important feature of eq. 1 is that all ions of a given m/z rotate at the same frequency, independent of their velocities.

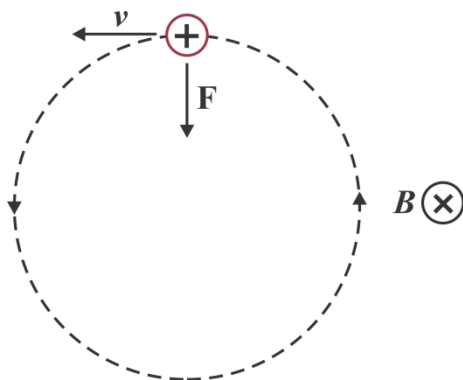


Figure 1.5. Illustration of the cyclotron motion of a positive ion of charge q moving with a velocity (v) in the presence of constant magnetic field (B) directed orthogonal to the motion of the ion. The ion experiences a Lorentz force $F = q (v \times B)$, which directs the ion to move in a counterclockwise orbit.

At this point, no signal is observed from mass spectrometer because the radius of the ion motion is very small. In order to produce a signal for the analyte ions trapped in the ICR cell, excitation of each single m/z is achieved by a swept RF pulse throughout the excitation plates of the ICR cell. If the frequency of the applied electric field matches their ω_c , the ions will absorb energy and thus they will move circularly with a bigger orbital radius but ω_c will remain same. Shown in Figure 1.6 is the spiral trajectory of excited analyte ions with the same m/z and ω_c . As they consistently pass the detection plates of the ICR cell which are parallel to the magnetic axis, the orbiting ions accelerate an alternating current (image current) on the plates (Figure 1.6). The amount of this current is proportional to the number of ions in the ICR cell during the frequency of the alternating current matches the ω_c of the ions. FT converts the detected image current

from the time domain signal into the frequency domain and a mass spectrum can be generated as ω_c is related to m/z .

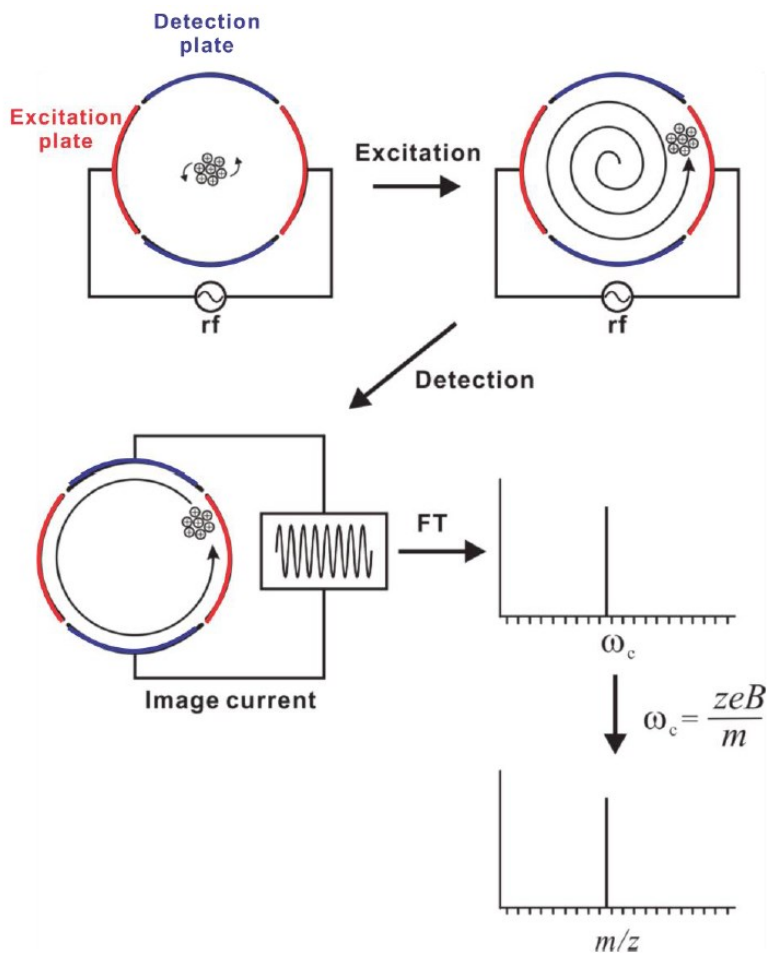


Figure 1.6. Illustration of excitation, image current detection and the production of mass spectrum by FTICR.

A noteworthy feature of FTICR is its ultrahigh resolution which comes from the concept that all ions of a given m/z rotate at the same value of ω_c which is free of their kinetic energy. The resolution of an FTICR mass spectrometer can routinely reach value of hundreds of thousands. The resolving power is directly proportional to the magnetic field

strength and the acquisition time. The acquisition time is the length of the detection phase and it is determined by the dataset size and the frequency of sampling. The longer the acquisition time (larger dataset size), the higher the resolution of the instrument. Thus, high vacuum (10⁻¹⁰ mbar) is required in the cell region of FTICR mass spectrometer, to nullify collisions with gas particles and deactivation of the ions.

1.2.2.2 Quadrupole-IMS-TOF mass spectrometer

Shown in Figure 1.7a is a schematic diagram of the Synapt G2 quadrupole-IMS-TOF mass spectrometer (Waters UK Ltd., Manchester, UK) equipped with a nanoESI source used in this present work (Chapter 3). Briefly, small droplets produced by nanoESI are first introduced into the mass spectrometer through a “Z-spray source”. It is used to minimize neutral contamination and improves the signal-to-noise. The resulting gaseous ions are transferred through a quadrupole mass filter to the ion mobility section of the instrument (Triwave). Later, the mobility separated analyte ions are detected by an orthogonal acceleration TOF mass analyzer (QuanTOF) which is equipped with a high field pusher and a dual-stage reflection.

The other Waters Synapt G2-S nanoESI-quadrupole-IMS-TOF mass spectrometer used in this study (Chapter 3) is shown in Figure 1.7b. Overall, the operation scheme of the Synapt G2-S is quite similar to Synapt G2, but it is an updated generation with a newly improved “step-wave” design in the ion source of the instrument for improved transmission. This feature is suitable for resolving pick for large molecular weight protein and proteomics analysis where the complexity of the sample can be minimized by the ion mobility separation.

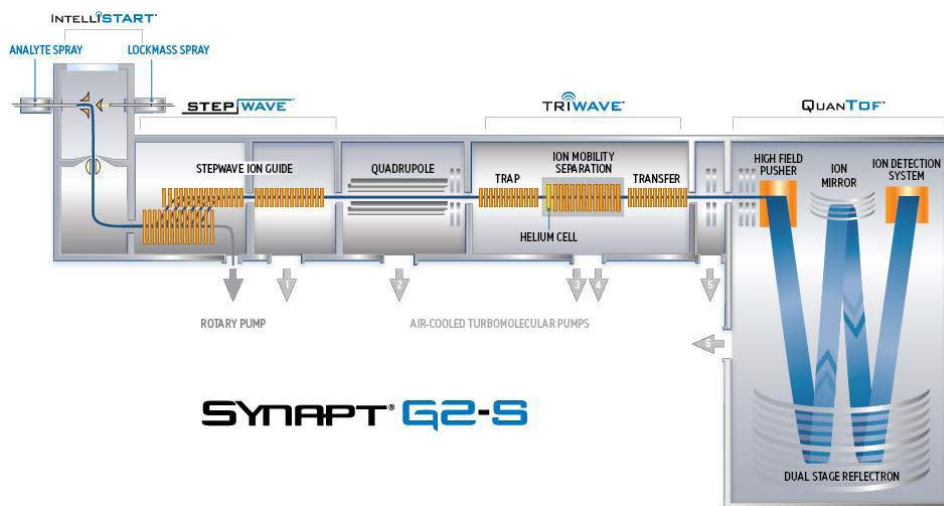
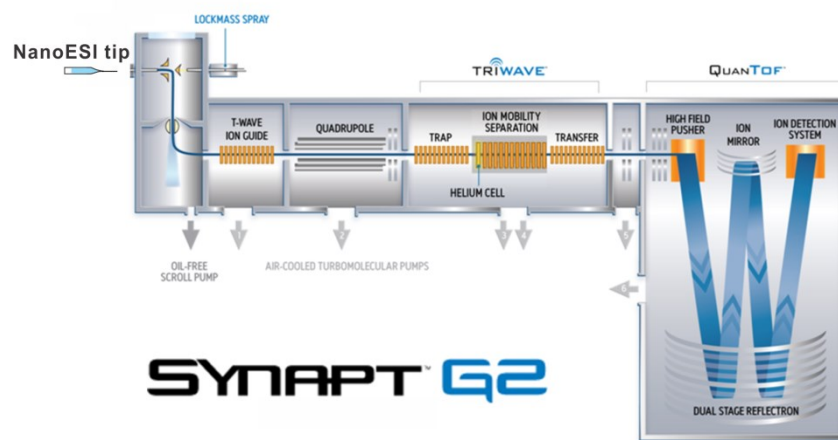


Figure 1.7. Schematic diagrams of (a) Waters Synapt G2 nanoESI-quadrupole -IMS-TOF mass spectrometer and (b) Waters Synapt G2-S nanoESI-quadrupole-IMS-TOF mass spectrometer used in this present study. Figures were adapted from the Waters user’s manual.

Both of the Waters Synapt G2 and G2-S nanoESI-quadrupole-IMS-TOF mass spectrometers were used in this study for their high sensitivity, broad mass range, and high IMS efficiency which enables separating samples based on size, shape, and charge,

as well as mass. A brief overview of three main parts of the Synapt mass spectrometer is provided.

1.2.2.2.1 Quadrupole

The quadrupole in the instrument consists of four cylindrical metal rods which are accurately positioned in a radial array and the diametrically opposed rods are paired. A direct current (DC) and a RF potential, 180 degrees out of phase, are commonly employed to each pair of rods.⁷⁶ In the Synapt mass spectrometer, the quadrupole consists two parts, one is a quadrupole prefilter followed by another quadrupole mass filter. (Figure 1.8). The use of prefilter improves the absolute sensitivity by reducing the effects of fringing fields at the entry to the quadrupole.

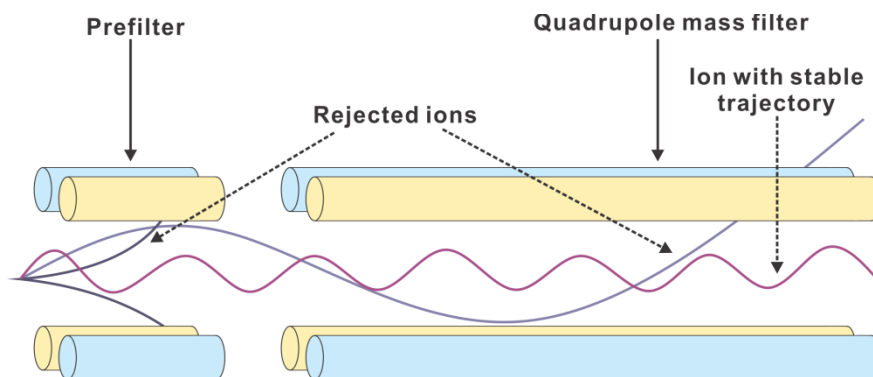


Figure 1.8. Schematic representation of the quadrupole in the Waters Synapt G2 Q-IMS-TOF mass spectrometer.

The quadrupole functions in RF only mode which transmits and passes ions over a wide m/z range to the following components of the instrument in the MS-TOF mode. In the MS/MS-TOF mode, the quadrupole functions with both RF and DC. Depending on the particular voltage and frequency applied, analyte ions of a specific m/z can be picked out

and move through the full length of the rods; other ions outside the m/z range are expelled out by hitting the rods.

1.2.2.2.2 Triwave

The Triwave part of the Waters Synapt G2 or G2-S mass spectrometer comprises of three T-wave ion guides (Trap, IMS and Transfer). Each of these ion guides comprises a series of planar electrodes. Opposite phases of a RF voltage are employed to nearby electrodes and provide a radially confining potential barrier. In the presence of gas, ion axial motion through the ion guide can be slowed or stopped because of the presence of axial traps generated by the ring geometry. To trigger ions through the gas, a DC voltage is superimposed on the RF employed to a pair of adjacent electrodes in a duplicating sequence along the length of the device. The series of potential hills produced are applied to the next pair of electrodes downstream at regular time intervals which provides a continuous sequence of T-waves. The ions within the device are forced to move away from the potential hills and accordingly they are carried through the device with the waves, reducing their transit time. Ions with enough mobility are rapidly pushed through the device by the T-Waves whereas ions with low mobility experience higher friction from the bath gas causing them to be decelerated.

In the MS-TOF mode, the Trap T-Wave is generally engaged in trapping and accumulating ions. Later, ions are released in a group into the IMS T-Wave thus IMS is performed. A high-pressure helium-filled cell at the front of the IMS T-Wave cell is used to reduce scattering and/or fragmentation of ions. The Transfer T-Wave pushes the mobility separated ions to the QuantTOF part for detection. However in the MS/MS-TOF

mode, collision-induced dissociation (CID) can be performed in both the trap and transfer regions (~10⁻³ mbar).

1.2.2.2.3 TOF

In case of TOF analyzers, one of the physical properties that are assessed during an analysis is the ions' flight time.⁷⁷ Mass to charge ratio (m/z) values are determined by measuring the time that ions take to pass through a field-free region between the source and the detector, according to eq 1.2:

$$m/z = t^2 \frac{2eV_s}{L^2} \quad (1.2)$$

where, m represents the mass of the ion, z is the charge of the ion, e is the elementary charge, V_s is the acceleration potential, t is the flight time and L is the length of the flight tube. Equation 2 shows that m/z can be calculated from a measurement of t . Low mass ions reach the detector faster than heavy mass ions. TOF analyzers are of two types: linear TOF analyzer and reflectron TOF analyzer. The linear TOF analyzer has a limitation. Here ions of the same m/z value may reach the detector at different times. This is because of the initial energy distribution, which results in peak broadening and poor resolution.

Waters Synapt G2 or G2-S mass spectrometer uses a reflectron TOF analyzer. This TOF analyzer counterbalances the energy distribution of ions by using consecutive sets of electric grids of increasing potential and it deflects the ions and reverses their flight direction directing them back through the flight tube. Based on their kinetic energy, ions of the same m/z enter the field at different heights; ions with more kinetic energy and high velocity enter the field more deeply than ions with low kinetic energy. Therefore, the faster ions spend more time in the reflectron and reach the detector at the same time

as the slower ions with the same m/z . This effect changes mass resolution with minimal losses in sensitivity.

After a detailed description of the basic principles and instrumentations of ESI-MS, an introduction of different areas of studying non-covalent protein-ligand interactions by ESI-MS is given in the following section 1.3.

1.3 Quantification of Interactions of Non-Covalent Complexes by MS-Based Techniques

1.3.1 Desorption Electrospray Ionization Mass Spectrometry (DESI-MS)

1.3.1.1 Conventional DESI-MS

In 2004, desorption electrospray ionization (DESI) was first introduced by Graham Cooks and co-workers from Purdue University.⁷⁸ Use of sample without preparation is the major feature of DESI-MS.⁷⁸ During the last decade, DESI has got the attention of many researchers and it has become a popular and powerful tool for developing ambient ionization methods. It has gained popularity because of its robustness and applicability to broad range and quality of analyte types. Not only that, the low cost for building a DESI source is another reason why it is widely used recently.⁷⁹ The ionization mechanism of DESI-MS is very similar to ESI-MS. This is why mass spectra obtained from DESI-MS look similar to those produced by ESI-MS. In addition, DESI-MS is capable of featuring all the beneficial characteristics of ESI-MS (i.e., sensitivity, selectivity, and speed of analysis), hence, it has been increasingly applied to direct identification of pharmaceutical compounds, explosives, proteins and a range of various biological materials.⁸⁰ So, it is crucial to understand the ionization processes in DESI.

A brief overview of DESI is described below with its mechanism. Shown in Figure 1.9 is a schematic representation of a typical DESI instrument.

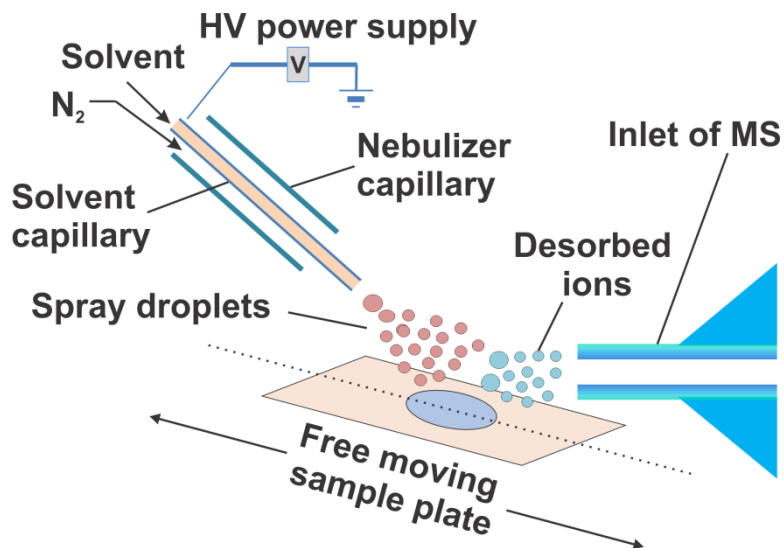


Figure 1.9. Schematic representation of typical DESI instrument, it is adapted from reference.⁷⁸

There are four major steps for the production of gaseous analyte ions from a typical DESI instrument. The process is named as “droplet pick-up” mechanism.⁸¹

(a) High velocity charged ESI droplets formation: A high voltage is applied to solvent solution which produces high velocity jet of charged ESI droplets. It is ordinarily a mixture of H₂O with organic solvent⁸² along with surrounding nebulizing gas. The solvent spray generally consists of droplets which vary in size ranging from 1 to 10 μm and velocity ≥ 100 m/s. The size and velocity of droplets depend on the capillary diameter, the employed voltage, the surrounding gas velocity, composition and most importantly flow rate of the spray solvent.^{83,84} Once the solvent droplets have been made, they start to reduce in velocity because of collisions with atmospheric molecules. The distance covered by primary droplets from the solvent capillary to the sample surface, is

generally few millimeters. Hence, the size and velocity of the primary droplets are almost the same as the initial values when they reach the sample surface.⁸⁴

(b) A thin film of liquid layer forms on the sample surface: While impacting on the sample surface, the solvent spray forms a thin liquid film on the top. The solvent solution collected on the sample surface experiences secondary droplet formation and emission happens through solvent evaporation under the strong surrounding gas flow. Hence, there is an equilibrium attained on the sample surface in between solvent deposited and evaporated from the surface. This process plays a crucial role for stability and reproducibility of the analysis.⁸⁵

(c) Desorption of analyte from sample surface to liquid phase: After forming a thin layer of liquid, analyte droplets dissolve on the sample surface. Here the analyte solubility plays a significant role during the sample extraction process from the surface. The signal and mass spectra in the DESI instrument are directly dependent on the solubility of analyte.^{79,82,86} In the meantime, primary droplets impacting the thin liquid film result in the production of secondary droplets containing analyte, which is the desorption process. Thus, the solid sample dried on the surface is successfully transferred to secondary droplets flying to the mass spectrometer inlet.⁸⁷

(d) Formation of secondary droplets from the sample surface: Secondary droplets are produced by the transfer of momentum from the high velocity primary droplets which are composed of liquid from both the thin liquid film on the sample surface and the primary spray droplets. The parameters in the DESI instruments, such as capillary tip distance from the sample surface and the surrounding gas velocity, can influence the desorption process and the formation of secondary droplets.⁸¹ In addition, Flow rate of gas, solvent

flow rate and some other instrumental parameters also affect the droplet evaporation. These parameters need to be optimized for successful generation of analytical results. Hence, the combination of all of these instrumental parameters with optimization is necessary for effective production of secondary droplets from the sample surface with sufficient energy that can reach the MS inlet. Later, highly charged secondary droplets experience the same ionization process to generate gas phase analyte ions as droplets produced by ESI (e.g., IEM and CRM) for effective detection.^{88,89}

1.3.1.2 Liquid sample DESI

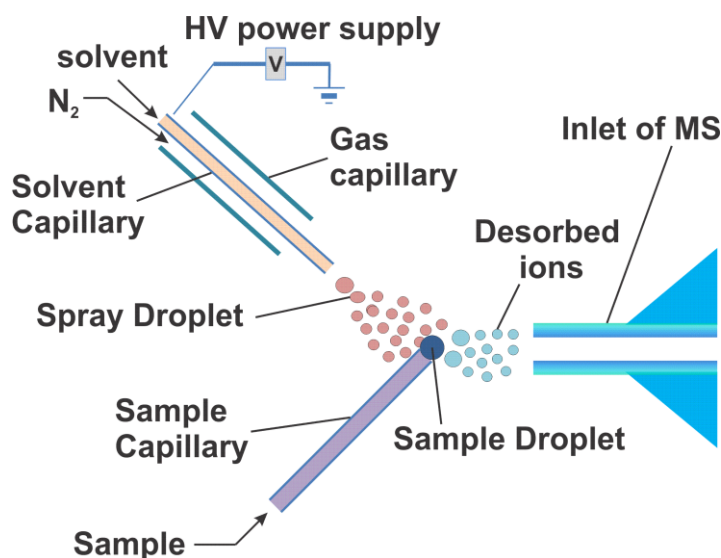


Figure 1.10. Schematic representation of the liquid sample DESI used in this study.

Conventional DESI MS features has drawback which is related to presence of high molecular mass of the molecules (i.e., proteins) in the analyte solution. It reduces the instrumental signal, because of the unsuccessful desorption of protein ions from the surface of the sample.⁹⁰⁻⁹² In order to resolve this problem, liquid sample DESI can be employed to analyze proteins. There was a report that ~150 kDa proteins were effectively

detected using liquid sample DESI where noncovalent interaction of protein-ligand complex was conserved during DESI ionization process.⁹³ Hence, it is worth to analyze and study the potential of DESI in quantifying protein-ligand interactions. Shown in Figure 1.10 is the representation of the liquid sample DESI.

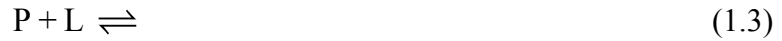
In liquid sample DESI, the sample solution is delivered by the sample capillary rather than using dry sample on the surface, (Chapter 2). The mechanism of ionization of liquid sample DESI is the similar as droplet pick-up mechanism of conventional DESI MS which was discussed in section 1.3.1.1. However, there is a difference between the solution phase dissolution of dried sample and the mixing of liquid sample with solvent spray solution.

Conventional DESI showed its ability to study analyte with less sample preparation and high tolerability of sample matrix to non-volatile salts.⁷⁸ In the same way, it was hypothesized that liquid sample DESI may get over the major shortcomings of the ESI-MS assay, which is generally carried out using limited types of volatile buffers e.g. aqueous ammonium carbonate, aqueous ammonium acetate solutions etc.⁶² As a result, analyte becomes incompatible with most of the nonvolatile “physiological” buffers, such as Tris-HCl, phosphate buffered saline (PBS), citrate, HEPES etc in conventional ESI-MS assay. These buffers are crucial for protein stability in solution and they reduce the protein aggregation.⁹⁴ In addition, liquid sample DESI can produce multiply charged gas phase protein ions and non-covalent protein complexes without substantial unfolding of the proteins.⁹³ Hence, the target of the Chapter 2 is to evaluate the reliability of liquid sample DESI for the protein-carbohydrate binding quantification and comparing the

results with values obtained by regular nanoESI-MS in aqueous ammonium acetate solutions.

1.3.2 Direct ESI-MS Binding Assay

The direct ESI-MS binding assay is established on the direct detection of free and ligand-bound protein ions by ESI-MS. For a reversible interaction between monovalent protein (P) and a monovalent ligand (L), eq 1.3 shows 1:1 ratio complex where the association constant (K_a) is calculated by using eq 1.4:



$$K_a = \frac{[PL]_{eq}}{[P]_{eq}[L]_{eq}} \quad (1.4)$$

where $[PL]_{eq}$, $[P]_{eq}$ and $[L]_{eq}$, are the equilibrium concentrations of PL complex, free P and L, respectively. They can be calculated from the initial concentrations of P and L in solution, which are $[P]_0$ and $[L]_0$. At equilibrium eqs 1.5-1.7 represent the concentration ratio of PL and P. The ratio (R) of the total abundance (Ab) of PL to P ions (i.e., PL^{n+} , P^{n+}) measured in the gas phase by ESI-MS is expected to be equivalent to the ratio of the concentrations of PL and P in solution at equilibrium.⁷⁹

$$[P]_0 = [P]_{eq} + [PL]_{eq} \quad (1.5a)$$

$$[L]_0 = [L]_{eq} + [PL]_{eq} \quad (1.5b)$$

$$R = \frac{Ab(PL)}{Ab(P)} = \frac{[PL]_{eq}}{[P]_{eq}} \quad (1.6)$$

$$[PL]_{eq} = \frac{R[P]_0}{1+R} \quad (1.7)$$

K_a value for 1:1 monovalent protein-ligand complex is determined from R , $[P]_0$ and $[L]_0$ using eq 1.8.

$$K_a = \frac{R}{[L]_0 - \frac{R}{1+R}[P]_0} \quad (1.8)$$

In cases for a multivalent protein (P) that can sequentially add up to q ligand molecules, the following q interactions are considered, eq 1.9:



.....



For the simplest case, it is assumed that all q binding sites are equivalent, with identical binding constants. More complicated cases have been discussed elsewhere.⁹⁵ The equilibrium concentrations, $[P]_{eq}$, $[PL]_{eq}$, ..., $[PLq]_{eq}$, can be found from relative abundance of the representing ions observed in the mass spectrum and eq 1.10a. These values can be used to find the equilibrium concentration of L (eq 1.10):

$$[P]_0 = [P]_{eq} + [PL]_{eq} + [PL_2]_{eq} \cdots \quad (1.10a)$$

$$[L]_0 = [L]_{eq} + [PL]_{eq} + 2[PL_2]_{eq} \cdots \quad (1.10b)$$

K_a can be determined from eq 1.12, which is based on the eq 1.11, where i is the number of occupied binding sites:⁹⁵

$$K_i = K_a (q - i + 1) / i \quad (1.11)$$

$$K_i = \frac{[PL_i]_{eq}}{[PL_{(i-1)}]_{eq} [L]_{eq}} \quad (1.12)$$

Average K_a can be found from the binding constant determined for each of the binding reactions.

However, ESI-MS binding measurements are usually limited to particular range of R values from 0.05 to 20 and P and L concentrations from 0.1 to 1000 μM which follows that K_a values compatible with the direct ESI-MS binding assay range from approximately 10^3 to 10^7 M^{-1} .⁹⁶ On the other hand, interactions with large K_a values can be examined using competitive binding approach and direct ESI-MS measurements.

1.3.3 Indirect ESI-MS Assays

Sometime protein-carbohydrate interactions cannot be studied using the *direct* ESI-MS assay. Because of protein heterogeneity or high molecular weight which makes protein peaks unresolvable due to instrumental limitations (mass range and mass resolution). In that case, *indirect* ESI-MS assay comes to play a vital role in studying protein-carbohydrate interactions. In addition, *direct* ESI-MS assay method is incompatible with the analysis of membrane proteins or insoluble cellular receptors. In such cases, a combination of *direct* ESI-MS with competitive protein or ligand binding can be helpful to quantify these interactions. These types of indirect ESI-MS assays have been elaborately described in this thesis. The *proxy protein* ESI-MS method⁹⁷ demonstrated the ability to quantify carbohydrate interactions with high molecular weight proteins (Chapters 3).

Few other ESI-MS based strategies are available to quantify protein-ligand interactions. These methods rely on measuring free ligand concentration at equilibrium in solution. Depending on ESI-MS analysis of the relative abundance of the ligand (L) to the internal standard (IS), which corresponds to ligand (L), but does not have interaction to the target

protein (P), the dependence of free ligand concentration ([L]) in solution on the initial protein concentration ([P]₀) can be obtained to find the K_a of P-L interaction.⁹⁸ In another way, this method can be modified to use a reference ligand (L_{ref}), with known binding affinity for P, to determine the binding affinities from the relative abundance of the L to L_{ref} by ESI-MS.⁹⁹

To understand the *indirect* ESI-MS assay, the *proxy protein* ESI-MS method is described in the following section for a single ligand and a ligand library.

1.3.3.1 Proxy protein ESI-MS assay

The implementation of the *proxy protein* ESI-MS method for ligand (L) binding to P_T with three equivalent binding sites was described previously.⁹⁷ Below, is a brief overview of the implementation of the method for monovalent P_{proxy} and P_T binding to a single L and a library of ligands (L₁, L₂, ..., L_x).

(a) Application to a single ligand

As discussed above and elsewhere, the *proxy protein* ESI-MS method relies on changes in the relative abundance of L-bound P_{proxy} upon addition of P_T to solution.⁹⁷ The relevant association reactions for the competitive binding of a monovalent P_{proxy} and monovalent P_T to L are given by eqs 1.13 and 1.14, respectively:



The abundance ratio of L-bound to free P_{proxy} ions (i.e., R_{proxy}), as measured by ESI-MS and which is taken to be equal to the concentration ratio (i.e., [P_{proxy}L]/[P_{proxy}]) eq 1.15, is related to the association constant for the P_{proxy}L interaction (i.e., K_{a,proxy}) by eq 1.16:

$$R_{\text{proxy}} = \frac{[\text{P}_{\text{proxy}}\text{L}]}{[\text{P}_{\text{proxy}}]} \quad (1.15)$$

$$K_{\text{a,proxy}} = \frac{[\text{P}_{\text{proxy}}\text{L}]}{[\text{P}_{\text{proxy}}][\text{L}]} = \frac{R_{\text{proxy}}}{[\text{L}]} \quad (1.16)$$

The addition of P_T to the solution (and the concomitant formation of P_TL complex, eq 1.14 results in a reduction in the concentration of free L in solution and, in turn, a difference in the apparent R_{proxy} (*i.e.*, ΔR_{proxy}) measured in the absence and presence of P_T (*i.e.*, $\Delta R_{\text{proxy}} = R_{\text{proxy}} - R_{\text{proxy,PT}}$). The association constant for the P_TL complex (*i.e.*, $K_{\text{a,PT}}$), eq 17:

$$K_{\text{a,PT}} = \frac{[\text{P}_T\text{L}]}{[\text{P}_T][\text{L}]} \quad (1.17)$$

can be determined from the magnitude of $R_{\text{proxy,PT}}$ measured at a known concentration of P_T and the relevant equations of mass balance, eqs 1.18a-c:

$$[\text{L}]_0 = [\text{L}] + [\text{P}_{\text{proxy}}\text{L}] + [\text{P}_T\text{L}] \quad (1.18a)$$

$$[\text{P}_{\text{proxy}}]_0 = [\text{P}_{\text{proxy}}] + [\text{P}_{\text{proxy}}\text{L}] \quad (1.18b)$$

$$[\text{P}_T]_0 = [\text{P}_T] + [\text{P}_T\text{L}] \quad (1.18c)$$

The $[\text{L}]$ term can be calculated from eq 1.19a:

$$[\text{L}] = \frac{R_{\text{proxy,PT}}}{K_{\text{a,proxy}}} = \frac{R_{\text{proxy}} - \Delta R_{\text{proxy}}}{K_{\text{a,proxy}}} \quad (1.19a)$$

and the $[P_{\text{proxy}}L]$ can be calculated by eq 1.19b:

$$[P_{\text{proxy}}L] = \frac{[P_{\text{proxy}}]_o R_{\text{proxy,PT}}}{R_{\text{proxy,PT}} + 1} \quad (1.19b)$$

Substituting eqs 1.19a and 1.19b into eq 1.18a gives the following expression for $[P_T L]$, eq 1.20:

$$[P_T L] = [L]_o - \frac{[P_{\text{proxy}}]_o R_{\text{proxy,PT}}}{R_{\text{proxy,PT}} + 1} - \frac{R_{\text{proxy,PT}}}{K_{a,\text{proxy}}} \quad (1.20)$$

The $[P_T]$ term is found by combining eqs 1.18c and 1.7 to give eq 1.21:

$$[P_T] = [P_T]_o - [L]_o + \frac{[P_{\text{proxy}}]_o R_{\text{proxy,PT}}}{R_{\text{proxy,PT}} + 1} + \frac{R_{\text{proxy,PT}}}{K_{a,\text{proxy}}} \quad (1.21)$$

It follows that $K_{a,\text{PT}}$ can be calculated from eq 1.22:

$$K_{a,\text{PT}} = \frac{\frac{[L]_o K_{a,\text{proxy}}}{R_{\text{proxy,PT}}} - \frac{[P_{\text{proxy}}]_o K_{a,\text{proxy}} - 1}{R_{\text{proxy,PT}} + 1}}{[P_T]_o - [L]_o + \frac{R_{\text{proxy,PT}}}{K_{a,\text{proxy}}} + \frac{[P_{\text{proxy}}]_o R_{\text{proxy,PT}}}{R_{\text{proxy,PT}} + 1}} \quad (1.22)$$

(b) Application to a ligand library

For a library of ligands (L_1, L_2, \dots, L_x) eq 1.22 can be rewritten for calculating $K_{a,\text{PT},x}$:

$$K_{a,\text{PT},x} = \frac{\left(\frac{[L_x]_o K_{a,\text{proxy},x}}{R_{\text{proxy,PT},x}} - \frac{[P_{\text{proxy}}]_o K_{a,\text{proxy},x} - 1}{1 + \sum_x R_{\text{proxy,PT},x}} \right)}{\left([P_T]_o - \sum_x \left([L_x]_o - \frac{[P_{\text{proxy}}]_o R_{\text{proxy,PT},x}}{1 + \sum_x R_{\text{proxy,PT},x}} - \frac{R_{\text{proxy,PT},x}}{K_{a,\text{proxy},x}} \right) \right)} \quad (1.23)$$

Like all other techniques, ESI-MS assay also has its own limitations and a more detailed discussion is provided in the following section.

1.4 Potential limitation of the direct ESI-MS binding assay

The direct ESI-MS has several limitations. There are several physical or chemical processes that can affect the abundance ratio of bound and unbound proteins during ESI process and transportation of ions that can lead to incorrect K_a values and binding stoichiometry. There are three common errors associated with ESI-MS measurements: (1) non-uniform response factors, (2) nonspecific binding, and (3) in-source dissociation. These are briefly described below.

1.4.1 Non-uniform response factors

ESI-MS is efficient in ionization and detection, so the abundances of free protein and bound protein complex ions in gas phase measured by ESI-MS are involved with their solution concentrations through response factors (RF), eq 1.24:

$$\frac{[PL]_{eq}}{[P]_{eq}} = \frac{Ab(PL)/RF_{PL}}{Ab(P)/RF_P} = RF_{P/PL} \frac{Ab(PL)}{Ab(P)} \quad (1.24)$$

here RF_{PL} and RF_P are the response factors of PL and P, respectively, and the $RF_{P/PL}$ is the ratio of RF_P to RF_{PL} , which is also denoted as the relative response factor. The absolute RF values relate to many factors, such as the structure, size and most importantly surface properties of PL and P as well as the instrumental parameters and solution composition of the sample used in the measurement. So, consistent RF values of PL and P (i.e., $RF_{P/PL} \approx 1$) are important assumption for ESI-MS assay. Here the size of ligand L is insignificant compared to the size of protein; so it is assumed that PL and P have similar size and surface properties.¹⁰⁰⁻¹⁰⁵

Different strategies have been developed to minimize the consequences of non-uniform response factors for determining binding affinity constants (K_a). One approach is to correct $RF_{P/PL}$ values of a proper binding model to interpret with titration results of experiment.¹⁰⁶⁻¹⁰⁹ This method needs to fit several parameters to adjust for a binding model to its titration data, so, good quality experimental results are required to derive reliable K_a values.¹⁰⁸ At the same time, it is important to realize the underlying assumption to apply this approach: $RF_{P/PL}$ has no dependence on concentration in the range that is investigated. It is also necessary to use an internal standard (IS), that has similar properties (e.g. MW and surface activity) to the target analyte P which has no binding to L.¹⁰⁹ This method is preferred as the abundance of the IS ions can reflect the variation of $RF_{P/PL}$ in concentrations along with ESI instability and other factors.

1.4.2 Nonspecific binding

Previously it was shown that, during the ESI process, free L can form nonspecific complexes with P along with specific PL complexes, as the ESI droplets dried up.^{110,111} Nonspecific ligand binding is directly related to the concentration of free L and, accordingly, it is more pronounced when measuring low affinity protein ligand interactions because high L concentrations are usually required to produce measureable amount of the PL complexes.¹¹¹ Thus, nonspecific PL formation which influences the measured abundances of the P and PL ions can introduce error into the R and K_a values. In Figure 1.11 is the schematic presentation of the formation of nonspecific protein-ligand interaction during the ESI process. This development process can be understood through the CRM of ESI (section 1.2.1).

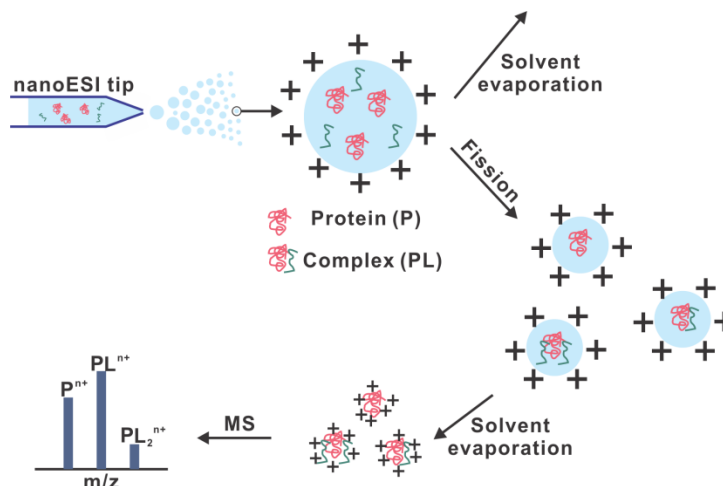


Figure 1.11. Schematic representation of the formation of nonspecific protein-ligand interactions (false positive), reproduced from reference 96.

In the CRM model, initial parent droplets are shrinking to smaller size while solvent evaporates until they reach the Rayleigh limit. Parent droplets experience Coulomb fission beyond this point to release a jet spray of smaller and multiply charged progeny droplets. These nanodroplets have analyte molecules, and form gaseous analyte ions after solvent evaporation. If two or more analyte molecules exist in a single nanodroplet, nonspecific complexes can be formed because of nonspecific intermolecular interactions occurring during the ionization process. Hence, there is a chance of formation of nonspecific complexes between L with P and PL in the presence of high concentration of L in solution. These processes obscure the true binding stoichiometry of P and L in bulk solution and lead to false positive signal and add error to K_a values measured by ESI-MS. This problem can be reduced by lowering the initial concentration of ligand. However, it is not always possible to avoid nonspecific binding when high concentration of ligand is essential to produce detectable signal of weakly bound protein-ligand complexes. Several

strategies have been developed to effectively correct this nonspecific binding in the ESI-MS process.^{111,112} The reference protein method is a straightforward and effective method to correct ESI mass spectra quantitatively for nonspecific binding.¹¹¹ The method requires adding of a reference protein (P_{ref}), which has no specific binding with P or L, in the solution. The distribution of nonspecific bound molecules on mass spectra is similar to Poisson distribution and it suggests that the nonspecific binding consequence of ligand to protein is a random process and has similar effect on every protein species present in solution phase. The presence or absence of nonspecific binding can be found from the appearance of $P_{ref}L_q$ ions corresponding to P_{ref} bound to one or multiple molecules of L to form complexes. Hence, the fractional abundance of nonspecific interaction in bound and unbound state of P_{ref} can give a quantitative value for the nonspecific binding measurement contributing to apparent intensities of free and specifically bound proteins. For proteins with one binding site, the contribution from nonspecific binding to the apparent binding affinity can be presented by eqs 1.25a and 1.25b where abundances of P ($Ab_{app}(P)$) and PL ($Ab_{app}(PL)$) can be correlated by the following eqs:

$$Ab(P) = Ab_{app}(P) / f_0 \quad (1.25a)$$

$$Ab(PL) = [Ab_{app}(PL) - f_1 Ab(P)] / f_0 \quad (1.25b)$$

here f_0 is the fraction of free P and f_1 is the fraction of P bound nonspecifically to one molecule of L. These fractions can be found from the abundances of free and ligand-bound forms of P_{ref} measurement by eqs 1.26a and 1.26b:

$$f_0 = Ab(P_{ref}) / [Ab(P_{ref}) + Ab(P_{ref}L)] \quad (1.26a)$$

$$f_1 = Ab(P_{ref}L) / [Ab(P_{ref}) + Ab(P_{ref}L)] \quad (1.26b)$$

In the same way, the “true” abundance of a multiple binding sites containing protein (PL_q) can be calculated from the abundance measurement of PL_q and $P_{ref}L_q$ species by the following eqs 1.27a and 1.27b:

$$Ab(PL_q) = [Ab_{app}(PL_q) - f_1 Ab(PL_{q-1}) - \dots] / f_0 \quad (1.27a)$$

$$f_q = Ab(P_{ref}L_q) / [Ab(P_{ref}) + Ab(P_{ref}L) + \dots + Ab(P_{ref}L_q)] \quad (1.27b)$$

here f_q is the fraction of P bound to q molecules of L by nonspecific interaction. This method has been successfully used to correct nonspecific interactions of neutral and charged molecules, such as carbohydrates, peptides, amino acids and divalent metal ions to various proteins by ESI-MS measurements.^{111,113,114}

1.4.3 In-source dissociation

While using ESI-MS for noncovalent protein-ligand interactions studies, in-source collision-induced dissociation commonly causes reduction in abundance of PL complex ions.¹¹¹ As a consequence of these events, the R value becomes smaller and results in the decrease in the magnitude of K_a value. The R value is the ratio of abundances of the ligand-bound protein to free protein, In some cases, PL complex ions influenced by in-source dissociation event may not adequate enough to obtain measurable signals.¹¹⁵ Commonly, weak protein-ligand interactions are more prone to dissociation due to different ion source parameters, most commonly voltage differences in high pressure regions that can regulate internal energy of complex ions and modify the R value. Besides that, proper selection of the ion source and instrumental parameters can influence the gas-phase stability of the PL complex being examined. All these things play crucial roles in in-source dissociation events.

To reduce the in-source dissociation of gaseous complex ions, several precautions can be taken such as, low source temperatures in the sampling capillary region, low voltages through lens elements, and short accumulation time. These can minimize the problem for obtaining more reliable binding affinity with less false negative error. Sometime these conditions influence signal intensities in the instrument. So, instrumental parameters need to be adjusted to reduce dissociation of complex ions, and acquire mass spectra with good signal to noise ratio (S/N) at the same time. There are some other options, such as addition of small organic molecules (i.e., imidazole¹¹⁶ and amino acids¹¹⁷) into analyte solutions and incorporation of solvent vapors (i.e., sulfur hexafluoride¹¹⁸, water and organic solvents¹¹⁹) into the ion source during ESI-MS process that can minimize in-source dissociation. For example, Konermann and co-workers described that they could not detect and identify any signal for the trypsin (Tryp) – benzamidine (Benz) complex ions using direct ESI-MS assay.¹²⁰ After a few years, the Klassen group demonstrated that addition of a small molecule, e.g., imidazole, could stabilize the (Tryp-Benz) complex in the gas phase using ESI-MS.¹¹⁶ The stabilization effect of imidazole is assumed to be the effect of increased evaporation cooling by removal of imidazole from PL ions during the ionization process. Thus, it decreases the internal energy of gas phase PL ions and hence, reduces the dissociation of PL complex ions.¹¹⁶ Instead of adding small molecule additives into ESI solutions, switching of the ambient gas composition at the ionization region could also protect protein-ligand interaction from in-source dissociation. As for example, water and organic vapors (e.g. methanol, ethanol, acetonitrile, acetone),¹¹⁹ SF₆ vapor.¹¹⁸

The Klassen group also introduced a competitive binding assay technique named as the reference ligand method, to quantify protein-ligand interactions that are highly prone to breakdown and cannot be detected by ESI-MS.¹¹⁵ This method uses direct ESI-MS analysis with a reference ligand (L_{ref}). The L_{ref} binds specifically to P, at the same binding site as L, with known binding affinity. Thus it forms a stable protein-ligand complex in the gas phase. The fraction of P bound to L_{ref} , can be determined directly from the ESI mass spectrum and it is related to the fraction of P bound to L in the ESI solution which enables the affinity of P for L to be determined in indirect way. This method is useful for the analysis of kinetically unstable PL interactions in the gas phase.¹²¹

1.5 The Present Work

This thesis focuses on the development of mass spectrometry methods to study protein-glycan interactions. In Chapter 2 the goal of the project was to validate the method and assess the reliability of liquid sample DESI for the quantification of protein-carbohydrate interaction in aqueous ammonium acetate solutions. The binding affinities of tri- and tetrasaccharide ligands for lysozyme (Lyz), a glycosyl hydrolase, and a single chain variable fragment (scFv) of a monoclonal antibody were evaluated by liquid sample DESI-MS. These results were compared with those measured using ITC and the direct ESI-MS assay. Overall, liquid sample DESI was shown as a newly developed ionization source which can be used to quantify protein-carbohydrate interaction in solution. Protein and ligands can be premixed in solution or can be sprayed from separate sample delivery nozzles to study the effect of mixing time.

The goal of Chapter 3 was to develop a method to screen oligosaccharide libraries against carbohydrate-binding proteins using the proxy protein ESI-MS assay. In the field of

glycomics, comprehensive identification and characterization of protein-oligosaccharide interactions represent very important goals. So, rapid and quantitative screening tools are required for these purposes and electrospray ionization mass spectrometry (ESI-MS) assay offers a new way for screening oligosaccharide libraries against protein targets. It was shown recently that direct ESI-MS binding assay can be applied for protein screening against oligosaccharide library. In this present work, the *proxy protein* ESI-MS method, which combines direct ESI-MS protein-ligand binding assay and competitive protein binding, was developed to detect and quantify interactions of protein target (P_T) with components of the library (L_x), when direct detection of P_T by ESI-MS was not possible. P_T - L_x interactions were identified and quantified from the magnitude of the change in relative abundance of complex of *proxy* protein (P_{proxy}) with L_x (as measured by ESI-MS) upon addition of P_T to the solution. The C-terminal domain fragment of galectin-3 served as P_{proxy} and its affinity for all components of the library was measured by direct ESI-MS assay. The *Proxy protein* ESI-MS method was applied to screen small oligosaccharide libraries against the N-terminal fragment of the family 51 carbohydrate-binding module, a fucose-binding bacterial lectin from *Ralstonia solanacearum* and the P particle of human norovirus, to demonstrate the reliability and versatility of the assay.

Finally in Chapter 4, comparative studies of human milk oligosaccharides (HMOs) specificities of human galectin-1, 3 and 9 were described. Human milk oligosaccharides (HMOs) have a variety of biological functions such as blocking of binding of pathogenic microbes, including viruses and bacteria, and parasites to epithelial cell and serve as prebiotic. First, the interaction between three human galectins and 32 HMOs were

quantified by direct electrospray ionization mass spectrometry (ESI-MS) binding assay. Later, these results were compared with data obtained by glycan microarray screening. Glycan microarrays can be employed for purified proteins and protein complexes. In addition, this method can be used for glycan screening of cell extracts, bacteria, viruses and cells.¹²²⁻¹²⁸ Screening in this way is rapid, utilizes relatively small amounts of sample (50–100 fmol of individual glycan, $\sim 10 \mu\text{g mL}^{-1}$ of target protein)^{129,130} and it can provide a order of ligand affinities.^{45,122,128,131-133} However, glycan microarray binding data are known to exhibit a dependence on the size and nature of the linker along with density of glycans printed on the surface.¹³⁴ This technique is also prone to false negatives, particularly for low affinity interactions.^{48,130,135,136} Therefore, direct electrospray ionization mass spectrometry (ESI-MS) has been used to show that galectins have broad HMO specificity with association constants ranging from 10^3 to 10^5 M^{-1} which is not the case for microarray screening because this method is incapable of finding binding constants and insensitive to find binding for weak affinity ligands. In conclusion, the binding affinity of galectins to HMOs was found to be similar to binding affinity to histo-blood type oligosaccharides. Weak or no binding was established for galactooligosaccharides (GOS) and fructo-oligosaccharides (FOS).

1.6 References

- (1) Holgersson, J.; Gustafsson, A.; Breimer, M. E. *Immunol. Cell Biol.* **2005**, *83*, 694-708.
- (2) Varki, A. C.; Cummings, R. D.; Esko, J. D.; Freeze, H. H.; Stanley, P.; Bertozzi, C. R.; Hart, G. W.; Etzler, M. E. *Essentials of Glycobiology*; Cold Spring Harbor Laboratory Press: Cold Spring Harbor, NY, 2009.
- (3) Ghazarian, H.; Idoni, B.; Oppenheimer, S. B. *Acta Histochem.* **2011**, *113*, 236-247.
- (4) Ohtsubo, K.; Marth, J. D. *Cell* **2006**, *126*, 855-867.
- (5) Bode, L. *Nutr. Rev.* **2009**, *67*, S183-S191.
- (6) Sharon, N.; Lis, H. *Science* **1989**, *246*, 227-234.
- (7) Ofek, I.; Hasty, D. L.; Sharon, N. *FEMS Immunol. Med. Mic.* **2003**, *38*, 181-191.
- (8) Lis, N. S. a. H. *Sci. Am.* **1993**, *268*, 82-89.
- (9) Opdenakker, G.; Rudd, P. M.; Ponting, C. P.; Dwek, R. A. *FASEB J.* **1993**, *7*, 1330-1337.
- (10) Mody, R.; Joshi, S. H. a.; Chaney, W. *J. Pharmacol. Toxicol.* **1995**, *33*, 1-10.
- (11) Disney, M. D.; Seeberger, P. H. *Chem. Biol.* **2004**, *11*, 1701-1707.
- (12) Blomme, B.; Van Steenkiste, C.; Callewaert, N.; Van Vlierberghe, H. *J. Hepatol.* **2009**, *50*, 592-603.
- (13) El-Hawiet, A.; Kitova, E. N.; Klassen, J. S. *Glycobiology* **2015**, *25*, 845-854.
- (14) Feizi, T.; Mulloy, B. *Curr. Opin. Struc. Biol.* **2003**, *13*, 602-604.
- (15) Wormald, M. R.; Sharon, N. *Curr. Opin. Struc. Biol.* **2004**, *14*, 591-592.
- (16) Oppenheimer, S. B.; Alvarez, M.; Nnoli, J. *Acta Histochem.* **2008**, *110*, 6-13.

- (17) Schwartz-Albiez, R.; Laban, S.; Eichmüller, S.; Kirschfink, M. *Autoimmunity Rev.* **2008**, *7*, 491-495.
- (18) Goetz, J. A.; Mechref, Y.; Kang, P.; Jeng, M. H.; Novotny, M. V. *Glycoconjugate J.* **2009**, *26*, 117-131.
- (19) Patsos, G.; Hebbe-Viton, V.; Robbe-Masselot, C.; Masselot, D.; Martin, R. S.; Greenwood, R.; Paraskeva, C.; Klein, A.; Graessmann, M.; Michalski, J. C.; Gallagher, T.; Corfield, A. *Glycobiology* **2009**, *19*, 382-398.
- (20) Powlesland, A. S.; Hitchen, P. G.; Parry, S.; Graham, S. A.; Barrio, M. M.; Elola, M. T.; Mordoh, J.; Dell, A.; Drickamer, K.; Taylor, M. E. *Glycobiology* **2009**, *19*, 899-909.
- (21) Rek, A.; Krenn, E.; Kungl, A. J. *Brit. J. Pharmacol.* **2009**, *157*, 686-694.
- (22) Shida, K.; Misonou, Y.; Korekane, H.; Seki, Y.; Noura, S.; Ohue, M.; Honke, K.; Miyamoto, Y. *Glycobiology* **2009**, *19*, 1018-1033.
- (23) Mammen, M.; Choi, S.-K.; Whitesides, G. M. *Angew. Chem. Int. Edit.* **1998**, *37*, 2754-2794.
- (24) Klemm, J. D.; Schreiber, S. L.; Crabtree, G. R. *Annu. Rev. Immunol.* **1998**, *16*, 569-592.
- (25) Sacchettini, J. C.; Baum, L. G.; Brewer, C. F. *Biochemistry* **2001**, *40*, 3009-3015.
- (26) Drickamer, K.; Taylor, M. E. *Annu. Rev. Cell Biol.* **1993**, *9*, 237-264.
- (27) Liu, F.-T. *Clin. Immunol.* **2000**, *97*, 79-88.
- (28) Bundle, D. R.; Young, N. M. *Curr. Opin. Struc. Biol.* **1992**, *2*, 666-673.
- (29) García-Hernández, E.; Hernández-Arana, A. *Protein Sci.* **1999**, *8*, 1075-1086.
- (30) Dam, T. K.; Brewer, C. F. *Chem. Rev.* **2002**, *102*, 387-430.

- (31) García-Hernández, E.; Zubillaga, R. A.; Rojo-Domínguez, A.; Rodríguez-Romero, A.; Hernández-Arana, A. *Proteins* **1997**, *29*, 467-477.
- (32) Toone, E. J. *Curr. Opin. Struc. Biol.* **1994**, *4*, 719-728.
- (33) García-Hernández, E.; Zubillaga, R. A.; Rodríguez-Romero, A.; Hernández-Arana, A. *Glycobiology* **2000**, *10*, 993-1000.
- (34) Lemieux, R. U. *Accounts Chem. Res.* **1996**, *29*, 373-380.
- (35) Rand, R. P.; Fuller, N. L.; Butko, P.; Francis, G.; Nicholls, P. *Biochemistry* **1993**, *32*, 5925-5929.
- (36) Swaminathan, C. P.; Surolia, N.; Surolia, A. *J. Am. Chem. Soc.* **1998**, *120*, 5153-5159.
- (37) Schlichting, I. *Method Mol. Biol.* **2005**, 155-165.
- (38) Palmer, R.; Niwa, H. *Biochem. Soc. Trans.* **2003**, *31*, 973-979.
- (39) Staunton, D.; Owen, J.; Campbell, I. D. *Accounts Chem. Res.* **2003**, *36*, 207-214.
- (40) Karlsson, R. *J. Mol. Recognit.* **2004**, *17*, 151-161.
- (41) De Crescenzo, G.; Boucher, C.; Durocher, Y.; Jolicoeur, M. *Cel. Mol. Bioeng.* **2008**, *1*, 204-215.
- (42) Daghestani, H. N.; Day, B. W. *Sensors* **2010**, *10*, 9630-9646.
- (43) Schuck, P. *Annu. Rev. Bioph. Biom.* **1997**, *26*, 541-566.
- (44) Larsen, K.; Thygesen, M. B.; Guillaumie, F.; Willats, W. G. T.; Jensen, K. J. *Carbohydr. Res.* **2006**, *341*, 1209-1234.
- (45) Rillahan, C. D.; Paulson, J. C. *Annu. Rev. Biochem.* **2011**, *80*, 797-823.
- (46) Alvarez, R. A.; Blixt, O. *Method. Enzymol.* **2006**, *415*, 292-310.

- (47) Blixt, O.; Head, S.; Mondala, T.; Scanlan, C.; Huflejt, M. E.; Alvarez, R.; Bryan, M. C.; Fazio, F.; Calarese, D.; Stevens, J.; Razi, N.; Stevens, D. J.; Skehel, J. J.; van Die, I.; Burton, D. R.; Wilson, I. A.; Cummings, R.; Bovin, N.; Wong, C.-H.; Paulson, J. C. *P. Natl. Acad. Sci. USA* **2004**, *101*, 17033-17038.
- (48) Smith, D. F.; Song, X.; Cummings, R. D. *Method. Enzymol.* **2010**, *480*, 417-444.
- (49) Liu, Y.; Palma, A. S.; Feizi, T. *Biol. Chem.* **2009**, *390*, 647-656.
- (50) Park, S.; Gildersleeve, J. C.; Blixt, O.; Shin, I. *Chem. Soc. Rev.* **2013**, *42*, 4310-4326.
- (51) Grant, O. C.; Smith, H. M.; Firsova, D.; Fadda, E.; Woods, R. J. *Glycobiology* **2013**, cwt083.
- (52) Sridharan, R.; Zuber, J.; Connelly, S. M.; Mathew, E.; Dumont, M. E. *BBA-Biomembranes* **2014**, *1838*, 15-33.
- (53) Wishart, D. *Curr. Pharm. Biotechnol.* **2005**, *6*, 105-120.
- (54) Zuiderweg, E. R. *Biochemistry* **2002**, *41*, 1-7.
- (55) Meyer, B.; Peters, T. *Angew. Chem. Int. Edit.* **2003**, *42*, 864-890.
- (56) Ganem, B.; Li, Y. T.; Henion, J. D. *J. Am. Chem. Soc.* **1991**, *113*, 6294-6296.
- (57) Drummond, J. T.; Loo, R. R. O.; Matthews, R. G. *Biochemistry* **1993**, *32*, 9282-9289.
- (58) Drake, R. R.; Schwegler, E. E.; Malik, G.; Diaz, J.; Block, T.; Mehta, A.; Semmes, O. J. *Mol. Cell. Proteom.* **2006**, *5*, 1957-1967.
- (59) Deroo, S.; Hyung, S.-J.; Marcoux, J.; Gordiyenko, Y.; Koripella, R. K.; Sanyal, S.; Robinson, C. V. *ACS Chem. Biol.* **2012**, *7*, 1120-1127.

- (60) Rosu, F.; Gabelica, V.; Shin-ya, K.; De Pauw, E. *Chem. Commun.* **2003**, 2702-2703.
- (61) Gabelica, V.; Rosu, F.; De Pauw, E. *Anal. Chem.* **2009**, *81*, 6708-6715.
- (62) Kebarle, P.; Peschke, M. *Anal. Chim. Acta* **2000**, *406*, 11.
- (63) Kebarle, P.; Tang, L. *Anal. Chem.* **1993**, *65*, 972A-986A.
- (64) Taylor, G.; McEwan, A. *J. Fluid Mech.* **1965**, *22*, 1-15.
- (65) Iribarne, J. V.; Thomson, B. A. *J. Chem. Phys.* **1976**, *64*, 2287.
- (66) Thomson, B. A.; Iribarne, J. V. *J. Chem. Phys.* **1979**, *71*, 4451.
- (67) Dole, M.; Mack, L. L.; Hines, R. L.; Mobley, R. C.; Ferguson, L. D.; Alice, M. B. *J. Chem. Phys.* **1968**, *49*, 2240.
- (68) Kebarle, P.; Verkerk, U. H. *Mass Spectrom. Rev.* **2009**, *28*, 898-917.
- (69) Iavarone, A. T.; Williams, E. R. *J. Am. Chem. Soc.* **2003**, *125*, 2319.
- (70) Konermann, L.; Ahadi, E.; Rodriguez, A. D.; Vahidi, S. *Anal. Chem.* **2012**, *85*, 2-9.
- (71) Ahadi, E.; Konermann, L. *J. Phys. Chem. B* **2011**, *116*, 104-112.
- (72) Konermann, L.; Rodriguez, A. D.; Liu, J. *Anal. Chem.* **2012**, *84*, 6798-6804.
- (73) Marshall, A. G.; Hendrickson, C. L.; Jackson, G. S. *Mass Spectrom. Rev.* **1998**, *17*, 1-35.
- (74) Marshall, A. G.; Hendrickson, C. L. *Int. J. Mass Spectrom.* **2002**, *215*, 59-75.
- (75) Xian, F.; Hendrickson, C. L.; Marshall, A. G. *Anal. Chem.* **2012**, *84*, 708-719.
- (76) Hoffmann, E. D.; Charette, J.; Stroobant, V.; Brodbelt, J. *J. Am. Soc. Mass Spectrom.* **1997**, *8*, 1193-1194.
- (77) Guilhaus, M.; Selby, D.; Mlynski, V. *Mass Spectrom. Rev.* **2000**, *19*, 65-107.

- (78) Takats, Z.; Wiseman, J. M.; Gologan, B.; Cooks, R. G. *Science* **2004**, *306*, 471-473.
- (79) Badu-Tawiah, A.; Bland, C.; Campbell, D. I.; Cooks, R. G. *J. Am. Soc. Mass Spectrom.* **2010**, *21*, 572-579.
- (80) Ifa, D. R.; Wu, C.; Ouyang, Z.; Cooks, R. G. *The Analyst* **2010**, *135*, 669-681.
- (81) Takats, Z.; Wiseman, J. M.; Cooks, R. G. *J. Mass Spectrom.* **2005**, *40*, 1261-1275.
- (82) Green, F.; Salter, T.; Gilmore, I.; Stokes, P.; O'Connor, G. *The Analyst* **2010**, *135*, 731-737.
- (83) Olumee, Z.; Callahan, J. H.; Vertes, A. *J. Phys. Chem. A* **1998**, *102*, 9154-9160.
- (84) Venter, A.; Sojka, P. E.; Cooks, R. G. *Anal. Chem.* **2006**, *78*, 8549-8555.
- (85) Zivolic, F.; Zancanaro, F.; Favretto, D.; Ferrara, S. D.; Seraglia, R.; Traldi, P. *J. Mass Spectrom.* **2010**, *45*, 411-420.
- (86) Douglass, K. A.; Venter, A. R. *J. Mass Spectrom.* **2013**, *48*, 553-560.
- (87) Costa, A. B.; Cooks, R. G. *Chem. Commun.* **2007**, 3915-3917.
- (88) Thomson, B.; Iribarne, J. *J. Chem. Phys.* **1979**, *71*, 4451-4463.
- (89) Mack, L. L.; Kralik, P.; Rheude, A.; Dole, M. *J. Chem. Phys.* **1970**, *52*, 4977-4986.
- (90) Shin, Y.-S.; Drolet, B.; Mayer, R.; Dolence, K.; Basile, F. *Anal. Chem.* **2007**, *79*, 3514-3518.
- (91) Heaton, K.; Solazzo, C.; Collins, M. J.; Thomas-Oates, J.; Bergström, E. T. *J. Archaeol. Sci.* **2009**, *36*, 2145-2154.
- (92) Myung, S.; Wiseman, J. M.; Valentine, S. J.; Takats, Z.; Cooks, R. G.; Clemmer, D. E. *J. Phys. Chem. B* **2006**, *110*, 5045-5051.

- (93) Ferguson, C. N.; Benchaar, S. A.; Miao, Z.; Loo, J. A.; Chen, H. *Anal. Chem.* **2011**, *83*, 6468-6473.
- (94) Banerjee, S.; Mazumdar, S. *Int. J. Anal. Chem.* **2012**, 2012, 282574.
- (95) Tjernberg, A.; Carno, S.; Oliv, F.; Benkestock, K.; Edlund, P. O.; Griffiths, W. J.; Hallen, D. *Anal. Chem.* **2004**, *76*, 4325-4331.
- (96) Kitova, E. N.; El-Hawiet, A.; Schnier, P. D.; Klassen, J. S. *J. Am. Soc. Mass Spectrom.* **2012**, *23*, 431-441.
- (97) El-Hawiet, A.; Kitova, E. N.; Arutyunov, D.; Simpson, D. J.; Szymanski, C. M.; Klassen, J. S. *Anal. Chem.* **2012**, *84*, 3867-3870.
- (98) Wortmann, A.; Rossi, F.; Lelais, G.; Zenobi, R. *J. Mass Spectrom.* **2005**, *40*, 777-784.
- (99) Wortmann, A.; Jecklin, M. C.; Touboul, D.; Badertscher, M.; Zenobi, R. *J. Mass Spectrom.* **2008**, *43*, 600-608.
- (100) Soya, N.; Shoemaker, G. K.; Palcic, M. M.; Klassen, J. S. *Glycobiology* **2009**, *19*, 1224-1234.
- (101) Kitova, E. N.; Kitov, P. I.; Paszkiewicz, E.; Kim, J.; Mulvey, G. L.; Armstrong, G. D.; Bundle, D. R.; Klassen, J. S. *Glycobiology* **2007**, *17*, 1127-1137.
- (102) El-Hawiet, A.; Kitova, E. N.; Kitov, P. I.; Eugenio, L.; Ng, K. K. S.; Mulvey, G. L.; Dingle, T. C.; Szpacenko, A.; Armstrong, G. D.; Klassen, J. S. *Glycobiology* **2011**, *21*, 1217-1227.
- (103) Yanes, O.; Villanueva, J.; Querol, E.; Aviles, F. X. *Nat. Prot.* **2007**, *2*, 119-130.
- (104) Jecklin, M. C.; Touboul, D.; Jain, R.; Toole, E. N.; Tallarico, J.; Drueckes, P.; Ramage, P.; Zenobi, R. *Anal. Chem.* **2008**, *81*, 408-419.

- (105) Yanes, O.; Villanueva, J.; Querol, E.; Aviles, F. X. *Mol. Cell. Proteom.* **2005**, *4*, 1602-1613.
- (106) Wilcox, D. E. *Inorg. Chim. Acta* **2008**, *361*, 857-867.
- (107) Chitta, R. K.; Rempel, D. L.; Gross, M. L. *J. Am. Soc. Mass Spectrom.* **2005**, *16*, 1031-1038.
- (108) Gabelica, V.; Galic, N.; Rosu, F.; Houssier, C.; De Pauw, E. *J. Mass Spectrom.* **2003**, *38*, 491-501.
- (109) Mathur, S.; Badertscher, M.; Scott, M.; Zenobi, R. *Phys. Chem. Chem. Phys.* **2007**, *9*, 6187-6198.
- (110) Wang, W. J.; Kitova, E. N.; Klassen, J. S. *Anal. Chem.* **2005**, *77*, 3060-3071.
- (111) Sun, J. X.; Kitova, E. N.; Wang, W. J.; Klassen, J. S. *Anal. Chem.* **2006**, *78*, 3010-3018.
- (112) Kitova, E. N.; Soya, N.; Klassen, J. S. *Anal. Chem.* **2011**, *83*, 5160-5167.
- (113) Sun, J.; Kitova, E. N.; Sun, N.; Klassen, J. S. *Anal. Chem.* **2007**, *79*, 8301-8311.
- (114) Deng, L.; Sun, N.; Kitova, E. N.; Klassen, J. S. *Anal. Chem.* **2010**, *82*, 2170-2174.
- (115) El-Hawiet, A.; Kitova, E. N.; Liu, L.; Klassen, J. S. *J. Am. Soc. Mass Spectrom.* **2010**, *21*, 1893-1899.
- (116) Sun, J.; Kitova, E. N.; Klassen, J. S. *Anal. Chem.* **2007**, *79*, 416-425.
- (117) Zhang, H.; Lu, H.; Chingin, K.; Chen, H. *Anal. Chem.* **2015**, *87*, 7433-7438.
- (118) Bagal, D.; Kitova, E. N.; Liu, L.; El-Hawiet, A.; Schnier, P. D.; Klassen, J. S. *Anal. Chem.* **2009**, *81*, 7801-7806.
- (119) DeMuth, J. C.; Bu, J.; McLuckey, S. A. *Rapid Commun. Mass Spectrom.* **2015**, *29*, 973-981.

- (120) Clark, S. M.; Konermann, L. *Anal. Chem.* **2004**, *76*, 7077-7083.
- (121) Liu, L.; Kitova, E. N.; Klassen, J. S. *J. Am. Soc. Mass Spectrom.* **2011**, *22*, 310-318.
- (122) Oyelaran, O.; Gildersleeve, J. C. *Curr. Opin. Chem. Biol.* **2009**, *13*, 406-413.
- (123) Nimrichter, L.; Gargir, A.; Gortler, M.; Altstock, R. T.; Shtevi, A.; Weisshaus, O.; Fire, E.; Dotan, N.; Schnaar, R. L. *Glycobiology* **2004**, *14*, 197-203.
- (124) Dickinson, L. E.; Ho, C. C.; Wang, G. M.; Stebe, K. J.; Gerecht, S. *Biomaterials* **2010**, *31*, 5472-5478.
- (125) Šardžik, R.; Sharma, R.; Kaloo, S.; Voglmeir, J.; Crocker, P. R.; Flitsch, S. L. *Chem. Commun.* **2011**, *47*, 5425-5427.
- (126) Song, X.; Lasanajak, Y.; Xia, B.; Heimbürg-Molinaro, J.; Rhea, J. M.; Ju, H.; Zhao, C.; Molinaro, R. J.; Cummings, R. D.; Smith, D. F. *Nat. Methods* **2011**, *8*, 85-90.
- (127) Arndt, N. X.; Tiralongo, J.; Madge, P. D.; von Itzstein, M.; Day, C. J. *J. Cell. Biochem.* **2011**, *112*, 2230-2240.
- (128) Liang, P.-H.; Wu, C.-Y.; Greenberg, W. A.; Wong, C.-H. *Curr. Opin. Chem. Biol.* **2008**, *12*, 86-92.
- (129) Heimbürg-Molinaro, J.; Song, X.; Smith, D. F.; Cummings, R. D. *Curr. Protoc. Prot. Sci.* **2011**, 12.10. 11-12.10. 29.
- (130) Arthur, C. M.; Rodrigues, L. C.; Baruffi, M. D.; Sullivan, H. C.; Heimbürg-Molinaro, J.; Smith, D. F.; Cummings, R. D.; Stowell, S. R. *Galectins: Methods and Protocols* **2015**, 115-131.

- (131) Raman, R.; Raguram, S.; Venkataraman, G.; Paulson, J. C.; Sasisekharan, R. *Nat. Methods* **2005**, *2*, 817-824.
- (132) Liang, C.-H.; Wu, C.-Y. *Expert Rev Proteom.* **2009**, *6*, 631-645.
- (133) Drickamer, K.; Taylor, M. E. *Genome Biol.* **2002**, *3*, 1034.
- (134) Kilcoyne, M.; Gerlach, J. Q.; Kane, M.; Joshi, L. *Anal. Methods* **2012**, *4*, 2721-2728.
- (135) Grant, O. C.; Smith, H. M.; Firsova, D.; Fadda, E.; Woods, R. J. *Glycobiology* **2014**, *24*, 17-25.
- (136) Paulson, J. C.; Blixt, O.; Collins, B. E. *Nat. Chem. Biol.* **2006**, *2*, 238-248.

Chapter 2

Quantifying Protein-Carbohydrate Interactions Using Liquid Sample Desorption Electrospray Ionization Mass Spectrometry¹

2.1 Introduction

Non-covalent interactions between proteins and carbohydrates on the surfaces of cell, present as either part of membrane glycoproteins or glycolipids, are involved in many normal and pathological cellular processes, including catalysis, signaling and molecular recognition.¹ Studies of protein-carbohydrate interactions in vitro can provide fundamental insights into these important processes and guide the development of diagnostics and therapeutics for a variety of infections and diseases. There exist a number of analytical methods for the detection and characterization of protein-carbohydrate interactions. For example, glycan microarrays are now commonly used to screen libraries of carbohydrates for specific interactions with proteins,² while isothermal titration calorimetry (ITC),³ surface plasmon resonance (SPR),⁴ nuclear magnetic resonance (NMR) spectroscopy⁵ and enzyme-linked immunosorbent assays (ELISA)⁶ are extensively used to quantify the thermodynamics (and in some instances the kinetics) of protein-carbohydrate binding. In recent years, electrospray ionization mass spectrometry (ESI-MS) has emerged as a powerful method for detecting protein-carbohydrate complexes in solution and measuring the affinities of the interactions.⁷⁻¹⁸

In the direct ESI-MS binding assay, the protein-ligand binding equilibrium is determined by quantifying the relative abundances of the free and ligand-bound protein

¹ A version of this chapter has been published: Yao, Y., Shams-Ud-Doha, K., Daneshfar, R., Kitova, E. N., Klassen, J. S., *J. Am. Soc. Mass Spectrom.*, 2015, 26, 98-106.

ions in the gas phase.¹¹⁻¹³ The measurements are fast and can often be completed within a few minutes, the amount of sample consumed is low, typically picomoles of protein and nano- to picomoles of ligand, and there is no requirement for labeling or additional reagents, which makes the assay very versatile. Moreover, the direct ESI-MS assay is the only technique that directly measures binding stoichiometry. This feature is particularly beneficial to the study of protein-carbohydrate interactions, as many carbohydrate-binding proteins are composed of multiple subunits and possess multiple ligand binding sites. The ESI-MS assay also affords the opportunity to measure, simultaneously, the binding of multiple, distinct ligands, and is, therefore, well suited to carbohydrate library screening.¹⁶

A drawback of the ESI-MS assay, which is typically carried out using aqueous ammonium acetate solutions,¹⁹ is that it suffers from general incompatibility with nonvolatile “physiological” buffers, such as phosphate buffered saline (PBS), citrate, HEPES and Tris-HCl. Such buffers are often needed to keep the protein stable in solution and to minimize protein aggregation.²⁰ Several strategies have been proposed to allow ESI-MS analysis of solutions containing physiological buffers at relevant concentrations, including the use of high concentrations of ammonium acetate²¹ or carrying out ESI in the presence of a high velocity gas.²² A possible alternative approach involves separating the sample from the ESI process through the use of desorption electrospray ionization (DESI)²³⁻²⁵ or liquid sample DESI.²⁶⁻²⁹ In liquid sample DESI-MS, the liquid sample is ionized through collisions with charged droplets produced by ESI.^{26-27, 30} The ESI solution is typically a mixture of water and an organic solvent, such as acetonitrile or methanol.²⁸ Despite this, liquid sample DESI has been shown to produce multiply

charged gaseous ions of proteins and non-covalent protein complexes without inducing significant unfolding of the protein.²⁸ A variation of liquid sample DESI, known as reactive liquid sample DESI, was recently described and used to screen a library of compounds for specific binding to a target protein and to quantify the interactions.²⁷ In this approach, the ligands are introduced (consecutively) into the ESI spray solvent, rather than to the sample solution, which contained the target protein. The advantage of reactive liquid sample DESI is that the premixing of protein with ligands can be avoided.²⁷

The goal of the present study was to assess the reliability of liquid sample DESI for the quantification of protein-carbohydrate binding in aqueous ammonium acetate solutions. The affinities of tri- and tetrasaccharide ligands for lysozyme (Lyz), a glycosyl hydrolase, and a single chain variable fragment (scFv) of a monoclonal antibody were measured by liquid sample DESI-MS and the results compared with those measured using ITC and the direct ESI-MS assay.³¹⁻³³

2.2 Experimental section

2.2.1 Materials

Ubiquitin (Ubq, MW 8565 Da), lysozyme (from chicken egg white, Lyz, MW 14310 Da) and maltotriose (**L1**, MW 504.44 Da) were purchased from Sigma-Aldrich Canada (Oakville, Canada) and β -D-GlcNAc-(1 \rightarrow 4)- β -D-GlcNAc-(1 \rightarrow 4)-D-GlcNAc (**L2**, MW 627.59 Da) and β -D-GlcNAc-(1 \rightarrow 4)- β -D-GlcNAc-(1 \rightarrow 4)- β -D-GlcNAc-(1 \rightarrow 4)-D-GlcNAc (**L3**, MW 830.27 Da) were purchased from Dextra Science and Technology Centre (United Kingdom). The single chain variable fragment of Se155-4 (scFv, MW 26539 Da) was produced and purified as described previously³⁴⁻³⁵ and α -D-Galp-(1 \rightarrow 2)-

[α -D-Abep-(1 \rightarrow 3)]- α -D-Manp-OCH₃ (**L4**, MW 486.50 Da) and β -D-Glcp-(1 \rightarrow 2)-[α -D-Abep-(1 \rightarrow 3)]- α -D-Manp-OCH₃ (**L5**, MW 486.50 Da) were gifts from Prof. D. Bundle (University of Alberta). Stock solutions of each protein (in 50 mM ammonium acetate) and oligosaccharide (in deionized water) were prepared, and stored at -20 °C until needed. Sample solutions for ESI- and liquid sample DESI-MS analysis were prepared from the stock solutions of protein and oligosaccharide. Unless otherwise indicated, the sample solutions contained 20 mM ammonium acetate.

2.2.2 Mass spectrometry

All of the ESI- and liquid sample DESI-MS measurements were carried out in positive ion mode using a Synapt G2 quadrupole-ion mobility separation-time-of-flight (Q-IMS-TOF) mass spectrometer (Waters UK Ltd., Manchester, UK) equipped with a 8k quadrupole mass filter. All data were processed using MassLynx software (v4.1). For the ESI-MS measurements, nanoflow ESI (nanoESI) tips, produced from borosilicate capillaries (1.0 mm o.d., 0.68 mm i.d.) and pulled to ~ 5 μ m using a P-1000 micropipette puller (Sutter Instruments, Novato, CA, USA), were used. A platinum wire was inserted into the nanoESI tip and a Capillary voltage of 1.0 – 1.3 kV was applied to initiate the spray. A Cone voltage of 30 V was used and the source block temperature was maintained at 60 °C. The Trap and Transfer ion guides were maintained at 5 V and 2 V, respectively, and the argon pressure in these regions was 2.22×10^{-2} mbar and 3.36×10^{-2} mbar, respectively. For the liquid sample DESI-MS measurements, a modified OMNI SPRAY Ion Sources 2-D OS-6205 (Prosolia Inc., Indianapolis, IN, USA) was used. The liquid sample solution was delivered through a silica capillary (360 nm o.d., 100 nm i.d.) at a flow rate of 5-10 μ L h⁻¹ using a syringe pump (Chemyx Syringe Pumps Fusion 100,

Chemyx Inc, Stafford, TX, USA). The end of the silica capillary was positioned between the ESI tip and inlet of the mass spectrometer. The ESI solution flow rate was between 2 and 4 $\mu\text{L min}^{-1}$. Capillary and Cone voltages of 3.0 – 3.5 kV and 30 V, respectively, were used and the pressure of the N_2 nebulizing gas was 60 – 70 psi. The source block temperature was the same as for the ESI-MS measurements.

Prior to carrying out the liquid sample DESI-MS protein-carbohydrate binding measurements, several different spray solvent compositions were tested (deionized water, 20 mM ammonium acetate, 50/50 v/v water/methanol, 20/80 v/v water/acetonitrile, 50/50 v/v water/acetonitrile and 80/20 v/v water/acetonitrile) for the analysis of aqueous ammonium acetate solutions of Lyz or scFv, the two model carbohydrate-binding proteins used in this study. Ultimately, it was found that a 50/50 water/acetonitrile solution gave mass spectra with the highest signal-to-noise ratios. Shown in Figure 2.1 are representative liquid sample DESI mass spectra acquired in positive ion mode for aqueous ammonium acetate (20 mM) solutions containing Lyz (10 μM) or scFv (10 μM).

It can be seen that liquid sample DESI-MS produced abundant signal corresponding to the protonated ions of Lyz (Figure 2.1a) and scFv (Figure 2.1b). A 50/50 water/acetonitrile solution was used as the spray solvent for all of the liquid sample DESI-MS binding measurements reported in this study.

2.2.3 Isothermal titration calorimetry

The ITC measurements were carried out using a VP-ITC (MicroCal, Inc. USA). For each ITC experiment, the Lyz solution (0.1 - 0.2 mM) in the sample cell was titrated with a solution of **L2** or **L3** (2 mM); both the protein and ligand solutions were aqueous ammonium acetate (50 mM, pH 6.8) at 25 °C.

2.2.4 Data analysis

The general procedure for determining association constants (K_a) for protein-ligand interactions from ESI mass spectra has been described in detail elsewhere and only a brief description is given for the case where the protein has single ligand binding site.^{18, 36-37} The assay relies on the detection and quantification of the gas-phase ions of free and ligand-bound protein. The concentration ratio (R) of the ligand-bound protein (PL) to free protein (P) in solution is taken to be equal to the total abundance (Ab) of P and PL ions as measured by ESI-MS, eq 2.1. It follows that K_a can be calculated from eq 2.2:

$$R = \frac{\sum Ab(PL)}{\sum Ab(P)} = \frac{[PL]_{eq}}{[P]_{eq}} \quad (2.1)$$

$$K_a = \frac{R}{[L]_o - \frac{R[P]_o}{1+R}} \quad (2.2)$$

where $[P]_o$ and $[L]_o$ are the initial protein and ligand concentrations, respectively.

It was shown previously that, during the ESI process, free L can form so-called nonspecific complexes with P (and specific PL complexes), as the ESI droplets evaporate to dryness.³⁶⁻³⁷ The extent of nonspecific ligand binding is sensitive to the concentration of free L and, consequently, is more prevalent when measuring low affinity interactions because high L concentrations are needed to produce detectable concentrations of the PL complexes.³⁷ The formation of nonspecific PL interactions changes to the measured abundances of the P and PL ions and, thereby, introduces error into the R and K_a values. The reference protein method was developed to quantitatively correct ESI mass spectra for nonspecific binding.³⁷ The method involves the addition of reference protein (P_{ref}), which does not interact with P or L, to the solution. The presence of nonspecific binding

is established from the appearance of ions corresponding to P_{ref} bound to one or more molecules of L, i.e., $P_{\text{ref}}L_x$ complexes. As described in detail elsewhere, the contribution of nonspecific binding to the apparent (measured) abundances of P ($Ab_{\text{app}}(\text{P})$) and PL ($Ab_{\text{app}}(\text{PL})$) can be accounted for using eqs 2.3a and 2.3b:

$$Ab(\text{P}) = Ab_{\text{app}}(\text{P}) / f_0 \quad (2.3a)$$

$$Ab(\text{PL}^{n+}) = \{Ab_{\text{app}}(\text{PL}^{n+}) - f_1 Ab(\text{P}^{n+})\} / f_0 \quad (2.3b)$$

where f_0 is the fraction of free P and f_1 the fraction of P bound nonspecifically to one molecule of L. These fractions can be determined from the measured abundances of free and ligand-bound forms of P_{ref} , eqs 2.4a and 2.4b:

$$f_0 = Ab(\text{P}_{\text{ref}}) / \{Ab(\text{P}_{\text{ref}}) + Ab(\text{P}_{\text{ref}}\text{L})\} \quad (2.4a)$$

$$f_1 = Ab(\text{P}_{\text{ref}}\text{L}) / \{Ab(\text{P}_{\text{ref}}) + Ab(\text{P}_{\text{ref}}\text{L})\} \quad (2.4b)$$

To test the reliability of the reference protein method for correcting liquid sample DESI mass spectra for the occurrence of nonspecific carbohydrate-protein binding, control experiments were carried out on solutions containing a pair of proteins (Lyz and Ubq) and **L1**, which does not bind to either protein in solution.³¹⁻³² Shown in Figure 2.2 are liquid sample DESI mass spectra acquired in positive ion mode for aqueous 20 mM ammonium acetate solutions of Lyz (10 μM) and Ubq (10 μM) and **L1** at concentration of 15 μM (Figure 2.2a) or 40 μM (Figure 2.2b).

It can be seen that, in addition to the protonated ions of Lyz (at charge states +6 to +9) and Ubq (at charge states +4 to +6), ions corresponding to nonspecific complexes with **L1** are evident at both concentrations. Shown in the insets of Figures 2.2a and 2.2b are the normalized abundances of Lyz and Ubq in their free and bound (to **L1**) forms.

Notably, the distributions of both proteins are identical, within experimental error, at both concentrations of **L1**. These results confirm that the extent of nonspecific carbohydrate binding during the liquid sample DESI process is the same for the two proteins and, further, supports the use of the reference protein method for correcting liquid sample DESI mass spectra for nonspecific carbohydrate-protein binding.

2.3 Results and discussion

To test the reliability of liquid sample DESI-MS for quantifying protein-carbohydrate interactions, the affinities of the tri- and tetrassachride ligands, **L2** and **L3** for Lyz, and the trisaccharide ligands **L4** and **L5** for scFv were measured. The affinities of **L4** and **L5** for scFv were previously measured in this laboratory using the direct ESI-MS assay and found to be $1.2 \times 10^5 \text{ M}^{-1}$,³⁸ and $(5.0 \pm 1.0) \times 10^3 \text{ M}^{-1}$,³⁹ respectively. The affinities of **L2** and **L3** for Lyz have been measured using several different biophysical techniques. Values of $1.1 \times 10^5 \text{ M}^{-1}$ (**L2**) and $1.8 \times 10^5 \text{ M}^{-1}$ (**L3**) were obtained using fluorescence-based assay.⁴⁰ Quantitative ESI-MS studies have also been carried out - Oldham and coworkers measured affinities of $1.0 \times 10^5 \text{ M}^{-1}$ (**L2**) and $1.2 \times 10^5 \text{ M}^{-1}$ (**L3**),³¹ while Zenobi and coworkers found somewhat lower values (ranging from $2 \times 10^4 \text{ M}^{-1}$ to $5 \times 10^4 \text{ M}^{-1}$) for **L2**.³³ Given the range of the reported values for **L2**, the affinities of **L2** and **L3** for Lyz in aqueous ammonium acetate (50 mM, pH 6.8 and 25 °C) were measured using ITC, which is widely regarded as the gold standard method for quantifying the thermodynamics of protein-carbohydrate interactions. Shown in Figures 2.3 and 2.4 are the raw and integrated ITC data measured for binding of Lyz to **L2** and **L3**, respectively.

According to the best fit of a 1:1 binding model to the ITC data, the affinities of **L2** and **L3** for Lyz are $(9.0 \pm 0.3) \times 10^4 \text{ M}^{-1}$ and $(1.1 \pm 0.1) \times 10^5 \text{ M}^{-1}$, respectively. These results are in good agreement with the values obtained using the fluorescence-based assay⁴⁰ and those reported by Oldham and coworkers.³¹

2.3.1 Binding of Lyz to **L2** and **L3**

The affinities of **L2** and **L3** for Lyz in aqueous ammonium acetate (20 mM, pH 6.8 and 25 °C) were measured at three different ligand concentrations. Shown in Figures 2.5a and 2.5c are representative liquid sample DESI mass spectra acquired for solutions of Lyz (10 μM) with **L2** (15 μM) or **L3** (15 μM), respectively. Ubq (5 μM), which served as P_{ref} , was added to both solutions. For comparison purposes, ESI mass spectra were also acquired for these solutions (Figures 2.5b and 2.5d). From Figures 2.5a and 2.5c, it can be seen that liquid sample DESI produces ions corresponding to free Lyz and ligand-bound Lyz (i.e., the (Lyz + **L2**) or (Lyz + **L3**) complexes), at charge states +6 to +8, as well as free Ubq at charge states +4 and +5. Ion signal corresponding to the nonspecific (Ubq + **L2**) or (Ubq + **L3**) complexes was negligible. Similar results were obtained for solutions containing **L2** or **L3** at two other concentrations, 5 μM and 10 μM (data not shown). The K_a values, representing the average of the values obtained by liquid sample DESI-MS at the three ligand concentrations, are $(1.0 \pm 0.1) \times 10^5 \text{ M}^{-1}$ (**L2**) and $(9.9 \pm 0.6) \times 10^4 \text{ M}^{-1}$ (**L3**) (Table 2.1).

The ESI mass spectra obtained for aqueous ammonium acetate (20 mM) solutions of Lyz (10 μM), Ubq (5 μM), and **L2** (15 μM) or **L3** (15 μM) (Figures 2.5b and 2.5d, respectively) are qualitatively similar to the liquid sample DESI mass spectra, although the average charge states (ACS) of Lyz are slightly higher than those observed with liquid

sample DESI (*ACS* 6.98 (Figure 2.5a), 7.43 (Figure 2.5b), 7.02 (Figure 2.5c), 7.98 (Figure 2.5d)). The lower *ACS* values measured with liquid sample DESI-MS may be due to a subtle enhancement in the extent of proton transfer from the protein ions to acetonitrile in the gas phase. Acetonitrile has a relatively low gas phase basicity (178.8 kcal mol⁻¹), compared to ammonia (195.7 kcal mol⁻¹),⁴¹ but is present at a high concentration in the spray solvent (~9.6 M) and is expected to be present at relatively high concentrations in the spray droplets. The resulting acetonitrile vapour could affect proton transfer from the gaseous Lyz ions. Support for this explanation can be found in an observed decrease in *ACS* measured for Lyz when carrying out ESI in the presence of acetonitrile vapour (data not shown), a phenomenon also observed by Oldham and coworkers.⁴⁴⁻⁴⁵ The average K_a values obtained by ESI-MS at the three ligand concentrations are $(8.0 \pm 0.5) \times 10^4 \text{ M}^{-1}$ (**L2**) and $(6.3 \pm 0.5) \times 10^4 \text{ M}^{-1}$ (**L3**) (Table 2.1). Notably, the absolute affinities measured by liquid sample DESI-MS for **L2** and **L3** agree within a factor of 2 with the values determined from the ESI-MS measurements. More importantly, the liquid sample DESI-MS values are in excellent agreement with the affinities determined by ITC.

2.3.2 Binding of scFv to L4 and L5

The affinities of **L4** and **L5** for scFv in aqueous ammonium acetate (20 mM, pH 6.8 and 25 °C) were also measured at three different ligand concentrations. Shown in Figures 2.6a and 2.6c are representative liquid sample DESI mass spectra acquired for solutions of scFv (10 μM) with **L4** (15 μM) or **L5** (40 μM), respectively. Lyz (5 μM), which served as P_{ref} , was added to both solutions. For comparison purposes, ESI mass spectra were also acquired for these solutions (Figures 2.6b and 2.6d). In Figures 2.6a and 2.6c,

ion signal corresponding to protonated free scFv and the (scFv + **L4**) or (scFv + **L5**) complexes, at charge states +8 to +10, as well as free Lyz and the (Lyz + **L4**) or (Lyz + **L5**) complexes, at charge states +6 to +9, is evident. The appearance of ion signal for the (Lyz + **L4**) and (Lyz + **L5**) complexes indicates the occurrence of nonspecific carbohydrate-protein binding during ion formation.

Similar results were obtained for solutions at two other concentrations of **L4** (5 and 10 μM) and **L5** (20 and 30 μM). Following correction of the mass spectra for nonspecific binding, average K_a values of $(7.6 \pm 0.1) \times 10^4 \text{ M}^{-1}$ (**L4**) and $(5.7 \pm 0.2) \times 10^4 \text{ M}^{-1}$ (**L5**) were determined (Table 2.1). The ESI mass spectra measured for solutions of scFv (10 μM), Lyz (5 μM) with **L4** (15 μM) or **L5** (40 μM) (Figures 2.6b and 2.6d, respectively) are similar to the corresponding liquid sample DESI mass spectra (Figures 2.6a and 2.6c). However, the extent of nonspecific binding is less in the case of ESI - there was no significant signal corresponding to the nonspecific (Lyz + **L4**) complex and significantly less (Lyz + **L5**) detected. The reduced occurrence of nonspecific binding may be due to the small droplets produced with the nanoESI tips, compared to those formed in liquid sample DESI.⁴² The smaller nanoESI droplets will contain fewer ligand molecules and, therefore, produce less nonspecific binding, compared to the larger ESI droplets used for liquid sample DESI-MS. Following correction for nonspecific ligand binding, the affinities of **L4** and **L5** are found to be $(6.6 \pm 0.3) \times 10^4 \text{ M}^{-1}$ and $(5.0 \pm 0.1) \times 10^3 \text{ M}^{-1}$, respectively. Importantly, the affinities measured by liquid sample DESI-MS for **L4** and **L5** are in good agreement with the values determined using the direct ESI-MS assay.

Taken together, the results obtained for these model carbohydrate binding proteins demonstrate that absolute affinities for protein-carbohydrate interactions can be

accurately quantified using liquid sample DESI-MS. These findings further indicate that the lifetime of the ESI droplets that produce gaseous protein ions in liquid sample DESI-MS are sufficiently short that neither the presence of a high concentration of organic solvent in the ESI spray solution, nor the inevitable dilution of the sample (protein and ligand) solution by the solvent spray results in a measurable shift in the binding equilibrium.

2.3.3 Comparison of liquid sample DESI-MS and reactive liquid sample DESI-MS

It is also interesting to compare the affinity of **L2** for Lyz measured by liquid sample DESI-MS with the value determined by Loo and coworkers using reactive liquid sample DESI-MS.²⁷ Notably, the value measured using reactive liquid sample DESI-MS, $5.9 \times 10^3 \text{ M}^{-1}$, is eighteen times smaller than the value determined by liquid sample DESI-MS (and ITC). It has been suggested that the short time available for protein and ligand mixing in reactive liquid sample DESI (estimated to be <2 ms) might be insufficient for equilibration of the binding reaction.⁴³ To help rule out other alternative explanations, in particular the possibility of in-source dissociation, reactive liquid sample DESI-MS was carried in the present study to measure the affinity of **L2** for Lyz. The experimental and instrumental conditions were identical to those used for the liquid sample DESI measurements described above, with the exception that **L2** was absent in the sample solution but present in the spray solvent. Shown in Figure 2.7 is a representative reactive liquid sample DESI mass spectrum acquired for an aqueous ammonium acetate (20 mM) solution of Lyz (10 μM) and Ubq (5 μM); the spray solvent was a 50/50 water/acetonitrile solution containing **L2** (50 μM).

Ion signal corresponding to protonated and sodiated **L2** monomer, dimer and trimer was detected, along with protonated ions of Lyz and (Lyz + **L2**), at charge states +6 to +8, and Ubq and (Ubq + **L2**), at charge state +4. Following correction for nonspecific carbohydrate-protein binding, the K_a value was determined to be $(7.9 \pm 0.4) \times 10^3 \text{ M}^{-1}$, which is similar to the value reported by Loo and coworkers.²⁷ Given that the instrumental conditions were identical to those used for the liquid sample DESI-MS measurements, it can be concluded that the lower affinity is not due to artifacts associated with instrumental conditions, such as in-source dissociation of the protein-carbohydrate complexes. This finding further supports the suggestion that the lower affinity is, in fact, a kinetic artifact owing to the insufficient time in the droplets for the protein-ligand binding equilibrium to be established.²⁰

The differences in the appearances of the liquid sample DESI and ESI mass spectra can be rationalized by considering the differences in the initial composition of the droplets in each case. In the ESI-MS experiments, the initial droplets will contain concentrations of buffer that are similar to that found in bulk solution, with some enrichment in cations (Na^+ and K^+) expected as a result of the applied electric field.¹⁹ As a result of solvent evaporation, the concentration of buffer components in the droplets will further increase, with the highest concentrations found in the offspring droplets produced late in the ESI process.¹⁹ In contrast, in liquid sample DESI-MS, the initial ESI droplets are devoid of buffer and contain only water and acetonitrile. It is only through collisions with the sample solution that buffer components are transferred to the ESI droplets.

2.4 Conclusions

In summary, the application of liquid sample DESI-MS for quantifying protein-carbohydrate interactions in aqueous solutions is described. Notably, the affinities of tri- and tetrasaccharide ligands for Lyz and scFv measured using liquid sample DESI-MS are found to be in good agreement with values measured by ITC and the direct ESI-MS assay. It is also found that the reference protein method, which was originally developed to correct ESI mass spectra for the occurrence of nonspecific ligand-protein binding, can be used to correct liquid sample DESI mass spectra for nonspecific carbohydrate binding.

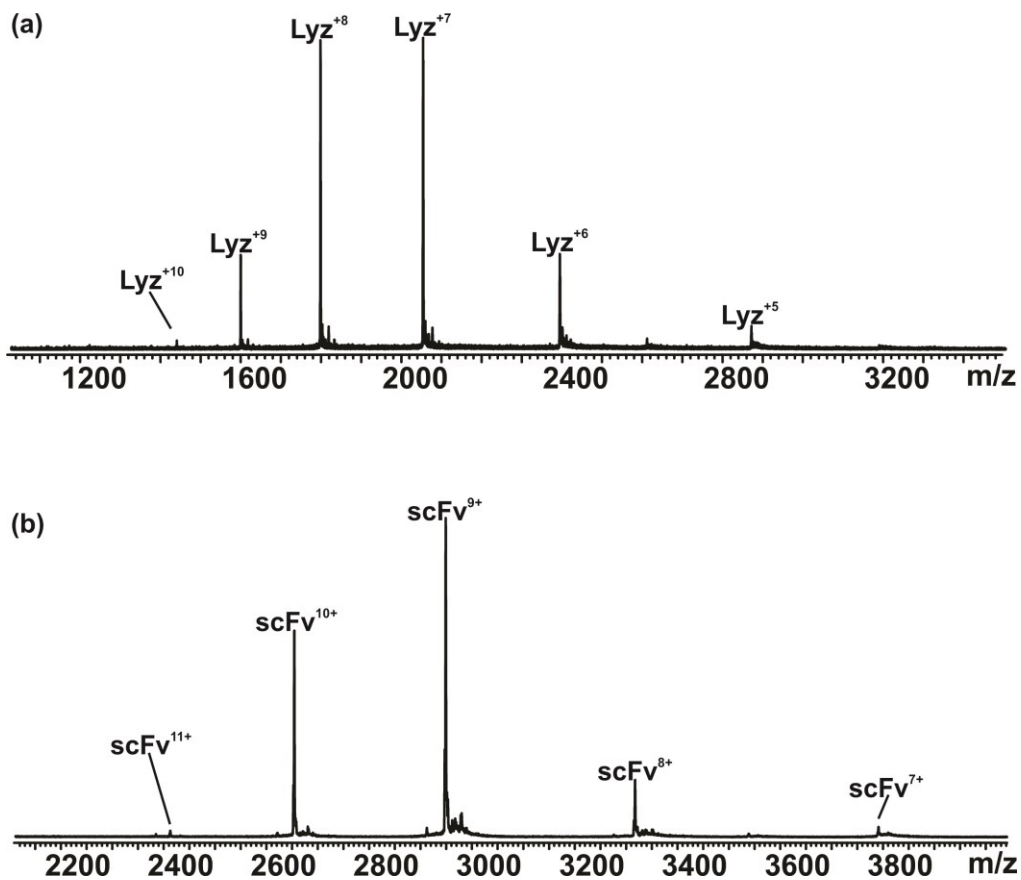


Figure 2.1. Representative liquid sample DESI mass spectra acquired in positive ion mode for aqueous ammonium acetate (20 mM) solutions containing (a) Lyz (10 μ M), and (b) scFv (10 μ M). The ESI spray solution was 50/50 water/acetonitrile.

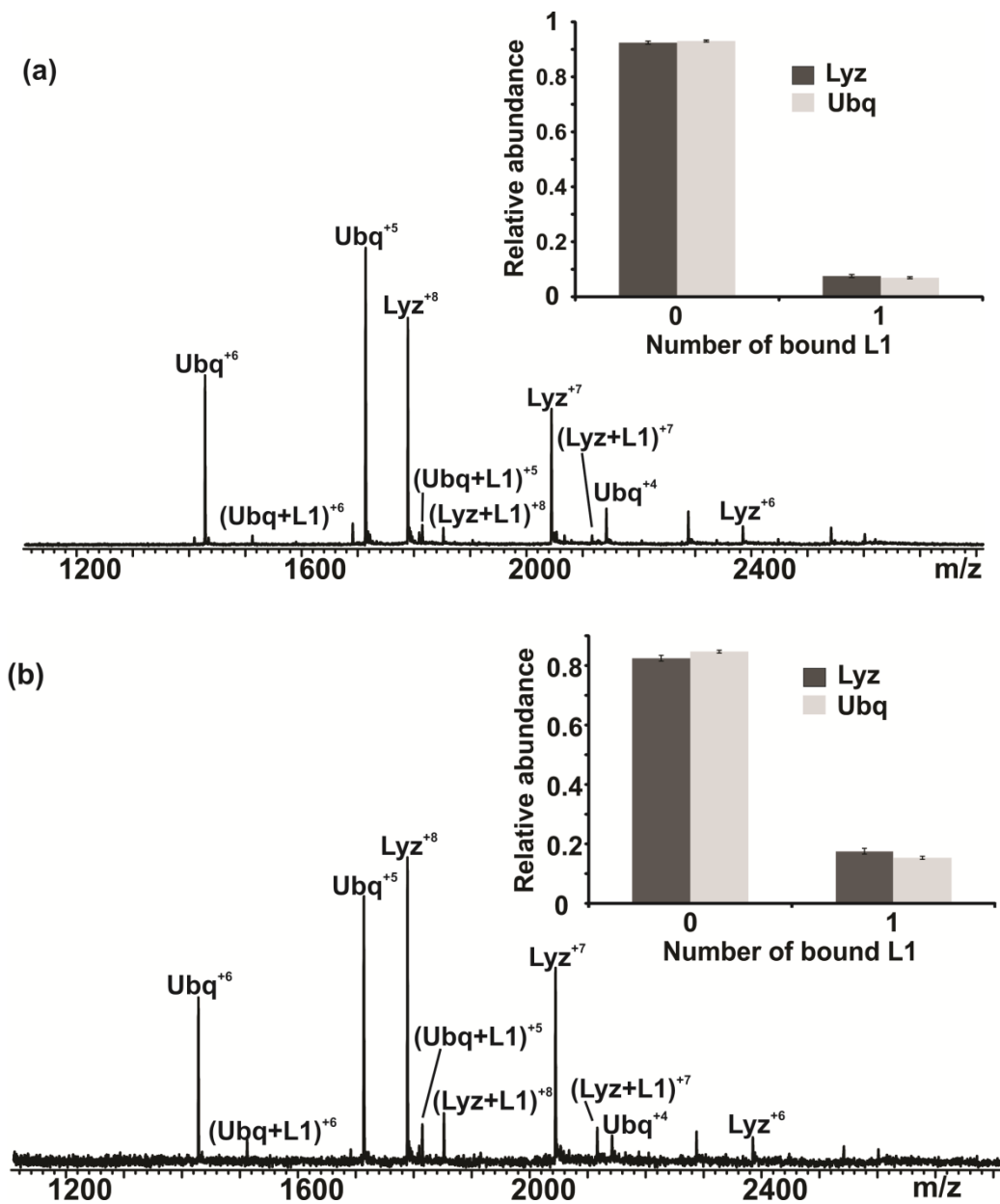


Figure 2.2. Representative liquid sample DESI mass spectra acquired in positive ion mode for aqueous ammonium acetate (20 mM, pH 6.8 and 25 °C) solutions containing Ubq (10 μM), Lyz (10 μM) and L1 at (a) 15 μM or (b) 40 μM concentrations. The ESI spray solution was 50/50 water/acetonitrile.

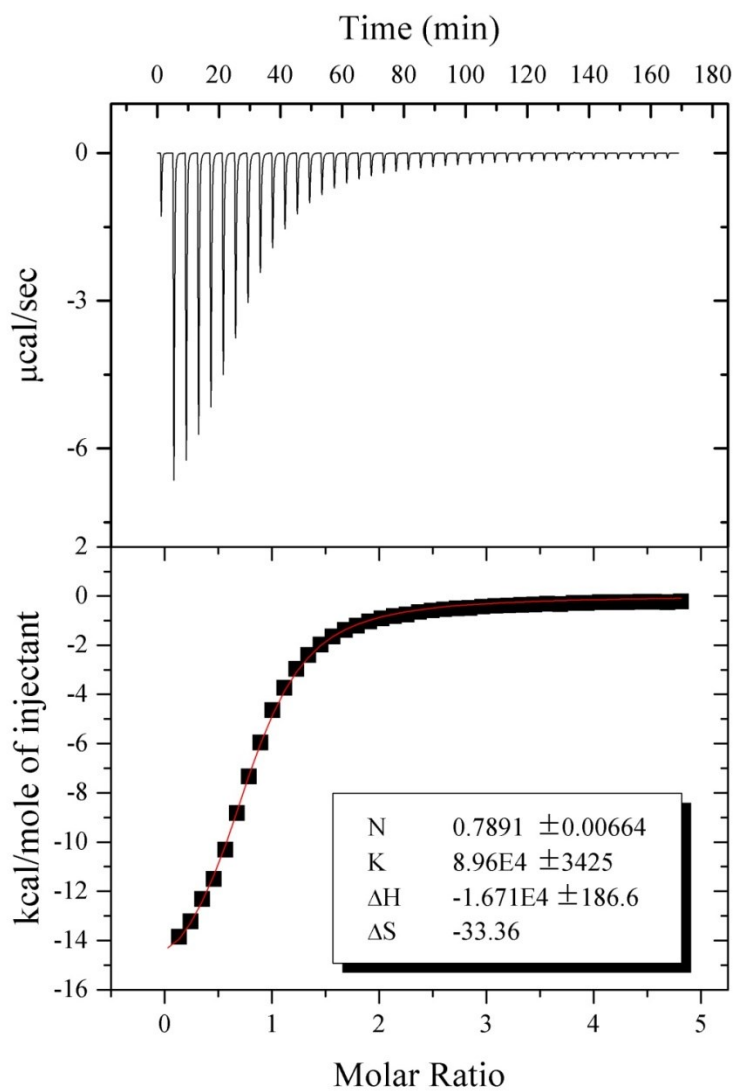


Figure 2.3. ITC data measured for the binding of Lyz (0.087 mM) to L2 (2.0 mM) in aqueous ammonium acetate (50 mM, pH 6.8 and 25 °C) solutions.

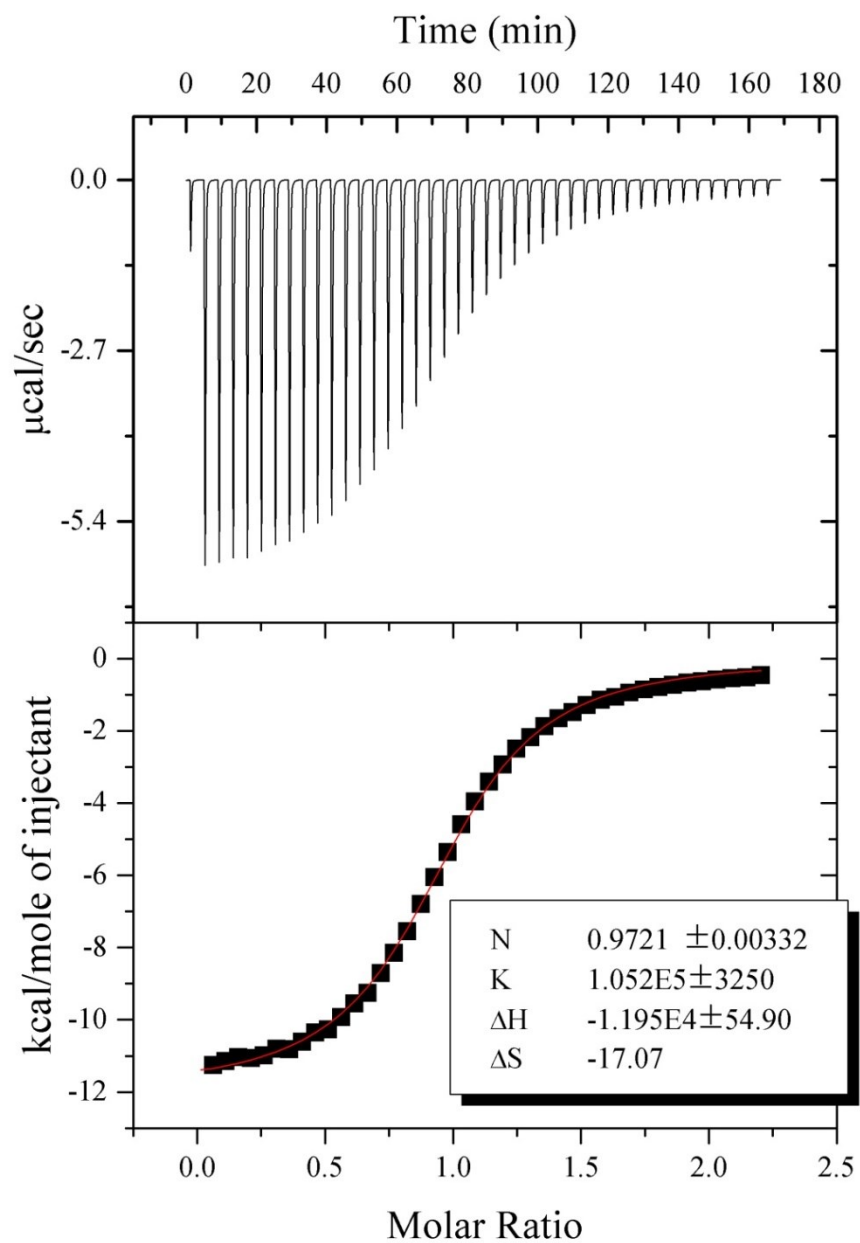


Figure 2.4. ITC data measured for the binding of Lyz (0.202 mM) to L3 (2.0 mM) in aqueous ammonium acetate (50 mM, pH 6.8 and 25 °C) solutions.

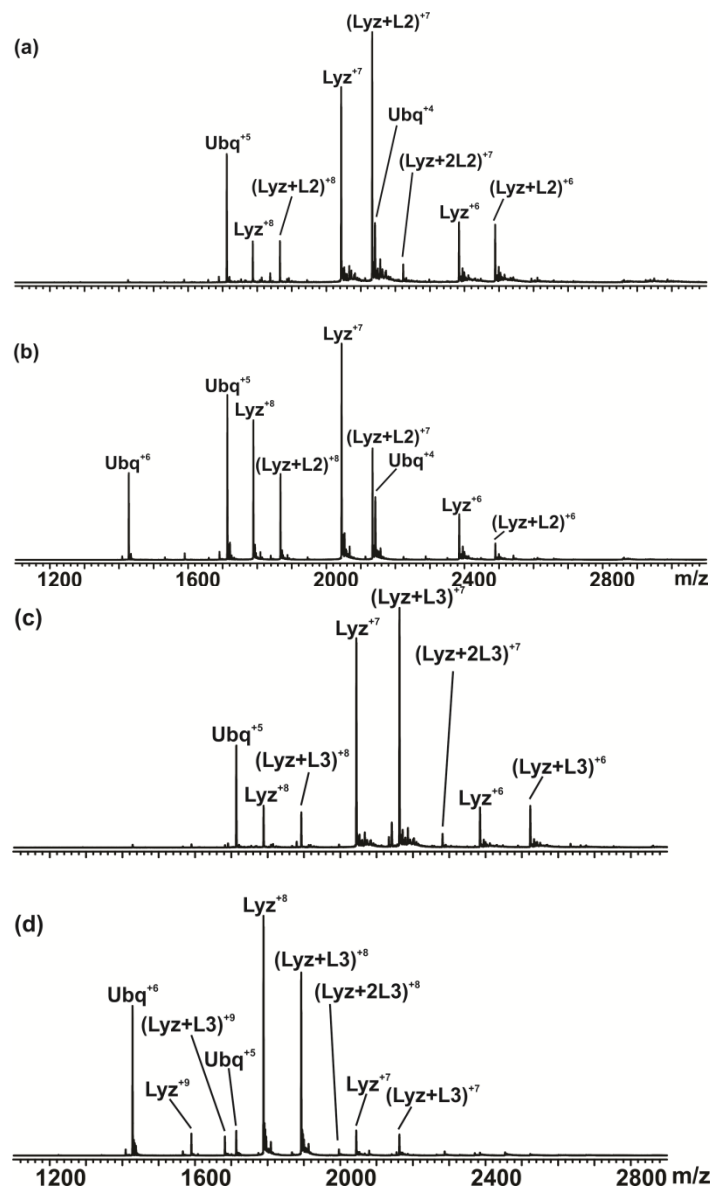


Figure 2.5. Representative (a), (c) liquid sample DESI and (b), (d) ESI mass spectra acquired in positive ion mode for aqueous ammonium acetate (20 mM, pH 6.8 and 25 °C) solutions containing Lyz (10 μ M), L2 (15 μ M) and Ubq (5 μ M) ((a) and (b)) or Lyz (10 μ M), L3 (15 μ M) and Ubq (5 μ M) ((c) and (d)). For the liquid sample DESI-MS measurements, the ESI spray solution was 50/50 water/acetonitrile.

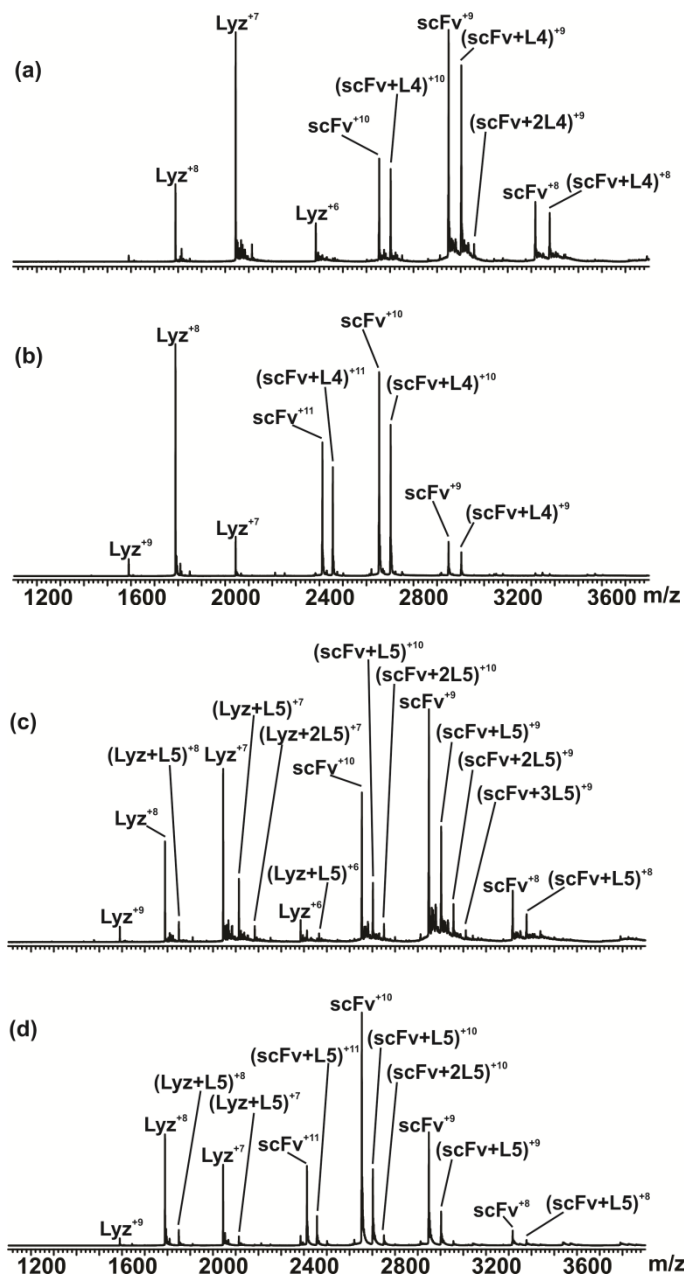


Figure 2.6. Representative (a), (c) liquid sample DESI and (b), (d) ESI mass spectra acquired in positive ion mode for aqueous ammonium acetate (20 mM, pH 6.8 and 25 °C) solutions containing scFv (10 μM), L4 (15 μM) and Lyz (5 μM) ((a) and (b)) or scFv (10 μM), L5 (40 μM) and Lyz (5 μM) ((c) and (d)). For the liquid sample DESI-MS measurements, the ESI spray solution was 50/50 water/acetonitrile.

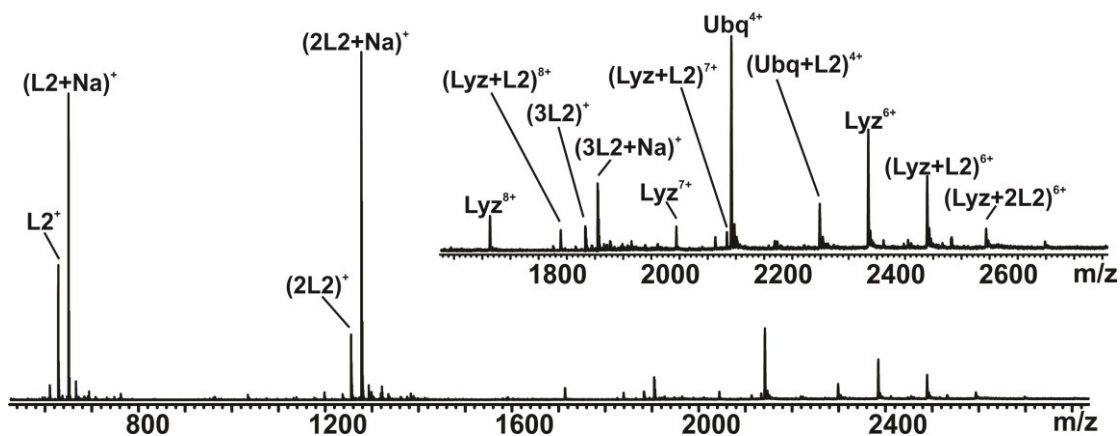


Figure 2.7. Representative reactive liquid sample DESI mass spectrum acquired in positive ion mode for an aqueous ammonium acetate (20 mM, pH 6.8 and 25 °C) solution containing Lyz (10 μ M) and Ubq (5 μ M) and an ESI spray solution (50/50 water/acetonitrile) that contained **L2** (50 μ M). The flow rates of both the sample and ESI spray solution were 5 μ L min^{-1} . All other instrumental conditions were identical to those used for the liquid sample DESI measurements.

Table 2.1. Comparison of association constants (K_a) measured by liquid sample DESI-MS, ESI-MS and ITC for the interactions of **L2** and **L3** with Lyz and **L4** and **L5** with scFv in aqueous ammonium acetate solutions at pH 6.8 and 25 °C.^a

Protein	Ligand	K_a (liquid sample DESI-MS)/M ⁻¹	K_a (ESI-MS)/M ⁻¹	K_a (ITC)/M ⁻¹
Lyz	L2	$(1.0 \pm 0.1) \times 10^5$	$(8.0 \pm 0.5) \times 10^4$	$(9.0 \pm 0.3) \times 10^4$
Lyz	L3	$(9.9 \pm 0.6) \times 10^4$	$(6.3 \pm 0.5) \times 10^4$	$(1.1 \pm 0.1) \times 10^5$
scFv	L4	$(7.6 \pm 0.1) \times 10^4$	$(6.6 \pm 0.3) \times 10^4$ $(1.2 \times 10^5)^b$	
scFv	L5	$(5.7 \pm 0.2) \times 10^3$	$(5.0 \pm 0.1) \times 10^3$	

a. Errors correspond to one standard deviation. b. Value taken from ref. 38.

2.5 References

- (1) Bewley, C. A., *Protein-carbohydrate Interactions in Infectious Diseases*. RSC Publishing: Cambridge, UK; **2006**.
- (2) Disney, M. D.; Seeberger, P.H., *Chem. Biol.* **2004**, 11, 1701-1707.
- (3) Leavitt, S.; Freire, E., *Curr. Opin. Struct. Biol.* **2001**, 11, 560-566.
- (4) Frostell, Å.; Vinterbäck, L.; Sjöbom, H., *Methods Mol. Biol.* **2013**, 1008, 139-165.
- (5) Zech, S. G.; Olejniczak, E.; Hajduk, P.; Mack, J.; McDermott, A. E., *J. Am. Soc. Mass Spectrom.* **2004** 126, 13948-13953.
- (6) Orosz, F.; Ovadi, J., *J. Immunol. Methods.* **2002**, 270, 155-162.
- (7) El-Hawiet, A.; Kitova, E. N.; Klassen, J. S. *Anal. Chem.* **2013**, 85, 7637-7644.
- (8) Lin, H.; Kitova, E. N.; Klassen, J. S. *J. Am. Soc. Mass Spectrom.* **2014**, 25, 104-110.
- (9) Han, L.; Kitov, P. I.; Kitova, E. N.; Tan, M.; Wang, L.; Xia, M.; Jiang, X.; Klassen, J.S. *Glycobiology.* **2013**, 23, 276-285.
- (10) El-Hawiet. A.; Kitova, E. N.; Arutyunov, D.; Szymanski, C. M.; Klassen, J. S. *Anal. Chem.* **2012**, 84, 3867–3870.
- (11) El-Hawiet, A.; Kitova, E. N.; Klassen, J. S. *Biochemistry*, **2012**, 51, 4244-4253.
- (12) Daniel, J. M.; Friess, S. D.; Rajagopalan, S.; Wendt, S.; Zenobi, R. *Int. J. Mass Spectrom.* **2002**, 216, 1-27.
- (13) Kitova, E. N.; El-Hawiet, A.; Schnier, P. D.; Klassen J. S. *J. Am. Soc. Mass Spectrom.* **2012**, 23, 431-441.

- (14) El-Hawiet, A.; Kitova, E. N.; Liu, L.; Klassen, J. S. *J. Am. Soc. Mass Spectrom.* **2010**, 21, 1893-1899.
- (15) Deng, L.; Sun N; Kitova, E. N.; Klassen, J. S. *Anal. Chem.* **2010**, 82, 2170-2174.
- (16) El-Hawiet, A., Shoemaker, G. K., Daneshfar, R., Kitova, E. N., Klassen, J. S. *Anal. Chem.* **2011**, 84, 50-58.
- (17) Loo, J. A. *Mass Spectrom. Rev.* **1997**, 16, 1-23.
- (18) Wang, W.; Kitova, E. N.; Klassen, J. S. *Anal. Chem.* **2003**, 75, 4945-4955.
- (19) Kebarle, P. *J. Mass Spectrom.* **2000**, 35, 804-817.
- (20) Banerjee, S.; Mazumdar, S. *Int. J. Anal. Chem.* **2012**, 2012, 282574.
- (21) Sterling, H., Batchelor, J., Wemmer, D., Williams, E. *J. Am. Soc. Mass Spectrom.* **2010**, 21, 1045-1049.
- (22) Yang P.; Cooks R. G.; Ouyang Z. *Anal. Chem.* **2005**, **77**, 6174-6183.
- (23) Takáts, Z.; Wiseman, J. M.; Gologan, B.; Cooks, R. G. *Science* **2004**, 306, 471-473.
- (24) Shin, Y.-S.; Drolet, B.; Mayer, R.; Dolence, K.; Basile, F. *Anal. Chem.* **2007**, 79, 3514-3518.
- (25) Lu, X.; Ning, B.; He, D.; Huang, L.; Yue, X.; Zhang, Q.; Huang, H.; Liu, Y.; He, L.; Ouyang, J. *J. Am. Soc. Mass Spectrom.* **2014**, 25, 454-463.
- (26) Miao, Z.; Chen, H. *J. Am. Soc. Mass Spectrom.* **2009**, 20, 10-19.
- (27) Liu, P.; Zhang, J.; Ferguson, C. N.; Chen, H.; Loo, J. A. *Anal. Chem.* **2013**, 85, 11966-11972.
- (28) Ferguson, C. N.; Benchaar, S. A.; Miao, Z.; Loo, J. A.; Chen, H. *Anal. Chem.* **2011**, 83, 6468-6473.

- (29) Moore, B. N.; Hamdy, O.; Julian, R. R. *Int. J. Mass Spectrom.* **2012**, 330–332, 220-225.
- (30) Takáts, Z.; Wiseman, J. M.; Cooks, R. G. *J. Mass Spectrom.* **2005**, 40, 1261-1275.
- (31) Veros, C. T.; Oldham, N. J. *Rapid Commun. Mass Spectrom.* **2007**, 21, 3505-3510.
- (32) Sun, N.; Soya, N.; Kitova, E.; Klassen, J. *J. Am. Soc. Mass Spectrom.* **2010**, 21, 472-481.
- (33) Jecklin, M.; Touboul, D.; Bovet, C.; Wortmann, A.; Zenobi, R. *J. Am. Soc. Mass Spectrom.* **2008**, 19, 332-343.
- (34) Zdanov, A.; Li, Y.; Bundle, D. R.; Deng, S. J.; MacKenzie, C. R.; Narang, S. A.; Young, N. M.; Cygler, M. *Proc. Natl. Acad. Sci.* **1994**, 91, 6423-6427.
- (35) Rademacher, C.; Shoemaker, G. K.; Kim, H.-S.; Zheng, R. B.; Taha, H.; Liu, C.; Nacario, R. C.; Schriemer, D. C.; Klassen, J. S.; Peters, T.; Lowary, T. L. *J. Am. Chem. Soc.* **2007** 129, 10489-10502.
- (36) Wang, W.; Kitova, E. N.; Klassen, J. S. *Anal. Chem.* **2005**, 77, 3060-3071.
- (37) Sun, J.; Kitova, E. N.; Wang, W.; Klassen, J. S. *Anal. Chem.* **2006**, 78, 3010-3018.
- (38) Daneshfar, R.; Kitova, E. N.; Klassen, J. S. *J. Am. Chem. Soc.* **2004**, 126, 4786-4787.
- (39) Kitova, E. N.; El-Hawiet, A.; Klassen, J. S. *J. Am. Soc. Mass Spectrom.* **2014**, 25(11), 1908-1916.
- (40) Schindler, M.; Assaf, Y.; Sharon, N.; Chipman, D. M. *Biochemistry* **1977**, **16**, 423-431.

- (41) Hunter, E. P.; Lias, S. G. *J. Phys. Chem. Ref. Data* **1998**, 27, 413-656.
- (42) Venter, A.; Sojka, P. E.; Cooks, R. G. *Anal. Chem.* **2006**, 78, 8549-8555.
- (43) Miao, Z.; Wu, S.; Chen, H. *J. Am. Soc. Mass Spectrom.* **2010**, 21, 1730-1736.
- (44) Hopper, J. T. S.; Sokratous, K.; Oldham, N.J. *Anal. Biochem.* **2012**, 421, 788-790.
- (45) Hopper, J. T. S., Oldham, N. J. *Anal. Chem.* **2011**, 83, 7472-7479.

Chapter 3

Screening Oligosaccharide Libraries against Lectins

Using the Proxy Protein ESI-MS assay*

3.1 Introduction

A wide variety of carbohydrate structures, present as glycoproteins or glycolipids, are found on the surfaces of all living cells.¹⁻⁵ Non-covalent interactions between proteins and these cell surface carbohydrates (glycans) mediate many important biological processes, including cell adhesion, signaling and migration, the immune response and bacterial and viral infections.⁶⁻¹¹ Free, water-soluble oligosaccharides, originating from microbial or dietary sources, such as human milk, may also interact with water-soluble and membrane proteins and mediate biological processes.¹²⁻¹⁶ Given their critical roles in a wide range of biochemical and cellular processes, the identification and characterization of protein-glycan interactions is of fundamental importance to the development of a comprehensive understanding of biology. Moreover, a more complete appreciation of these biologically-relevant interactions could serve as the basis for the development of new glycomimetics and other non-carbohydrate drugs for the treatment of a variety of human diseases and conditions.^{17,18}

There are a variety of binding assays, including isothermal titration calorimetry (ITC), frontal affinity chromatography-mass spectrometry (FAC-MS), fluorescence polarization (FP), surface plasmon resonance (SPR) and nuclear magnetic resonance

*A version of this chapter has been submitted: Shams-Ud-Doha, K. (equal contribution), Han, L. (equal contribution), Kitova, E. N., Klassen, J. S., *Anal. Chem.*, (revision requested and resubmitted).

(NMR) spectroscopies that allow for the detection of protein-carbohydrate interactions *in vitro*.¹⁹⁻²⁴ These techniques (and others) can also be used to measure the association constants (K_a) for protein-carbohydrate binding. The enthalpy of association can be quantified directly using ITC and the corresponding kinetic parameters (on and off rate constants) are accessible through time-resolved techniques, such as SPR spectroscopy.^{23,25} There are a number of established methods for screening carbohydrate libraries against proteins and protein complexes, such as SPR, FAC-MS, FP and saturation transfer difference (STD) NMR; each method having particular strengths and weaknesses.²⁶⁻³⁰ Glycan microarrays, which can be applied to not only purified proteins and protein complexes, but also cell extracts, bacteria, viruses and cells, currently represent the dominant technology for glycan screening.³¹⁻³⁷ Glycan microarray screening is rapid, utilizes relatively small amounts of sample (50–100 fmol of individual glycan, $\sim 10 \mu\text{g mL}^{-1}$ of target protein)^{38,39} and can, in some instances, provide a ranking of ligand affinities.^{31,37,40-43} However, microarray binding data are known to exhibit a dependence on the size/nature of the linker and density of glycans printed on the surface.⁴⁴ The technique is also prone to false negatives, particularly in the case of low affinity interactions.^{39,45-47}

Recently, electrospray ionization mass spectrometry (ESI-MS) has emerged as a reliable method for detecting and quantifying protein-carbohydrate interactions *in vitro*.⁴⁸⁻⁵⁰ The direct ESI-MS assay, which is based on the direct detection of free and ligand-bound proteins, allows for determination of the binding stoichiometry and affinity of protein-carbohydrate complexes (as well as other types of non-covalent biomolecular complexes).⁵¹⁻⁵³ With the ability to monitor multiple binding equilibria simultaneously,

ESI-MS is also well suited for screening libraries.⁵⁴⁻⁵⁶ However, because the implementation of the direct ESI-MS assay requires detection of both the free and ligand-bound protein ions, its application is generally restricted to relatively low molecular weight (MW) proteins, typically less than ~150 kDa.⁵⁷ Heterogeneity in protein structure may also hinder the implementation of the assay. Two different ESI-MS strategies have been developed for the detection of protein-carbohydrate interactions in cases where direct ESI-MS detection of the protein and protein-ligand complex(es) is not possible. In the catch-and-release (CaR)-ESI-MS assay, carbohydrate ligands are identified following their release (as ions) from gaseous ions of the corresponding protein-ligand complexes upon collisional activation.⁵⁸⁻⁶⁰ The assay was recently shown to be amenable to screening carbohydrate libraries (containing in excess of 200 components) against proteins and protein complexes with MWs as high as ~1 MDa.^{61,62} While it has been shown that the CaR-ESI-MS assay can be used to rank ligand affinities (based on the relative abundances of the released ligands), it is generally not possible to determine absolute affinities.⁶¹ The *proxy protein* ESI-MS method is an alternative approach that is based on competitive protein binding.⁵⁷ This method employs a *proxy* protein (P_{proxy}), which binds specifically to the ligand of interest with known affinity and is readily detectable by ESI-MS.^{57,61,62} The relative abundance of ligand-bound P_{proxy} , which is measured directly by ESI-MS, reflects the amount of ligand that is bound to the target protein (P_{T}) and the affinity of the ligand for P_{T} can be calculated from the difference in the relative abundances of ligand-bound P_{proxy} measured in the absence and presence of P_{T} .⁵⁷

Although the *proxy protein* ESI-MS method was originally developed for detecting and quantifying binding between a P_T and a single ligand, the assay can, in principle, be extended to libraries of compounds and, thus, serve as a rapid and quantitative screening technique. The goal of the present work was to demonstrate the feasibility of using the *proxy protein* ESI-MS method for carbohydrate library screening. Experimental design considerations are discussed, along with a mathematical framework for data analysis in cases where the assay is implemented using a monovalent P_{proxy} and a monovalent or multivalent (with equivalent and independent binding sites) P_T. To illustrate the implementation of the *proxy protein* ESI-MS assay, small libraries of human milk oligosaccharides (HMOs) and histo-blood group antigen (HBGA) oligosaccharides were screened against an N-terminal fragment of the family 51 carbohydrate-binding module, a fucose-binding lectin from *Ralstonia solanacearum* and the human norovirus (huNoV) VA387 P particle (24-mer of the protruding domain of the capsid protein). Comparison of the data with results of direct ESI-MS binding measurements (interactions and affinities) served to assess the reliability of the assay.

3.2 Experimental

3.2.1 Proteins

The recombinant fragment of the C-terminus (residues 107–250) carbohydrate recognition domain of human galectin-3 (Gal-3C, MW 16,330 Da) was a gift from Prof. C. Cairo (University of Alberta).⁶³ The His-tag anchored N-terminal fragment (residues 65–233) of the family 51 carbohydrate-binding module (CBM, MW 20,735 Da) was a gift from Prof. A. Boraston (University of Victoria).⁶⁴ The fucose-binding bacterial lectin from *Ralstonia solanacearum* (RSL) (trimer, MW 29,329 Da)⁶⁵ was a gift from Prof. A.

Imberty (CERMAV-CNRS). Bovine ubiquitin (MW 8,565 Da), purchased from Sigma-Aldrich Canada (Oakville, Canada), and a single chain fragment (scFv, MW 26,539 Da) of the monoclonal antibody Se155-4, which was produced using recombinant technology,⁶⁶ served as reference proteins (P_{ref}) to correct the mass spectra for the occurrence of nonspecific carbohydrate-protein binding during the ESI process.⁶⁷ The P dimer (MW 69,312 Da) and P particle (24-mer, MW 865,036 Da) of huNoV VA387 were gifts from Prof. M. Tan (Cincinnati Children's Hospital Medical Center). All proteins were dialyzed against an aqueous solution of 200 mM ammonium acetate (pH 6.8) using Amicon 0.5 mL microconcentrator (EMD Millipore, Billerica, MA) with a MW cut-off of 10 kDa and stored at -20 °C until needed. The concentrations of protein stock solutions were estimated by UV absorption (280 nm).

3.2.2 Oligosaccharides

The structures of the twenty oligosaccharides (**L1 – L20**) used in this study are shown in Figure 3.1. Compounds **L1 - L3**, **L5**, **L16** and **L20** were gifts from Prof. T. Lowary (University of Alberta);⁶⁸⁻⁷⁰ **L4**, **L6**, **L12**, **L14**, **L15**, **L18**, **L19** were purchased from Elicityl SA (Crolles, France); **L7-L11**, **L13**, **L17** were purchased from IsoSep (Tullinge, Sweden). Stock solutions of each oligosaccharide were prepared by dissolving a known mass of compound in a known volume of ultra-filtered water (Milli-Q, Millipore, Billerica, MA) to achieve a final concentration of ~1 mM. The stock solutions were stored at -20 °C until needed.

3.2.3 Mass spectrometry

The ESI-MS binding assays were carried out in positive ion mode using three different mass spectrometers equipped with nanoflow ESI (nanoESI) sources. In all cases,

nanoESI was performed by applying a voltage of ~1 kV to a platinum wire inserted into the nanoESI tip, which was produced from a borosilicate glass capillary (1.0 mm o.d., 0.68 mm i.d.) pulled to ~5 μm o.d. using a P-1000 micropipette puller (Sutter Instruments, Novato, CA).

A 9.4T ApexQe Fourier-transform ion cyclotron resonance (FT-ICR) mass spectrometer (Bruker-Daltonics, Billerica, MA) was used to quantify the affinities of **L1-L20** for Gal3C, **L1-L3** for CBM, **L2, L4, L5, L7-L10, L14, L15** and **L17** for RSL and **L8** and **L13** for the P dimer of huNoV VA387. The nanoESI droplets were sampled through a stainless steel capillary (250 – 300 V) heated by N₂ gas at 90 °C. Gaseous ions were transferred into the first funnel (150 V) and skimmer (20 V), transmitted through the second funnel (7.5 V) and skimmer (5.0 V), and then accumulated in the hexapole for 0.5-0.9 s. The ions were then transferred through the quadrupole to the ion cyclotron resonance cell for detection. The pressure in the ICR cell was $\sim 10^{-10}$ mbar. Data acquisition was performed using the Apex Control software (version 4.0, Bruker-Daltonics). The time-domain signal, consisting of the sum of 50 transients containing 128k data points per transient, was subjected to one zero-fill prior to Fourier transformation.

Library screening of RSL was performed on a Synapt G2 quadrupole-ion mobility separation-time of flight (Q-IMS-TOF) mass spectrometer (Waters, Manchester, UK), while library screening of CBM and huNoV P particle VA387 were carried out using a Synapt G2S Q-IMS-TOF mass spectrometer (Waters, Manchester, UK). The source temperature and gas flow rates were 60 °C and 2 mL min⁻¹, respectively, for both instruments. The cone, trap and transfer voltages were 30 V, 5 V and 2 V, respectively,

for both instruments. MassLynx software (version 4.1) was used for data acquisition and processing.

3.2.4 Proxy protein ESI-MS assay

The implementation of the *proxy protein* ESI-MS method for ligand (L) binding to P_T with three equivalent binding sites was described previously.⁵⁷ Below, is a brief overview of the implementation of the method for monovalent P_{proxy} and P_T binding to a single L and a library of ligands (L₁, L₂, ..., L_x).

a. Application to a single ligand

As discussed above and elsewhere, the *proxy protein* ESI-MS method relies on changes in the relative abundance of L-bound P_{proxy} upon addition of P_T to solution.⁵⁷ The relevant association reactions for the competitive binding of a monovalent P_{proxy} and monovalent P_T to L are given by eqs 3.1a and 3.1b, respectively:



The abundance ratio of L-bound to free P_{proxy} ions (*i.e.*, R_{proxy}), as measured by ESI-MS and which is taken to be equal to the concentration ratio (*i.e.*, $[P_{\text{proxy}}L]/[P_{\text{proxy}}]$) eq 3.2, is related to the association constant for the P_{proxy}L interaction (*i.e.*, $K_{\text{a,proxy}}$) by eq 3.3:

$$R_{\text{proxy}} = \frac{[P_{\text{proxy}}L]}{[P_{\text{proxy}}]} \quad (3.2)$$

$$K_{\text{a,proxy}} = \frac{[P_{\text{proxy}}L]}{[P_{\text{proxy}}][L]} = \frac{R_{\text{proxy}}}{[L]} \quad (3.3)$$

The addition of P_T to the solution (and the concomitant formation of P_TL complex, eq 1b) results in a reduction in the concentration of free L in solution and, in turn, a difference in

the apparent R_{proxy} (*i.e.*, ΔR_{proxy}) measured in the absence and presence of P_T (*i.e.*, ΔR_{proxy} = $R_{\text{proxy}} - R_{\text{proxy,PT}}$). The association constant for the $P_T L$ complex (*i.e.*, $K_{a,PT}$), eq 3.4:

$$K_{a,PT} = \frac{[P_T L]}{[P_T][L]} \quad (3.4)$$

can be determined from the magnitude of $R_{\text{proxy,PT}}$ measured at a known concentration of P_T and the relevant equations of mass balance, eqs 3.5a-c:

$$[L]_o = [L] + [P_{\text{proxy}} L] + [P_T L] \quad (3.5a)$$

$$[P_{\text{proxy}}]_o = [P_{\text{proxy}}] + [P_{\text{proxy}} L] \quad (3.5b)$$

$$[P_T]_o = [P_T] + [P_T L] \quad (3.5c)$$

The $[L]$ term can be calculated from eq 3.6a:

$$[L] = \frac{R_{\text{proxy,PT}}}{K_{a,\text{proxy}}} = \frac{R_{\text{proxy}} - \Delta R_{\text{proxy}}}{K_{a,\text{proxy}}} \quad (3.6a)$$

and the $[P_{\text{proxy}} L]$ can be calculated by eq 3.6b:

$$[P_{\text{proxy}} L] = \frac{[P_{\text{proxy}}]_o R_{\text{proxy,PT}}}{R_{\text{proxy,PT}} + 1} \quad (3.6b)$$

Substituting eqs 1.6a and 1.6b into eq 1.5a gives the following expression for $[P_T L]$, eq 3.7:

$$[P_T L] = [L]_o - \frac{[P_{\text{proxy}}]_o R_{\text{proxy,PT}}}{R_{\text{proxy,PT}} + 1} - \frac{R_{\text{proxy,PT}}}{K_{a,\text{proxy}}} \quad (3.7)$$

The $[P_T]$ term is found by combining eqs 3.5c and 3.7 to give eq 3.8:

$$[P_T] = [P_T]_o - [L]_o + \frac{[P_{\text{proxy}}]_o R_{\text{proxy,PT}}}{R_{\text{proxy,PT}} + 1} + \frac{R_{\text{proxy,PT}}}{K_{a,\text{proxy}}} \quad (3.8)$$

It follows that $K_{a,PT}$ can be calculated from eq 3.9a:

$$K_{a,PT} = \frac{\frac{[L]_o K_{a,proxy}}{R_{proxy,PT}} - \frac{[P_{proxy}]_o K_{a,proxy}}{R_{proxy,PT} + 1} - 1}{[P_T]_o - [L]_o + \frac{R_{proxy,PT}}{K_{a,proxy}} + \frac{[P_{proxy}]_o R_{proxy,PT}}{R_{proxy,PT} + 1}} \quad (3.9a)$$

or eq 3.9b, in which $R_{proxy,PT}$ is replaced with ΔR_{proxy} :

$$K_{a,PT} = \frac{\frac{[L]_o K_{a,proxy}}{R_{proxy} - \Delta R_{proxy}} - \frac{[P_{proxy}]_o K_{a,proxy}}{R_{proxy} - \Delta R_{proxy} + 1} - 1}{[P_T]_o - [L]_o + \frac{R_{proxy} - \Delta R_{proxy}}{K_{a,proxy}} + \frac{[P_{proxy}]_o (R_{proxy} - \Delta R_{proxy})}{R_{proxy} - \Delta R_{proxy} + 1}} \quad (3.9b)$$

The magnitude of $K_{a,PT}$ can, in principle, be determined from a single ESI mass spectrum acquired for a solution containing P_{proxy} , P_T and L at known concentrations, provided that ΔR_{proxy} can be precisely measured. In practice, however, it is more reliable to carry out measurements at multiple P_T concentrations.

b. Application to a library of ligands

The relevant association reactions for the interactions of monovalent P_{proxy} and P_T with a library of ligands (L_1, L_2, \dots, L_x) are given by eqs 3.10 and 3.11:



.

.

.





The association constant for a given $P_T L_x$ complex (*i.e.*, $K_{a,P_T,x}$) can be calculated from $R_{\text{proxy},P_T,x}$, the apparent $R_{\text{proxy},x}$ (eqs 3.12a and 3.12b) and mass balance considerations, eqs 3.12c-e:

$$R_{\text{proxy},x} = \frac{[P_{\text{proxy}} L_x]}{[P_{\text{proxy}}]} = \frac{Ab(P_{\text{proxy}} L_x)}{Ab(P_{\text{proxy}})} \text{ when } [P_T] = 0 \quad (3.12a)$$

$$R_{\text{proxy},P_T,x} = \frac{[P_{\text{proxy}} L_x]}{[P_{\text{proxy}}]} = \frac{Ab(P_{\text{proxy}} L_x)}{Ab(P_{\text{proxy}})} \text{ when } [P_T] > 0 \quad (3.12b)$$

$$[L_x]_0 = [L_x] + [P_{\text{proxy}} L_x] + [P_T L_x] \quad (3.12c)$$

$$[P_{\text{proxy}}]_0 = [P_{\text{proxy}}] + \sum_x [P_{\text{proxy}} L_x] \quad (3.12d)$$

$$[P_T]_0 = [P_T] + \sum_x [P_T L_x] \quad (3.12e)$$

A given $[L_x]$ term can be found from $R_{\text{proxy},P_T,x}$ or $\Delta R_{\text{proxy},P_T,x}$ ($\Delta R_{\text{proxy},x} = R_{\text{proxy},x} - R_{\text{proxy},P_T,x}$) and the known association constant for the $P_{\text{proxy}} L_x$ complex (*i.e.*, $K_{a,\text{proxy},x}$), eq 3.13:

$$[L_x] = \frac{R_{\text{proxy},P_T,x}}{K_{a,\text{proxy},x}} = \frac{R_{\text{proxy},x} - \Delta R_{\text{proxy},x}}{K_{a,\text{proxy},x}} \quad (3.13)$$

Rearranging of eqs 12c-e, allows for the $[P_T L_x]$ and $[P_T]$ terms to be calculated from eqs 3.14 and 3.15, respectively:

$$[P_T L_x] = [L_x]_o - \frac{[P_{\text{proxy}}]_o R_{\text{proxy,PT,x}}}{1 + \sum_x R_{\text{proxy,PT,x}}} - \frac{R_{\text{proxy,PT,x}}}{K_{\text{a,proxy,x}}} \quad (3.14)$$

$$[P_T] = [P_T]_o - \sum_x \left([L_x]_o - \frac{[P_{\text{proxy}}]_o R_{\text{proxy,PT,x}}}{1 + \sum_x R_{\text{proxy,PT,x}}} - \frac{R_{\text{proxy,PT,x}}}{K_{\text{a,proxy,x}}} \right) \quad (3.15)$$

It follows that the general expression for $K_{\text{a,PT,x}}$, eq 3.16a:

$$K_{\text{a,PT,x}} = \frac{[P_T L_x]}{[P_T][L_x]} \quad (3.16a)$$

can be rewritten as eq 3.16b:

$$K_{\text{a,PT,x}} = \frac{\left(\frac{[L_x]_o K_{\text{a,proxy,x}}}{R_{\text{proxy,PT,x}}} - \frac{[P_{\text{proxy}}]_o K_{\text{a,proxy,x}}}{1 + \sum_x R_{\text{proxy,PT,x}}} - 1 \right)}{\left([P_T]_o - \sum_x \left([L_x]_o - \frac{[P_{\text{proxy}}]_o R_{\text{proxy,PT,x}}}{1 + \sum_x R_{\text{proxy,PT,x}}} - \frac{R_{\text{proxy,PT,x}}}{K_{\text{a,proxy,x}}} \right) \right)} \quad (3.16b)$$

As in the case of interactions of P_{proxy} and P_T with single L , $R_{\text{proxy,PT,x}}$ can be expressed using $R_{\text{proxy,x}}$ and $\Delta R_{\text{proxy,x}}$ values, eq 3.16c:

$$K_{\text{a,PT,x}} = \frac{\frac{[L_x]_o K_{\text{a,proxy,x}}}{R_{\text{proxy,x}} - \Delta R_{\text{proxy,x}}} - \frac{[P_{\text{proxy}}]_o K_{\text{a,proxy,x}}}{1 + \sum_x (R_{\text{proxy,x}} - \Delta R_{\text{proxy,x}})} - 1}{\left([P_T]_o - \sum_x \left([L_x]_o - \frac{R_{\text{proxy,x}} - \Delta R_{\text{proxy,x}}}{K_{\text{a,proxy,x}}} - \frac{[P_{\text{proxy}}]_o (R_{\text{proxy,x}} - \Delta R_{\text{proxy,x}})}{1 + \sum_x (R_{\text{proxy,x}} - \Delta R_{\text{proxy,x}})} \right) \right)} \quad (3.16c)$$

In order to apply the *proxy* ESI-MS assay, experimental conditions must be such that the addition of P_T leads to measurable changes of $R_{\text{proxy,x}}$. To aid in identifying

optimal conditions for the implementation of the *proxy protein* ESI-MS assay, numerical simulations were carried out (Maple 14, Maplesoft, Waterloo, Canada) to assess the influence of concentration (P_{proxy} , P_{T} and L) and affinity ($K_{\text{a,proxy}}$ and $K_{\text{a,PT}}$) on the magnitude of R_{proxy} and, more importantly, on the resulting change in R_{proxy} upon addition of P_{T} (*i.e.*, $\Delta R_{\text{proxy}} = R_{\text{proxy}} - R_{\text{proxy,PT}}$), for a monovalent P_{T} and P_{proxy} binding competitively to a single L . Shown in Figure 3.6 are plots of R_{proxy} versus $[P_{\text{T}}]_0$, calculated for initial L concentrations of 10 μM , 20 μM and 50 μM , $[P_{\text{T}}]_0$ concentrations ranging from 0 to 100 μM , $K_{\text{a,T}}$ values ranging from 1×10^3 to $1 \times 10^6 \text{ M}^{-1}$, and $K_{\text{a,proxy}}$ values of 10^3 M^{-1} , 10^4 M^{-1} , 10^5 M^{-1} and 10^6 M^{-1} . In all cases, $[P_{\text{proxy}}]_0$ was 5 μM (which is a typical protein concentration used for ESI-MS measurements). The corresponding plots of ΔR_{proxy} versus $[P_{\text{T}}]_0$ are shown in Figure 3.7.

Several conclusions can be drawn from inspection of Figures 3.6 and 3.7. First, $K_{\text{a,proxy}}$ should be $\geq 10^4 \text{ M}^{-1}$ such that the initial value of R_{proxy} (in the absence of P_{T}) is >0.2 at the highest L concentrations that is likely to be used in the ESI-MS library screening measurements (*i.e.*, $\sim 50 \mu\text{M}$ for each library component). The requirement for $R_{\text{proxy}} > 0.2$ is approximate and comes from a consideration of the experimental uncertainty in the R_{proxy} values. Statistical analysis of ESI mass spectra acquired for solutions containing free and ligand-bound protein (data not shown) suggests that the uncertainty in R_{proxy} (and $R_{\text{proxy,PT}}$) values is typically 5-10%, which, by propagation of error, translates to an absolute error of ~ 0.05 - 0.1 in ΔR_{proxy} . Importantly, this analysis is independent of the magnitude of $K_{\text{a,PT}}$. In practice, larger values of R_{proxy} (but less than ~ 10), which can be achieved using a P_{proxy} with a larger $K_{\text{a,proxy}}$ or using higher $[L]_0$, allow for more reliable determinations of ΔR_{proxy} . For $R_{\text{proxy}} > 10$, which corresponds to $>90\%$ of P_{proxy} being L -

bound, the uncertainty increases due to the low abundance of the free P_{proxy} ions. Secondly, it can be seen from Figure 3.7, that the magnitude of ΔR_{proxy} increases with $[P_{\text{T}}]_0$. Consequently, the use of a high $[P_{\text{T}}]_0$ is beneficial when probing low affinity ($K_{\text{a,PT}} < 10^4 \text{ M}^{-1}$) interactions. However, for high affinity interactions ($K_{\text{a,PT}} > 10^5 \text{ M}^{-1}$), ΔR_{proxy} reaches a maximum value, corresponding to the situation where L is predominantly bound to P_{T} , at relatively low $[P_{\text{T}}]_0$. As a result, there is no advantage to using high $[P_{\text{T}}]_0$ for high affinity interactions. Thirdly, measurable ΔR_{proxy} values (> 0.05) can, in principle, be achieved for $K_{\text{a,PT}} > 10^3 \text{ M}^{-1}$ (Figure 3.7). Consequently, the *proxy protein* ESI-MS assay can be used to detect and quantify low affinity P_{T} -L interactions

While the plots shown in Figures 3.6 and 3.7 were calculated for the competitive binding of P_{proxy} and P_{T} to a single L, they also provide guidance on appropriate concentrations of P_{proxy} and library components. An additional consideration when applying the *proxy protein* ESI-MS assay for library screening is the possibility of differences in $K_{\text{a,proxy}}$ for the different library components (*i.e.*, $K_{\text{a,proxy,x}}$). In cases where all components of the library bind to P_{proxy} with similar affinities (within an order of magnitude), equimolar library solutions are ideal since the trend in affinities can be deduced directly from the trend in $\Delta R_{\text{proxy,x}}$ values (normalized for the initial $R_{\text{proxy,x}}$ value). In cases, where the $K_{\text{a,proxy,x}}$ vary substantially, non-equimolar or “tailored” solutions can be used, whereby the concentrations of individual components are adjusted in order to achieve optimal $R_{\text{proxy,x}}$ values.

3.3 Results and Discussion

A series of control experiments were carried out to test the reliability of the *proxy protein* ESI-MS method for carbohydrate library screening. The different P_T's and carbohydrate libraries used are described below.

As a starting point, a simple, three-component oligosaccharide mixture (**L1** – **L3**) was screened against the recombinant family 51 CBM protein. The HBGA oligosaccharide-binding properties of CBM have recently been studied by ESI-MS and it was found that **L2** and **L3** are ligands, while **L1** is a non-binder (Table 3.2).⁶² Next, a 14-component library (**L2**, **L4** – **L15**, **L17**) was screened against RSL, which is a homotrimeric, L-fucose binding lectin produced by bacterium *Ralstonia solanacearum*.⁷¹ X-ray crystallography data show that each monomer of the RSL trimer possesses two fucose binding sites.⁷¹ Based on ITC binding measurements performed on α -Me-fucoside and α -L-Fuc-(1→2)- β -D-Gal-(1→4)- β -D-Glc (**L17**), it was concluded that the two binding sites are equivalent and independent.⁷¹ Binding studies carried out on RSL with a variety of fucose-containing oligosaccharides using SPR spectroscopy revealed affinities ranging from 10^4 – 10^6 M⁻¹.⁷¹ In the present study, the affinities of **L2**, **L4** – **L15**, **L17** (reported as intrinsic (per binding site) affinities) for RSL were measured using the direct ESI-MS assay (Table 3.2) and representative binding data, for RSL interacting with **L7** and with **L17**, are shown in Figure 3.8. RSL does not bind to **L6** and **L11-L13**, which lack α -L-fucose, and these compounds served as negative controls. Finally, a 10-component library (**L1** - **L3**, **L5**, **L8**, **L13**, **L16**, **L18** – **L20**) was screened against the huNoV P particle, which predominantly exists as a 24-mer (with MW of ~865 kDa) in solution.^{72,73} The huNoV P particle was shown to bind type A, type B and type H HBGAs, as well as some

HMO structures, but with low affinity, typically $10^2 - 10^3 \text{ M}^{-1}$.⁶² The affinities of **L1 - L3, L5, L16** and **L18 - L20** for the related P dimer (which is the building block of the P particle) were measured in an earlier study (Table 3.2)^{62,74} and the affinities of **L8** and **L13** for the P dimer were measured in the present study (Figure 3.9 and Table 3.2); oligosaccharide **L16** was reported not to bind.⁶² It was shown previously that the intrinsic affinities of HBGA oligosaccharides for the P particle and P dimer in these two proteins are similar, within a factor of two.⁶²

A C-terminal fragment of human galectin 3 (Gal-3C), which possesses a single carbohydrate binding site, served as P_{proxy} for all of the screening measurements reported in this study. Galectin 3, as well as other galectins, recognizes Gal β 1-3/4GlcNAc disaccharides, namely type 1 and 2 LacNAc,⁷⁵ and these structural motifs are present in many HMOs and HBGA oligosaccharides. Although the oligosaccharide binding properties of galectin 3 have been the subject of multiple studies,⁷⁶ reliable affinity data for galectin 3 (or Gal-3C) are not available for the majority of the oligosaccharides considered in the present study (*i.e.*, **L1-L20**). Therefore, quantitative binding measurements, carried out using the direct ESI-MS assay, were performed on **L1-L20** and Gal-3C; the affinities, which are shown in Table 3.2, range from 10^4 M^{-1} to 10^5 M^{-1} . Representative binding data measured for Gal-3C interacting with **L7** and with **L17** are shown in Figure 3.10.

(a) Screening a three-component library against CBM

Shown in Figure 3.2a is a representative ESI mass spectrum acquired for a 200 mM aqueous ammonium acetate solution (pH 6.8, 25 °C) of Gal-3C (5 μM), P_{ref} (4 μM) and **L1, L2** and **L3** (10 μM each). Protonated ions corresponding to free Gal-3C and the 1:1

complexes of Gal-3C with each of the three oligosaccharides were identified, *i.e.*, P_{proxy}^{q+} and $(P_{\text{proxy}} + L_x)^{q+}$, where $x = 1, 2, 3$ and $q = 8, 9$. Due to the relatively low concentration of individual oligosaccharides, as well as their relatively high affinities for Gal-3C, the occurrence of nonspecific binding was expected to be low. This was confirmed by the absence of detectable signal corresponding to Gal-3C bound to two or more oligosaccharides and the very low abundances of the corresponding $(P_{\text{ref}} + L_x)^{q+}$ ions (Figure 3.2a). Similar results were obtained for all measurements performed using this library and, consequently, no correction for nonspecific binding was made to the $R_{\text{proxy},x}$ values. Shown in Figure 3.2b is a representative ESI mass spectrum acquired for a solution identical to the one describe above, but with the addition of 23 μM CBM. From a visual comparison of the two mass spectra, it can be seen that the addition of CBM resulted in decrease in the relative abundances of the ions corresponding to Gal-3C bound to **L2** and **L3**. In contrast, no significant change in the relative abundance of **L1**-bound Gal-3C was evident. Based on these observations alone, it can be concluded that **L2** and **L3** are ligands for CBM and **L1** is a non-binder. Measurements were performed at six other CBM concentrations (4, 8, 9, 12, 15 and 18 μM). Plotted in Figure 3.2c are the abundance ratios of **L1**-, **L2**- and **L3**-bound Gal-3C to free Gal-3C, *i.e.*, $R_{\text{proxy},1}$, $R_{\text{proxy},2}$ and $R_{\text{proxy},3}$, respectively, versus CBM concentration. Inspection of the plots reveal that, at concentrations $\geq 8 \mu\text{M}$, the addition of CBM produced measurable changes in $R_{\text{proxy},2}$ and $R_{\text{proxy},3}$. For example, at the highest CBM concentration (23 μM), the $\Delta R_{\text{proxy},2}$ and $\Delta R_{\text{proxy},3}$ values are 0.44 ± 0.03 and 0.62 ± 0.04 , respectively. These values translate to affinities of $(6.0 \pm 0.4) \times 10^4 \text{ M}^{-1}$ (**L2**) and $(5.1 \pm 0.4) \times 10^4 \text{ M}^{-1}$ (**L3**), respectively. These values are similar in magnitude to the average affinities determined from the affinities

calculated at each of the CBM concentrations ($\geq 8 \mu\text{M}$) investigated - $(5.8 \pm 1.6) \times 10^4 \text{ M}^{-1}$ (**L2**) and $(5.1 \pm 1.2) \times 10^4 \text{ M}^{-1}$ (**L3**). Moreover, these values are in good agreement with reported affinities, $(5.6 \pm 0.3) \times 10^4 \text{ M}^{-1}$ and $(7.0 \pm 0.3) \times 10^4 \text{ M}^{-1}$, respectively (Figure 3.2d).⁶² In contrast to what was observed for $R_{\text{proxy},2}$ and $R_{\text{proxy},3}$, $R_{\text{proxy},1}$ showed no significant dependence on CBM concentration (slope of -0.0014 ± 0.0010 for a linear curve fit to the data). The absence of a detectable interaction between **L1** and CBM is consistent with results of a previous binding study.⁶²

(b) Screening a fourteen-component library against RSL.

The *proxy protein* method was then used to screen a 14-component library (**L2**, **L4** – **L15**, **L17**) against RSL. Shown in Figure 3.3a is a representative ESI mass spectrum acquired for a 200 mM aqueous ammonium acetate solution (pH 6.8, 25 °C) of Gal-3C (8 μM), P_{ref} (3 μM) and the 14-component library (24 μM each). Signal corresponding to free Gal-3C and the corresponding 1:1 complexes with each of the fourteen oligosaccharides was detected (Figure 3.3a). Shown in Figure 3.3b is a mass spectrum acquired for the same solution as described above but with the addition of RSL at a concentration of 11 μM . From a comparison of the mass spectra shown in Figures 3.3a and 3.3b, it can be seen that the addition of RSL resulted in a decrease in the relative abundances of the complexes of Gal-3C with seven of the oligosaccharides (**L2**, **L5**, **L7** – **L10** and **L17**). Plotted in Figure 3.3c are the $R_{\text{proxy},x}$ values determined at RSL concentrations of 0 μM , 3 μM , 6 μM , 8 μM , 9 μM , and 11 μM . It can be seen that measurable changes in $R_{\text{proxy},x}$ are observed for the seven oligosaccharides at RSL concentrations $\geq 6 \mu\text{M}$. For example, at an RSL concentration of 11 μM , the corresponding $\Delta R_{\text{proxy},x}$ values are: 0.79 ± 0.09 ($\Delta R_{\text{proxy},2}$), 1.63 ± 0.1 ($\Delta R_{\text{proxy},5}$), $1.38 \pm$

0.10 ($\Delta R_{\text{proxy},7}$), 0.38 ± 0.06 ($\Delta R_{\text{proxy},8}$), 0.13 ± 0.03 ($\Delta R_{\text{proxy},9}$), 0.11 ± 0.04 ($\Delta R_{\text{prox},10}$), 0.44 ± 0.01 ($\Delta R_{\text{proxy},17}$). In contrast, the $R_{\text{proxy},x}$ values of **L4**, **L6** and **L11 – L15** showed no significant dependence on RSL concentration: 0.1 ± 0.1 ($\Delta R_{\text{proxy},4}$), 0.09 ± 0.11 ($\Delta R_{\text{proxy},6}$), 0.04 ± 0.03 ($\Delta R_{\text{proxy},11}$), 0.03 ± 0.02 ($\Delta R_{\text{proxy},12}$), 0.04 ± 0.03 ($\Delta R_{\text{proxy},13}$), 0.07 ± 0.06 ($\Delta R_{\text{proxy},14}$), -0.03 ± 0.06 ($\Delta R_{\text{proxy},15}$). Based on these results, it is concluded that **L2**, **L5**, **L7 – L10** and **L17** are ligands of RSL, while **L4**, **L6** and **L11 – L15** are non-binders. However, based on the results of direct ESI-MS measurements, only **L6** and **L11-L13** are non-binders; **L4**, **L14** and **L15** exhibit affinities of $(1.0 \pm 0.1) \times 10^4 \text{ M}^{-1}$, $(3.5 \pm 0.1) \times 10^4 \text{ M}^{-1}$, $(1.0 \pm 0.1) \times 10^4 \text{ M}^{-1}$, respectively, for RSL (Table 3.3). Shown in Figure 3.3d are the average affinities determined for **L2**, **L5**, **L7 – L10** and **L17**. Notably, the values agree, within a factor of three, with the intrinsic affinities measured for RSL (Figure 3.3d).

These false negative results obtained for **L4**, **L14** and **L15** can be explained by the fact that, under the concentrations used for the screening measurements, most of the RSL binding sites are occupied by the highest affinity ligands. Consequently, the interactions involving the lower affinity ligands are at low concentration and, therefore, difficult to reliably detect. For example, for the 11 μM RSL solution it is predicted from numerical modeling that **L4**, **L14** and **L15** occupy less than 6% of the RSL binding sites. To further support this explanation for the false negatives, the screening measurements were repeated in the absence of the highest affinity RSL ligands (**L2**, **L5**, **L7**, **L8** and **L17**). Shown in Figures 3.4a and 3.4b are representative ESI mass spectra acquired for 200 mM aqueous ammonium acetate solutions (pH 6.8, 25 °C) of Gal-3C (8 μM), P_{ref} (2.5 μM) and the 9-component library (**L4**, **L6**, and **L9–L15**, 24 μM each) in the absence

and presence of RSL (11 μM), respectively. Comparison of the two mass spectra reveals that the relative abundances of the complexes corresponding to Gal-3C bound to **L4**, **L14** and **L15**, as well as **L9**, **L10**, exhibit a noticeable decrease upon addition of RSL to solution. These results indicate that these six oligosaccharides are ligands for RSL. Consistent with the results described above, no significant change in relative abundances was observed for **L6**, **L11** – **L13**. The influence of RSL concentration on relative abundance of bound Gal-3C is more clearly seen in Figure 3.4c, where the $R_{\text{proxy},x}$ values are plotted versus the concentration of RSL. The average intrinsic affinities determined for **L4**, **L9**, **L10**, **L14** and **L15** are shown in Figure 3.4d, along with the intrinsic affinities measured for RSL. In all cases the values agree, within a factor two.

(c) Screening a ten-component non-equimolar library against huNoV P particle.

As a final and very challenging (due to the low oligosaccharide affinities) test of the *proxy protein* ESI-MS method, the assay was used to screen a 10-component library (**L1**–**L3**, **L5**, **L8**, **L13**, **L16** and **L18** – **L20**) against the hNoV P particle. Given the high MW of the P particle, ~ 865 kDa, the direct detection of oligosaccharide-bound P particle complexes by ESI-MS was not possible with the available instrumentation.⁶⁰ Because the affinities of **L1**, **L8**, **L13** and **L16** for Gal-3C are significantly lower than those of the other six oligosaccharides (Table 3.2), the concentrations of the library components were tailored (40 μM for **L1**, **L8**, **L13** and **L16**, and 10 μM for **L2**, **L3**, **L5** and **L18**–**L20**). Shown in Figures 3.5a and 3.5b are representative ESI mass spectra acquired for a 200 mM aqueous ammonium acetate solution (pH 6.8, 25 $^{\circ}\text{C}$) of Gal-3C (5 μM), P_{ref} (3 μM) and the 10-component library in the absence and presence (7.8 μM) of P particle, respectively. In both ESI mass spectra, ion signal corresponding to the protonated P_{proxy}^{q+}

and $(P_{\text{proxy}} + L_x)^{q+}$ ions, where $x = 1-3,5,8,13,16$ and $18-20$ and $q = 7 - 9$, was detected. Abundant signal corresponding to $(P_{\text{ref}} + L_x)^{q+}$ ions, where $x = 1-3,5,8,13,16$ and $18-20$ and $q = 5$ and 6 , indicated a significant contribution from non-specific binding to the mass spectrum. Following correction for non-specific binding,⁶⁷ the changes in relative abundances of the Gal-3C complexes of eight of the oligosaccharides (**L1-L3**, **L5**, **L8**, **L18 – L20**) were indicative of binding. Analogous measurements were carried out at P particle concentrations of $1.2 \mu\text{M}$, $2.4 \mu\text{M}$, $4.8 \mu\text{M}$ and $6.2 \mu\text{M}$. The corresponding plots of $R_{\text{proxy},x}$ values versus P particle concentration are shown in Figure 3.5c. It can be seen that, while the initial $R_{\text{proxy},x}$ values ($0.5 - 3.2$) are well suited to the implementation of the *proxy protein* method, the changes in $R_{\text{proxy},x}$ upon addition of $7.8 \mu\text{M}$ P particle (the highest concentration tested) ranged from only 3% to 17% (due to the low affinities). The concentration of the P particle stock solution precluded the use of higher concentrations. Despite the small $\Delta R_{\text{proxy},x}$ values, the average affinities determined for **L1-L3**, **L5**, **L8**, **L18 – L20** are found to agree within a factor of three with the affinities measured using direct ESI-MS assay for the corresponding hNoV P dimer (Figure 3.5d).⁷⁴ Moreover, the absence of detectable binding for **L13** and **L16** to the P particle is consistent with the results of the binding measurements performed on the P dimer (Table 3.2).⁶²

3.4 Conclusions

The use of the *proxy protein* ESI-MS method for the rapid and quantitative screening of carbohydrate libraries against lectins is described. Specific interactions between components of the carbohydrate library and a P_T are identified from changes in the relative abundances of the carbohydrate complexes of P_{proxy} , which binds to all components of the library with known affinity, upon introduction of P_T to the solution.

The affinity of an identified interaction can be calculated from the magnitude of the change in relative abundance of a given P_{proxy} -ligand complex. A mathematical framework for the implementation of the method in the case of monovalent P_{proxy} and monovalent and multivalent (multiple equivalent and independent binding sites) P_T , as well as general experimental design considerations are given. Application of the method to screen small libraries of oligosaccharides against three lectins (CBM, RSL and hNoV P particle, serve to demonstrate the reliability and versatility of the assay for the simultaneous detection and quantification of both low and high affinity interactions. Finally, it should be noted that, although relatively small libraries were used in the present study, implementation of the assay using higher resolution MS instruments is expected to allow for the use of multiple P_{proxy} . This, in turn, will allow for libraries containing a larger number of components to be screened.

Figure captions

Figure 3.1. Structures of the oligosaccharides **L1** – **L20**. Monosaccharide key: Glucose (●), galactose (◐), N-acetylgalactosamine (◑), N-acetylglucosamine (■), sialic acid(◆), fucose (▲).

Figure 3.2. ESI mass spectra acquired in positive ion mode for 200 mM aqueous ammonium acetate solutions (pH 6.8 and 25 °C) containing Gal-3C (5 μM), P_{ref} (4 μM), and a three-component library (**L1**, **L2** and **L3**, 10 μM each) with (a) 0 μM and (b) 23 μM CBM. (c) Plots of the abundance ratios of **L1**- (■), **L2**- (●) and **L3**-bound Gal-3C (▲) to free Gal-3C (*i.e.*, $R_{\text{proxy},x}$) versus CBM concentration (0 – 23 μM) measured under the same solution conditions as described for (a). Solid curves correspond to the apparent $R_{\text{proxy},x}$ calculated from the average affinity (K_a , Table 3.2). (d) Comparison of the affinities **L1** – **L3** for CBM measured using the *proxy protein* method (■) with those measured using *direct* ESI-MS assay (▨). Errors correspond to one standard deviation.

Figure 3.3. ESI mass spectra acquired in positive ion mode for 200 mM aqueous ammonium acetate solutions (pH 6.8 and 25 °C) containing Gal-3C (8 μM), P_{ref} (3 μM), and a fourteen-component library (**L2**, **L4** – **L15**, **L17**, 24 μM each) with (a) 0 μM and (b) 11 μM RSL. (c) Plots of the abundance ratios of **L17**- (■), **L12**- (◆), **L11**- (●), **L14**- (◆), **L2**- (■), **L5**- (▲), **L7**- (●), **L4**- (●), **L9**- (●), **L15**- (●), **L10**- (■), **L13**- (◆), **L8**- (◆) and **L6**-bound Gal-3C (■) to free Gal-3C (*i.e.*, $R_{\text{proxy},x}$) versus RSL trimer concentration (0 – 11 μM) measured under the same solution conditions as described for (a). Solid curves correspond to the apparent $R_{\text{proxy},x}$ calculated from the average affinity (K_a , Table 3.2). (d) Comparison of intrinsic affinities of **L2**, **L4** – **L15**, **L17** for RSL measured using

the *proxy protein* method (■) with those measured using *direct* ESI-MS assay (▨). Errors correspond to one standard deviation.

Figure 3.4. ESI mass spectra acquired in positive ion mode for 200 mM aqueous ammonium acetate solutions (pH 6.8 and 25 °C) containing Gal-3C (8 μM), P_{ref} (2 μM), and a fourteen-component library (L6 - L15, 24 μM each) with (a) 0 μM and (b) 11 μM RSL. (c) Plots of the abundance ratios of L4- (■), L6- (◆), L9- (●), L10- (▲), L11- (●), L12- (x), L13- (■), L14- (▲) and L15-bound Gal-3C (●) to free Gal-3C (i.e., $R_{\text{proxy},x}$) versus RSL concentration measured under the same solution conditions as described for (a). Solid curves correspond to the apparent $R_{\text{proxy},x}$ calculated from the average affinity (K_a , Table 3.2). (d) Comparison of intrinsic affinities of L6 - L15 for RSL measured using the *proxy protein* method (■) with those measured using *direct* ESI-MS assay (▨). Errors correspond to one standard deviation.

Figure 3.5. ESI mass spectra acquired in positive ion mode for 200 mM aqueous ammonium acetate solutions (pH 6.8 and 25 °C) containing Gal-3C (5 μM), P_{ref} (4 μM) and a ten-component library (L1, L8, L13 and L16, 40 μM each; L2, L3, L5 and L18–L20, 10 μM each each) with (a) 0 μM and (b) 7.8 μM P particle. (c) Plots of the abundance ratios of L1- (■), L2- (■), L3- (◆), L5- (●), L8- (x), L13- (▲), L16- (●), L18- (x) and L19- (■) and L20-bound Gal-3C (▲) to free Gal-3C ($R_{\text{proxy},x}$) versus P particle concentration measured under the same solution conditions as described for (a). Solid curves correspond to the apparent $R_{\text{proxy},x}$ calculated from the average affinity (K_a , Table 3.2). (d) Comparison of intrinsic affinities of L1-L3, L5, L8, L13, L16, L18–L20 for P particle measured using the *proxy protein* method (■) with those measured using *direct* ESI-MS assay for P dimer (▨). Errors correspond to one standard deviation.

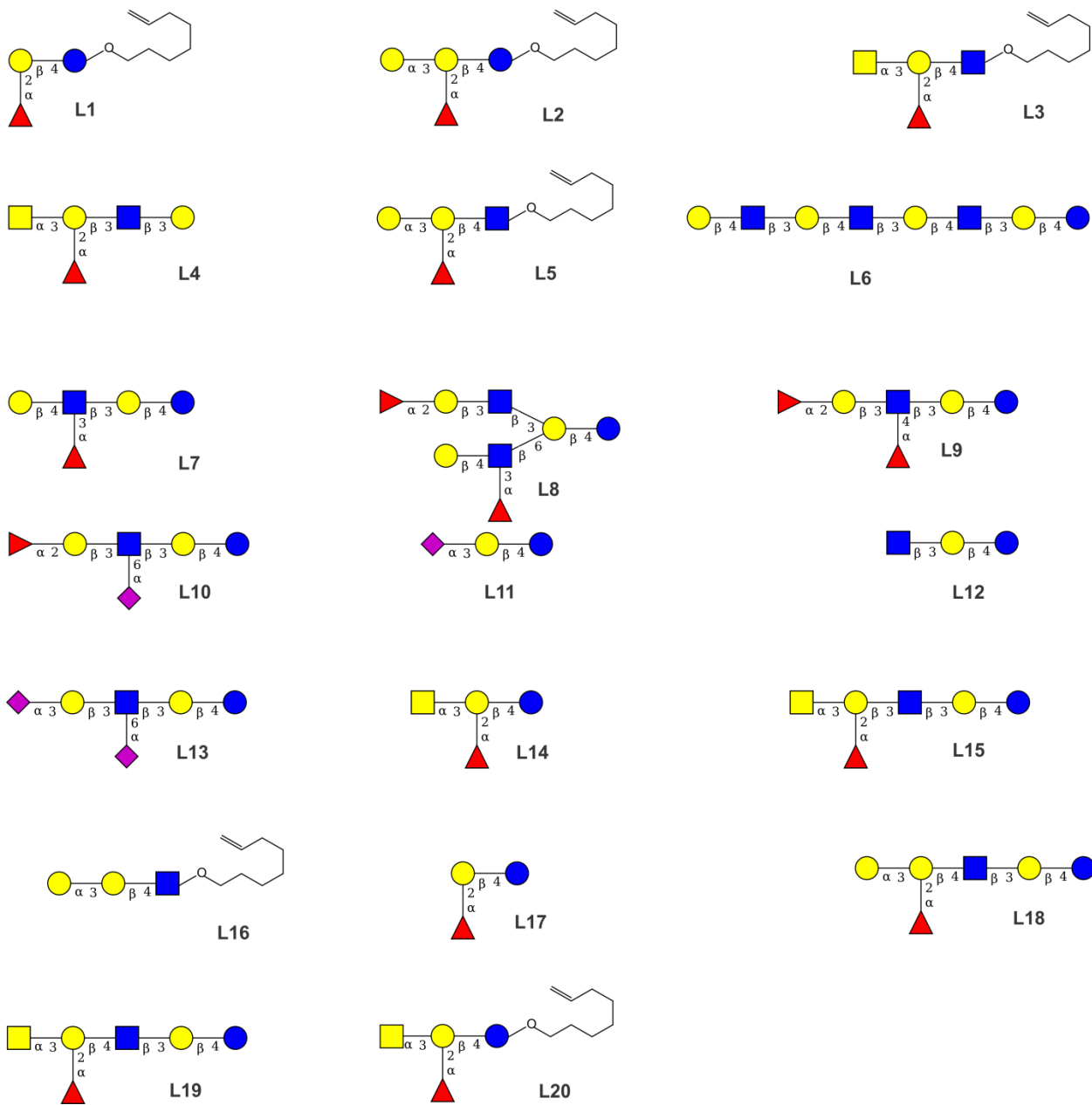


Figure 3.1.

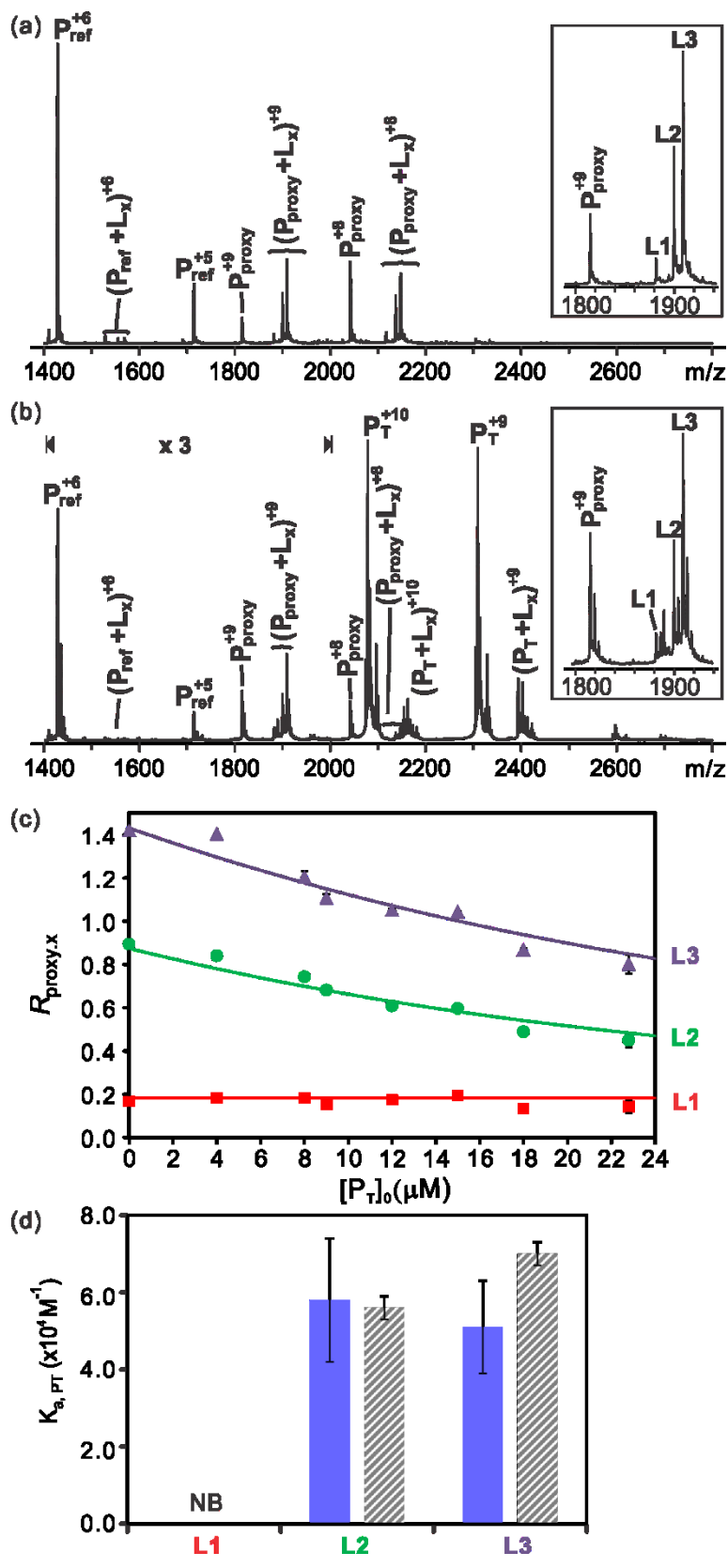


Figure 3.2.

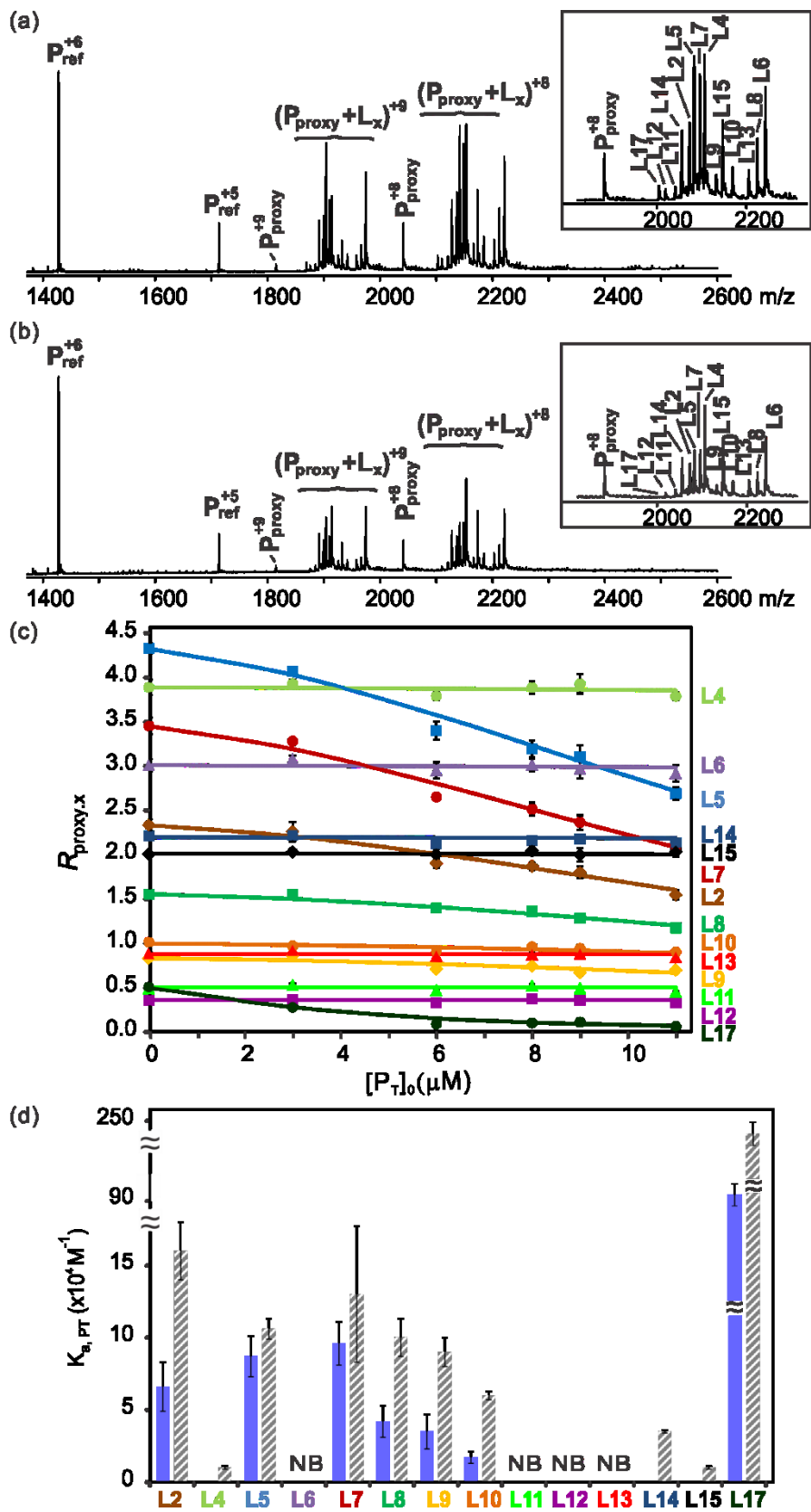


Figure 3.3.

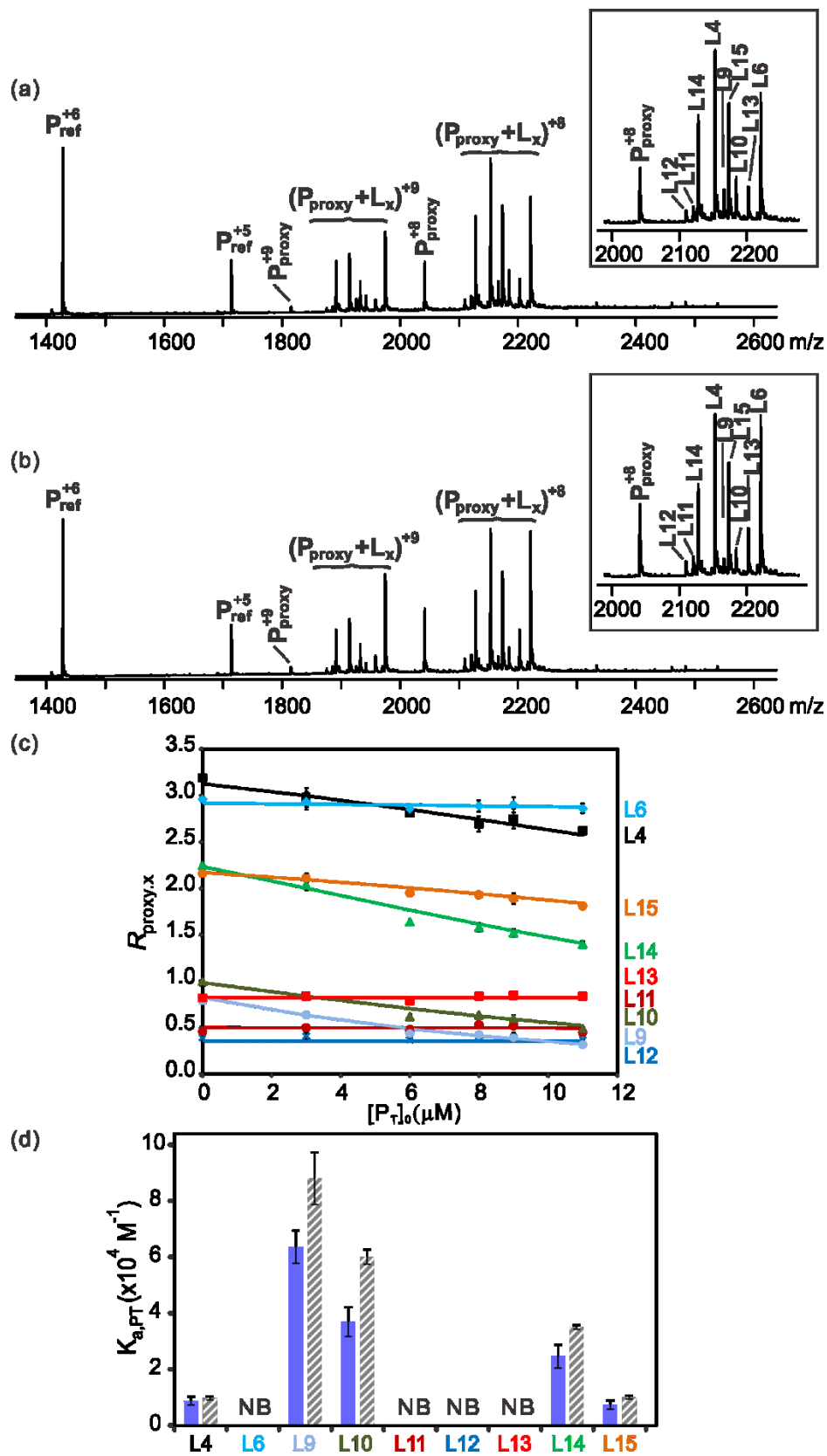


Figure 3.4.

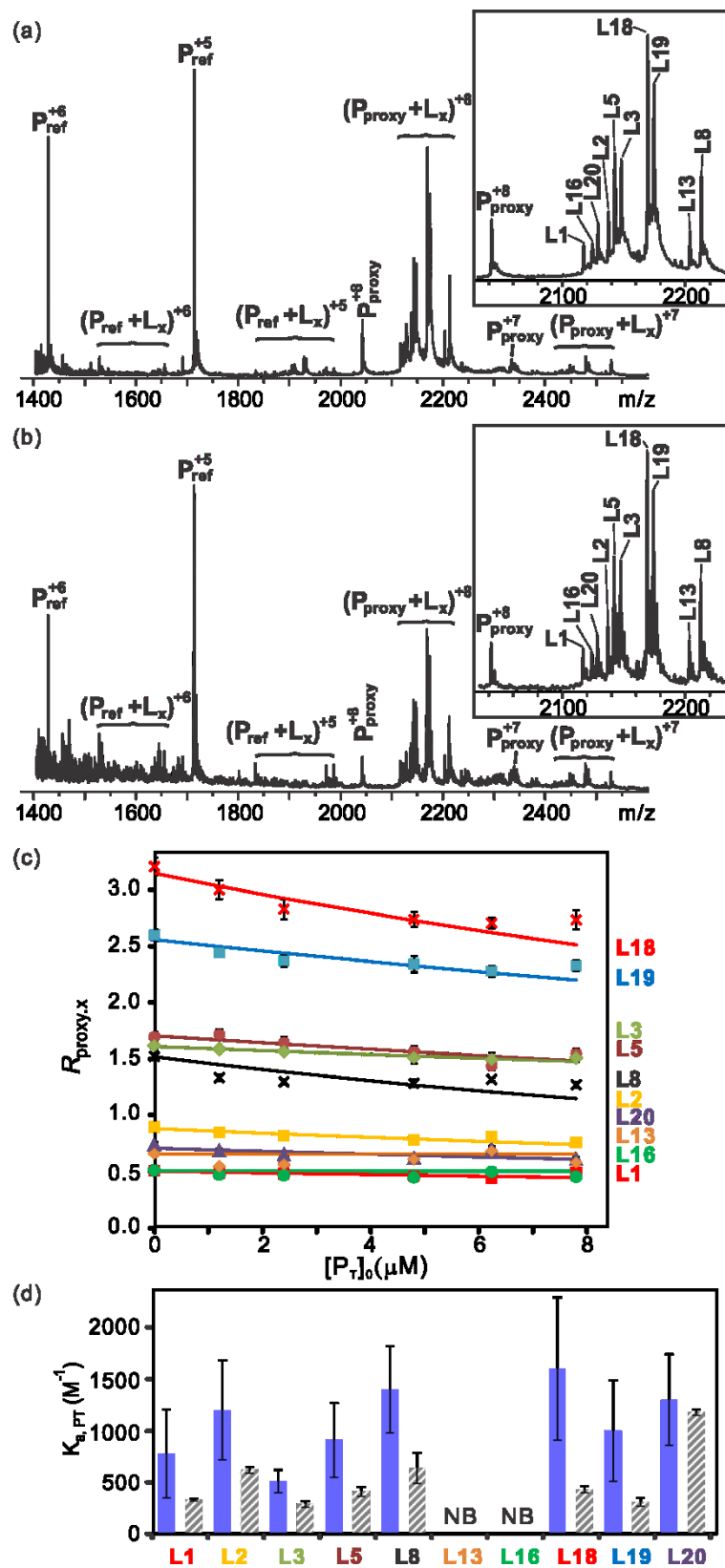


Figure 3.5.

Table 3.1. Structures of oligosaccharides used in this study (**L1 – L20**).

Oligosaccharide	Structure
L1	α -L-Fuc-(1→2)- β -D-Gal-(1→4)- β -D-Glc-O(CH ₂) ₆ CH=CH ₂
L2	α -D-Gal-(1→3)-[α -L-Fuc-(1→2)]- β -D-Gal-(1→4)- β -D-Glc-O(CH ₂) ₆ CH=CH ₂
L3	α -D-GalNAc-(1→3)-[α -L-Fuc(1→2)]- β -D-Gal-(1→4)- β -D-GlcNAc-O(CH ₂) ₆ CH=CH ₂
L4	α -D-GalNAc-(1→3)-[α -L-Fuc-(1→2)]- β -D-Gal-(1→3)- β -D-GlcNAc-(1→3)- β -D-Gal
L5	α -D-Gal-(1→3)-[α -L-Fuc-(1→2)]- β -D-Gal-(1→4)- β -D-GlcNAc-O(CH ₂) ₆ CH=CH ₂
L6	β -D-Gal-(1→4)- β -D-GlcNAc-(1→3)- β -D-Gal-(1→4)- β -D-GlcNAc-(1→3)- β -D-Gal-(1→4)- β -D-Glc
L7	β -D-Gal-(1→4)-[α -L-Fuc-(1→3)]- β -D-GlcNAc-(1→3)- β -D-Gal-(1→4)- β -D-Glc
L8	β -D-Gal-(1→4)-[α -L-Fuc-(1→3)]- β -D-GlcNAc-(1→6)-[α -L-Fuc-(1→2)- β -D-Gal-(1→3)- β -D-GlcNAc-(1→3)]- β -D-Gal-(1→4)- β -D-Glc
L9	α -L-Fuc-(1→2)- β -D-Gal-(1→3)-[α -L-Fuc-(1→4)]- β -D-GlcNAc-(1→3)- β -D-Gal(1→4)- β -D-Glc

- L10** α -L-Fuc-(1→2)-β-D-Gal-(1→3)-[α-D-Neu5Ac-(2→6)]-β-D-GlcNAc-(1→3)-β-D-Gal-(1→4)-β-D-Glc
- L11** α -D-Neu5Ac-(2→3)-β-D-Gal(1→4)-β-D-Glc
- L12** β-D-GlcNAc(1→3)-β-D-Gal(1→4)-β-D-Glc
- L13** α -D-Neu5Ac-(2→3)-β-D-Gal-(1→3)-[α-D-Neu5Ac-(2→6)]-β-D-GlcNAc-(1→3)-β-D-Gal-(1→4)-β-D-Glc
- L14** α -D-GalNAc-(1→3)-[α-L-Fuc-(1→2)]-β-D-Gal-(1→4)-β-D-Glc
- L15** α -D-GalNAc-(1→3)-[α-L-Fuc-(1→2)]-β-D-Gal-(1→3)-β-D-GlcNAc-(1→3)-β-D-Gal-(1→4)-β-D-Glc
- L16** α -D-Gal-(1→3)-β-D-Gal-(1→4)-β-D-GlcNAc-O(CH₂)₆CH=CH₂
- L17** α -L-Fuc-(1→2)-β-D-Gal-(1→4)-β-D-Glc
- L18** α -D-Gal-(1→3)-[α-L-Fuc(1→2)]-β-D-Gal-(1→4)-β-D-GlcNAc-(1→3)-β-D-Gal-(1→4)-β-D-Glc
- L19** α -D-GalNAc-(1→3)-[α-L-Fuc(1→2)]-β-D-Gal-(1→4)-β-D-GlcNAc-(1→3)-β-D-Gal-(1→4)-β-D-Glc
- L20** α -D-GalNAc-(1→3)-[α-L-Fuc-(1→2)]-β-D-Gal-(1→4)-D-Glc
-

Table 3.2. Association constants, K_a (units of 10^4 M^{-1}) for binding of HBGA and HMO oligosaccharides ($L_x = L1 - L20$) to Gal-3C, RSL, huNoV P dimer and CBM measured at 25 °C and pH 6.8 by the direct ESI-MS assay.^a

L_x	Gal-3C	RSL ^b	P dimer ^b	CBM
L1	1.4 ± 0.1^c	n.d. ^e	0.033 ± 0.003^c	$< 0.02^c$
L2	10.2 ± 0.4^c	16.0 ± 2.4	0.060 ± 0.005^c	5.6 ± 0.3^c
L3	17.4 ± 1.4^c	n.d. ^e	0.029 ± 0.003^c	7.0 ± 0.3^c
L4	14.1 ± 0.3	1.0 ± 0.1	n.d. ^e	n.d. ^e
L5	22.3 ± 1.7^c	10.6 ± 0.7	0.041 ± 0.005^c	n.d. ^e
L6	13.0 ± 1.0	NB ^f	n.d. ^e	n.d. ^e
L7	12.0 ± 0.8	13.0 ± 4.7	n.d. ^e	n.d. ^e
L8	5.8 ± 0.1	10.0 ± 1.3	0.064 ± 0.015	n.d. ^e
L9	4.2 ± 0.1	9.0 ± 1.0	n.d. ^e	n.d. ^e
L10	4.0 ± 0.1	6.0 ± 0.3	n.d. ^e	n.d. ^e
L11	2.0 ± 0.1	NB ^f	n.d. ^e	n.d. ^e
L12	1.5 ± 0.1	NB ^f	n.d. ^e	n.d. ^e
L13	3.3 ± 0.2	NB ^f	NB ^f	n.d. ^e
L14	8.4 ± 0.2	3.5 ± 0.1	n.d. ^e	n.d. ^e
L15	9.0 ± 0.6	1.0 ± 0.1	n.d. ^e	n.d. ^e
L16	1.20 ± 0.04^c	n.d. ^e	NB ^{c,f}	n.d. ^e
L17	2.1 ± 0.2	240 ± 30	n.d. ^e	n.d. ^e
L18	36.4 ± 1.6	n.d. ^e	0.043 ± 0.003^d	n.d. ^e

L19	26.0 ± 1.5	n.d. ^e	0.031 ± 0.004^d	n.d. ^e
L20	6.4 ± 0.6	n.d. ^e	0.120 ± 0.008^d	n.d. ^e

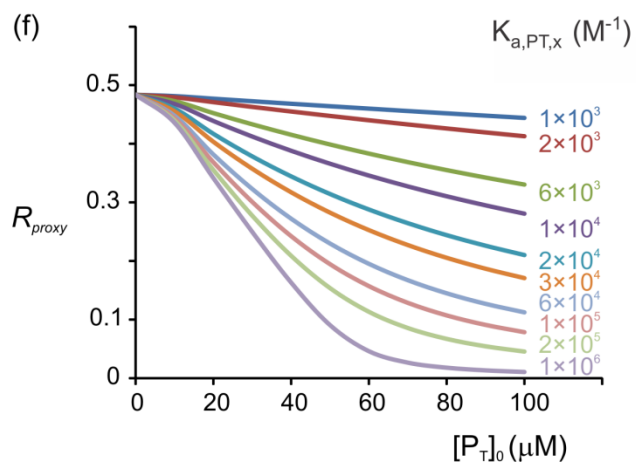
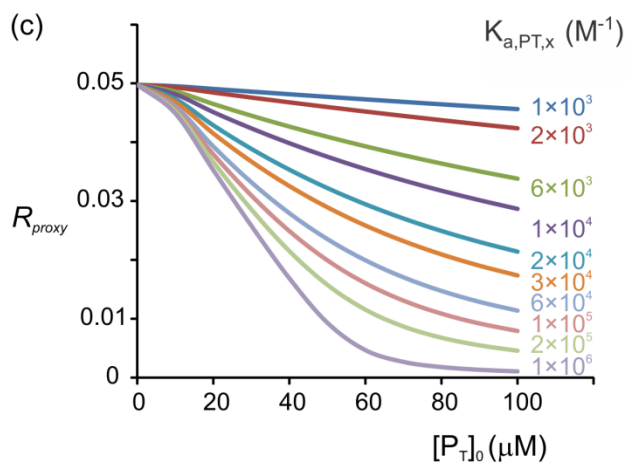
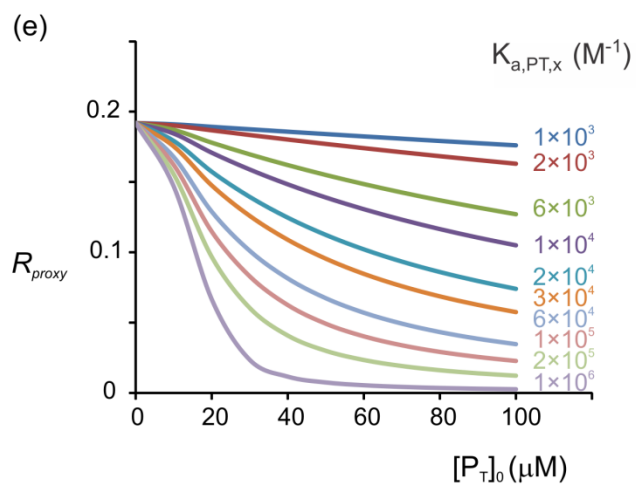
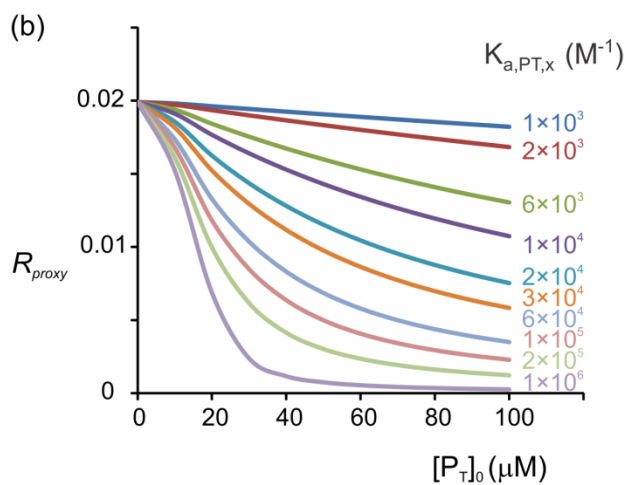
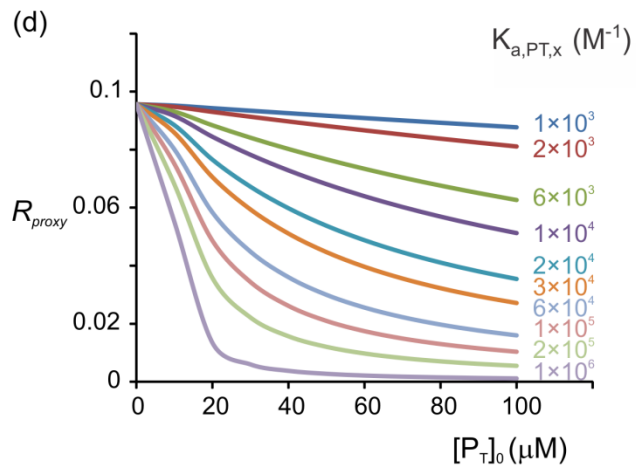
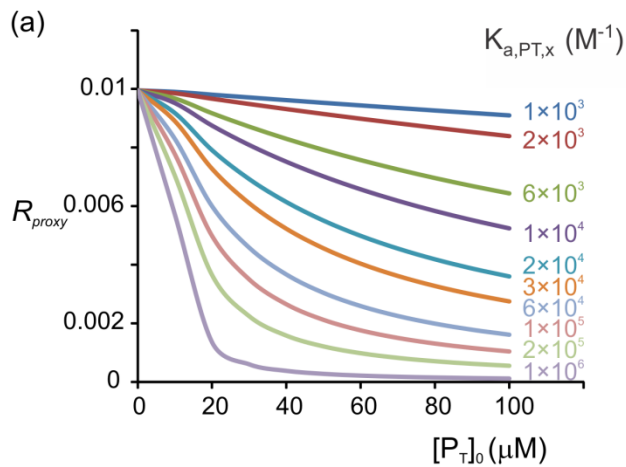
a. Uncertainties correspond to one standard deviation. b. K_a values for RSL (six binding sites) and huNoV P dimer (two binding sites) correspond to intrinsic (per binding site) association constants. c. Values are adapted from Han et al. 2015. d. Values calculated from apparent K_a in reference Han et al. 2013. e. n.d. \equiv not determined. f. NB \equiv no binding detected.

Table 3.3. Intrinsic association constants (units of 10^4 M^{-1}) for binding to RSL and the P particle measured at 25 °C and pH 6.8 by the *proxy protein* ESI-MS assay.^a

L_x	RSL^c	RSL^d	huNoV P particle^e
L1	n.d. ^f	n.d. ^f	0.078 ± 0.043
L2	6.6 ± 1.7	n.d. ^f	0.120 ± 0.048
L3	n.d. ^f	n.d. ^f	0.051 ± 0.011
L4	NB ^b	0.9 ± 0.2	n.d. ^f
L5	8.7 ± 1.4	n.d. ^f	0.091 ± 0.036
L6	NB ^b	NB ^b	n.d. ^f
L7	9.6 ± 1.5	n.d. ^f	n.d. ^f
L8	4.2 ± 1.1	n.d. ^f	0.140 ± 0.042
L9	3.5 ± 1.2	6.4 ± 0.6	n.d. ^f
L10	1.7 ± 0.4	3.7 ± 0.5	n.d. ^f
L11	NB ^b	NB ^b	n.d. ^f
L12	NB ^b	NB ^b	n.d. ^f
L13	NB ^b	NB ^b	NB ^b
L14	NB ^b	2.5 ± 0.4	n.d. ^f
L15	NB ^b	0.7 ± 0.2	n.d. ^f
L16	n.d. ^f	n.d. ^f	NB ^b
L17	92 ± 26	n.d. ^f	n.d. ^f
L18	n.d. ^f	n.d. ^f	0.160 ± 0.069
L19	n.d. ^f	n.d. ^f	0.100 ± 0.049

L20	n.d. ^f	n.d. ^f	0.130 ± 0.044
------------	-------------------	-------------------	-------------------

a. Uncertainties correspond to one standard deviation. b. NB \equiv no binding detected. c. Average of values measured at 8 μ M, 9 μ M and 11 μ M RSL for the 14-component library. d. Average of values measured at 3 μ M, 8 μ M, 9 μ M and 11 μ M RSL for the 9-component library. e. Average of values measured at 2.4 μ M, 4.8 μ M, 6.2 μ M and 7.8 μ M P particle for the 10-component library. f. n.d. \equiv not determined.



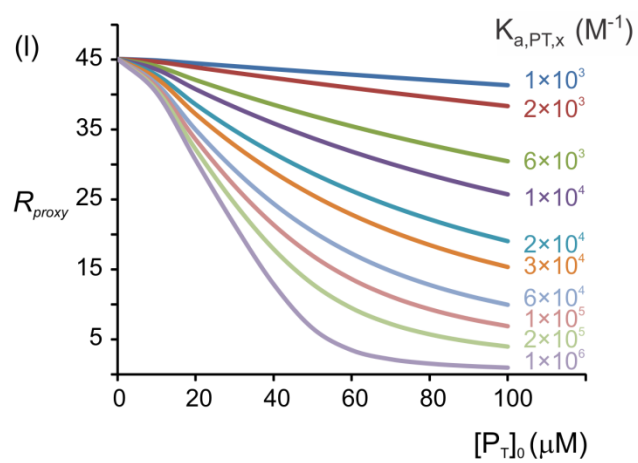
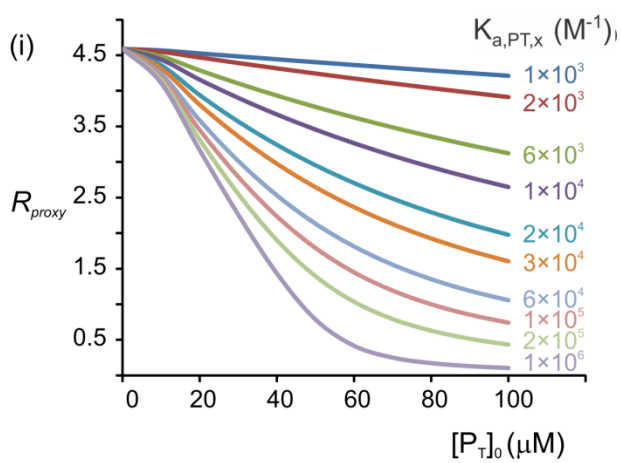
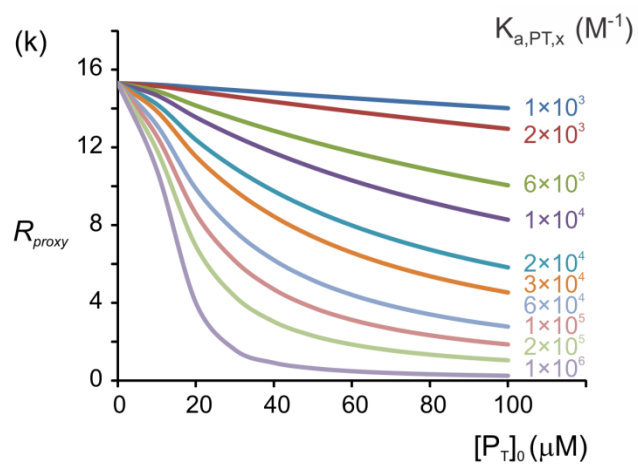
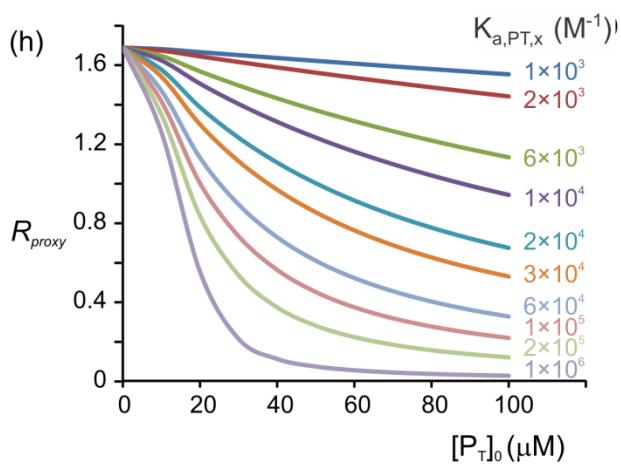
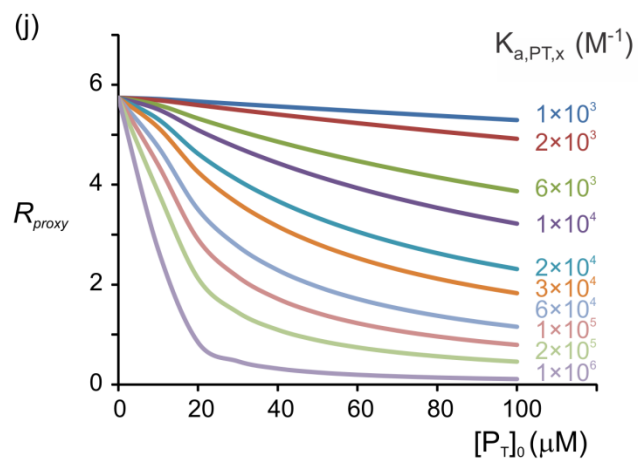
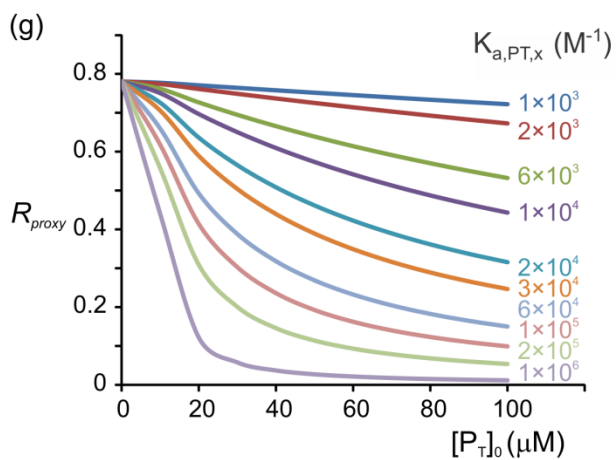
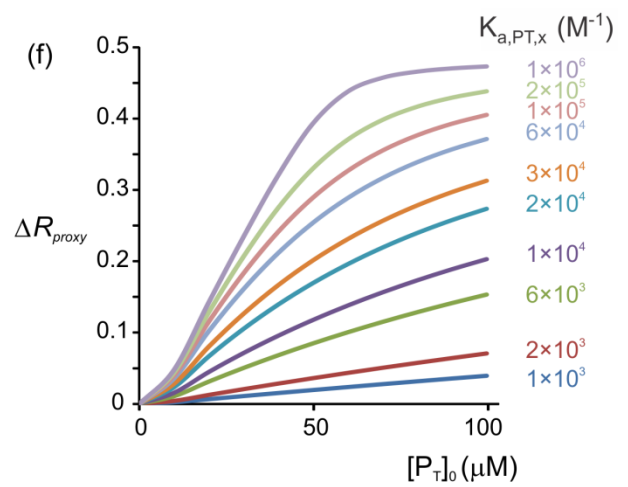
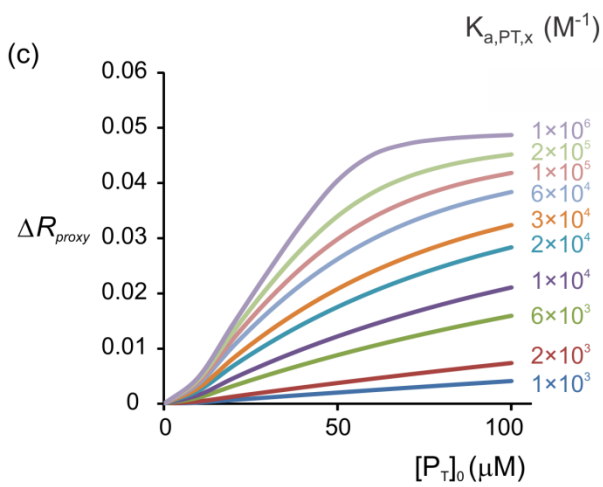
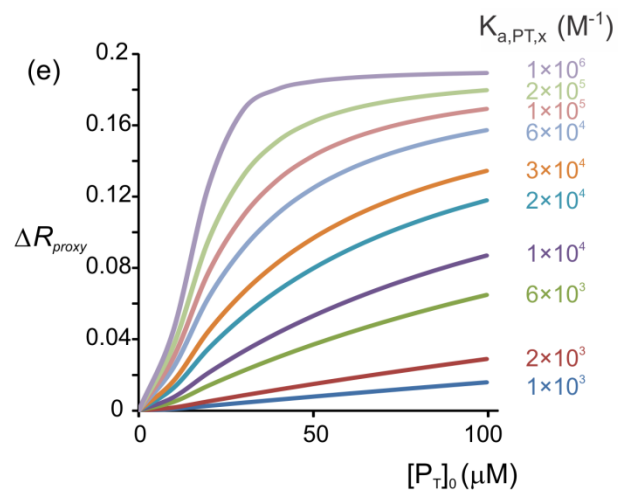
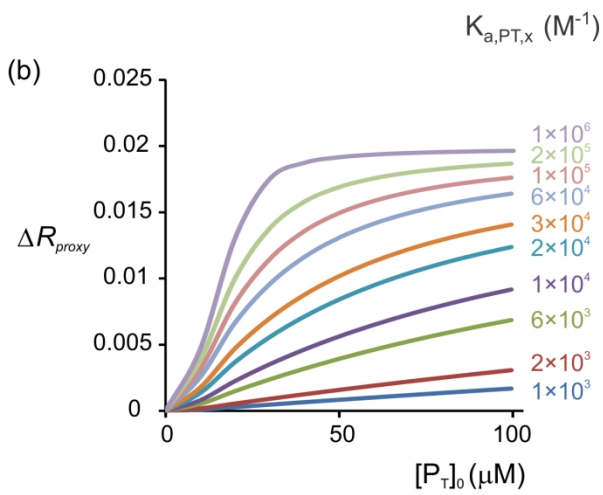
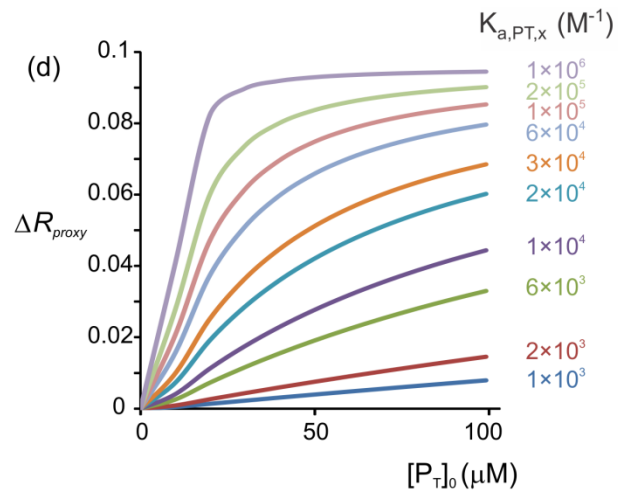
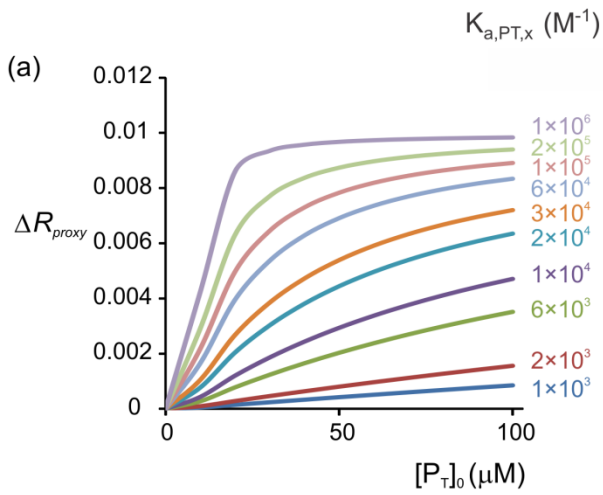


Figure 3.6. Calculated plots of R_{proxy} versus $[P_T]_0$. Initial conditions used for the numerical simulations: $[P_{proxy}]_0 = 5 \mu\text{M}$, $[L]_0 = 10 \mu\text{M}$ (a, d, g, j), $20 \mu\text{M}$ (b, e, h, k) and $50 \mu\text{M}$ (c, f, i, l). $K_{a,proxy} = 10^3 \text{ M}^{-1}$ (a-c), 10^4 M^{-1} (d-f), 10^5 M^{-1} (g-i), 10^6 M^{-1} (j-l). $[P_T]_0$ values are shown on the x-axis. $K_{a,PT,x}$ ranged (from top to bottom) from 1×10^3 (blue), 2×10^3 (red), 6×10^3 (green), 1×10^4 (purple), 2×10^4 (light blue), 3×10^4 (orange), 6×10^4 (pale blue), 1×10^5 (pink), 2×10^5 (light green) to 1×10^6 (light purple).



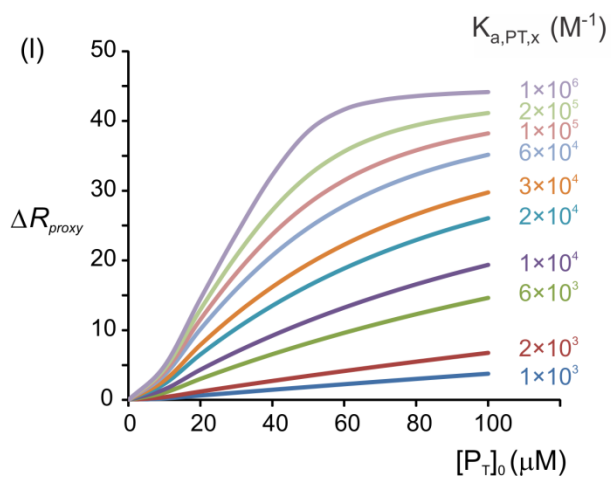
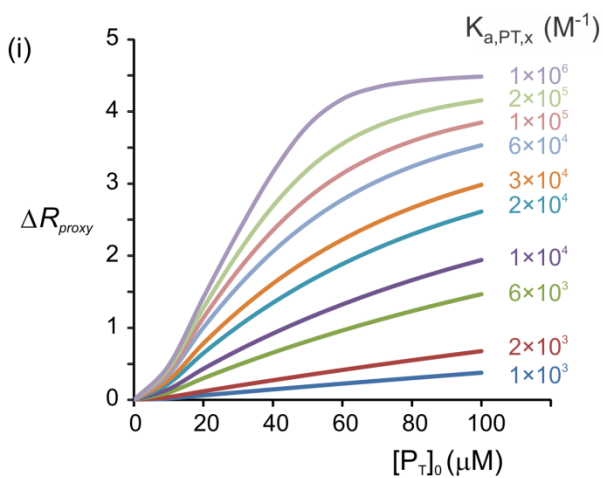
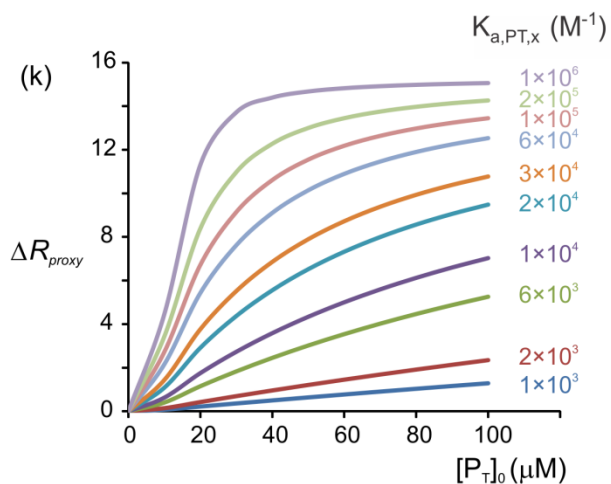
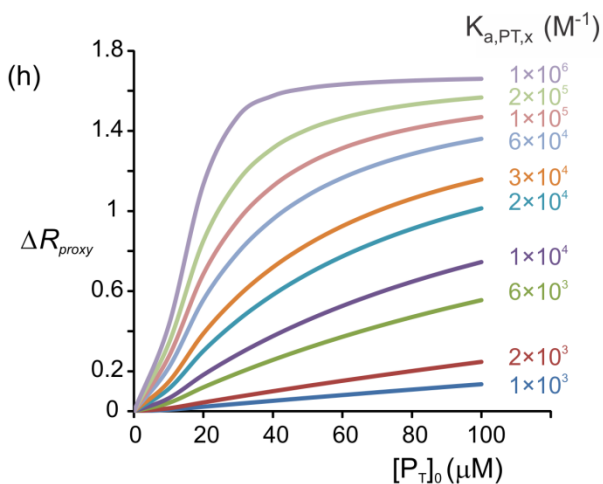
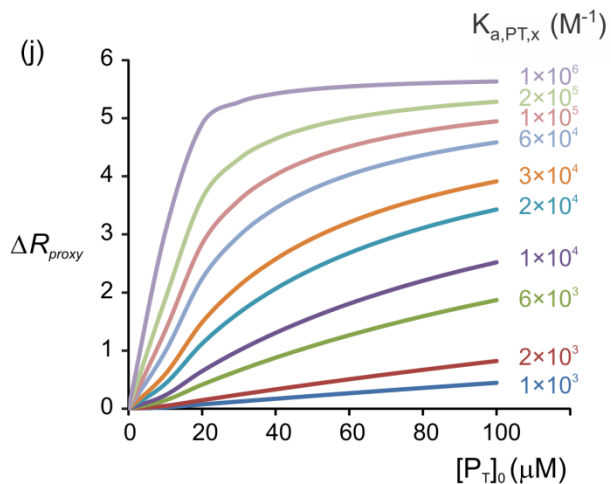
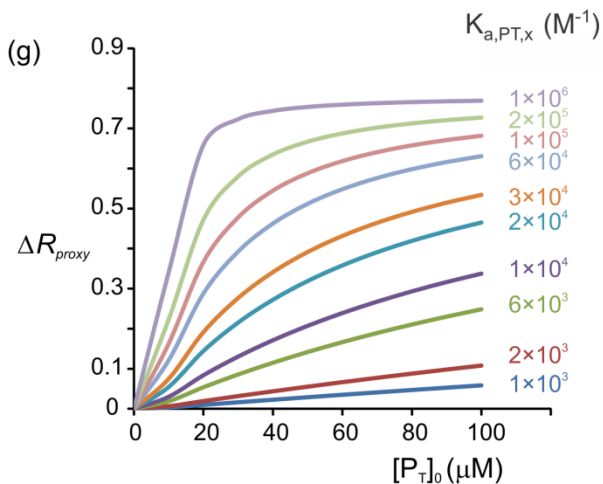


Figure 3.7. Calculated plots of ΔR_{proxy} versus $[P_T]_0$. Initial conditions used for numerical simulations: $[P_{proxy}]_0 = 5 \mu\text{M}$, $[L]_0 = 10 \mu\text{M}$ (a, d, g, j), $20 \mu\text{M}$ (b, e, h, k) and $50 \mu\text{M}$ (c, f, i, l). $K_{a,proxy} = 10^3 \text{ M}^{-1}$ (a-c), 10^4 M^{-1} (d-f), 10^5 M^{-1} (g-i), 10^6 M^{-1} (j-l). $[P_T]_0$ values are shown on the x-axis. $K_{a,PT,x}$ ranged (from top to bottom) from 1×10^3 (blue), 2×10^3 (red), 6×10^3 (green), 1×10^4 (purple), 2×10^4 (light blue), 3×10^4 (orange), 6×10^4 (pale blue), 1×10^5 (pink), 2×10^5 (light green) to 1×10^6 (light purple).

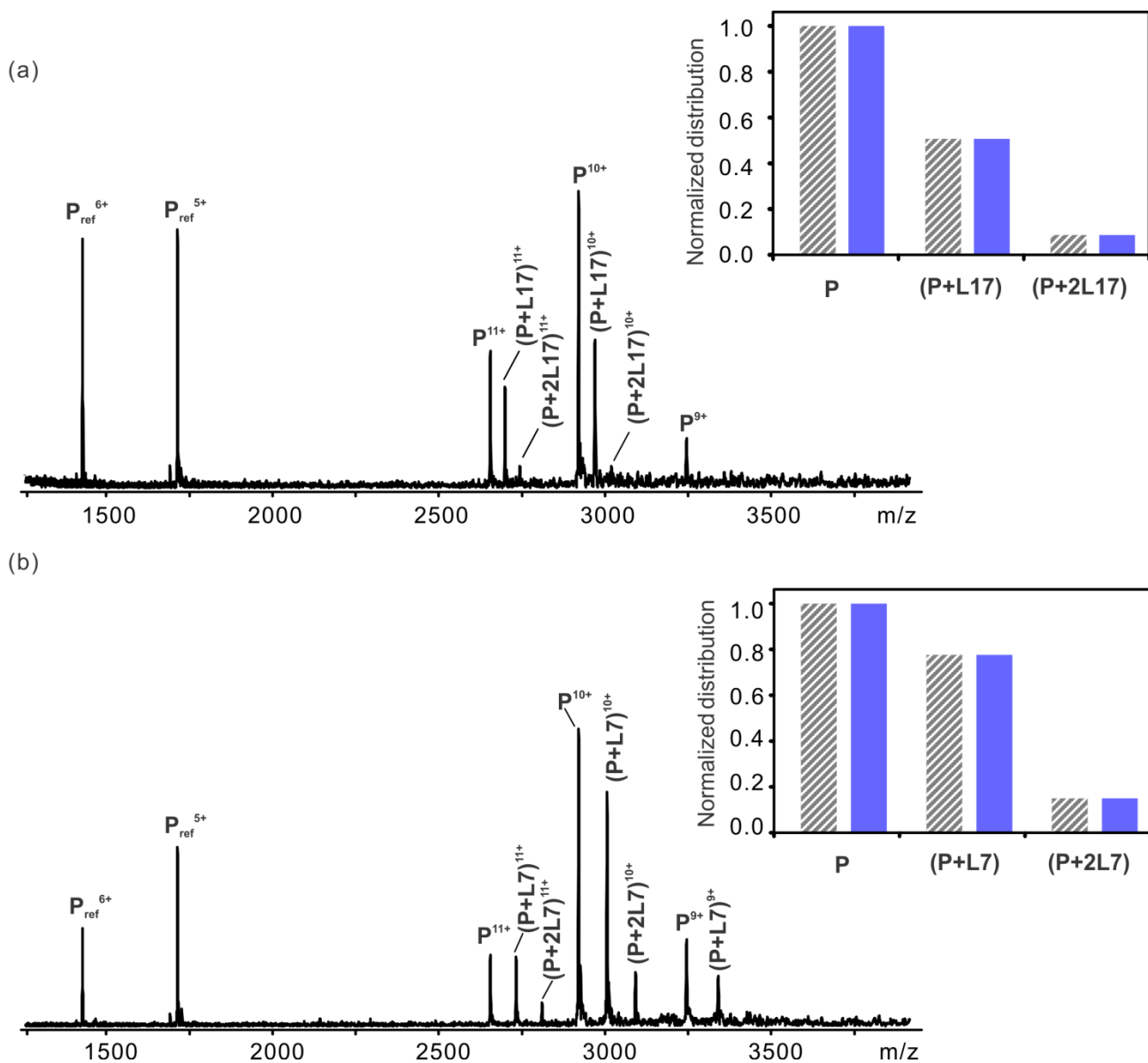


Figure 3.8. ESI mass spectra in positive ion mode for a 30 mM aqueous ammonium acetate solution (pH 6.8, 25 °C) of RSL (P, 1.3 μM) and P_{ref} (1 μM) with (a) 0.8 μM L17 or (b) 2 μM L7. Insets show normalized distribution of free and ligand-bound RSL before (▨) and after (■) correction for nonspecific ligand binding.

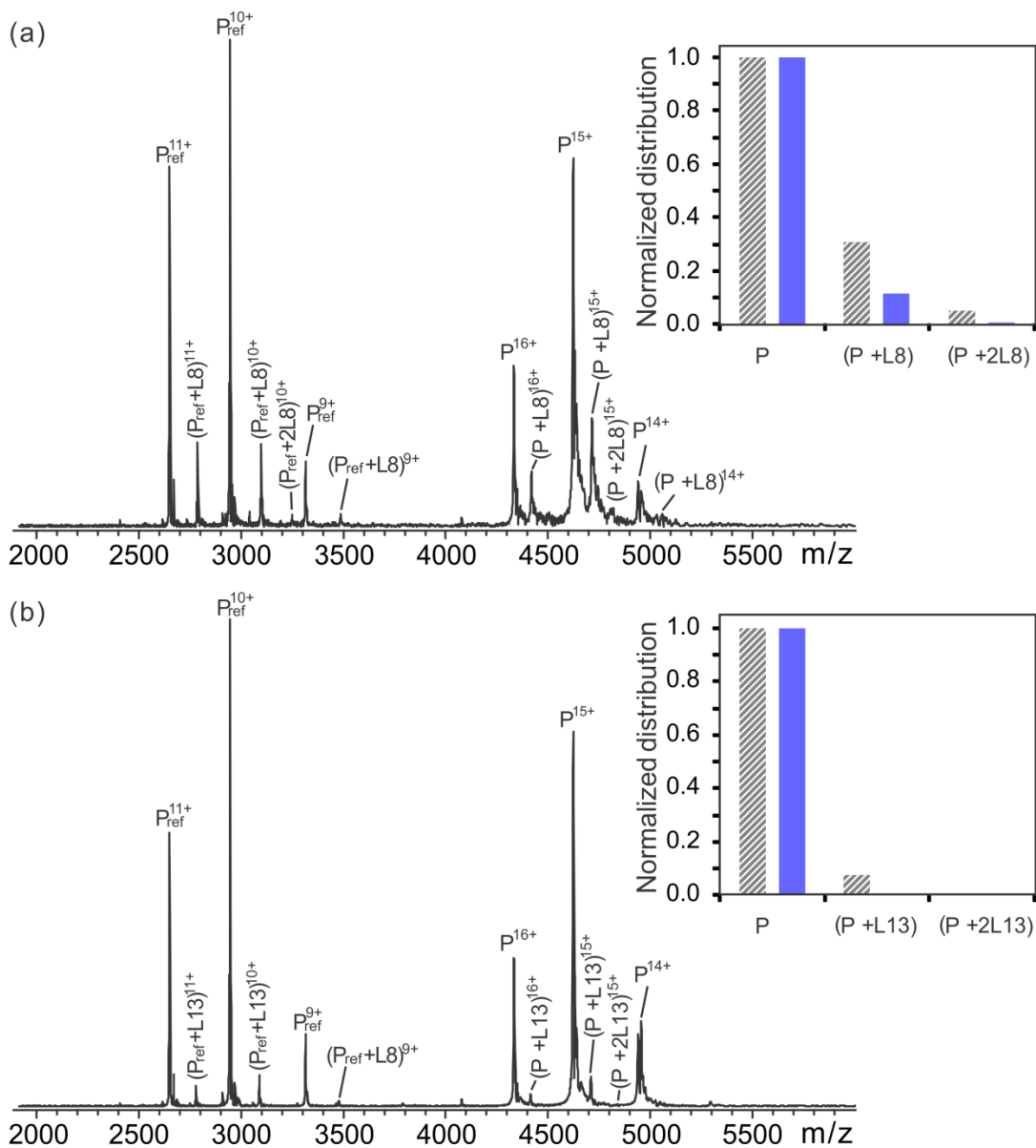


Figure 3.9. ESI mass spectra in positive ion mode for a 10 mM aqueous ammonium acetate solution (pH 6.8, 25 °C) of VA387 P dimer (P, 12 μ M) and P_{ref} (10 μ M) with (a) 80 μ M **L8**, or (b) 80 μ M **L13**. Insets show normalized distribution of free and ligand-bound P dimer before (▨) and after (■) correction for nonspecific ligand binding.

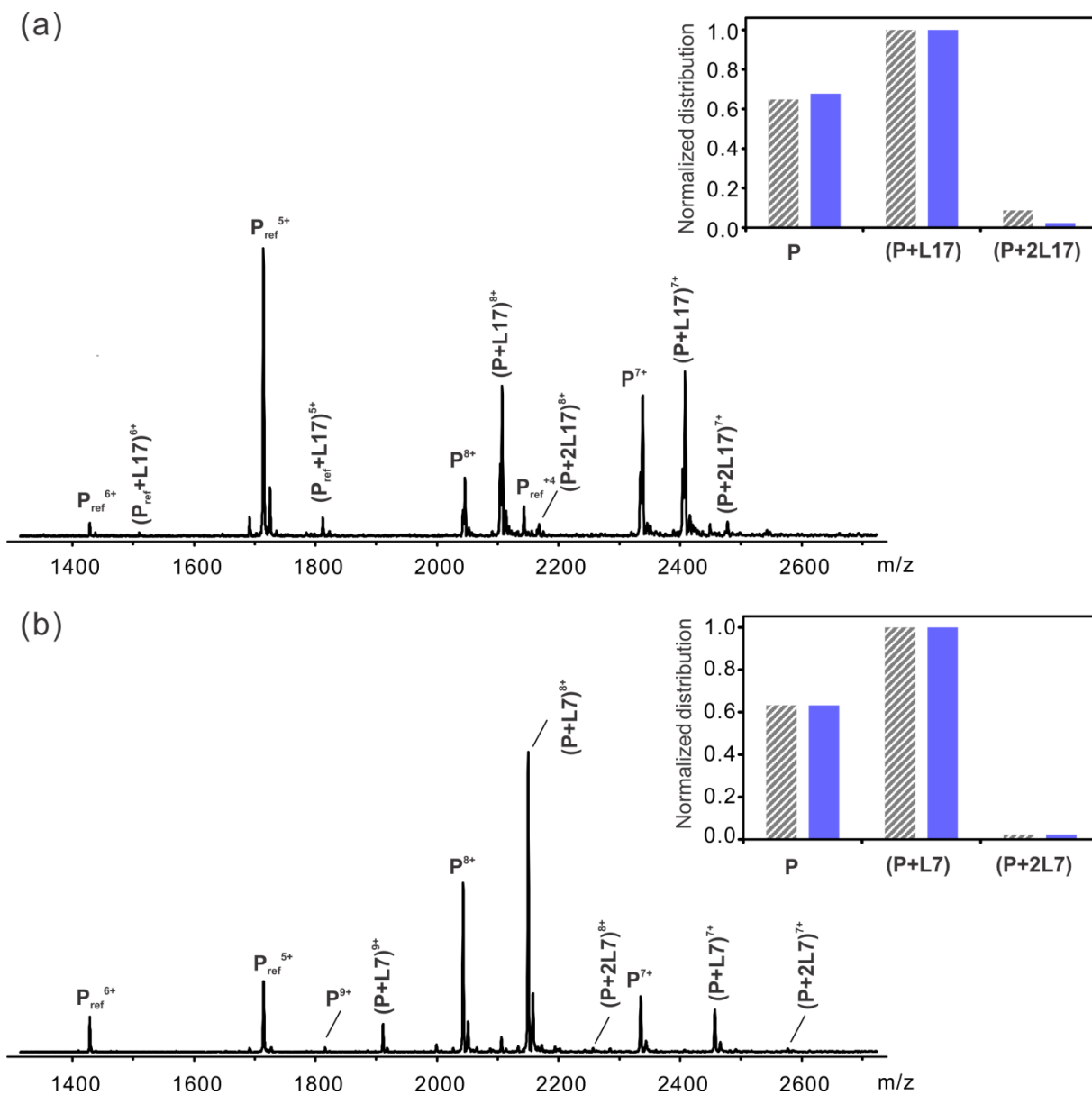


Figure 3.10. ESI mass spectra in positive ion mode for a 30 mM aqueous ammonium acetate solution (pH 6.8, 25 °C) of Gal-3C (P, 5 μ M) and P_{ref} (5 μ M) with (a) 40 μ M L17 or (b) 20 μ M L7. Insets show normalized distribution of free and ligand-bound RSL before (▨) and after (■) correction for nonspecific ligand binding.

3.5 References

- (1) Ohtsubo, K.; Marth, J. D. *Cell* **2006**, 126, 855-867.
- (2) Hakomori, S. *Curr. Opin. Hematol.* **2003**, 10, 16-24.
- (3) Sharon, N.; Lis, H. *Sci. Am.* **1993**, 268, 82-89.
- (4) Varki, A., Sharon, N. In *Essentials of Glycobiology, 2nd edition*; Varki, A., Cummings, R. D., Esko, J. D., Freeze, H. H., Stanley, P., Bertozzi, C. R., Hart, G. W., Etzler, M. E., Eds; Cold Spring Harbor (NY): Cold Spring Harbor Laboratory Press; **2009**, Part 1.
- (5) Dwek, R. A. *Chem. Rev.* **1996**, 96, 683-720.
- (6) Schulze, H.; Sandhoff, K. *BBA-Mol. Cell. Biol. L.* **2014**, 1841, 799-810.
- (7) Meyer, S.; van Liempt, E.; Imberty, A.; van Kooyk, Y.; Geyer, H.; Geyer, R.; van Die, I. *J. Biol. Chem.* **2005**, 280, 37349-37359.
- (8) Janes, P. W.; Ley, S. C.; Magee, A. I.; Kabouridis, P. S. *Semin. Immunol.* **2000**, 12, 23-34.
- (9) Lis, H.; Sharon, N. *Chem. Rev.* **1998**, 98, 637-674.
- (10) Lee, Y. C.; Lee, R. T. *Accounts Chem. Res.* **1995**, 28, 321-327.
- (11) Cohen, M. *Biomolecules* **2015**, 5, 2056-2072.
- (12) Bode, L. *Nutr. Rev.* **2009**, 67, S183-S191.
- (13) Hickey, R. M. *Int. Dairy J.* **2012**, 22, 141-146.
- (14) Newburg, D. S.; Ruiz-Palacios, G. M.; Morrow, A. L. *Annu. Rev. Nutr.* **2005**, 25, 37-58.
- (15) Bode, L.; Jantscher-Krenn, E. *Adv. Nutr.* **2012**, 3, 383S-391S.

- (16) Ruiz-Palacios, G. M.; Cervantes, L. E.; Ramos, P.; Chavez-Munguia, B.; Newburg, D. S. *J. Biol. Chem.* **2003**, 278, 14112-14120.
- (17) Ernst, B.; Magnani, J. L. *Nat. Rev. Drug Discov.* **2009**, 8, 661-677.
- (18) Magnani, J. L. *Glycoscience: Biology and Medicine* **2015**, 1517-1522.
- (19) Cooper, M. A. *Nat. Rev. Drug Discov.* **2002**, 1, 515-528.
- (20) de Azevedo, J.; Walter, F.; Dias, R. *Curr. Drug Targets* **2008**, 9, 1071-1076.
- (21) Slon-Usakiewicz, J. J.; Ng, W.; Dai, J.-R.; Pasternak, A.; Redden, P. R. *Drug Discov. Today* **2005**, 10, 409-416.
- (22) Meyer, B.; Peters, T. *Angew. Chem. Int. Edit.* **2003**, 42, 864-890.
- (23) Smith, E. A.; Thomas, W. D.; Kiessling, L. L.; Corn, R. M. *J. Am. Chem. Soc.* **2003**, 125, 6140-6148.
- (24) Rossi, A. M.; Taylor, C. W. *Nat. Protoc.* **2011**, 6, 365-387.
- (25) Myszka, D. G. *Curr. Opin. Biotech.* **1997**, 8, 50-57.
- (26) Boer, A. R.; Hokke, C. H.; Deelder, A. M.; Wuhrer, M. *Glycoconjugate J.* **2008**, 25, 75-84.
- (27) Mehta-D'souza, P. In *Galectins: Methods and Protocols*, Stowell, R. S.; Cummings, D. R., Eds.; Springer New York: New York, NY, **2015**, 105-114.
- (28) del Carmen Fernández-Alonso, M.; Díaz, D.; Alvaro Berbis, M.; Marcelo, F.; Jimenez-Barbero, J. *Curr. Protein Pept. Sci.* **2012**, 13, 816-830.
- (29) Rillahan, C. D.; Brown, S. J.; Register, A. C.; Rosen, H.; Paulson, J. C. *Angew. Chem. Int. Edit.* **2011**, 50, 12534-12537.
- (30) Ng, E. S. M.; Yang, F.; Kameyama, A.; Palcic, M. M.; Hindsgaul, O.; Schriemer, D. C. *Anal. Chem.* **2005**, 77, 6125-6133.

- (31) Oyelaran, O.; Gildersleeve, J. C. *Curr. Opin. Chem. Biol.* **2009**, 13, 406-413.
- (32) Nimrichter, L.; Gargir, A.; Gortler, M.; Altstock, R. T.; Shtevi, A.; Weissshaus, O.; Fire, E.; Dotan, N.; Schnaar, R. L. *Glycobiology* **2004**, 14, 197-203.
- (33) Dickinson, L. E.; Ho, C. C.; Wang, G. M.; Stebe, K. J.; Gerecht, S. *Biomaterials* **2010**, 31, 5472-5478.
- (34) Šardžik, R.; Sharma, R.; Kaloo, S.; Voglmeir, J.; Crocker, P. R.; Flitsch, S. L. *Chem. Commun.* **2011**, 47, 5425-5427.
- (35) Song, X.; Lasanajak, Y.; Xia, B.; Heimbürg-Molinaro, J.; Rhea, J. M.; Ju, H.; Zhao, C.; Molinaro, R. J.; Cummings, R. D.; Smith, D. F. *Nat. Methods* **2011**, 8, 85-90.
- (36) Arndt, N. X.; Tiralongo, J.; Madge, P. D.; von Itzstein, M.; Day, C. J. *J. Cell. Biochem.* **2011**, 112, 2230-2240.
- (37) Liang, P.-H.; Wu, C.-Y.; Greenberg, W. A.; Wong, C.-H. *Curr. Opin. Chem. Biol.* **2008**, 12, 86-92.
- (38) Heimbürg-Molinaro, J.; Song, X.; Smith, D. F.; Cummings, R. D. *Curr. Protoc. Protein Sci.* **2011**, 64: 12.10. 11-12.10. 29.
- (39) Arthur, C. M.; Rodrigues, L. C.; Baruffi, M. D.; Sullivan, H. C.; Heimbürg-Molinaro, J.; Smith, D. F.; Cummings, R. D.; Stowell, S. R. In *Galectins: Methods and Protocols*, Stowell, R. S.; Cummings, D. R., Eds.; Springer New York: New York, NY, **2015**, 115-131.
- (40) Raman, R.; Raguram, S.; Venkataraman, G.; Paulson, J. C.; Sasisekharan, R. *Nat. Methods* **2005**, 2, 817-824.
- (41) Liang, C.-H.; Wu, C.-Y. *Expert Rev. Proteom.* **2009**, 6, 631-645.

- (42) Rillahan, C. D.; Paulson, J. C. *Annu. Rev. Biochem.* **2011**, 80, 797-823.
- (43) Drickamer, K.; Taylor, M. E. *Genome Biol.* **2002**, 3, 1034.
- (44) Kilcoyne, M.; Gerlach, J. Q.; Kane, M.; Joshi, L. *Anal. Methods* **2012**, 4, 2721-2728.
- (45) Grant, O. C.; Smith, H. M.; Firsova, D.; Fadda, E.; Woods, R. J. *Glycobiology* **2014**, 24, 17-25.
- (46) Paulson, J. C.; Blixt, O.; Collins, B. E. *Nat. Chem. Biol.* **2006**, 2, 238-248.
- (47) Smith, D. F.; Song, X.; Cummings, R. D. *Method Enzymol.* **2010**, 480, 417-444.
- (48) Daniel, J. M.; Friess, S. D.; Rajagopalan, S.; Wendt, S.; Zenobi, R. *Int. J. Mass Spectrom.* **2002**, 216, 1-27.
- (49) Schug, K. A. *Com. Chem. High T. Scr.* **2007**, 10, 301-316.
- (50) Heck, A. J.; van den Heuvel, R. H. *Mass Spectrom. Rev.* **2004**, 23, 368-389.
- (51) El-Hawiet, A.; Kitova, E. N.; Liu, L.; Klassen, J. S. *J. Am. Soc. Mass Spectrom.* **2010**, 21, 1893-1899.
- (52) Lin, H.; Kitova, E. N.; Klassen, J. S. *J. Am. Soc. Mass Spectrom.* **2014**, 25, 104-110.
- (53) Liu, L.; Kitova, E. N.; Klassen, J. S. *J. Am. Soc. Mass Spectrom.* **2011**, 22, 310-318.
- (54) Kitova, E. N.; El-Hawiet, A.; Klassen, J. S. *J. Am. Soc. Mass Spectrom.* **2014**, 25, 1908-1916.
- (55) El-Hawiet, A.; Shoemaker, G. K.; Daneshfar, R.; Kitova, E. N.; Klassen, J. S. *Anal. Chem.* **2012**, 84, 50-58.

- (56) Leney, A. C.; Fan, X.; Kitova, E. N.; Klassen, J. S. *Anal. Chem.* **2014**, 86, 5271-5277.
- (57) El-Hawiet, A.; Kitova, E. N.; Arutyunov, D.; Simpson, D. J.; Szymanski, C. M.; Klassen, J. S. *Anal. Chem.* **2012**, 84, 3867-3870.
- (58) El-Hawiet, A.; Kitova, E. N.; Klassen, J. S. *Anal. Chem.* **2013**, 85, 7637-7644.
- (59) Zhang, Y. X.; Liu, L.; Daneshfar, R.; Kitova, E. N.; Li, C. S.; Jia, F.; Cairo, C. W.; Klassen, J. S. *Anal. Chem.* **2012**, 84, 7618-7621.
- (60) Han, L.; Kitova, E. N.; Tan, M.; Jiang, X.; Klassen, J. S. *J. Am. Soc. Mass Spectrom.* **2014**, 25, 111-119.
- (61) Han, L.; Tan, M.; Xia, M.; Kitova, E. N.; Jiang, X.; Klassen, J. S. *J. Am. Chem. Soc.* **2014**, 136, 12631-12637.
- (62) Han, L.; Kitova, E. N.; Tan, M.; Jiang, X.; Pluvinage, B.; Boraston, A. B.; Klassen, J. S. *Glycobiology* **2015**, 25, 170-180.
- (63) Diehl, C.; Genheden, S.; Modig, K.; Ryde, U.; Akke, M. *J. Biomol. NMR* **2009**, 45, 157-169.
- (64) Higgins, M. A.; Ficko-Blean, E.; Meloncelli, P. J.; Lowary, T. L.; Boraston, A. B. *J. Mol. Biol.* **2011**, 411, 1017-1036.
- (65) Arnaud, J.; Tröndle, K.; Claudinon, J.; Audfray, A.; Varrot, A.; Römer, W.; Imberty, A. *Angew. Chem. Int. Edit.* **2014**, 53, 9267-9270.
- (66) Zdanov, A.; Li, Y.; Bundle, D. R.; Deng, S.-J.; MacKenzie, C. R.; Narang, S. A.; Young, N. M.; Cygler, M. *P. Natl. Acad. Sci. USA* **1994**, 91, 6423-6427.
- (67) Sun, J. X.; Kitova, E. N.; Wang, W. J.; Klassen, J. S. *Anal. Chem.* **2006**, 78, 3010-3018.

- (68) Meloncelli, P. J.; Lowary, T. L. *Aust. J. Chem.* **2009**, 62, 558-574.
- (69) Meloncelli, P. J.; Lowary, T. L. *Carbohydr. Res.* **2010**, 345, 2305-2322.
- (70) Meloncelli, P. J.; West, L. J.; Lowary, T. L. *Carbohydr. Res.* **2011**, 346, 1406-1426.
- (71) Kostlánová, N.; Mitchell, E. P.; Lortat-Jacob, H.; Oscarson, S.; Lahmann, M.; Gilboa-Garber, N.; Chambat, G.; Wimmerová, M.; Imberty, A. *J. Biol. Chem.* **2005**, 280, 27839-27849.
- (72) Tan, M.; Hegde, R. S.; Jiang, X. *J. Virol.* **2004**, 78, 6233-6242.
- (73) Tan, M.; Jiang, X. *J. Virol.* **2005**, 79, 14017-14030.
- (74) Han, L.; Kitov, P. I.; Kitova, E. N.; Tan, M.; Wang, L.; Xia, M.; Jiang, X.; Klassen, J. S. *Glycobiology* **2013**, 23, 276-285.
- (75) Urashima, T.; Asakuma, S.; Leo, F.; Fukuda, K.; Messer, M.; Oftedal, O. T. *Adv. Nutr.* **2012**, 3, 473S-482S.
- (76) Arthur, C. M.; Baruffi, M. D.; Cummings, R. D.; Stowell, S. R. In *Galectins: Methods and Protocols*, Stowell, R. S.; Cummings, D. R., Eds.; Springer New York: New York, NY, **2015**, 1-35.

Chapter 4

Comparative Studies of Human Milk Oligosaccharide Specificities of Human Galectin-1, 3, 9

4.1 Introduction

Human milk contains a variety of bioactive components, including proteins, glycoproteins, fat globules and free oligosaccharides (referred to as human milk oligosaccharides, HMOs.)^{1,2} HMOs are present in human milk at concentrations of 7-12 g/L,³ they promote good bacteria growth,⁴ serve as antiadhesive antimicrobials in intestinal and urinary pathogens, modulate immune response and regulate gene expression in intestinal epithelial cells.⁵⁻¹³ Recently specific interactions of HMOs with bacterial toxins were demonstrated¹⁴ and the anti-allergic properties of acidic HMOs linked to stimulating production of cytokines were proposed.¹⁵ While HMOs mainly are present in the intestinal tracts of infants, they can reach systemic circulation and therefore have effects outside of the gastrointestinal tract on local and systemic levels.¹⁰ Putative host binding partners of HMOs are involved in intestinal immune system and include C-type lectins, siglecs and galectins.¹⁶

Several HMOs have similar structures as cell surface glycans which serve as ligands for galectin. Galectins, evolutionarily conserved β -galactose-binding lectins consisting of ~130 amino acids, play important roles in a variety of physiological and pathological processes, such as inflammation, cell proliferation, the cell cycle, transcription processes and cell apoptosis.¹⁷ Galectins can be found in the extracellular space, on the cell surface, in the cytoplasm, and even in the nucleus. Extracellular galectins may mediate cell-cell

or cell–matrix adhesion by recognizing cell surface glycoproteins and glycolipids or glycosylated extracellular matrix.¹⁸ During the infection process, galectins have diverse effects on cells involved in innate immune responses, including macrophages, dendritic cells, neutrophils, eosinophils and mast cells. Galectins can modulate T cell homeostasis by signaling cascades triggered by their binding and lattice formation at the T cell surface and leading to secretion of pro- and anti-inflammatory cytokines.¹⁹ Based on exacerbated or depressed immune function, resulting effects can be beneficial or detrimental for pathological conditions such as inflammatory, allergic and autoimmune disorders, and cancer.²⁰⁻²² The ability of some galectins to modulate the differential expression of cytokine genes in leukocytes may signify an important role for galectins in the adaptive immune response,²³ in particular T2-type allergic response.

Human galectins exist in three different types, dimeric (1, 2, 7, 10 and 13), tandem (4, 8, 9 and 12) or chimera (3) and they possess unique physiological properties.²⁴⁻²⁸ Each galectin recognizes different glycan receptors^{29,30} although most of the members of galectin family bind to glyconjugates containing lactose (Gal β 1-4Glc) and N-acetyllactosamine (LacNAc). Galectins 1, 3 and 9 belong to different types and represent each different class of galectin. They are produced in intestinal cells and are present at low concentration in the blood. They were shown to bind to glycoproteins (complex N-linked glycan inherited in protein) and glycans containing N-acetyllactosamine and lactose containing oligosaccharides. Galectin 1 exists in solution as a dimer, has two identical binding sites.³¹ Galectin-9 N- and C-terminal CRD parts have different carbohydrate binding sites³² where each terminal has single binding site in their structure.³² Galectin 3 has single binding site.³³ The affinities for a small number of HMOs for human galectins

1, 2, 3, 7, 8, 9 have been previously measured by frontal affinity chromatography (FAC)³⁴ then by fluorescence anisotropy assay for galectin 3.³³ In addition, different research groups reported galectin-glycan interactions using commercially available few simple glycans.³⁴⁻³⁸

Recently HMOs binding properties were studied using glycan array technology³⁹ where HMO were modified to print on the glass slides and structural characterization was described by using multistage mass spectrometry and computational approaches.⁴⁰⁻⁴² While it is established that human galectins, except galectin 2 recognize HMOs, there are little quantitative binding data with some disagreement between different methods. Moreover, each human milk oligosaccharide contains a free-reducing end⁴³⁻⁴⁵ which might be the reason for arising binding data disagreement. It may possibly relate to the modification done in proteins and oligosaccharides to detect binding. Using glycan array technique, screening is quick and requires comparatively small amounts of sample by glycan array method⁴⁶⁻⁴⁸ nonetheless binding data are known to display a dependence on the size/nature of the linker and amount of glycans printed on the surface.⁴⁹ Also false negatives, particularly for low affinity interactions are commonly observed by this technique.^{46,50-52}

For the last several years direct ESI-MS binding assay was developed to become reliable technique to quantify protein-carbohydrate affinities. Important features of the assay are that interactions occur in solution and no chemical modification is needed.⁵³⁻⁵⁵ With the goals to quantify and to extend the affinity measurements to a larger number of HMO structures, the direct ESI-MS binding assay was used to screen thirty-two HMOs against

galectin 1 and two human galectin fragments, N-terminal fragment of galectin 9 and C-terminal fragment of galectin 3 in this study.

4.2 Materials and Methods

4.2.1 Oligosaccharides

The structures of the 32 oligosaccharides (**L1 – L32**) used in this study are shown in Figure 4.1 and Table 4.1. **L1, L5, L6, L12, L17, L19, L21, L26-L28, L29, L31, L32** were purchased from Elicityl SA (Crolles, France); **L2-L4, L7, L9-L11, L13-L16, L13-L16, L18, L20, L22-L24** and **L25** were purchased from IsoSep (Tullinge, Sweden); **L8** was obtained from Dextra (Reading, UK) and **L30** from Sigma-Aldrich Canada (Oakville, ON, Canada). **L33** was purchased from Elicityl SA (Crolles, France) which is present in the core of many HMO structure. Four fructo-oligosaccharides (FOS) **L34-L37** (Elicityl code, **Fru111-Fru114**) were also purchased from Elicityl SA (Crolles, France). Stock solutions of each oligosaccharide were prepared by dissolving a known mass of compound in a known volume of ultra-filtered water (Milli-Q, Millipore, Billerica, MA) to achieve a final concentration of ~1 mM. Galacto-oligosaccharides (GOS) were purchased from FrieslandCampina Domo (Amersfoort, The Netherlands); both of the sample (Vivinal GOS syrup and Vivinal GOS 90 powder) are available in syrup and dry powder form. Vivinal GOS 90 powder was dissolved in ultra-filtered Milli-Q water to make a stock solution to achieve a final concentration ~ 26.76 g/L. This stock solution is diluted to use in the experiment. Similarly, 125 µL of highly concentrated Vivinal GOS syrup was diluted 10 times with ultra-filtered Milli-Q water to make a stock solution. This solution is further diluted multiple times during experiment. The stock solutions were stored at -20 °C until needed.

4.2.2 Proteins

S-carboxyamidomethylated oxidation resistant (C2S substituted) recombinant human galectin-1 (Dimer, Gal-1, MW 29500 Da) was gifts from Prof. S. Sato (Université Laval, Quebec).⁵⁶ C2S substitution was done for improving stability and it does not alter affinity of Gal-1 for glycan.⁵⁷ The recombinant fragment of the C-terminus (residues 107–250) carbohydrate recognition domain of human galectin-3 (Gal-3C, MW 16,330 Da)⁵⁸ and recombinant fragment of N-terminus (residues 1–148) carbohydrate recognition domain of human galectin-9 (Gal-9N, MW 18509 Da)⁵⁹ was a gift from Prof. C. Cairo (University of Alberta).

4.2.3 Mass spectrometry

The ESI-MS binding assays were carried out in positive ion mode using a 9.4T ApexQe FTICR mass spectrometer (Bruker, Billerica, MA) and a Synapt G2 quadrupole-ion mobility separation-time-of-flight (Q-IMS-TOF) mass spectrometer (Waters UK Ltd., Manchester, UK). For these instruments, nanoflow ESI (nanoESI) was performed using borosilicate glass tips (1.0 mm o.d., 0.68 mm i.d.) pulled to ~5 μm o.d. at one end using a P-2000 micropipette puller (Sutter Instruments, Novato, CA). A capillary voltage of ~1.0 kV was applied to a Pt wire in the nanoESI tip to carry out ESI. A brief description of the instrumental conditions used for the two mass spectrometers is given below.

ApexQe 9.4T FTICR mass spectrometer. The ESI source was fitted with a metal sampling capillary (0.5 mm i.d.) which is maintained at 280 V. Nitrogen gas was used as a drying gas at a flow rate of 2.0 L min⁻¹ and 90 °C. Ions were carried through the first funnel and skimmer at 150 V and 20 V, respectively, and then ions were transmitted through the second funnel and skimmer at 7.6 V and 5.3 V, respectively. Electrostatically the ions

were stored temporarily in an rf hexapole for 0.6 s. They were further stored in a hexapole collision cell for 0.5 s. Following accumulation, the ions were transferred into the ion cell for detection. The front and back trapping plate voltage of the cell were maintained at 0.9 and 1.0 V, respectively, throughout the full experiment. The typical instrument base pressure for was $\sim 1 \times 10^{-10}$ mbar. Analysis and data acquisition were executed using ApexControl, version 4.0 (Bruker Daltonics). For each acquisition a minimum of 30 transients with 128K data points per transient were used.

Synapt G2 mass spectrometer. Mass spectra were acquired using a sampling cone voltage of 30 V and an extraction cone voltage of 2 V. The source wave velocity and wave height were 200 m/s and 0.2 V, respectively. Gas flow rates were 2 mL min⁻¹ in trap, 180 mL min⁻¹ in helium cell, 90 mL min⁻¹ in ion mobility cell. Backing pressure of the source was 3.2 mbar and the block temperature was 70 °C. Ions were transmitted using Trap and Transfer ion guides where Trap (5V) and Transfer (2V) voltage were kept fixed. At least 150 scans were collected for every acquisition. Data acquisition and processing were carried out using MassLynx (v 4.1).

4.2.4 ESI-MS affinity measurements for Ka value determination

For binding of the galectins to each of the thirty two HMOs (L1-L32) the apparent association constants ($K_{a, app}$) were quantified by the direct ESI-MS assay.^{53,55,60,61} All measurements were performed using six replicate measurements with a minimum of two different concentrations for each protein and HMO. For correcting the nonspecific carbohydrate- protein binding during the ionization process a reference protein (P_{ref}) was added to the mixture to correct the mass spectra.⁶⁵ Later, $K_{a,app}$ was calculated from the

abundance ratio (R_q) of the ligand bound (PL_q) to free protein (P) after correction for nonspecific binding (eq 4.1a). If initial concentrations of protein ($[P]_0$) and ligand ($[L]_0$) are known then $K_{a,app}$ can be measured by eq 4.1b:

$$R_q = \frac{Ab(PL_q)}{Ab(P)} = \frac{[PL_q]}{[P]} \quad (4.1a)$$

$$K_{a,app} = \frac{[PL_1]}{[P][L]} = \frac{R_1}{[L]_0 - \frac{\sum_{1 \leq q \leq 5} q R_q}{1 + \sum_{1 \leq q \leq 5} R_q} [P]_0} \quad (4.1b)$$

4.3 Results and Discussions

Galectins binds with galactose residue (Gal) and most of the HMOs contain Gal in the β configuration (β -galactoside) in the form of lacto-N-biose I [Gal(β 1-4)GlcNAc, Type 1] and/or N-acetyllactosamine [Gal(β 1-3)GlcNAc, Type 2] in their structure.⁴³ Structurally, HMOs contain GlcNAc (N-acetylglucosamine), Gal (galactose), Fuc (fucose), and/or Neu5Ac (N-acetylneuraminic acid) residues as monosaccharide components. Among tested HMOs 10 compounds containing α -D-Neu5Ac(2-3/6) linkages are acidic oligosaccharides and 22 HMOs are neutral. According to Kobata et al. 2010, two histo-blood group oligosaccharides found in minor amount in blood group A secretor individuals, AT5 tetra (**L31**), AT1 hexa (**L32**), were tested for binding with galectins. Cummings RD et al. 2009 showed a comparison of sequences of human galectins where amino acid residues involved in carbohydrate binding are highly conserved in all galectins, eight polar (His45, Asn47, Arg49, Asn62, Glu72, Arg74) and two non-polar (Val60, Trp69).

HMO-binding specificity of Galectins

Galectin-1 (Gal-1) forms a noncovalent homodimer in solution. It contains single CRD and it is sensitive to oxidation because of six conserved cysteine residues to its dimerization location.⁶² Oxidation causes inactivation and loss of its hemagglutinin activity. It was described that mild treatment of galectin-1 by *S*-carboxyamidomethylation with iodoacetamide makes it resistant to oxidation along with preservation of its biological functions.⁶³ In this study, we used carboxyamidomethylated Gal-1 to prevent oxidation. Recently it has been reported that specificity of Gal-1 for glycan depends on both structures and mode of representation in solution or solid phase.⁶⁴ Solution-based method such as equilibrium gel filtration assay and isothermal titration calorimetry showed that single or poly N-acetylglucosamine sequence does not have much influence on glycan binding capacity of Gal-1.²⁸ Using our method, ESI-MS-binding measurement also showed similar results. For Type 2 LacNac containing HMOs, **L6** has one N-acetylglucosamine unit whereas **L1** and **L8** have two N-acetylglucosamine units each and **L5** has three units but all of their apparent binding affinities ($K_{a, 1}$) are moderately strong and those are of similar strength ($\sim 10^4 \text{ M}^{-1}$) whereas Type 1 LacNac containing HMO, **L9** has one unit of N-acetylglucosamine and interestingly binding affinity is stronger ($\sim 10^5 \text{ M}^{-1}$) than Type 2 LacNac containing HMOs. Lack of Type 1 or 2 LacNac doesn't have any influence on binding since **L19** also shows moderate affinity ($\sim 10^4 \text{ M}^{-1}$) for Gal-1. None of these HMOs have fucosylation or sialylation in their side chain. On the other hand, Gal-1 dimer has more preference for poly N-acetylglucosamine in solid phase assays. It means surface immobilization of glycan helps to understand more about the glycan specificities nature of Gal-1. Surface immobilization has little

importance for studying galectin and HMO interaction as HMOs present as free unit in human milk and free-reducing end lactose unit might play role in modulation of biological activities.

Representative ESI mass spectra acquired for a solution of Gal-1 (3 μM) and 5 μM and 10 μM **L34** (Figure 4.2) in 30 mM aqueous ammonium acetate solution (pH 6.8, 25 °C) reveal that the presence of ions corresponding to the (G1 + $q\text{L3}$) complexes, at charge states +9 – +11, where $q = 1$ (Figure 4.2). The appearance of nonspecific ($\text{P}_{\text{ref}} + q\text{L3}$) ions, where $q = 1$, at charge states +5 and +6, indicates the occurrence of nonspecific binding of **L3** to the Gal-1 complexes during the ESI process. The distribution of **L3** bound specifically to (G1 + $q\text{L3}$) was obtained following correction of the mass spectrum using the P_{ref} method⁶⁵ (inset Figure 4.2). All binding affinities for gal-1 reported in the Table 4.1 are apparent (first binding site).

According to Noll et al. 2016, Gal-1 binding to the HM-SGM-v2 array was weak and broad, with a little preference for branched glycans terminating in Type 1 or Type 2 LacNAc which is not consistent with our result. Linear structure ligands such as: **L1**, **L5**, **L6**, **L9** and **L11** exhibits affinities of $(4.5 \pm 0.8) \times 10^4 \text{ M}^{-1}$, $(2.5 \pm 0.3) \times 10^4 \text{ M}^{-1}$, $(2.4 \pm 0.1) \times 10^4 \text{ M}^{-1}$, $(11.5 \pm 0.2) \times 10^4 \text{ M}^{-1}$ and $(3.9 \pm 0.2) \times 10^4 \text{ M}^{-1}$. Branched structure ligands **L2**, **L4**, **L7**, **L13**, **L14**, **L22**, **L23**, **L28** and **L29** exhibits affinities of $(0.6 \pm 0.02) \times 10^4 \text{ M}^{-1}$, $(0.74 \pm 0.1) \times 10^4 \text{ M}^{-1}$, $(1.4 \pm 0.3) \times 10^4 \text{ M}^{-1}$, $(0.3 \pm 0.1) \times 10^4 \text{ M}^{-1}$, $(0.4 \pm 0.1) \times 10^4 \text{ M}^{-1}$, $(0.3 \pm 0.2) \times 10^4 \text{ M}^{-1}$, $(0.3 \pm 0.1) \times 10^4 \text{ M}^{-1}$, $(0.8 \pm 0.1) \times 10^4 \text{ M}^{-1}$ and $(0.3 \pm 0.1) \times 10^4 \text{ M}^{-1}$ respectively. However, **L8** has strong affinity of $(5.9 \pm 0.4) \times 10^4 \text{ M}^{-1}$. Figure 4.5a shows the direct ESI-MS ($K_{\text{a1,app}}$, M^{-1}) affinities compared to RFU values obtained from HM-SGM-v2 microarray for Gal-1 and 4.5b shows the linear relationship of direct

ESI-MS ($K_{a1,app}$, M^{-1}) affinities and RFU value at highest concentration of 200 $\mu\text{g/ml}$. Binding affinity for **L9** is moderately high (11.5 ± 0.2) $\times 10^4 M^{-1}$ compared to the RFU value. In Figure 4.5c similar comparison was made using defined HMG microarray to ESI-MS affinities. Linear relationship was shown in 4.5d for direct ESI-MS ($K_{a1,app}$, M^{-1}) affinities and RFU value at highest concentration of 200 $\mu\text{g/ml}$. Defined HMG microarray contains both ‘open-ring’ and ‘closed-ring’ structures at the reducing end lactose. ‘Closed-ring’ structure HMOs were derivatized in the similar way as ‘open-ring’ HMOs. It was assumed that ‘closed-ring’ reducing end was essential for HMOs binding. However this structural modification has little influence on the improvement of RFU value. Thus, it explains why HMO binding cannot be improved for Gal-1 through this modification. Glycan microarray Chart ID and structure for all HMOs are given in Table 4.6 and 4.7. Figure 4.20a represents the similar comparison made with the selected HMOs from CFG glycan microarray data V 5.0.

Human galectin 3 (Gal-3C) is one of the best studied galectins with many functions. In this study, a C-terminal fragment of human galectin 3 (Gal-3C) was used. It possesses a single CRD along with a large amino terminal domain and thus forms noncovalent monomer in solution. Gal-3C recognizes both Type 1 and Type 2 LacNac. It has multifaceted specificity for small oligosaccharides. The addition of Neu5Ac(α 2-3/6) changes binding affinity. The addition of GalNAc(α 1-3), similar as blood group A or B determinants, improve binding affinity by 10-25 fold. The addition of GlcNAc(β 1-3) with an additional Gal residue, similar as poly-N-acetyl-lactosaminoglycans also improve binding affinity.⁶⁶

In ESI mass spectra obtained for a solution of Gal-3C (G3, 8 μM) and 20 μM and 40 μM **L3** (Figure 3) in 30 mM aqueous ammonium acetate solution (pH 6.8, 25 $^{\circ}\text{C}$) reveal that the presence of ions corresponding to the ($\text{G3} + q\text{L3}$) complexes, at charge states +7 – +9, where $q = 1-2$. The appearance of nonspecific ($\text{P}_{\text{ref}} + q\text{L3}$) ions, where $q = 1$, at charge states +5 and +6, indicates the occurrence of nonspecific binding of **L3** to the Gal-3C complexes during the ESI process. The distribution of **L3** bound specifically to ($\text{G3} + q\text{L3}$) was obtained following correction of the mass spectrum using the P_{ref} method (inset Figure 4.3a and 4.3b).⁶⁵

Hirabayashi et al. 2002 described the oligosaccharides specificities of several galectins using frontal affinity chromatography. Reported binding affinity of whole galectin-3 was few times higher than Gal-3C. All available HMOs from the oligosaccharide list from Hirabayashi et al. 2002 are in good agreement (Table 4.1). Fluorescence Anisotropy (FA) was also used to describe several oligosaccharides specificities of Gal-3C. Interestingly, binding affinities were overestimated by this method. **L3, L6, L7, L9, L13, L15, L16, L18, L19** and **L30** shows binding affinities of $127 \times 10^4 \text{M}^{-1}$, $154 \times 10^4 \text{M}^{-1}$, $238 \times 10^4 \text{M}^{-1}$, $103 \times 10^4 \text{M}^{-1}$, $303 \times 10^4 \text{M}^{-1}$, $164 \times 10^4 \text{M}^{-1}$, $104 \times 10^4 \text{M}^{-1}$, $59 \times 10^4 \text{M}^{-1}$, $105 \times 10^4 \text{M}^{-1}$ and $36 \times 10^4 \text{M}^{-1}$ respectively.^{33, 66} Nonspecific binding may be the reason for overestimation of affinities.

In this study, direct ESI-MS binding data was compared to RFU values obtained from glycan microarray reported in Noll et al. 2016 using HM-SGM-v2 array and defined HMG microarray for Gal-3C and 32 HMOs. However, whole galectin-3 was used in microarray study and data agreement from the direct comparison between two methods may not depicts the overall specificities of the HMOs. Glycan microarray data described

the binding preference of Gal-3 for minimum three repeating Type 2 LacNAc unit containing HMO structure whereas direct ESI-MS data shows good binding affinity for both linear and branched structure HMOs containing Type 1 and Type 2 LacNAc with Gal-3C. Overall, binding specificities are strong and broad except for some specific linkages which completely destroy the binding of HMOs (**L24-L29**). Interestingly it agrees with the previously reported values obtained by frontal affinity chromatography.³⁴ Data comparison from direct ESI-MS with HM-SGM-v2 microarray and defined HMG microarray show very poor agreement. Hirabayashi et al. 2002 showed weaker binding affinities for whole Gal-3 compared to Gal-3C. It can be justified by the comparisons of the binding affinities by glycan microarray method and ESI-MS method in the Figure 4.6. Figure 4.20b represents the similar comparison made with the selected HMOs from CFG glycan microarray data V 5.0. This comparison shows some similar trend in ESI-MS vs microarray data. However, values obtained from microarray data are poor and very similar to background level. So it can be concluded that, RFU values obtained for Gal-3C CFG glycan microarray data V 5.0 are not reliable.³⁹

Glycan microarray studies described that the oligosaccharide ligands for tandem repeat Gal-9 are still unclear because of two non-identical CRDs. So, high concentration (20 $\mu\text{g/ml}$ and 200 $\mu\text{g/ml}$) of whole Gal-9 was not used in glycan microarray studies. But biochemical studies have found that both the N-terminal CRD (NCRD) and C-terminal CRD (CCRD) of human galectin-9 show high affinity for repeating Type 2 LacNAc residues (poly-*N*-acetyllactosamine).³⁴

ESI mass spectra acquired for solution of Gal-9N (G9, 10 μM) and 8 μM and 15 μM **L3** (Figure 4.4) in 30 mM aqueous ammonium acetate solution (pH 6.8, 25 °C)

reveal that the presence of ions corresponding to the (G9 + $q\mathbf{L3}$) complexes, at charge states +7 – +9, where $q = 1-2$. The appearance of nonspecific ($P_{\text{ref}} + q\mathbf{L3}$) ions, where $q = 0$, at charge states +5 and +6, indicates the occurrence of nonspecific binding of $\mathbf{L3}$ to the Gal-9N complexes during the ESI process. The distribution of $\mathbf{L3}$ bound specifically to (G9 + $q\mathbf{L3}$) was obtained following correction of the mass spectrum using the P_{ref} method (inset Figure 4.4a and 4.4b).⁶⁵

Hirabayashi et al. 2002 reported the oligosaccharides specificities of both whole Gal-9 and Gal-9N using frontal affinity chromatography where reported binding affinity of whole Gal-9 was few times higher than Gal-9N due to presence of two non-identical CRD (N-terminal and C-terminal) in this tandem repeat galectin. It was reported that both of the CRDs are required for biological activity.²⁶ All available HMOs binding affinities from Hirabayashi et al. 2002 are in good agreement with ESI-MS data (Table 4.1).

Data obtained from ESI-MS study for gal-9N was compared with HM-SGM-v2 microarray and defined HMG microarray data obtained for Gal-9 and same HMOs. Due to difference in nature of the galectins used in both methods, values are in poor agreement. Glycan microarray affinities are mostly at background level for whole Gal-9. Figure 4.20c showed the comparison of ESI-MS data with CFG glycan microarray data V 5.0. ESI-MS study showed high affinity for several HMOs and no affinity for other HMOs. It depicts the specificity of Gal-9N for various HMOs.

Galacto-oligosaccharide (GOS) and fructo-oligosaccharide (FOS) binding specificity of Galectins

Galacto-oligosaccharide (GOS) and fructo-oligosaccharide (FOS) are soluble non-digestible carbohydrates which have core molecular structural similarities with HMOs.

Both of the GOS and FOS respectively contain chain of galactose and chain of fructose with glucose at the end. GOS boosts the growth of Bifidobacteria and Lactobacilli,⁶⁷⁻⁶⁹ and thus contributes to the natural defences of human.⁷⁰⁻⁷³ It also plays a role in normal gut transit⁷⁴⁻⁷⁷ and enhancement of mineral absorption.⁷⁸⁻⁸² FOS is included in food products and infant formulas because of its prebiotic effect, i.e., stimulatory effects on the growth of nonpathogenic intestinal microbes.⁸³ Mixture of GOS and FOS has been suggested as an alternative to HMOs for infant formula supplementation.⁸⁴

Noll et al. 2016 described that, semi-purified GOS fractions has no binding with galectins on the defined HMO microarray. Here they suggested that there is less chance of modulation of galectins activities by HMOs. While testing the binding affinity of both FOS and GOS with three available galectins (Gal-1, Gal-3C and Gal-9N) glycan array data was taken into account, and interestingly bindings of variable strength were found.

ESI-MS binding measurements were performed on available 3 galectins and individual FOSs (**L34-L37**) in 30 mM aqueous ammonium acetate solution (pH 6.8, 25 °C). The structures of **L34-L37** are given in Figure 4.12. Representative ESI mass spectra acquired for solution containing Gal-3C and **L34** are shown in Figure 4.10. Figures 4.18 for Gal-1 and **L34**; Figure 4.19 for Gal-9N and **L34** represent two other galectins. After correction of the mass spectra for the presence of nonspecific FOS-protein binding during the ESI process,⁶⁵ $K_{a,app}$ values were calculated from the relative abundances of the free and ligand-bound protein ions (Table 4.2).

Data investigation from the Table 4.2 reveals that the both of the Gal-1 and Gal-9N have binding with the 4 FOSs present in the study. Nevertheless, Gal-3C doesn't show binding with any of them. Measured affinities are relatively low, with $K_{a,app}$ ranging

from 2000 M^{-1} to 4000 M^{-1} for Gal-1 and 100 M^{-1} to 1000 M^{-1} for Gal-9N. Inspection of the ESI mass spectra acquired for a solution of Gal-3C ($5 \text{ }\mu\text{M}$) and $20 \text{ }\mu\text{M}$ and $40 \text{ }\mu\text{M}$ **L34** (Figure 4.10) in 30 mM aqueous ammonium acetate solution ($\text{pH } 6.8$, $25 \text{ }^\circ\text{C}$) reveal that the presence of ions corresponding to the $(\text{G3} + q\text{L34})$ complexes, at charge states $+7 - +9$, where $q = 1$ (Figure 7). The appearance of nonspecific ($\text{P}_{\text{ref}} + q\text{L34}$) ions, where $q = 1$, at charge states $+5$ and $+6$, indicates the occurrence of nonspecific binding of **L34** to the Gal-3C complexes during the ESI process. The distribution of **L34** bound specifically to $(\text{G3} + q\text{L34})$ was obtained following correction of the mass spectrum using the P_{ref} method⁶⁵ (inset Figure 4.10a and 4.10b). It can be seen that there is no visible binding was observed after nonspecific binding correction.

Similarly, ESI-MS binding measurements were carried out on available 3 galectins and Vivinal GOS 90 powder (G_{px}) and Vivinal GOS syrup (G_{sx}). GOS mixtures were diluted before performing the ESI-MS experiments. GOS content of the Vivinal GOS 90 powder is 69% whereas it is 59% on dry matter weight of Vivinal GOS syrup (Product data sheet from FrieslandCampina Domo). Due to the lack of known concentration of GOSs in mixture, binding affinity ($\text{K}_{\text{a,app}}$, M^{-1}) calculations were not possible. However, it is possible to calculate the abundance ratio (R) of the ligand bound (PL_q) to free protein (P) after correction for nonspecific binding.

Shown in Figures 4.8 and 4.9 are ESI mass spectra acquired for the Gal-3C ($5 \text{ }\mu\text{M}$) with 0.05 g/L and 0.1 g/L Vivinal GOS 90 powder and 6000 and 1200 time diluted Vivinal GOS syrup respectively. Protonated ions corresponding to G3-L_x (where, $\text{L}_x = \text{GOS1-GOS6}$) complexes, at charge states $+7 - +9$ were detected in both cases for dry powder and syrup. The distributions of specifically bound L_x , obtained from the mass

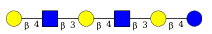
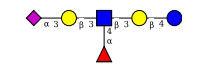
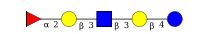
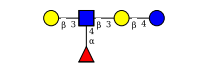


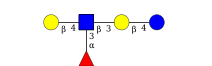
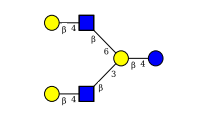

spectra following correction for nonspecific binding (inset, Figures 8a, 8b and 9a, 9b) confirms that L_x can bind to gelatins. Interestingly, total 6 different GOS were detected as complex with galectins. For example, at G_{px} concentration of 0.1 g/L, the corresponding R values are in the range of 0.02 ± 0.00 to 0.12 ± 0.01 whereas ~ 1200 times diluted G_{sx} show R values are in the range of 0.05 ± 0.01 to 0.58 ± 0.04 for different component of L_x (Figure 8b and 9b) for Gal-3C. Similar results were obtained for other two galectins (Gal-1 and Gal-9N) bound to L_x (Figures 4.14 – 4.17).

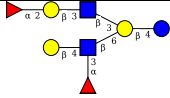
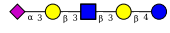
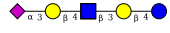
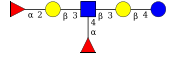
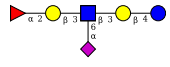
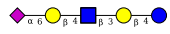
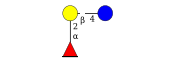
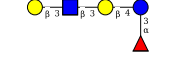


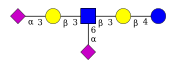
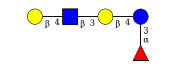
From the above discussion, it can be concluded that further studies are required using whole galectin-3 and whole galectin-9 to reliably comment on the binding specificities of oligosaccharide using ESI-MS method. It is apparent that ESI-MS is more sensitive, reliable and versatile for protein-carbohydrate binding measurement. But it was not thoroughly studied how glycan conjugation affects the interaction in glycan microarray studies. Further studies are required to comment on the effect of glycan conjugation on the binding affinities.

4.4 Conclusions

In summary, the affinities of 32 of the most abundant HMOs for Gal-1, Gal-3C and Gal-9N were quantified for the first time using direct ESI-MS. It was found that each lectin binds to the majority of the HMOs tested in this study, even though binding affinities are very diverse for HMOs. In addition, study of GOS and FOS binding with galectin shows weak affinity. These results suggest that distinct nature of interaction HMOs might have influence on immunomodulation and benefit of child health. Moreover, comparison of the ESI-MS to glycan microarray study shows the binding data reliability of the ESI-MS over glycan microarray for study of glycan-protein interaction.

Table 4.1. Apparent association constants, $K_{a,app}$ (units of 10^4 M^{-1}) for binding of the HMOs (**L1 – L32**) to Gal3C, Gal1 and Gal9N determined in 20 mM aqueous ammonium acetate at 25 °C and pH 7.2 by the direct ESI-MS assay.^{1,2,3}

Structure	HMO	Gal3C		Gal1		Gal9N	
		$K_{a, app} (\text{M}^{-1})$	$K_a (\text{M}^{-1})$	$K_{a1, app} (\text{M}^{-1})$	$K_a (\text{M}^{-1})$	$K_{a, app} (\text{M}^{-1})$	$K_a (\text{M}^{-1})$
		(ESI-MS)	Others ^{1,2}	(ESI-MS)	Others ^{1,2}	(ESI-MS)	Others ^{1,2}
	L1	9.3 ± 0.2		4.5 ± 0.8		7.0 ± 0.8	
	L2	6.6 ± 0.2		0.6 ± 0.02		35.6 ± 0.2	
	L3	8.6 ± 0.1	20^1	1.32 ± 0.3	1.7^1	24.7 ± 2.0	26.3^1
	L4	12.0 ± 0.6	5^1	0.74 ± 0.1	NB ¹	41.5 ± 2.0	25.6^1
	L5	13.0 ± 1.0		2.5 ± 0.3		3.5 ± 0.1	
	L6	9.2 ± 0.3	13^1	2.4 ± 0.1	2^1	12.0 ± 0.5	24.4^1
	L7	12.0 ± 0.8	11^1	1.4 ± 0.3	NB ¹	13.5 ± 0.8	10.6^1
	L8	6.3 ± 0.4		5.9 ± 0.4		0.9 ± 0.1	
	L9	6.0 ± 0.1	10^1	11.5 ± 0.2	1.6^1	6.3 ± 0.3	20.8^1

Structure	HMO	Gal3C		Gal1		Gal9N	
		$K_{a, app} (M^{-1})$ (ESI-MS)	$K_a (M^{-1})$ Others ^{1,2}	$K_{a1, app} (M^{-1})$ (ESI-MS)	$K_a (M^{-1})$ Others ^{1,2}	$K_{a, app} (M^{-1})$ (ESI-MS)	$K_a (M^{-1})$ Others ^{1,2}
	L10	5.8 ± 0.1		2.4 ± 0.2		1.4 ± 0.3	
	L11	5.6 ± 0.2		3.9 ± 0.2		7.0 ± 1.1	
	L12	5.4 ± 0.2		1.8 ± 0.2		1.0 ± 0.1	
	L13	4.2 ± 0.1		0.3 ± 0.1		6.6 ± 1.1	
	L14	4.0 ± 0.1		0.4 ± 0.1		1.1 ± 0.1	
	L15	2.2 ± 0.1		0.4 ± 0.1		13.0 ± 1.2	
	L16	2.1 ± 0.2	1.1 ¹	1.9 ± 0.1	NB ¹	NB	NB ¹
	L17	2.1 ± 0.2		1.5 ± 0.1		1.2 ± 0.1	
	L18	2.0 ± 0.1	0.4 ¹	1.9 ± 0.2	NB ¹	NB	0.3 ¹
	L19	1.5 ± 0.1		0.8 ± 0.1		4.8 ± 0.4	
	L20	3.3 ± 0.2		0.4 ± 0.1		NB	
	L21	1.3 ± 0.1		1.6 ± 0.2		0.6 ± 0.1	

Structure	HMO	Gal3C		Gal1		Gal9N	
		$K_{a, app} (M^{-1})$ (ESI-MS)	$K_a (M^{-1})$ Others ^{1,2}	$K_{a1, app} (M^{-1})$ (ESI-MS)	$K_a (M^{-1})$ Others ^{1,2}	$K_{a, app} (M^{-1})$ (ESI-MS)	$K_a (M^{-1})$ Others ^{1,2}
	L22	1.0 ± 0.1		0.3 ± 0.2		0.7 ± 0.1	
	L23	0.2 ± 0.1		0.3 ± 0.1		1.7 ± 0.2	
	L24	NB		0.4 ± 0.1		NB	
	L25	NB	NB ¹	0.6 ± 0.1	NB ¹	NB	NB ¹
	L26	NB		0.2 ± 0.0		NB	
	L27	NB		0.2 ± 0.1		NB	
	L28	NB		0.8 ± 0.1		NB	
	L29	NB		0.3 ± 0.1		NB	
	L30	0.2 ± 0.1	0.4 ¹	0.9 ± 0.1	NB ¹	0.3 ± 0.1	1.0 ¹
	L31	8.4 ± 0.2		1.3 ± 0.1		11 ± 0.6	
	L32	9.0 ± 0.6		0.5 ± 0.1		20 ± 0.4	

¹Hirabayashi et al. 2002, ³ Errors correspond to one standard deviation

Table 4.2. Association constants ($K_{a,app}$) measured by ESI-MS for the interactions of ligand **L34-L37** with Gal1, Gal-3C and Gal-9N in aqueous ammonium acetate solutions at pH 6.8 and 25 °C.^a

Elicityl Code	Ligand	$K_{a1,app}$	$K_{a,app}$	$K_{a,app}$
		(Gal-1)/M ⁻¹	(Gal-3C)/M ⁻¹	(Gal-9N)/M ⁻¹
Fru111	L34	$(2.3 \pm 0.3) \times 10^3$	NB	$(0.3 \pm 0.1) \times 10^3$
Fru112	L35	$(2.4 \pm 0.8) \times 10^3$	NB	$(0.2 \pm 0.05) \times 10^3$
Fru113	L36	$(2.7 \pm 0.2) \times 10^3$	NB	$(0.2 \pm 0.05) \times 10^3$
Fru114	L37	$(3.5 \pm 0.7) \times 10^3$	NB	$(0.7 \pm 0.3) \times 10^3$

a. Errors correspond to one standard deviation. b. NB = No binding

Figure captions

Figure 4.1. Structures of the oligosaccharides **L1 – L32**. Monosaccharide key: Glucose (●), galactose (○), N-acetylgalactosamine (■), N-acetylglucosamine (■), sialic acid(◆), fucose (▲).

Figure 4.2. ESI mass spectra in positive ion mode for a 30 mM aqueous ammonium acetate solution (pH 6.8, 25 °C) of Gal-1 (G1, 3 μM) and P_{ref} (2 μM) with (a) 5 μM **L3** or (b) 10 μM **L3**. Insets show normalized distribution of free and ligand-bound Gal-1 before (■) and after (■) correction for nonspecific ligand binding.

Figure 4.3. ESI mass spectra in positive ion mode for a 30 mM aqueous ammonium acetate solution (pH 6.8, 25 °C) of Gal-3C (G3, 8 μM) and P_{ref} (3 μM) with (a) 20 μM **L3** or (b) 40 μM **L3**. Insets show normalized distribution of free and ligand-bound Gal-3C before (■) and after (■) correction for nonspecific ligand binding.

Figure 4.4. ESI mass spectra in positive ion mode for a 30 mM aqueous ammonium acetate solution (pH 6.8, 25 °C) of Gal-9N (G9, 10 μM) and P_{ref} (2 μM) with (a) 8 μM **L3** or (b) 15 μM **L3**. Insets show normalized distribution of free and ligand-bound Gal-9N before (■) and after (■) correction for nonspecific ligand binding.

Figure 4.5. Summary of the comparison of the ESI-MS ($K_{a,app}$, M^{-1}) and RFU value obtained from HMO microarray for Gal-1. HM-SGM-v2 microarray data compared to ESI-MS ($K_{a,app}$, M^{-1}) are presented at (a) three concentration (2, 20 and 200 μg/ml) (b) one highest concentration (200 μg/ml) available. Defined HMG microarray compared to ESI-MS ($K_{a,app}$, M^{-1}) are presented at (c) three concentration (2, 20 and 200 μg/ml) (d) one highest concentration (200 μg/ml) available. Chart ID for HM-SGM-v2 are taken from supplementary data on Table 4.6 and Chart

ID for Defined HMG microarray are taken from supplementary data on Table 4.7. Errors correspond to one standard deviation.

Figure 4.6. Summary of the comparison of the ESI-MS ($K_{a,app}$, M^{-1}) and RFU value obtained from HMO microarray for Gal-3C. HM-SGM-v2 microarray data compared to ESI-MS ($K_{a,app}$, M^{-1}) are presented at (a) three concentration (2, 20 and 200 $\mu\text{g/ml}$) (b) one highest concentration (200 $\mu\text{g/ml}$) available. Defined HMG microarray compared to ESI-MS ($K_{a,app}$, M^{-1}) are presented at (c) three concentration (2, 20 and 200 $\mu\text{g/ml}$) (d) one highest concentration (200 $\mu\text{g/ml}$) available. Chart ID for HM-SGM-v2 are taken from supplementary data on Table 4.6 and Chart ID for Defined HMG microarray are taken from supplementary data on Table 4.7. Errors correspond to one standard deviation.

Figure 4.7. Summary of the comparison of the ESI-MS ($K_{a,app}$, M^{-1}) and RFU value obtained from HMO microarray for Gal-9N. HM-SGM-v2 microarray data compared to ESI-MS ($K_{a,app}$, M^{-1}) are presented at (a) two concentration (2 and 20 $\mu\text{g/ml}$) (b) one highest concentration (20 $\mu\text{g/ml}$) available. Defined HMG microarray compared to ESI-MS ($K_{a,app}$, M^{-1}) are presented at (c) one concentration (2 $\mu\text{g/ml}$) (d) one highest concentration (2 $\mu\text{g/ml}$) available. Chart ID for HM-SGM-v2 are taken from supplementary data on Table 4.6 and Chart ID for Defined HMG microarray are taken from supplementary data on Table 4.7. Errors correspond to one standard deviation.

Figure 4.8. ESI mass spectra in positive ion mode for a 30 mM aqueous ammonium acetate solution (pH 6.8, 25 °C) of Gal-3C (G3, 5 μM) and P_{ref} (2 μM) with (a) 0.05 g/L or (b) 0.1 g/L diluted solution of Vivinal GOS 90 powder. Insets show normalized distribution of free and ligand-bound Gal-3C before (■) and after (●) correction for nonspecific ligand binding.

Figure 4.9. ESI mass spectra in positive ion mode for a 30 mM aqueous ammonium acetate solution (pH 6.8, 25 °C) of Gal-3C (G3, 5 μ M) and P_{ref} (2 μ M) with (a) \sim 6000 times or (b) \sim 1200 times diluted solution of Vivinal GOS syrup. Insets show normalized distribution of free and ligand-bound Gal-3C before (■) and after (■) correction for nonspecific ligand binding.

Figure 4.10. ESI mass spectra in positive ion mode for a 30 mM aqueous ammonium acetate solution (pH 6.8, 25 °C) of Gal-3C (G3, 5 μ M) and P_{ref} (3 μ M) with (a) 20 μ M **L34** or (b) 40 μ M **L34**. Insets show normalized distribution of free and ligand-bound Gal-3C before (■) and after (■) correction for nonspecific ligand binding.

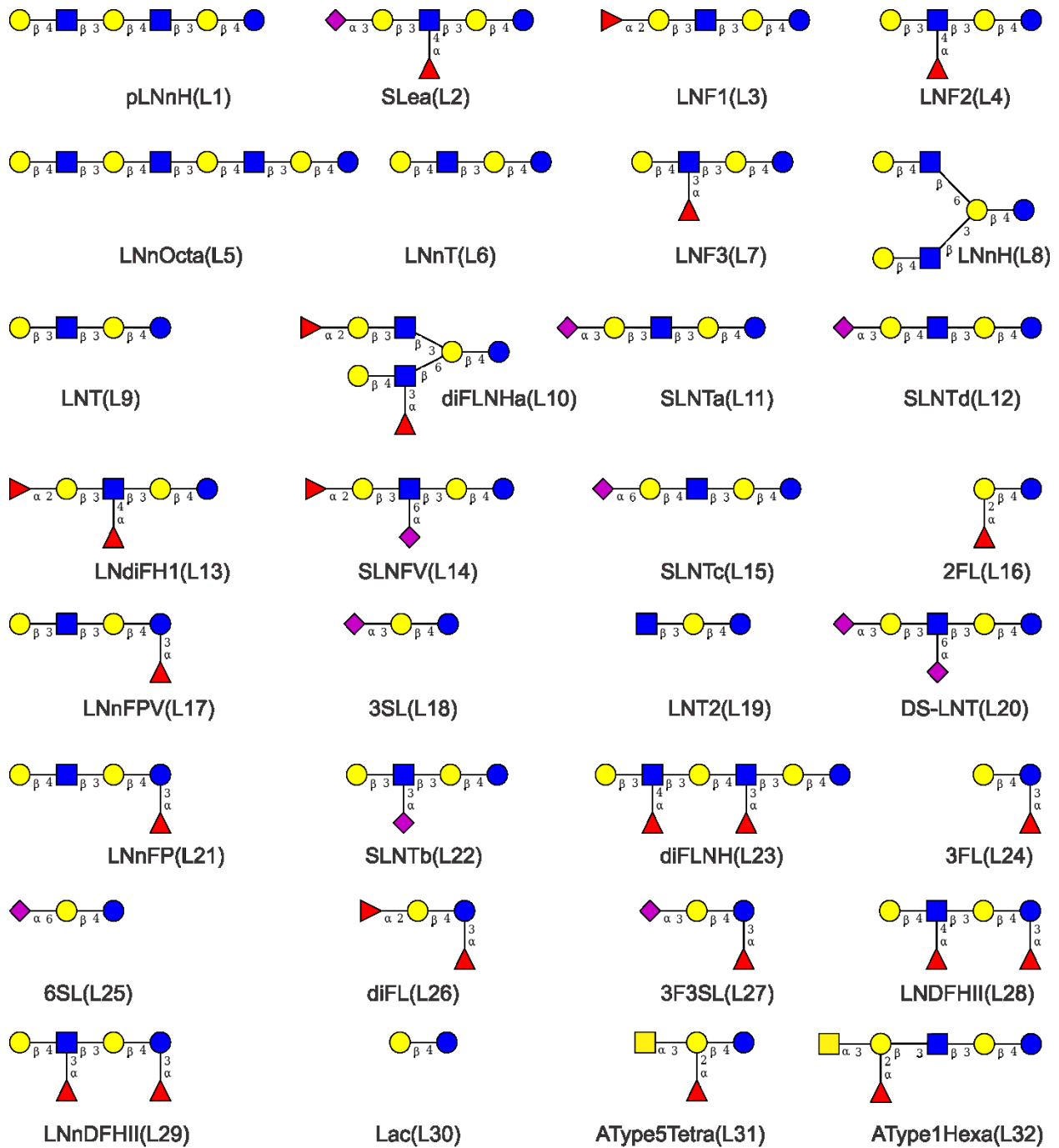


Figure 4.1.

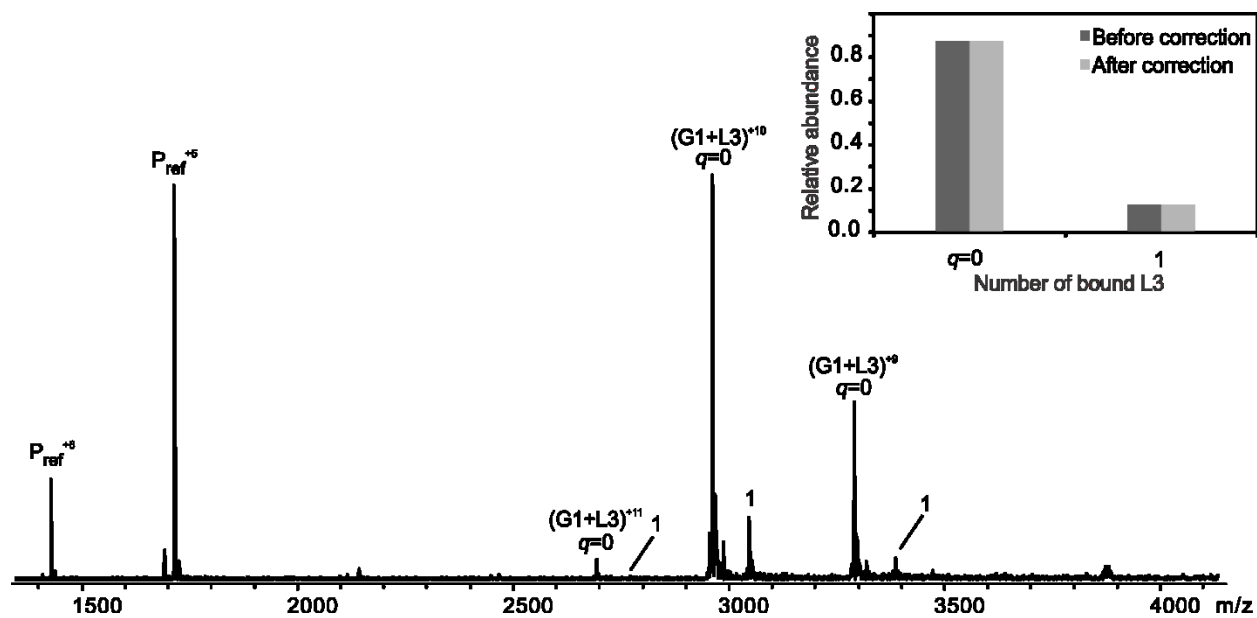
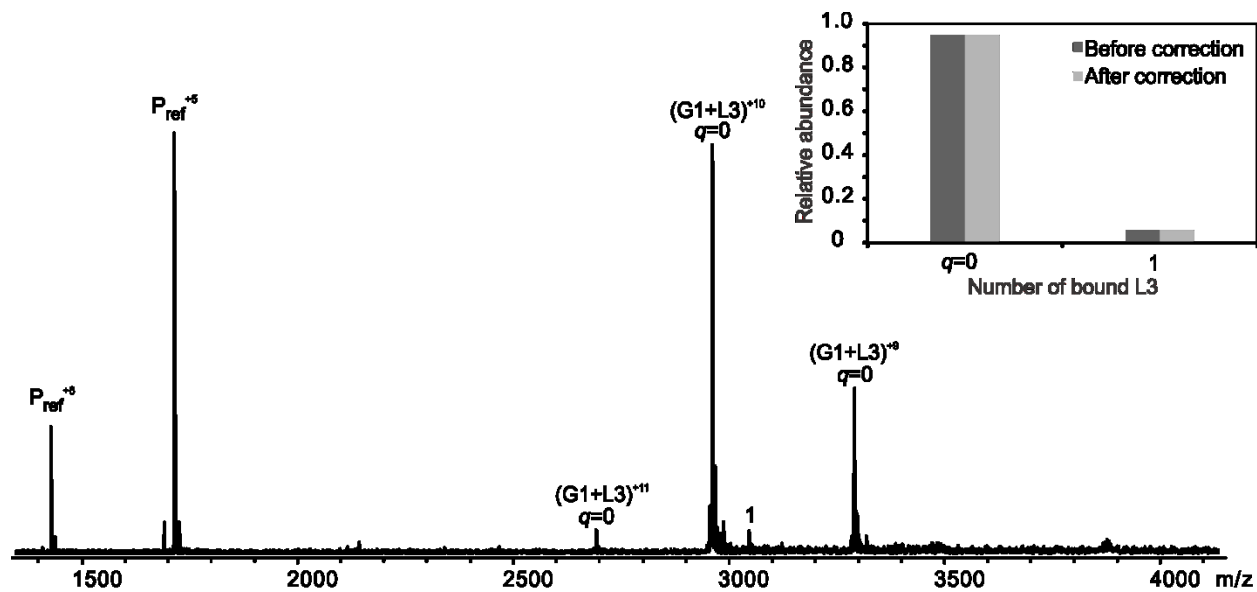


Figure 4.2.

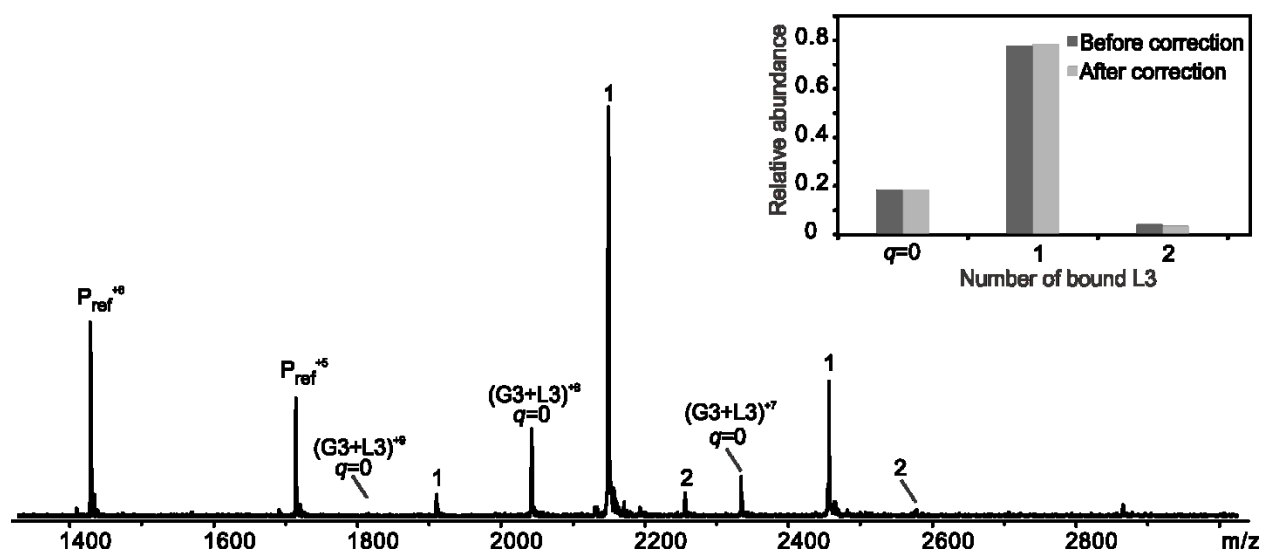
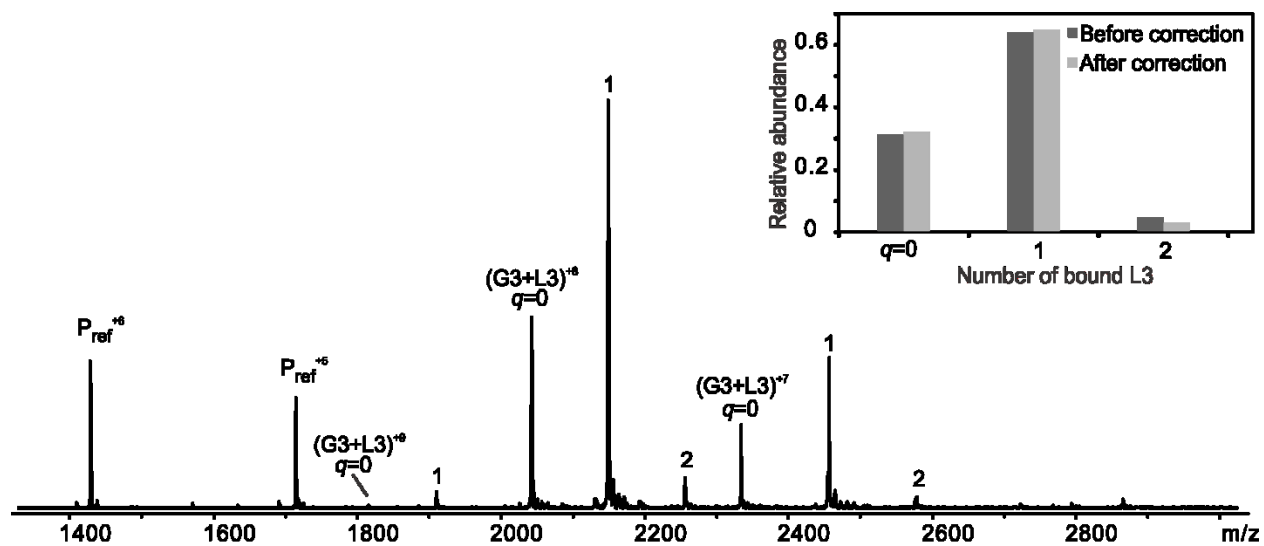


Figure 4.3.

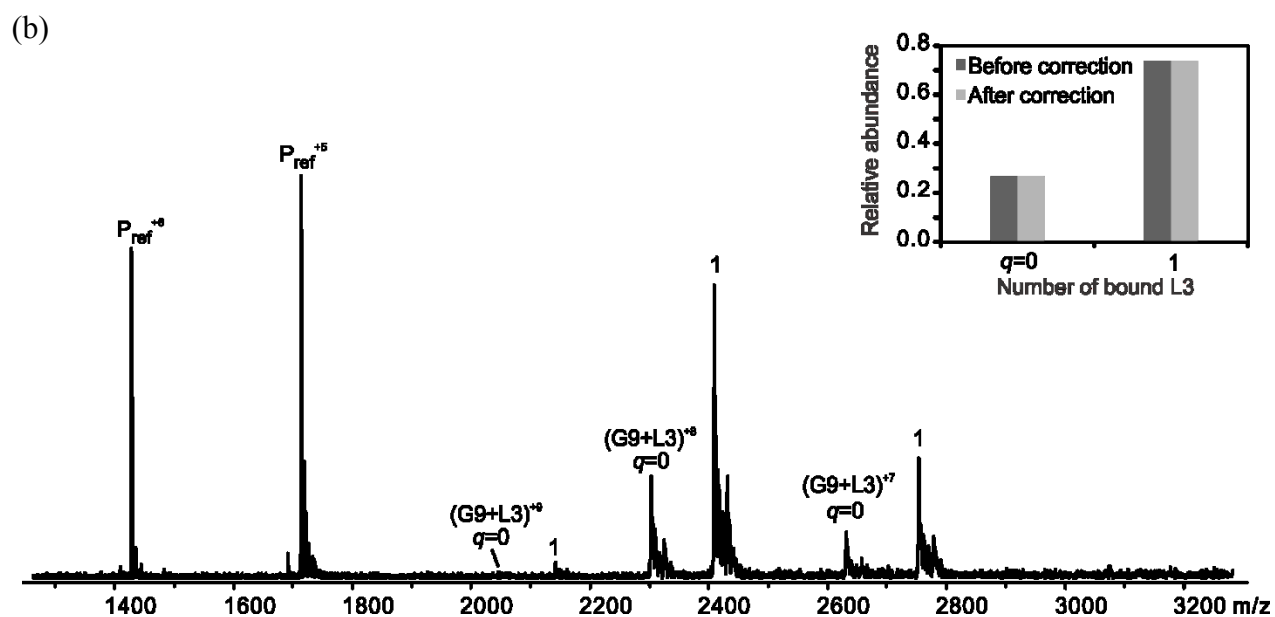
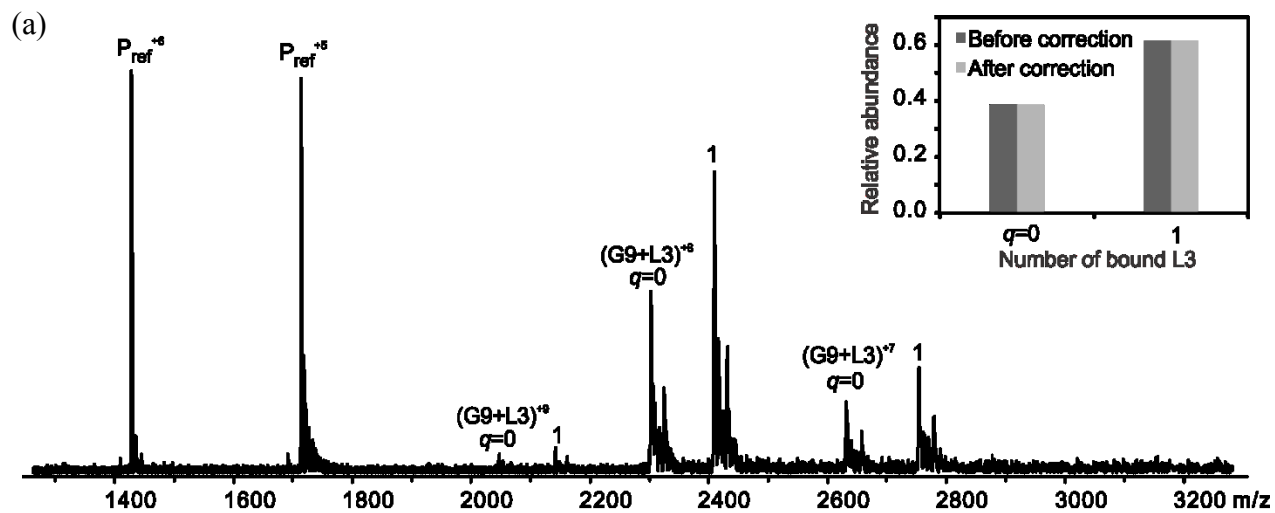


Figure 4.4.

Gal-1

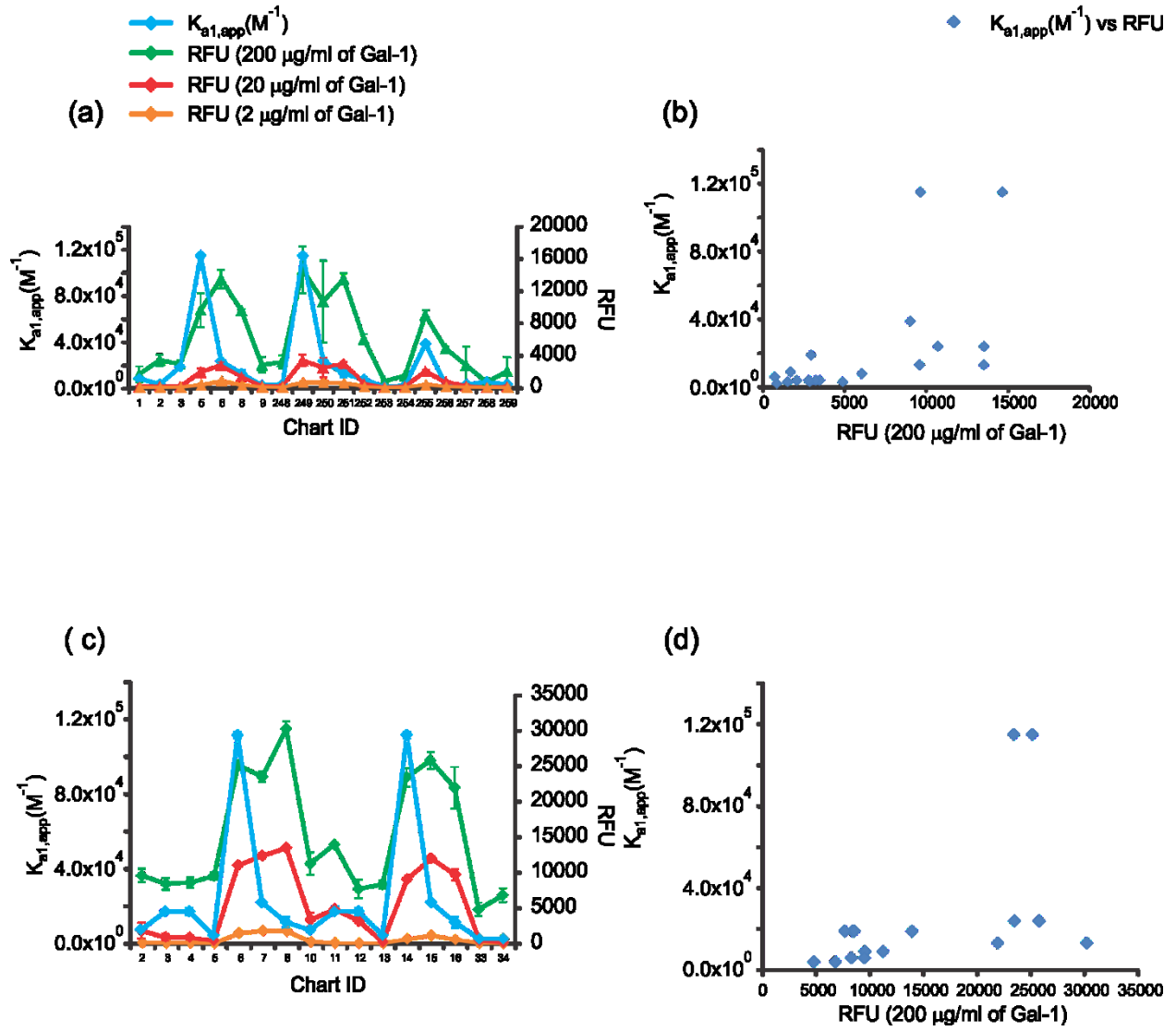


Figure 4.5.

Gal-3C

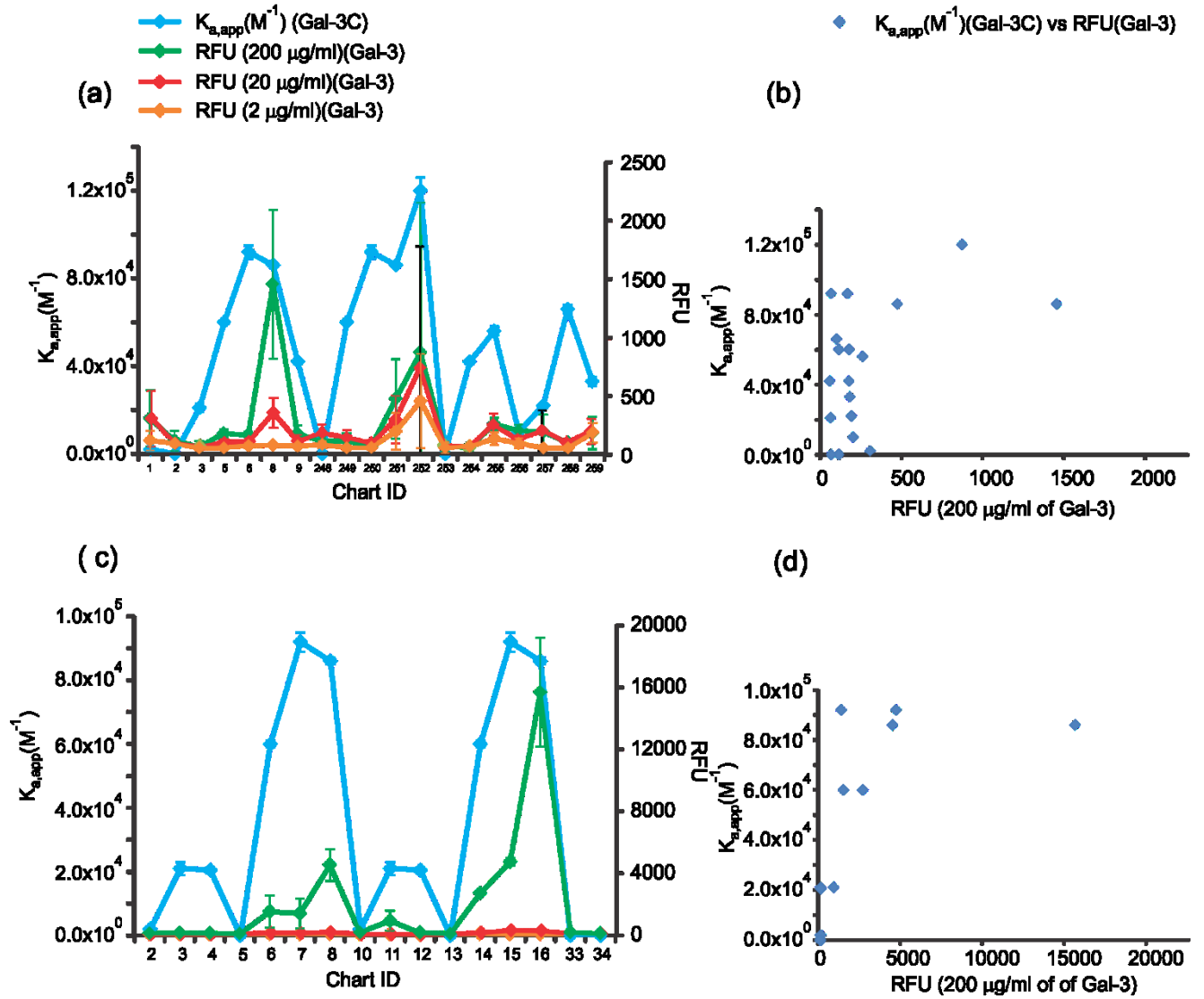


Figure 4.6.

Gal-9N

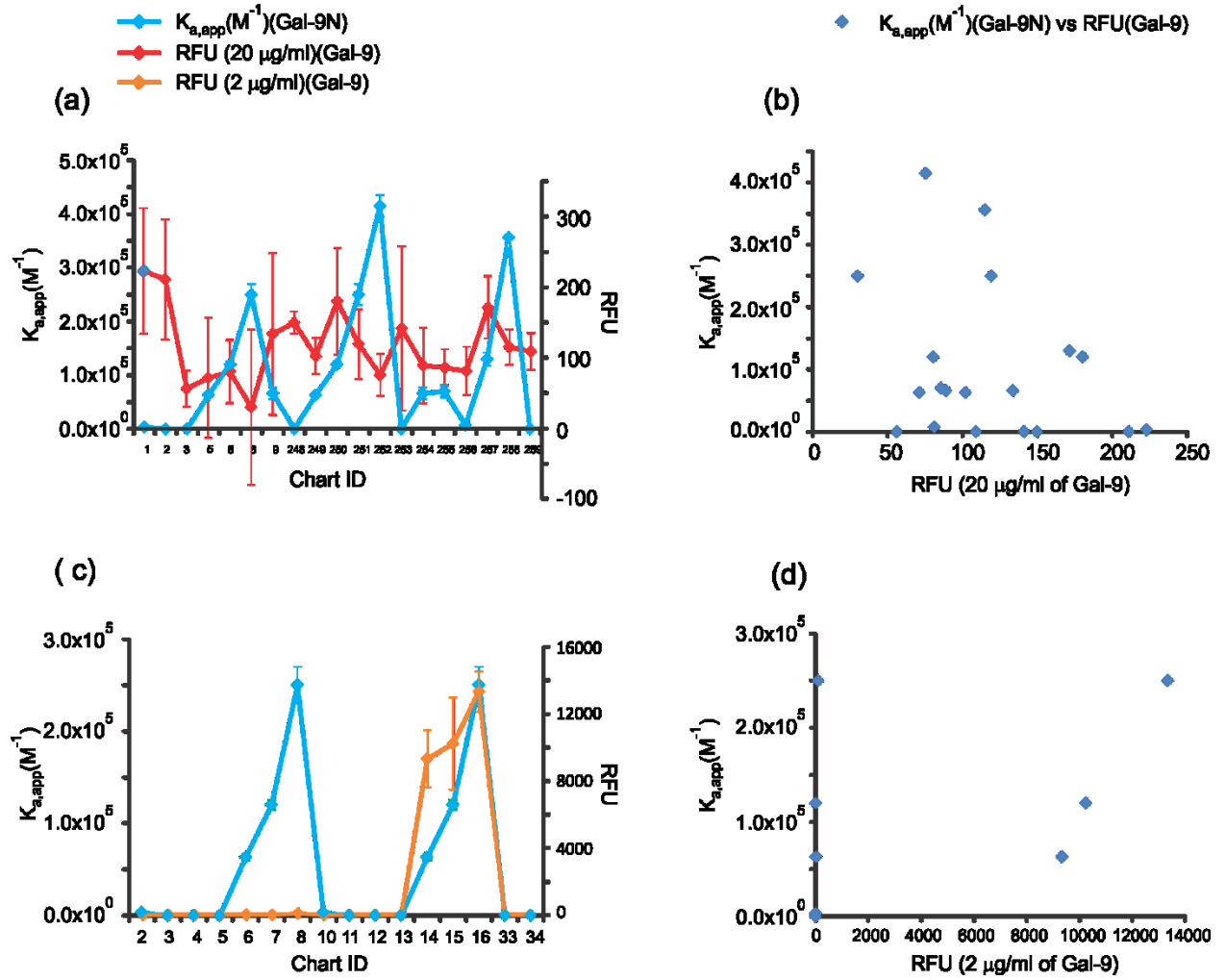


Figure 4.7.

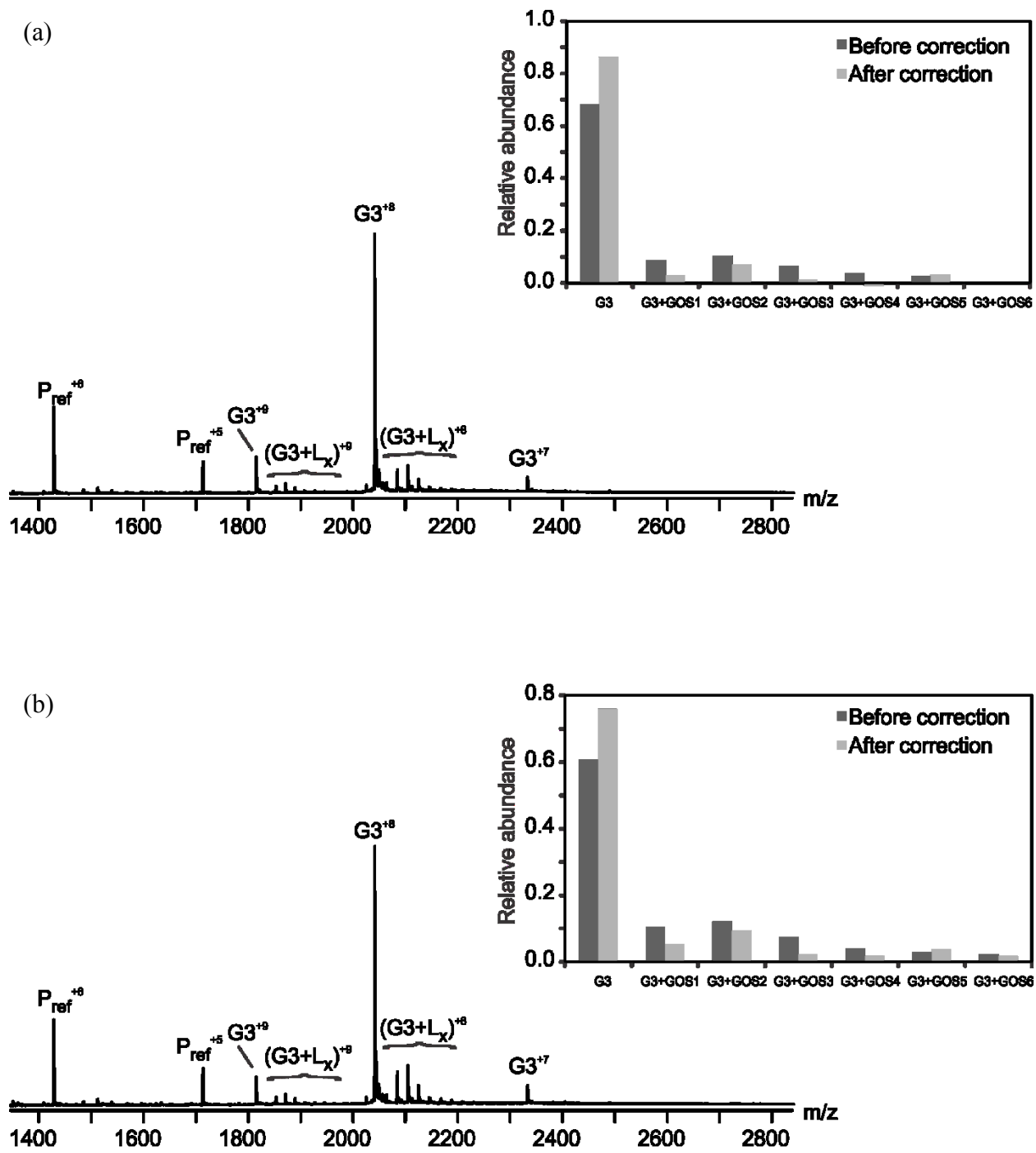


Figure 4.8.

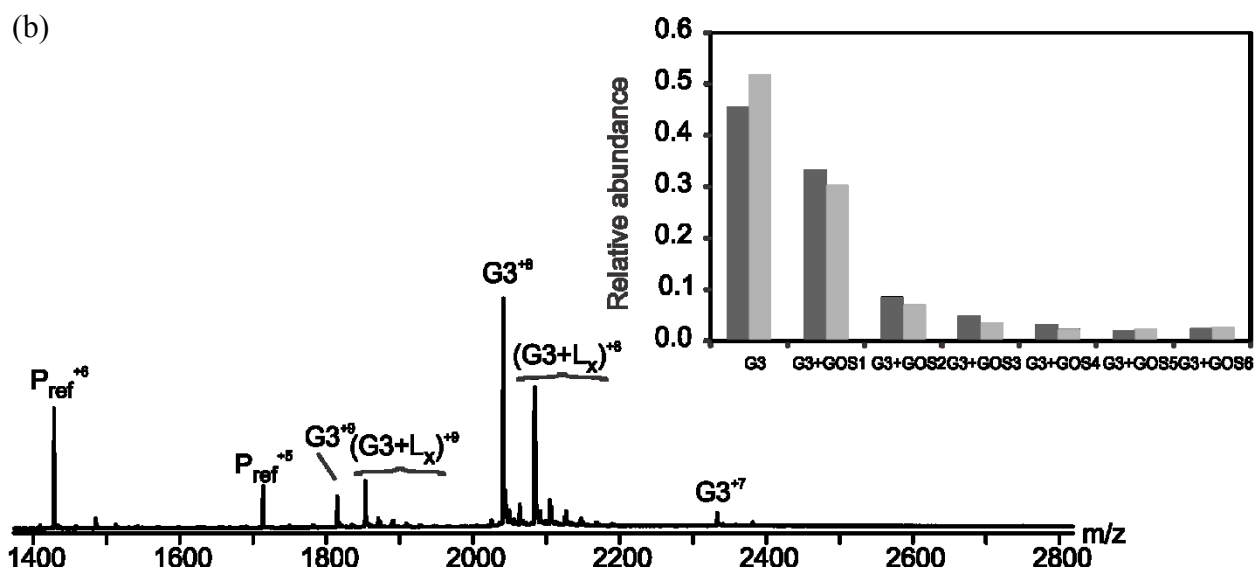
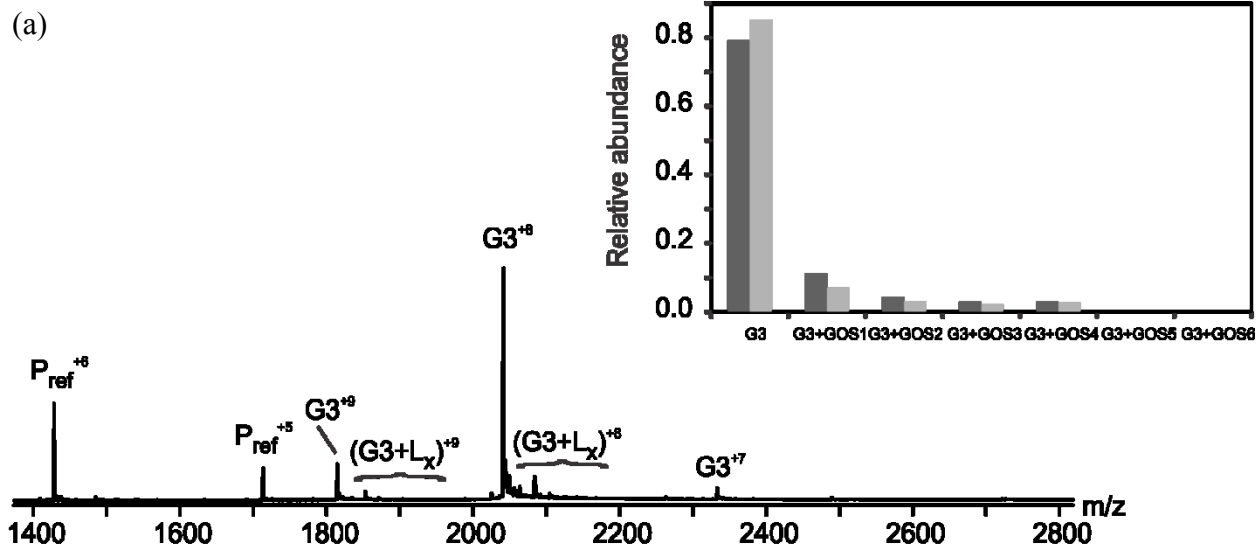


Figure 4.9.

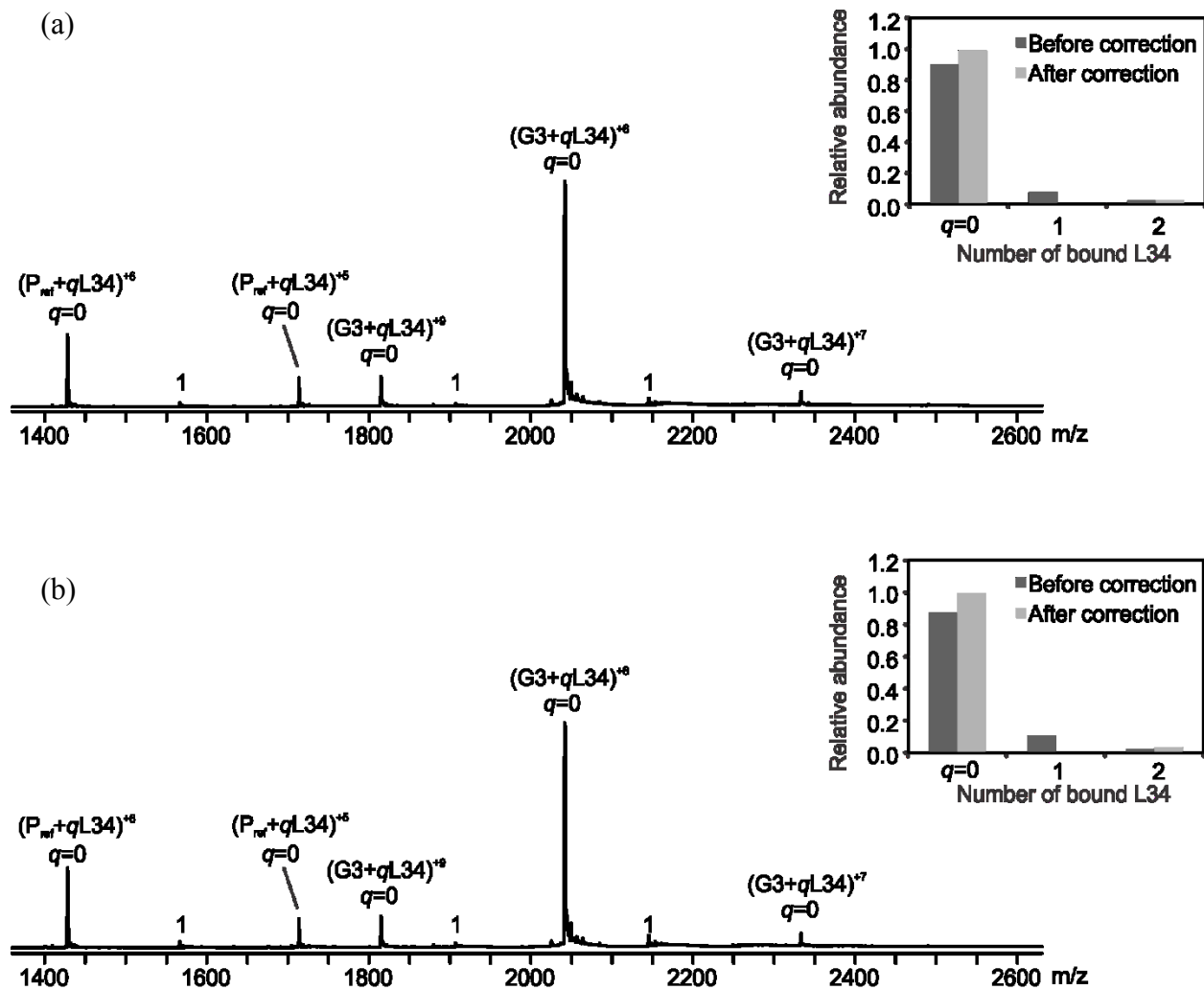


Figure 4.10.

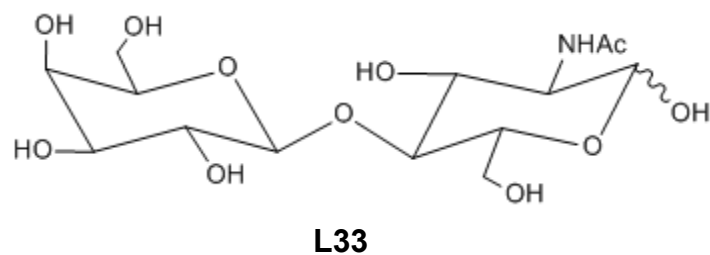
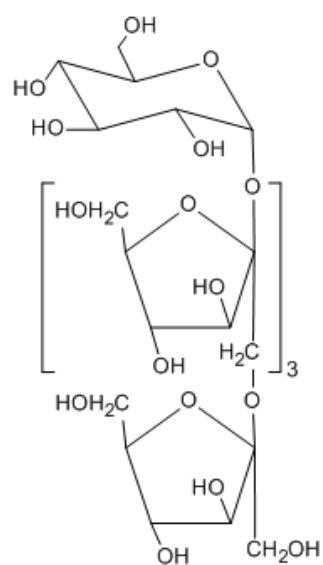


Figure 4.11. Structure of the **L33** (β -D-Gal-(1 \rightarrow 4)- β -D-GlcNAc).

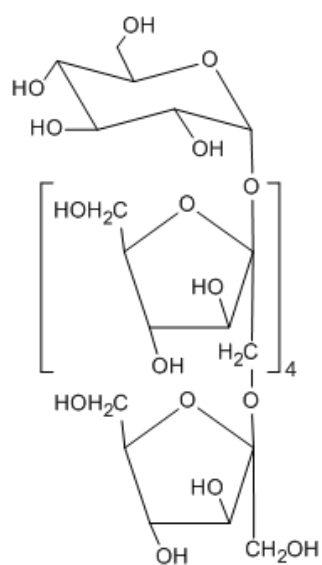
Table 4.3. Association constants (K_a) measured by ESI-MS for the interactions of ligand **L33** with Gal1, Gal-3C and Gal-9N in aqueous ammonium acetate solutions at pH 6.8 and 25 °C.^a

Elicityl Code	Ligand	K_a (Gal-1)/M ⁻¹	K_a (Gal-3C)/M ⁻¹	K_a (Gal-9N)/M ⁻¹
Gly008	L33	$(2.3 \pm 0.3) \times 10^3$	$(1.3 \pm 0.1) \times 10^4$	$(2.3 \pm 0.1) \times 10^4$

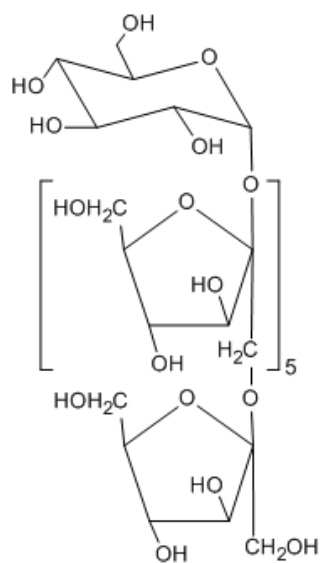
a. Errors correspond to one standard deviation. b. NB = No binding



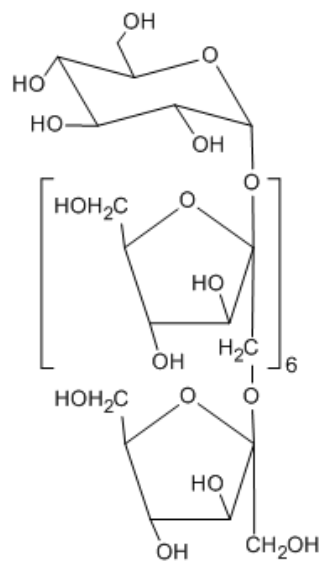
L34



L35



L36



L37

Figure 4.12. Structure of the of fructo-oligosaccharides; **L34** (β -D-Fru-(2 \rightarrow 1)-[β -D-Fru-(2 \rightarrow 1)]₃- α -D-Glc), **L35** (β -D-Fru-(2 \rightarrow 1)-[β -D-Fru-(2 \rightarrow 1)]₄- α -D-Glc), **L36**(β -D-Fru-(2 \rightarrow 1)-[β -D-Fru-(2 \rightarrow 1)]₅- α -D-Glc), **L37** (β -D-Fru-(2 \rightarrow 1)-[β -D-Fru-(2 \rightarrow 1)]₆- α -D-Glc).

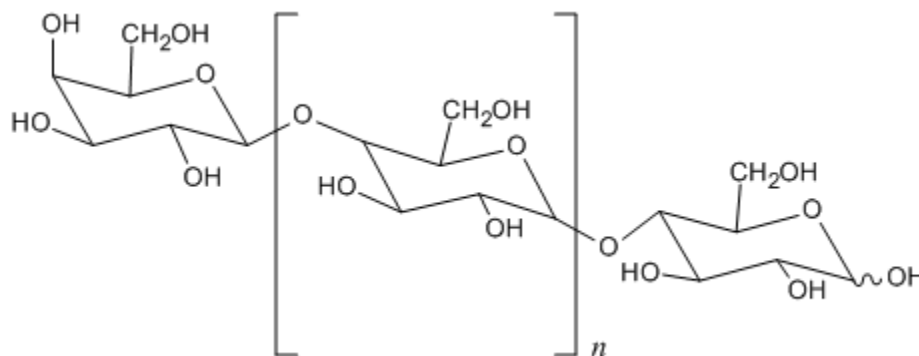


Figure 4.13. Structure of galacto-oligosaccharides ($n = 0-6$).

HMO classification:

Different HMOs are formed by the addition of diverging number of Neu5Ac and Fuc units. Our library contains total 32 HMOs. HMOs contain lactose at reducing end and they are further naturally modified to contain N-acetylglucosamine (GlcNAc), galactose (Gal), fucose (Fuc) and/or sialic acid (as N-acetylneuraminic acid; Neu5Ac).

Among them SLea (L2), LNF1 (L3), LNF2 (L4), LNT (L9), LSa (L11), LND1 (L13), SLNFV (L14), LNnFPV (L17), DS-LNT (L20), LSb (L22), LNDFHII (L28) and AT1 hexa (L32) are of type 1; pLNnH (L1), LNnOcta (L5), LNnT (L6), LNF3 (L7), LNnH (L8), sLNTd(L12), LSc (L15), LNnFP (L21) and LNnDFHII (L29) are of type 2 HMOs; diFLNHa (L10), diFLNH (L23); others 9 HMOs, 2FL (L16), 3SL (L18), LNT2 (L19), 3FL (L24), 6SL (L25), LDFT (L26), 3F3SL (L27), Lac (L30) and AT5 tetra (L31) are not included in neither type1/2 due to the absence of β -D-Gal(1-3/4)GlcNAc core in their structure.

10 HMOs containing α -D-Neu5Ac(2 \rightarrow 3/6) linkages are acidic oligosaccharides and rests of the 22 HMOs are neutral in nature. According to Urashima et al. 2012, HMOs contain 13 core groups in their structures. Among them 7 core groups are present in available 32 HMOs which are shown in table 4.1.

Among 32 HMOs, 5 HMOs are connected by α -L-Fuc (1 \rightarrow 2) at non-reducing end (Gal) of LNF1 (L3), LND1 (L13), SLNFV (L14), 2FL (L16), LDFT(L26); 8 HMOs are connected by α -L-Fuc(1 \rightarrow 3/4) to GlcNAc of SLea(L2), LNF2 (L4), LNF3 (L7), diFLNH_a (L10), LND1 (L13), diFLNH (L23), LNDFHII (L28), LNnDFHII (L29); 7 HMOs are connected by α -L-Fuc(1 \rightarrow 3) to the reducing end of Glc of LNnFPV (L17), LNnFP (L21), 3FL (L24), 6SL (L26), 3F3SL (L27), LNDFHII (L28), LNnDFHII (L29). Similarly, there are 9 HMOs where α -D-Neu5Ac(2 \rightarrow 3/6) is connected to the nonreducing end (Gal) of SLea (L2), LS_a (L11), sLNTd (L12), SLNFV (L14), LS_c (L15), 3SL (L18), DS-LNT (L20), LS_b (L22), 6SL (L25), 3F3SL (L27); Neu5Ac α (2-6) are connected to GlcNAc of 3 HMOs SLNFV (L14), DS-LNT (L20), LS_b (L22); Several HMOs: pLNnH (L1), LNnOcta (L5), LNnH (L8) represent repeating type 2 LacNAc units whereas diFLNH_a (L10) and diFLNH (L23) represent both type 1 and type 2 LacNAc alternatively. Table 4.5 shows the location of type 1 and type 2 LacNAc in HMO structures. Finally, 2 HMOs AT5 tetra (L31), AT1 hexa (L32) were found in minor amount in blood group A secretor individuals.

Table 4.4. The 7 core structures available in HMOs used in this study[‡]

Core	Structure	#HMO
Lactose	β -D-Gal(1→4)- β -D-Glc	L1, L16, L18, L19, L24, L25, L26, L27, L30, L31
Lacto- <i>N</i> - tetraose	β -D-Gal(1→3)- β -D-GlcNAc(1→3)- β -D-Gal(1→4)- β -D-Glc	L2, L3, L4, L9, L11, L13, L14, L17, L20, L22, L28, L32
Lacto- <i>N</i> - neotetraose	β -D-Gal(1→4)- β -D-GlcNAc(1→3)- β -D-Gal(1→4)- β -D-Glc	L6, L7, L12, L15, L21, L29
Lacto- <i>N</i> - hexose	β -D-Gal(1→4)- β -D-GlcNAc(1→6)-[β -D-Gal(1→3)- β -D-GlcNAc(1→3)]- β -D-Gal(1→4)- β -D-Glc	L10
Lacto- <i>N</i> - neohexose	β -D-Gal(1→4)- β -D-GlcNAc(1→6)-[β -D-Gal(1→4)- β -D-GlcNAc(1→3)]- β -D-Gal(1→4)- β -D-Glc	L8
<i>para</i> -Lacto- <i>N</i> - hexose	β -D-Gal(1→3)- β -D-GlcNAc(1→3)- β -D-Gal(1→4)- β -D-GlcNAc(1→3)- β -D-Gal(1→4)- β -D-Glc	L23
<i>para</i> -Lacto- <i>N</i> - neohexose	β -D-Gal(1→4)- β -D-GlcNAc(1→3)- β -D-Gal(1→4)- β -D-GlcNAc(1→3)- β -D-Gal(1→4)- β -D-Glc	L5

[‡] Urashima et al. 2012

Table 4.5. Structures of HMOs used in this study (L1 – L32)*, †

HMO #	Structure	Abbreviation
L1	β -D-Gal-(1→4)- β -D-GlcNAc(1→3)- β -D-Gal(1→4)- β -D-GlcNAc(1→3)- β -D-Gal(1→4)- β -D-Glc	pLNnH
L2	α -D-Neu5Ac(2→3)- β -D-Gal(1→3)-[α -L-Fuc(1→4)]- β -D-GlcNAc(1→3)- β -D-Gal(1→4)- β -D-Glc	SLea
L3	α -L-Fuc(1→2)- β -D-Gal(1→3)- β -D-GlcNAc(1→3)- β -D-Gal(1→4)- β -D-Glc	LNF1
L4	β -D-Gal(1→3)-[α -L-Fuc(1→4)]- β -D-GlcNAc(1→3)- β -D-Gal(1→4)- β -D-Glc	LNF2
L5	β -D-Gal-(1→4)- β -D-GlcNAc-(1→3)- β -D-Gal-(1→4)- β -D-GlcNAc-(1→3)- β -D-Gal-(1→4)- β -D-GlcNAc-(1→3)- β -D-Gal-(1→4)- β -D-Glc	LNnOcta
L6	β -D-Gal(1→4)- β -D-GlcNAc(1→3)- β -D-Gal(1→4)- β -D-Glc	LNnT
L7	β -D-Gal-(1→4)-[α -L-Fuc-(1→3)]- β -D-GlcNAc-(1→3)- β -D-Gal-(1→4)- β -D-Glc	LNF3
L8	β -D-Gal(1→4)- β -D-GlcNAc(1→6)-[β -D-Gal(1→4)- β -D-GlcNAc(1→3)]- β -D-Gal(β 1→4)- β -D-Glc	LNnH
L9	β -D-Gal(1→3)- β -D-GlcNAc(1→3)- β -D-Gal(1→4)- β -D-Glc	LNT
L10	β -D-Gal-(1→4)-[α -L-Fuc-(1→3)]- β -D-GlcNAc-(1→6)-[α -L-Fuc-(1→2)- β -D-Gal-(1→3)- β -D-GlcNAc-(1→3)]- β -D-Gal-(1→4)- β -D-Glc	diFLNHa
L11	α -D-Neu5Ac(2→3)- β -D-Gal(1→3)- β -D-GlcNAc(1→3)- β -D-	LSa

	Gal(1→4)-β-D-Glc	
L12	α-D-Neu5Ac(2→3)-β-D-Gal(1→4)-β-D-GlcNAc(1→3)-β-D-Gal(1→4)-β-D-Glc	sLNTd
L13	α-L-Fuc-(1→2)-β-D-Gal-(1→3)-[α-L-Fuc-(1→4)]-β-D-GlcNAc-(1→3)-β-D-Gal(1→4)-β-D-Glc	LND1
L14	α-L-Fuc-(1→2)-β-D-Gal-(1→3)-[α-D-Neu5Ac-(2→6)]-β-D-GlcNAc-(1→3)-β-D-Gal-(1→4)-β-D-Glc	SLNFV
L15	α-D-Neu5Ac(2→6)-β-D-Gal(1→4)-β-D-GlcNAc(1→3)-β-D-Gal(1→4)-β-D-Glc	LSc
L16	α-L-Fuc-(1→2)-β-D-Gal-(1→4)-β-D-Glc	2FL
L17	β-D-Gal(1→3)-β-D-GlcNAc(1→3)-β-D-Gal(1→4)-[α-L-Fuc(1→3)]-β-D-Glc	LNnFPV
L18	α-D-Neu5Ac-(2→3)-β-D-Gal(1→4)-β-D-Glc	3SL
L19	β-D-GlcNAc(1→3)-β-D-Gal(1→4)-β-D-Glc	LNT2
L20	α-D-Neu5Ac-(2→3)-β-D-Gal-(1→3)-[α-D-Neu5Ac-(2→6)]-β-D-GlcNAc-(1→3)-β-D-Gal-(1→4)-β-D-Glc	DS-LNT
L21	β-D-Gal(1→4)-β-D-GlcNAc(1→3)-β-D-Gal(1→4)-[α-L-Fuc(1→3)]-β-D-Glc	LNnFP
L22	α-D-Neu5Ac(2→6)-[β-D-Gal(1→3)]-β-D-GlcNAc(1→3)-β-D-Gal(1→4)-β-D-Glc	LSb
L23	β-D-Gal(1→3)-[α-L-Fuc(1→4)]-β-D-GlcNAc(1→3)-β-D-Gal(1→4)-[α-L-Fuc(1→3)]-β-D-GlcNAc(1→3)-β-D-Gal(1→4)-β-	diFLNH

	D-Glc	
L24	β -D-Gal(1→4)-[α -L-Fuc(1→3)]- β -D-Glc	3FL
L25	α -D-Neu5Ac(2→6)- β -D-Gal(1→4)- β -D-Glc	6SL
L26	α -L-Fuc(1→2)- β -D-Gal(1→4)-[α -L-Fuc(1→3)]- β -D-Glc	LDFT
L27	α -D-Neu5Ac(2→3)- β -D-Gal(1→4)-[α -L-Fuc(α 1→3)]- β -D-Glc	3F3SL
L28	β-D-Gal(1→3) -[α -L-Fuc(1→4)]- β-D-GlcNAc(1→3) - β -D-Gal(1→4)-[α -D-Fuc(1→3)]- β -D-Glc	LNDFHII
L29	β-D-Gal(1→4) -[α -L-Fuc(1→3)]- β-D-GlcNAc(1→3) - β -D-Gal(1→4)-[α -D-Fuc(1→3)]- β -D-Glc	LNnDFHII
L30	β -D-Gal-(1→4)- β -D-Glc	Lac
L31	α -D-GalNAc-(1→3)-[α -L-Fuc-(1→2)]- β -D-Gal-(1→4)- β -D-Glc	AT5 tetra
L32	α -D-GalNAc-(1→3)-[α -L-Fuc-(1→2)]- β-D-Gal-(1→3) - β -D- GlcNAc-(1→3) - β -D-Gal-(1→4)- β -D-Glc	AT1 hexa

*red color denotes lacto-N-biose I Type 1 LacNac, [Gal(β 1-3)GlcNAc] and blue color denotes Type 2 LacNac, N-acetyllactosamine [Gal(β 1-4)GlcNAc] in their structure (reference Urashima et al. 2012). † Reference Urashima et al. 2012.

Table 4.6. HMOs structures in HMG 260 microarray V2.0

Chart ID	Sample ID	Structure	HMO
1	HMO-1	Gal β 1-4Glc-AEAB	Lac
2	HMO-2	Gal β 1-4(Fuc α 1-3)Glc-AEAB	3-FL
3	HMO-3	Fuc α 1-2Gal β 1-4Glc-AEAB	2-FL
5	HMO-5	Gal β 1-3GlcNAc β 1-3Gal β 1-4Glc-AEAB	LNT
6	HMO-6	Gal β 1-4GlcNAc β 1-3Gal β 1-4Glc-AEAB	LNnT
8	HMO-8	Fuc α 1-2Gal β 1-3GlcNAc β 1-3Gal β 1-4Glc-AEAB	LNFP1
9	HMO-9	Fuc α 1-2Gal β 1-3(Fuc α 1-4)GlcNAc β 1-3Gal β 1-4Glc-AEAB	LND1
248	3FL	Gal β 1-4(Fuc α 1-3)Glc-AEAB	Lac
249	LNT	Gal β 1-3GlcNAc β 1-3Gal β 1-4Glc-AEAB	LNT2
250	LNnT	Gal β 1-4GlcNAc β 1-3Gal β 1-4Glc-AEAB	3SL
251	LNFP1	Fuc α 1-2Gal β 1-3GlcNAc β 1-3Gal β 1-4Glc-AEAB	3SL
252	LNFP1I	Gal β 1-3(Fuc α 1-4)GlcNAc β 1-3Gal β 1-4Glc-AEAB	6SL
253	LDFT	Fuc α 1-2Gal β 1-4(Fuc α 1-3)Glc-AEAB	6SL

Table 4.7. HMOs structures in Defined HMG microarray

Chart ID	Reducing end glucose structure	Structure	HMO
2	Open-Ring	Gal β 1-4Glc-AEAB	Lac
3	Open-Ring	Fuc α 1-2Gal β 1-4Glc-AEAB	2FL
4	Open-Ring	Neu5Ac α 2-3Gal β 1-4Glc-AEAB	3SL
5	Open-Ring	Neu5Ac α 2-6Gal β 1-4Glc-AEAB	6SL
6	Open-Ring	Gal β 1-3GlcNAc β 1-3Gal β 1-4Glc-AEAB	LNT
7	Open-Ring	Gal β 1-4GlcNAc β 1-3Gal β 1-4Glc-AEAB	LNnT
8	Open-Ring	Fuc α 1-2Gal β 1-3GlcNAc β 1-3Gal β 1-4Glc-AEAB	LNFP1
10	Closed-Ring	Gal β 1-4Glc-AEAB	GGLac
11	Closed-Ring	Fuc α 1-2Gal β 1-4Glc-AEAB	GG2FL
12	Closed-Ring	Neu5Ac α 2-3Gal β 1-4Glc-AEAB	GG3SL
13	Closed-Ring	Neu5Ac α 2-6Gal β 1-4Glc-AEAB	GG6SL
14	Closed-Ring	Gal β 1-3GlcNAc β 1-3Gal β 1-4Glc-AEAB	GGLNT
15	Closed-Ring	Gal β 1-4GlcNAc β 1-3Gal β 1-4Glc-AEAB	GGLNnT
16	Closed-Ring	Fuc α 1-2Gal β 1-3GlcNAc β 1-3Gal β 1-4Glc-AEAB	GGLNFP1
33	Open-Ring	Fuc α 1-3Gal β 1-4Glc-AEAB	3FL

Table 4.8. HMOs structures in CFG array V5.0

Chart ID	Structure	#HMO
66	Fuc(α 1-2)Gal(β 1-3)GlcNAc(β 1-3)Gal(β 1-4)Glc β -Sp8	LNF1
67	Fuc(α 1-2)Gal(β 1-3)GlcNAc(β 1-3)Gal(β 1-4)Glc β -Sp10	LNF1
78	Fuc(α 1-2)Gal(β 1-4)Glc β -Sp0	2FL
149	Gal(β 1-3)GlcNAc(β 1-3)Gal(β 1-4)Glc β -Sp10	LNT
165	Gal(β 1-4)GlcNAc(β 1-3)Gal(β 1-4)Glc β -Sp0	LNnT
166	Gal(β 1-4)GlcNAc(β 1-3)Gal(β 1-4)Glc β -Sp8	LNnT
172	Gal(β 1-4)Glc β -Sp0	Lac
173	Gal(β 1-4)Glc β -Sp8	Lac
186	GlcNAc(β 1-3)Gal(β 1-4)Glc β -Sp0	LNT2
264	Neu5Ac(α 2-3)Gal(β 1-4)Glc β -Sp0	3SL
265	Neu5Ac(α 2-3)Gal(β 1-4)Glc β -Sp8	3SL
273	Neu5Ac(α 2-6)Gal(β 1-4)Glc β -Sp0	6SL
274	Neu5Ac(α 2-6)Gal(β 1-4)Glc β -Sp8	6SL

Table 4.9. Spacer arm structures with code in CFG array V5.0

Code	Structure
Sp0	-CH ₂ CH ₂ NH ₂
Sp8	-CH ₂ CH ₂ CH ₂ NH ₂
Sp10	-NHCOCH ₂ NH

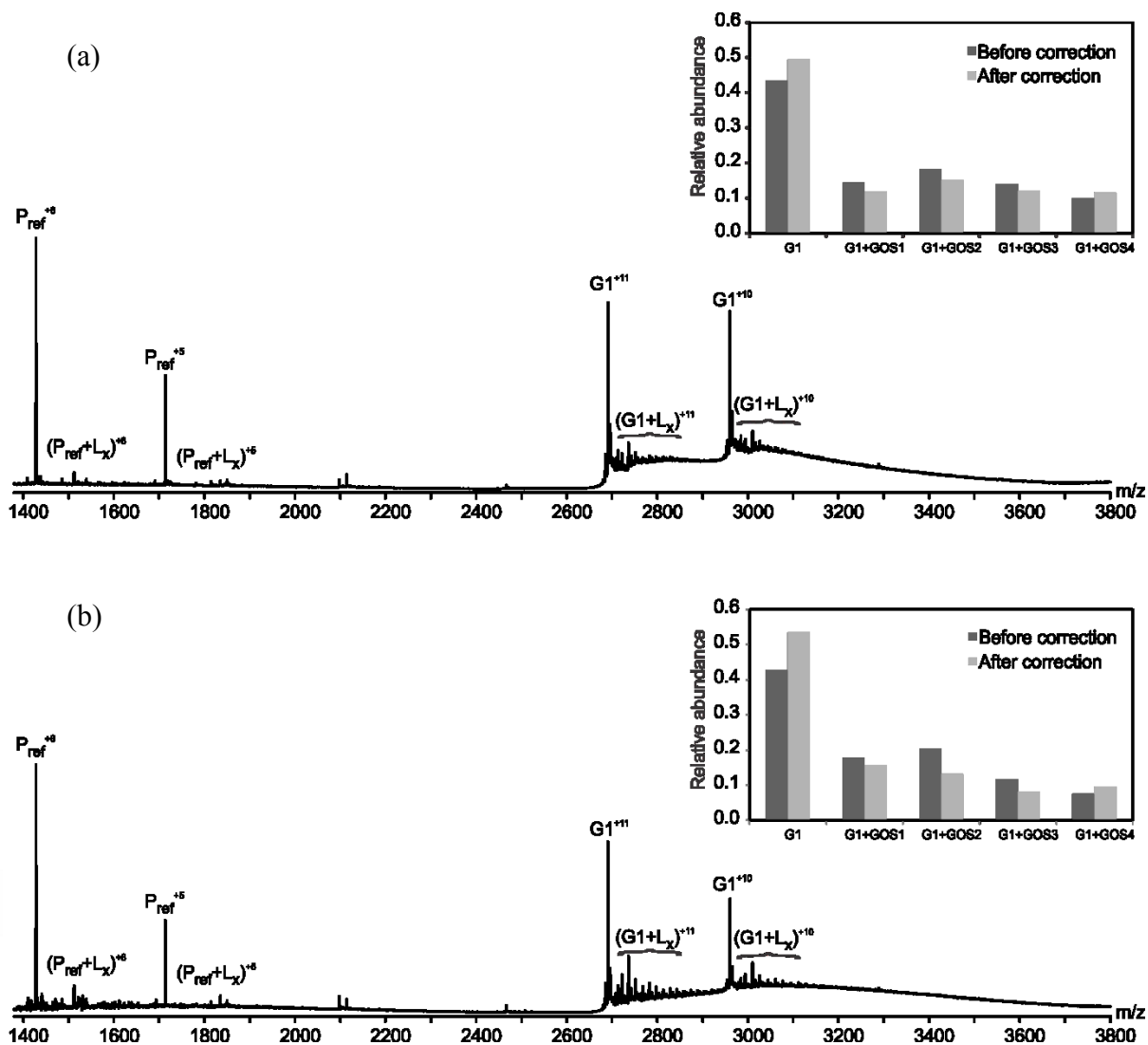


Figure 4.14. ESI mass spectra in positive ion mode for a 30 mM aqueous ammonium acetate solution (pH 6.8, 25 °C) of Gal-1 (G1, 6 μ M) and P_{ref} (1 μ M) with (a) 0.05 g/L or (b) 0.1 g/L diluted solution of Vivinal GOS 90 powder. Insets show normalized distribution of free and ligand-bound Gal-1 before (■) and after (■) correction for nonspecific ligand binding.

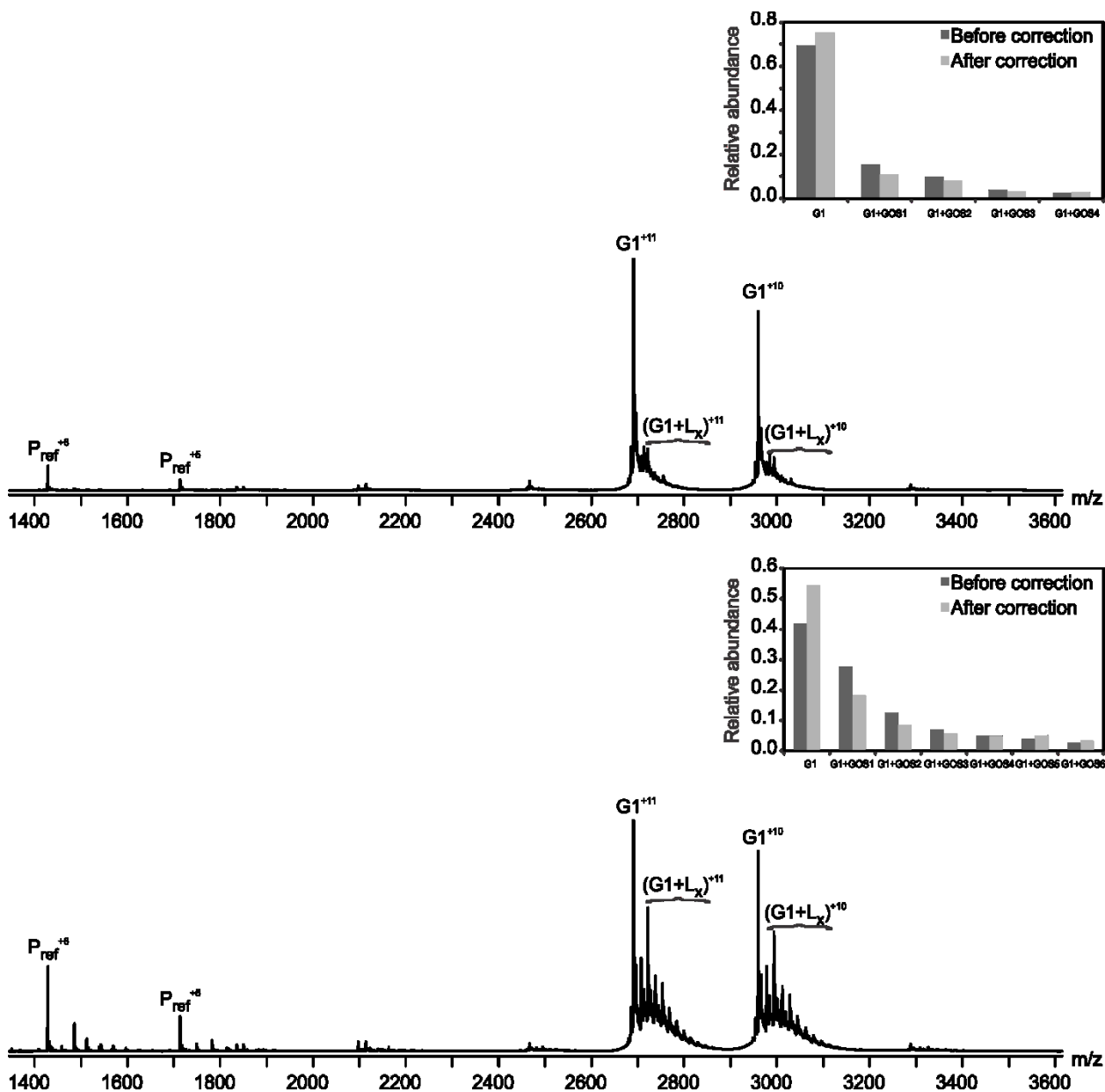


Figure 4.15. ESI mass spectra in positive ion mode for a 30 mM aqueous ammonium acetate solution (pH 6.8, 25 °C) of Gal-1 (G1, 6 μ M) and P_{ref} (1 μ M) with (a) ~ 6000 times or (b) ~ 2400 times diluted solution of Vivinal GOS syrup. Insets show normalized distribution of free and ligand-bound Gal-1 before (■) and after (■) correction for nonspecific ligand binding.

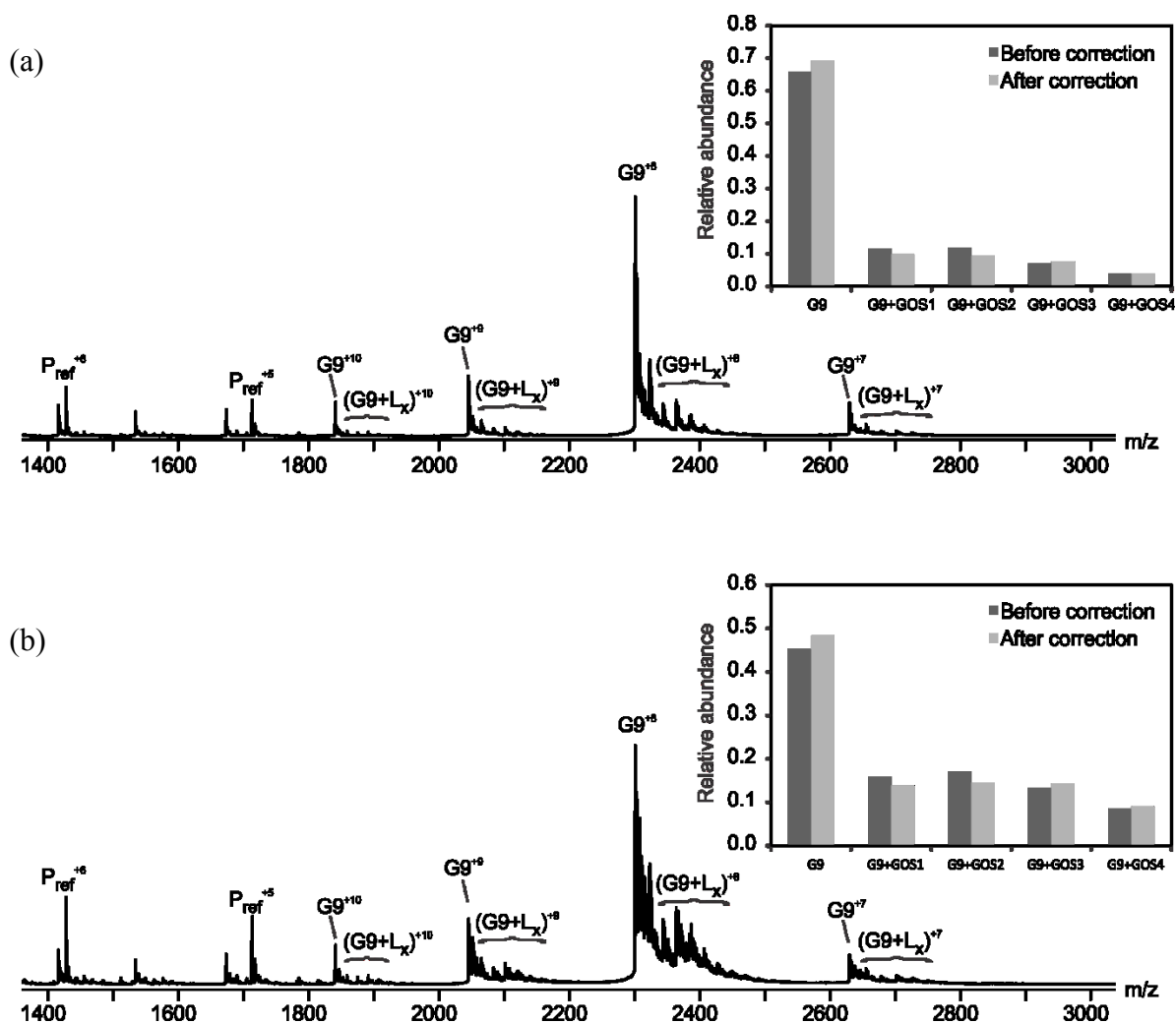


Figure 4.16. ESI mass spectra in positive ion mode for a 30 mM aqueous ammonium acetate solution (pH 6.8, 25 °C) of Gal-9N (G9, 10 μ M) and P_{ref} (0.7 μ M) with (a) 0.05 g/L or (b) 0.1 g/L diluted solution of Vivinal GOS 90 powder. Insets show normalized distribution of free and ligand-bound Gal-9N before (■) and after (■) correction for nonspecific ligand binding.

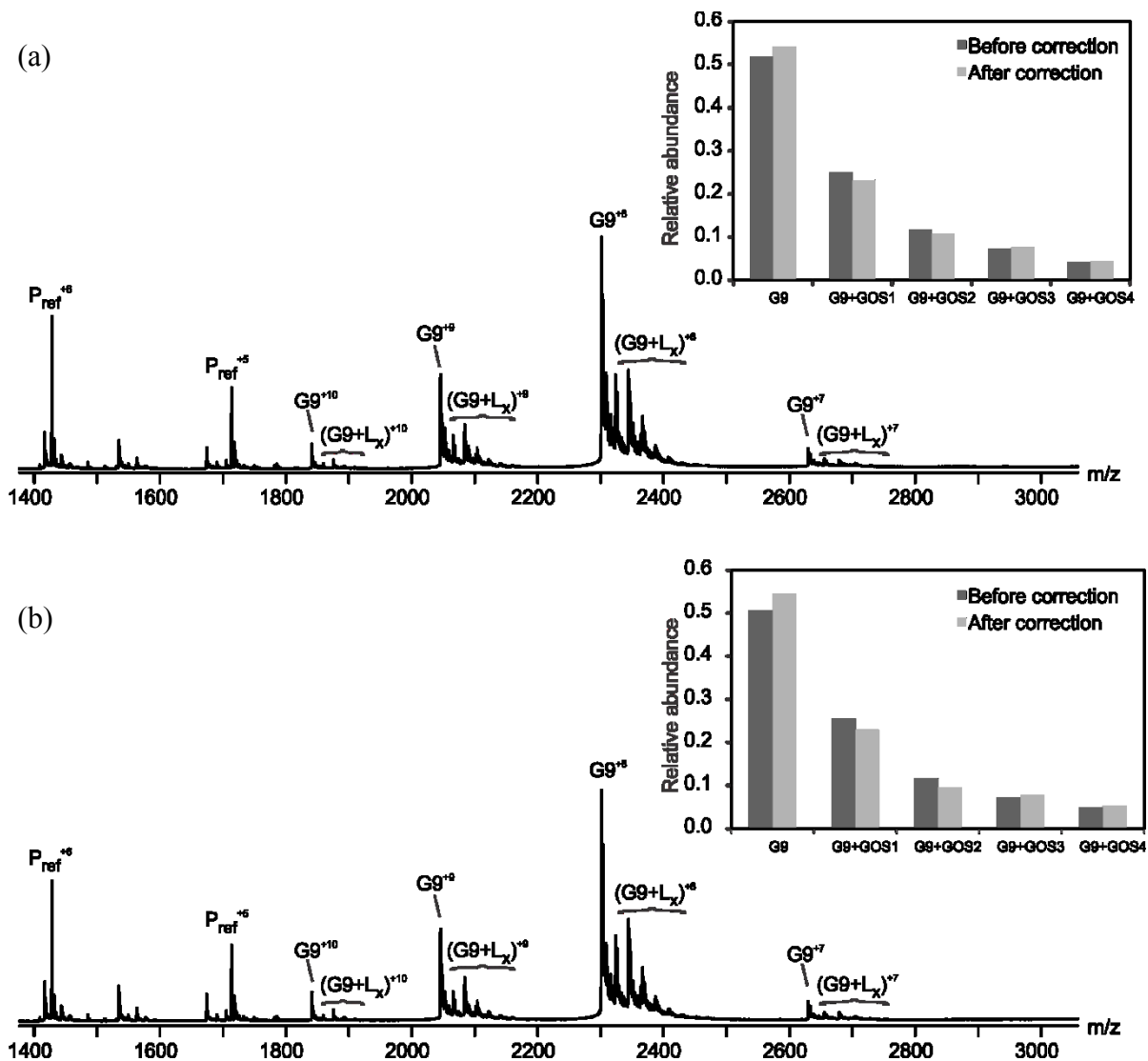


Figure 4.17. ESI mass spectra in positive ion mode for a 30 mM aqueous ammonium acetate solution (pH 6.8, 25 °C) of Gal-9 (G9, 10 μ M) and P_{ref} (1 μ M) with (a) ~ 2500 times or (b) ~ 2000 times diluted solution of Vivinal GOS syrup. Insets show normalized distribution of free and ligand-bound Gal-9N before (■) and after (■) correction for nonspecific ligand binding

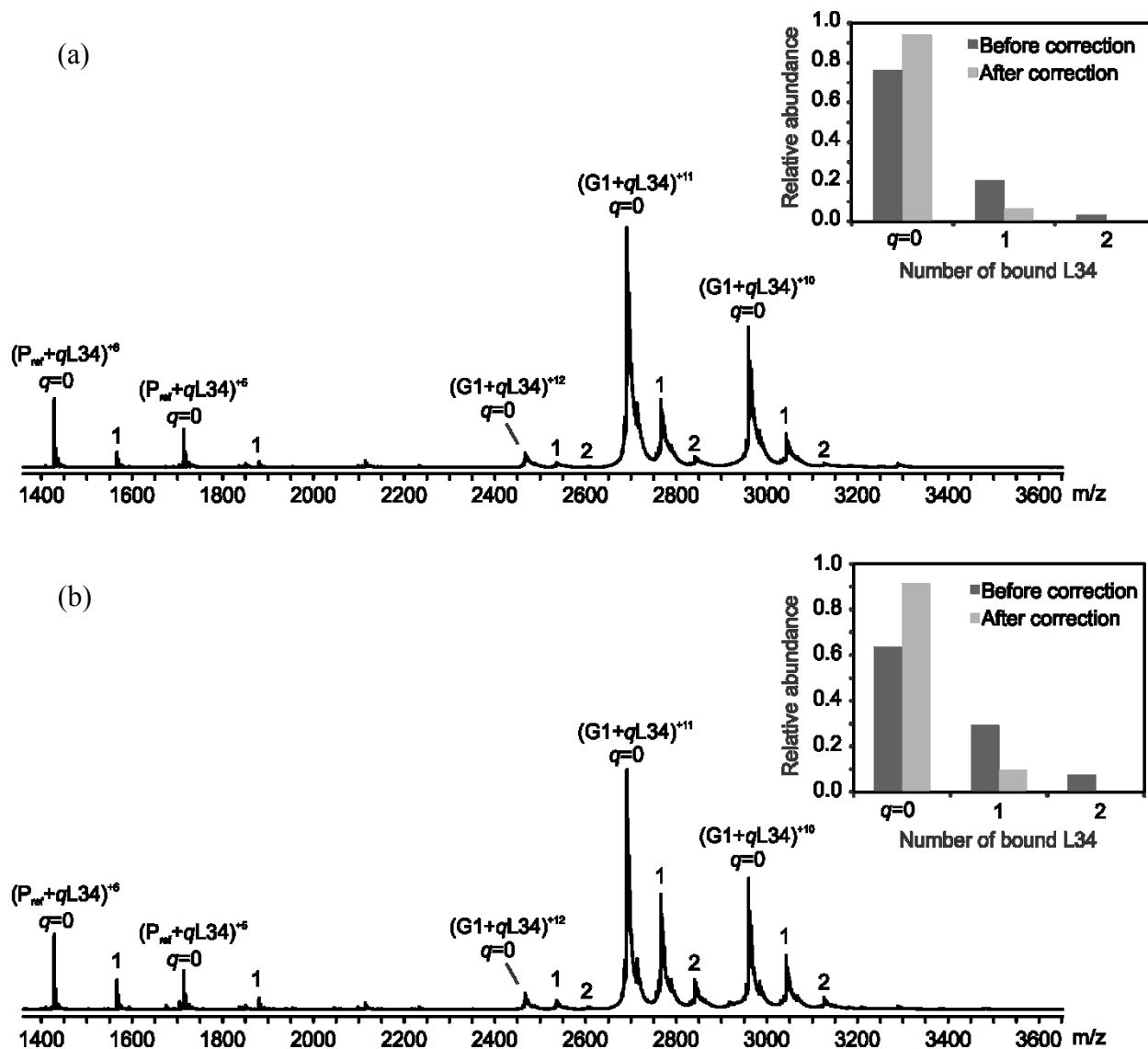


Figure 4.18. ESI mass spectra in positive ion mode for a 30 mM aqueous ammonium acetate solution (pH 6.8, 25 °C) of Gal-1 (G1, 6 μM) and P_{ref} (1 μM) with (a) 30 μM L34 or (b) 40 μM L34. Insets show normalized distribution of free and ligand-bound Gal-1 before (■) and after (■) correction for nonspecific ligand binding.

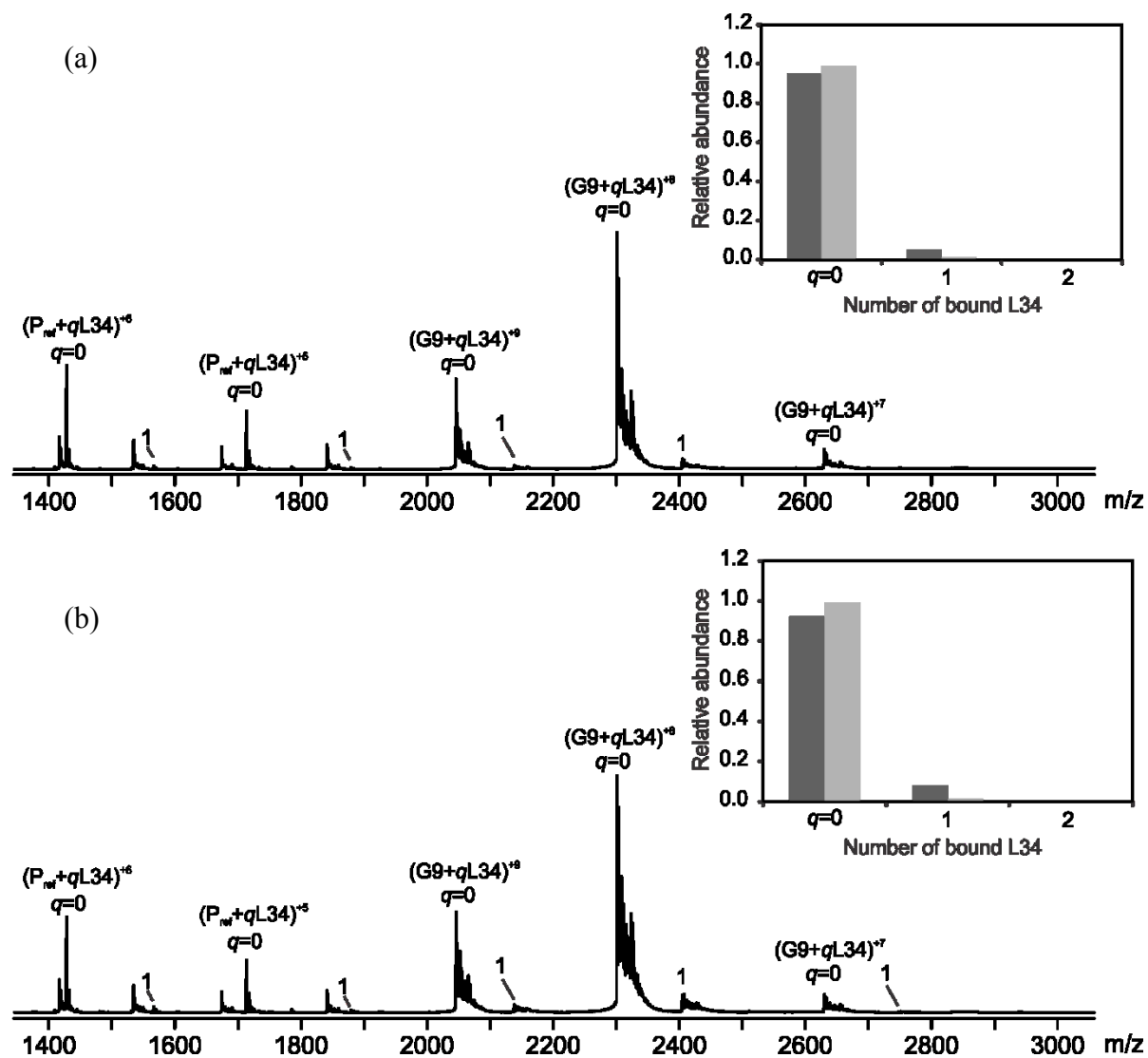


Figure 4.19. ESI mass spectra in positive ion mode for a 30 mM aqueous ammonium acetate solution (pH 6.8, 25 °C) of Gal-9N (G9, 10 μM) and P_{ref} (1 μM) with (a) 40 μM L34 or (b) 60 μM L34. Insets show normalized distribution of free and ligand-bound Gal-9N before (■) and after (■) correction for nonspecific ligand binding.

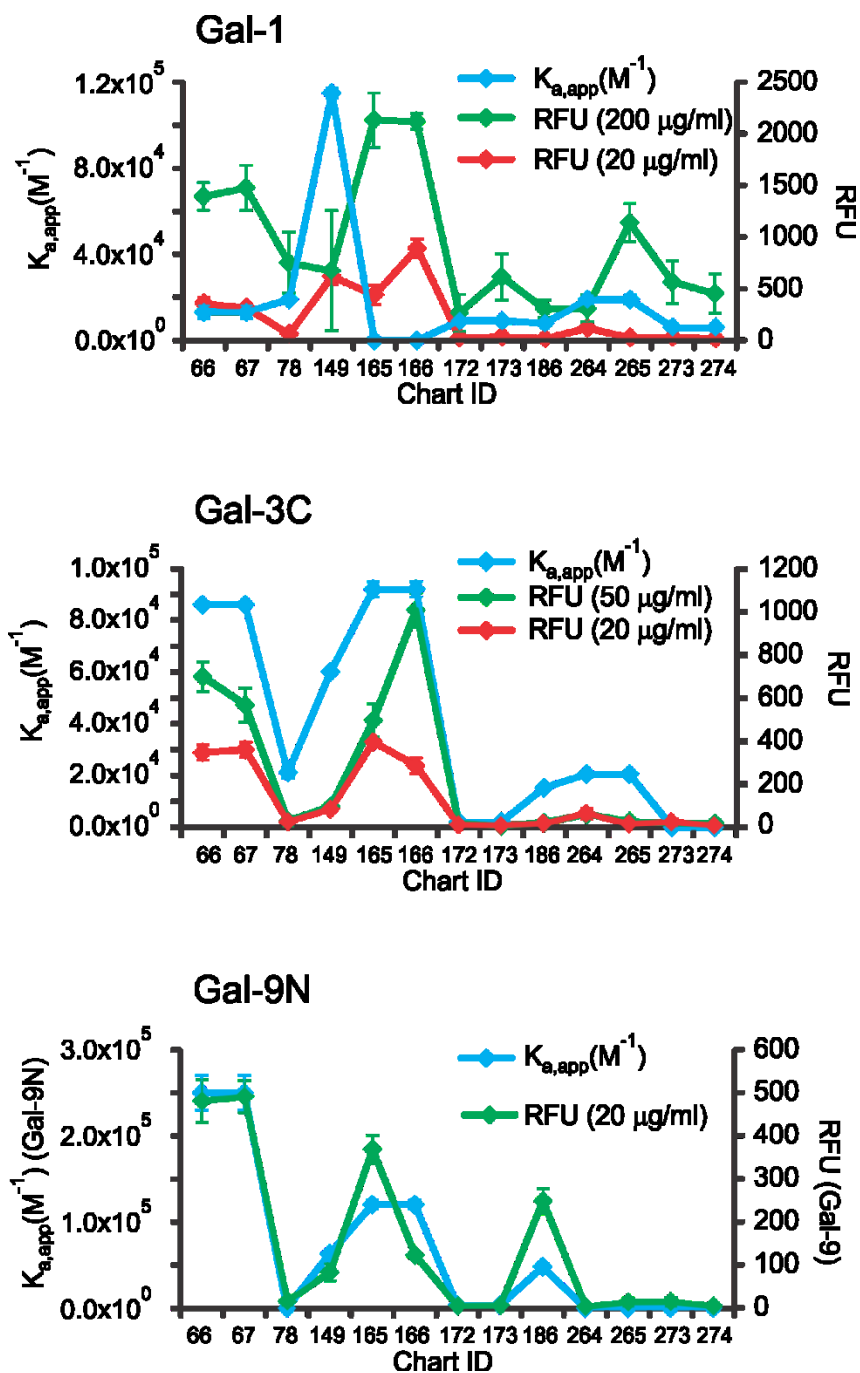


Figure 4.20. Comparison of binding affinity, $K_{a,app} (M^{-1})$ obtained from direct ESI-MS method to RFU value obtained from CFG glycan microarray data V 5.0 of (a) Gal-1, (b) Gal-3C and (c) Gal-9N. Concentration of each of the 3 galectins is given in the diagram for respective RFU value. Chart ID were taken from glycan microarray data V 5.0 and errors correspond to one standard deviation in the represented data.

4.5 References

- (1) Lara-Villoslada, F.; Olivares, M.; Sierra, S.; Rodríguez, J. M.; Boza, J.; Xaus, J. *Brit. J. Nutr.* **2007**, *98*, S96-S100.
- (2) Martín, R.; Langa, S.; Reviriego, C.; Jiménez, E.; Marín, M. L.; Xaus, J.; Fernández, L.; Rodríguez, J. M. *J. Pediatr.* **2003**, *143*, 754-758.
- (3) Wu, S.; Tao, N.; German, J. B.; Grimm, R.; Lebrilla, C. B. *J. Proteom. Res.* **2010**, *9*, 4138-4151.
- (4) Chichlowski, M.; German, J. B.; Lebrilla, C. B.; Mills, D. A. *Annu. Rev. Food Sci.* **2011**, *2*, 331-351.
- (5) Bode, L. *J. Nutr.* **2006**, *136*, 2127-2130.
- (6) Bode, L.; Jantscher-Krenn, E. *Adv. Nutr.* **2012**, *3*, 383S-391S.
- (7) Bode, L. *Glycobiology* **2012**, *22*, 1147-1162.
- (8) Bhargava, P.; Li, C.; Stanya, K. J.; Jacobi, D.; Dai, L.; Liu, S.; Gangl, M. R.; Harn, D. A.; Lee, C.-H. *Nat. Med.* **2012**, *18*, 1665-1672.
- (9) Gnoth, M. J.; Rudloff, S.; Kunz, C.; Kinne, R. K. *J. Biol. Chem.* **2001**, *276*, 34363-34370.
- (10) Goehring, K. C.; Kennedy, A. D.; Prieto, P. A.; Buck, R. H. *PloS One* **2014**, *9*, e101692.
- (11) Newburg, D. S.; Ruiz-Palacios, G. M.; Morrow, A. L. *Annu. Rev. Nutr.* **2005**, *25*, 37-58.
- (12) Rudloff, S.; Pohlentz, G.; Diekmann, L.; Egge, H.; Kunz, C. *Acta Paediatr.* **1996**, *85*, 598-603.

- (13) Obermeier, S.; Rudloff, S.; Pohlentz, G.; Lentze, M.; Kunz, C. *Isot. Environ. Healt. S.* **1999**, *35*, 119-125.
- (14) El-Hawiet, A.; Kitova, E. N.; Klassen, J. S. *Glycobiology* **2015**, *25*, 845-854.
- (15) Eiwegger, T.; Stahl, B.; Haidl, P.; Schmitt, J.; Boehm, G.; Dehlink, E.; Urbanek, R.; Szépfalusi, Z. *Pediat. Aller. Immunol.* **2010**, *21*, 1179-1188.
- (16) de Kivit, S.; Kraneveld, A. D.; Garssen, J.; Willemsen, L. E. *Eur. J. Phar.* **2011**, *668*, S124-S132.
- (17) Rabinovich, G. A.; Baum, L. G.; Tinari, N.; Paganelli, R.; Natoli, C.; Liu, F.-T.; Iacobelli, S. *Trend. Immunol.* **2002**, *23*, 313-320.
- (18) Hughes, R. C. *Biochimie* **2001**, *83*, 667-676.
- (19) Vasta, G. R. *Nat. Rev. Microbiol.* **2009**, *7*, 424-438.
- (20) Astorgues-Xerri, L.; Riveiro, M. E.; Tijeras-Raballand, A.; Serova, M.; Neuzillet, C.; Albert, S.; Raymond, E.; Faivre, S. *Cancer Treat. Rev.* **2014**, *40*, 307-319.
- (21) Song, L.; Tang, J.-w.; Owusu, L.; Sun, M.-Z.; Wu, J.; Zhang, J. *Clin. Chim. Acta* **2014**, *431*, 185-191.
- (22) Vladoiu, M. C.; Labrie, M.; St-Pierre, Y. *Int. J. Oncol.* **2014**, *44*, 1001-1014.
- (23) Rubinstein, N.; Alvarez, M.; Zwirner, N. W.; Toscano, M. A.; Ilarregui, J. M.; Bravo, A.; Mordoh, J.; Fainboim, L.; Podhajcer, O. L.; Rabinovich, G. A. *Cancer Cell* **2004**, *5*, 241-251.
- (24) Cerliani, J. P.; Stowell, S. R.; Mascanfroni, I. D.; Arthur, C. M.; Cummings, R. D.; Rabinovich, G. A. *J. Clin. Immunol.* **2011**, *31*, 10-21.
- (25) Di Lella, S.; Sundblad, V.; Cerliani, J. P.; Guardia, C. M.; Estrin, D. A.; Vasta, G. R.; Rabinovich, G. A. *Biochemistry* **2011**, *50*, 7842-7857.

- (26) Matsushita, N.; Nishi, N.; Seki, M.; Matsumoto, R.; Kuwabara, I.; Liu, F.-T.; Hata, Y.; Nakamura, T.; Hirashima, M. *J. Biol. Chem.* **2000**, *275*, 8355-8360.
- (27) Paclik, D.; Danese, S.; Berndt, U.; Wiedenmann, B.; Dignass, A.; Sturm, A. *PLoS One* **2008**, *3*, e2629.
- (28) Stowell, S. R.; Qian, Y.; Karmakar, S.; Koyama, N. S.; Dias-Baruffi, M.; Leffler, H.; McEver, R. P.; Cummings, R. D. *J. Immunol.* **2008**, *180*, 3091-3102.
- (29) Camby, I.; Le Mercier, M.; Lefranc, F.; Kiss, R. *Glycobiology* **2006**, *16*, 137R-157R.
- (30) Ilarregui, J.; Bianco, G.; Toscano, M.; Rabinovich, G. *Ann. Rheum. Dis.* **2005**, *64*, iv96-iv103.
- (31) López-Lucendo, M. F.; Solís, D.; André, S.; Hirabayashi, J.; Kasai, K.; Kaltner, H.; Gabius, H.-J.; Romero, A. *J. Mol. Biol.* **2004**, *343*, 957-970.
- (32) Yoshida, H.; Teraoka, M.; Nishi, N.; Nakakita, S.-i.; Nakamura, T.; Hirashima, M.; Kamitori, S. *J. Biol. Chem.* **2010**, *285*, 36969-36976.
- (33) Collins, P. M.; Bum-Erdene, K.; Yu, X.; Blanchard, H. *J. Mol. Biol.* **2014**, *426*, 1439-1451.
- (34) Hirabayashi, J.; Hashidate, T.; Arata, Y.; Nishi, N.; Nakamura, T.; Hirashima, M.; Urashima, T.; Oka, T.; Futai, M.; Muller, W. E. *BBA-Gen. Subjects* **2002**, *1572*, 232-254.
- (35) Bachhawat-Sikder, K.; Thomas, C. J.; Surolia, A. *FEBS Lett.* **2001**, *500*, 75-79.
- (36) Carlsson, S.; Carlsson, M. C.; Leffler, H. *Glycobiology* **2007**, *17*, 906-912.
- (37) Ideo, H.; Seko, A.; Ohkura, T.; Matta, K. L.; Yamashita, K. *Glycobiology* **2002**, *12*, 199-208.

- (38) Sparrow, C.; Leffler, H.; Barondes, S. *J. Biol. Chem.* **1987**, *262*, 7383-7390.
- (39) Noll, A. J.; Gourdine, J. P.; Yu, Y.; Lasanajak, Y.; Smith, D. F.; Cummings, R. D. *Glycobiology* **2016**, cww002.
- (40) Yu, Y.; Lasanajak, Y.; Song, X.; Hu, L.; Ramani, S.; Mickum, M. L.; Ashline, D. J.; Prasad, B. V.; Estes, M. K.; Reinhold, V. N. *Mol. Cell. Proteom.* **2014**, *13*, 2944-2960.
- (41) Ashline, D. J.; Yu, Y.; Lasanajak, Y.; Song, X.; Hu, L.; Ramani, S.; Prasad, V.; Estes, M. K.; Cummings, R. D.; Smith, D. F. *Mol. Cell. Proteom.* **2014**, *13*, 2961-2974.
- (42) Agravat, S. B.; Song, X.; Rojsajjakul, T.; Cummings, R. D.; Smith, D. F. *Bioinformatics* **2016**, *32*(10), 1471-1478.
- (43) Urashima, T.; Asakuma, S.; Leo, F.; Fukuda, K.; Messer, M.; Oftedal, O. T. *Adv. Nutr.* **2012**, *3*, 473S-482S.
- (44) Tao, N.; Wu, S.; Kim, J.; An, H. J.; Hinde, K.; Power, M. L.; Gagneux, P.; German, J. B.; Lebrilla, C. B. *J. Proteom. Res.* **2011**, *10*, 1548-1557.
- (45) Urashima, T.; Kitaoka, M.; Asakuma, S.; Messer, M. In *Adv. Dairy Chem.*; Springer, **2009**, 295-349.
- (46) Arthur, C. M.; Rodrigues, L. C.; Baruffi, M. D.; Sullivan, H. C.; Heimbürg-Molinari, J.; Smith, D. F.; Cummings, R. D.; Stowell, S. R. *Galectins: Methods and Protocols* **2015**, 115-131.
- (47) Heimbürg-Molinari, J.; Song, X.; Smith, D. F.; Cummings, R. D. *Curr. Prot. Protein Sci.* **2011**, 12.10. 11-12.10. 29.
- (48) Rillahan, C. D.; Paulson, J. C. *Annu. Rev. Biochem.* **2011**, *80*, 797-823.

- (49) Kilcoyne, M.; Gerlach, J. Q.; Kane, M.; Joshi, L. *Anal. Methods* **2012**, *4*, 2721-2728.
- (50) Paulson, J. C.; Blixt, O.; Collins, B. E. *Nat. Chem. Biol.* **2006**, *2*, 238-248.
- (51) Smith, D. F.; Song, X.; Cummings, R. D. *Methods Enzymol.* **2010**, *480*, 417-444.
- (52) Grant, O. C.; Smith, H. M.; Firsova, D.; Fadda, E.; Woods, R. J. *Glycobiology* **2014**, *24*, 17-25.
- (53) Wang, W. J.; Kitova, E. N.; Klassen, J. S. *Methods Enzymol.* **2003**, *362*, 376-397.
- (54) El-Hawiet, A.; Kitova, E. N.; Liu, L.; Klassen, J. S. *J. Am. Soc. Mass Spectrom.* **2010**, *21*, 1893-1899.
- (55) El-Hawiet, A.; Kitova, E. N.; Kitov, P. I.; Eugenio, L.; Ng, K. K. S.; Mulvey, G. L.; Dingle, T. C.; Szpacenko, A.; Armstrong, G. D.; Klassen, J. S. *Glycobiology* **2011**, *21*, 1217-1227.
- (56) Ouellet, M.; Mercier, S.; Pelletier, I.; Bounou, S.; Roy, J.; Hirabayashi, J.; Sato, S.; Tremblay, M. J. *J. Immunol.* **2005**, *174*, 4120-4126.
- (57) Hirabayashi, J.; Kasai, K. *J. Biol. Chem.* **1991**, *266*, 23648-23653.
- (58) Diehl, C.; Genheden, S.; Modig, K.; Ryde, U.; Akke, M. *J. Biomol. NMR* **2009**, *45*, 157-169.
- (59) Nagae, M.; Nishi, N.; Murata, T.; Usui, T.; Nakamura, T.; Wakatsuki, S.; Kato, R. *Glycobiology* **2009**, *19*, 112-117.
- (60) Kitova, E. N.; El-Hawiet, A.; Schnier, P. D.; Klassen, J. S. *J. Am. Soc. Mass Spectrom.* **2012**, *23*, 431-441.
- (61) El-Hawiet, A.; Kitova, E. N.; Klassen, J. S. *Biochemistry* **2012**, *51*, 4244-4253.
- (62) Cho, M.; Cummings, R. D. *Biochemistry* **1996**, *35*, 13081-13088.

- (63) Stowell, S. R.; Karmakar, S.; Arthur, C. M.; Ju, T.; Rodrigues, L. C.; Riul, T. B.; Dias-Baruffi, M.; Miner, J.; McEver, R. P.; Cummings, R. D. *Mol. Biol. Cell* **2009**, *20*, 1408-1418.
- (64) Leppänen, A.; Stowell, S.; Blixt, O.; Cummings, R. D. *J. Biol. Chem.* **2005**, *280*, 5549-5562.
- (65) Sun, J. X.; Kitova, E. N.; Wang, W. J.; Klassen, J. S. *Anal. Chem.* **2006**, *78*, 3010-3018.
- (66) Salomonsson, E.; Carlsson, M. C.; Osla, V.; Hendus-Altenburger, R.; Kahl-Knutson, B.; Öberg, C. T.; Sundin, A.; Nilsson, R.; Nordberg-Karlsson, E.; Nilsson, U. J. *J. Biol. Chem.* **2010**, *285*, 35079-35091.
- (67) Ben, X. M.; Li, J.; Feng, Z. T.; Shi, S. Y.; Lu, Y. D.; Chen, R.; Zhou, X. Y. *World J. Gastroenterol.* **2008**, *14*, 6564-6568.
- (68) Ben, X. M.; Zhou, X. Y.; Zhao, W. H.; Yu, W. L.; Pan, W.; Zhang, W. L.; Wu, S. M.; Van Beusekom, C. M.; Schaafsma, A. *Chinese Med. J-Peking* **2004**, *117*, 927-931.
- (69) Fanaro, S.; Marten, B.; Bagna, R.; Vigi, V.; Fabris, C.; Peña-Quintana, L.; Argüelles, F.; Scholz-Ahrens, K. E.; Sawatzki, G.; Zelenka, R. *J. Pediatr. Gastroenterol. Nutr.* **2009**, *48*, 82-88.
- (70) Arslanoglu, S.; Moro, G. E.; Schmitt, J.; Tandoi, L.; Rizzardi, S.; Boehm, G. *J. Nutr.* **2008**, *138*, 1091-1095.
- (71) Bruzzese, E.; Volpicelli, M.; Squeglia, V.; Bruzzese, D.; Salvini, F.; Bisceglia, M.; Lionetti, P.; Cinquetti, M.; Iacono, G.; Amarri, S. *Clin. Nutr.* **2009**, *28*, 156-161.

- (72) Shoaf, K.; Mulvey, G. L.; Armstrong, G. D.; Hutkins, R. W. *Infect. Immun.* **2006**, *74*, 6920-6928.
- (73) Sinclair, H. R.; de Slegte, J.; Gibson, G. R.; Rastall, R. A. *J. Agric. Food Chem.* **2009**, *57*, 3113-3119.
- (74) Costalos, C.; Kapiki, A.; Apostolou, M.; Papathoma, E. *Early Hum. Dev.* **2008**, *84*, 45-49.
- (75) Fanaro, S.; Boehm, G.; Garssen, J.; Knol, J.; Mosca, F.; Stahl, B.; Vigi, V. *Acta Paediatr.* **2005**, *94*, 22-26.
- (76) Schmelzle, H.; Wirth, S.; Skopnik, H.; Radke, M.; Knol, J.; Böckler, H.-M.; Brönstrup, A.; Wells, J.; Fusch, C. *J. Pediatric Gastroenterol. Nutr.* **2003**, *36*, 343-351.
- (77) Veereman-Wauters, G. *Brit. J. Nutr.* **2005**, *93*, S57-S60.
- (78) Chonan, O.; Watanuki, M. *J. Nutr. Sci. Vitam.* **1995**, *41*, 95-104.
- (79) Chonan, O.; Watanuki, M. *Int. J. Vit. Nutr. Res.* **1995**, *66*, 244-249.
- (80) van den Heuvel, E. G.; Schoterman, M. H.; Muijs, T. *J. Nutr.* **2000**, *130*, 2938-2942.
- (81) Weaver, C. M.; Martin, B. R.; Nakatsu, C. H.; Armstrong, A. P.; Clavijo, A.; McCabe, L. D.; McCabe, G. P.; Duignan, S.; Schoterman, M. H.; van den Heuvel, E. G. *J. Agr. Food Chem.* **2011**, *59*, 6501-6510.
- (82) Whisner, C. M.; Martin, B. R.; Schoterman, M. H.; Nakatsu, C. H.; McCabe, L. D.; McCabe, G. P.; Wastney, M. E.; van den Heuvel, E. G.; Weaver, C. M. *Brit. J. Nutr.* **2013**, *110*, 1292-1303.

- (83) Sabater-Molina, M.; Larqué, E.; Torrella, F.; Zamora, S. *J. Phys. Biochem.* **2009**, *65*, 315-328.
- (84) Oozeer, R.; van Limpt, K.; Ludwig, T.; Amor, K. B.; Martin, R.; Wind, R. D.; Boehm, G.; Knol, J. *Am. J. Clin. Nutr.* **2013**, *98*, 561S-571S.

Chapter 5

Conclusions and Future Work

5.1 Conclusions

This thesis describes the development and application of ESI-MS based techniques for quantitative determination of protein-carbohydrate interactions. The first project described in the chapter 2 focuses on the development of liquid sample desorption electrospray ionization method for quantifying protein-carbohydrate interactions. Second project which is described in the chapter 3 focuses on the development of *proxy protein* ESI-MS method for screening oligosaccharide libraries against lectins. Finally, the chapter 4 highlights the comparative studies of human milk oligosaccharides specificities of human galectin-1, 3, 9 where ESI-MS method was compared to glycan microarray method for its reliability and versatility in quantifying protein-carbohydrate interactions.

In chapter 2, the application of liquid sample DESI-MS for quantifying protein-carbohydrate interactions in aqueous solutions is described. Notably, the affinities of carbohydrate ligands measured using liquid sample DESI-MS are found to be in good agreement with values measured by ITC and the direct ESI-MS assay. It is also found that the reference protein method can be used to correct liquid sample DESI mass spectra for nonspecific carbohydrate binding. Reference protein method was originally developed to correct ESI mass spectra for the occurrence of nonspecific ligand-protein binding.

In chapter 3, *proxy protein* ESI-MS method for the rapid and quantitative screening of carbohydrate libraries against lectins is described. Specific interactions between components of the carbohydrate library and a target protein can be detected from

changes in the relative abundances of the carbohydrate complexes of *proxy protein*. It binds to all components of the library with known affinity, upon introduction of target protein to the solution. The affinity of an interaction can be calculated from the magnitude of the change in relative abundance of a given proxy protein-ligand complex. Application of the method to screen small libraries of oligosaccharides against three lectins (CBM, RSL and hNoV P particle), describes the reliability and versatility of the assay for the simultaneous detection and quantification of both low and high affinity interactions. Even though relatively small libraries were used in the present study, implementation of the assay using higher resolution MS instruments is expected to allow for the use of multiple proxy protein in future. This, in turn, will allow for libraries containing a larger number of components to be screened.

Finally chapter 4 describes the affinities of 32 of the most abundant HMOs for Gal-1, Gal-3C and Gal-9N which were quantified for the first time using direct ESI-MS. It was found that each lectin binds to the majority of the HMOs tested in this study, even though binding affinities are very different for each component of the HMO library. Comparing these affinity with the reported affinities by glycan microarray suggest that ESI-MS method is more reliable and versatile for quantifying protein- carbohydrate interaction. In addition, study of GOS and FOS binding with galectin shows weak affinity whereas glycan microarray reported no affinity in the same case. These results suggest that distinct nature of interaction HMOs might have influence on immunomodulation and benefit of child health. Further studies with more oligosaccharides against various lectins are required to compare ESI-MS method to glycan microarray method for reliable binding affinities measurements.

5.2 Future work

5.2.1 Application of Proxy Protein ESI-MS assay to screen large oligosaccharide libraries using new proxy proteins

In Chapter 3 *proxy protein* ESI-MS method was used to screen relatively small libraries of oligosaccharides. However, this method can be implemented for larger library (50-100 oligosaccharides) using multiple *proxy protein*. High resolution MS instrument can be used for this purpose which in turn, will allow reduce the time and complexity of the library screening process.

Galectins have poor or no affinity for several HMOs with specific glycan linkage. To implement the multiple *proxy protein* in a single system several other lectins were screened against HMOs containing specific linkage. Sialic acid α -D-Neu5Ac(2 \rightarrow 3/6) is common epitope present on the cell surface glycoprotein. A fungal galectin from *Agrocybe cylindracea* (ACG) shows broad binding specificity for β -galactose-containing glycans, more specifically α -D-Neu5Ac(2 \rightarrow 3)- β -D-Gal(1 \rightarrow 4)- β -D-Glc/GlcNAc trisaccharide sequences.¹ Another lectin from the mushroom *Polyporus squamosus* (PSL1a) possess a unique carbohydrate-binding specificity for sialylated glycan containing α -D-Neu5Ac(2 \rightarrow 6)- β -D-Gal(1 \rightarrow 4)- β -D-Glc/GlcNAc trisaccharide sequences.² Several HMOs have poor or no affinity for α -D-Neu5Ac(2 \rightarrow 3/6) linkage. So, affinity binding data acquired for specific HMOs will enhance the implementation of *proxy protein* ESI-MS method for large library of oligosaccharides in future.

5.2.2 Study of inhibitory effects of human milk oligosaccharides on galectin induced T cell death assay

Relevant extension of the work in chapter 4 can be done to investigate the inhibitory effects of human milk oligosaccharides on galectin induced T cell death assay. Human milk has nutritional value and it gives immune protection and other advantages to neonates.³ Human milk contains a large pool of free-reducing oligosaccharides. Among them lot of complex oligosaccharides are unique to human milk. These oligosaccharides block viral and bacterial attachment to epithelial cells of infants resulting in low risk of infection.⁴ Apart from protective properties of HMOs, they also show immunomodulatory effects.⁵

Galectins (galactose-binding lectins) are known to bind glycolipids and glycoproteins. It plays important roles in a variety of biological processes, such as inflammation, cell proliferation, the cell cycle, transcription processes, cell apoptosis.⁶ Given their biological importance in many diseases, including cancer, galectins are attractive pharmacological targets. Galectins can be found in the extracellular space, in the cell membrane, in the cytoplasm, and even in the nucleus. Extracellular galectins may mediate cell–cell or cell–matrix adhesion by recognizing cell surface glycoproteins and glycolipids or glycosylated extracellular matrix.⁷

Various human lectins have binding specificity for HMOs in the form of glycan epitopes. As for example, lots of complex glycans have affinities for siglecs and galectins. Galectins possess carbohydrate recognition domain (CRD) and show affinity for structure of N-acetylglucosamine (LacNAc).⁸⁻¹⁰ It has been 3 decades since galectins were discovered but understanding about their biological functions still continues to develop.

Also interference of HMOs in regulation of immunological processes by galectin is not clearly described to date.¹¹ It was mentioned earlier that HMOs can exist in the circulation at physiologically compatible concentration. Some HMOs have structural similarities with cell surface glycan and serve as ligand for galectin.

The affinities for a small number of HMOs for human galectins 1, 2, 3, 7, 8, 9 have been previously measured by frontal affinity chromatography (FAC)¹² and, more recently, by fluorescence anisotropy assay (for galectin 3).¹³ With the goal of addressing the immunomodulatory effects of HMOs, an extended affinity measurement experiment was performed for a larger number of HMO structures for galectins, by direct ESI-MS binding assay. Chapter 4 shows the affinities of 32 of the most abundant HMOs for Gal-1, Gal-3C and Gal-9N and these were quantified for the first time using direct ESI-MS. It can be hypothesized that, HMOs can modulate immune response by interacting with galectins. Galectin-1, -3 and -9 are reported to induce cell death by binding to distinct cell surface glycoprotein receptor and lactose can inhibit galectin dependent cell death.^{14,15} Human milk oligosaccharides contain lactose (Gal β 1-4Glc) at the reducing end so it is expected that, HMOs will show similar inhibitory effects by binding to galectin-1, -3 and -9.

In future, inhibitory effects of HMOs on cell surface binding of galectin and its induced T cell death assay can be studied.

Determination of galectin to T cell surface binding

Binding of biotinylated galectins to human T cell lines (MOLT-4, Jurkat, and CEM) or thymocytes is performed as described by Amano et al. 2003.¹⁶ Cells are incubated for 30 min at 4°C with increasing concentrations of biotinylated galectins to construct binding

curves, and galectin concentrations that give ~ 50% maximal binding are used for inhibition-binding assays with HMO fraction. Before running experiment with HMOs fractions they have to be characterized for specific content of oligosaccharides present in each fraction. Binding assays are performed at 4°C to minimize cell death. Cells are washed two times with PBS and stained with SA-FITC and 7-aminoactinomycin D (Molecular Probes) to detect galectin binding and dead cells, respectively. Flow cytometry data are acquired using a BD Biosciences BD-LSR I Analytic Flow Cytometer and analyzed with CellQuest software (BD Biosciences).

Inhibition of T cells death assay by galectins

Programmed cell death of lymphocyte is essential for normal immune development and regulation.¹⁷ Galectins regulates cell death either inside or outside of the cell. It binds specifically to glycoprotein receptor on cell surface to regulate cell death. Following a protocol described elsewhere assays can be performed.^{14, 18} T cells are incubated in RPMI nutrition media with the desired concentration of galectin-1, -3 and -9 and buffer control with or without specific concentration of HMOs fractions for 4 h at 37°C. Galectin can be dissociated with high concentration HMOs fraction and cell death can be detected by labeling with Annexin VGFP and propidium iodide (PI; Molecular Probes).

For detection of cells which contain subdiploid DNA, fixed permeabilized cells can be stained with PI and DNA content can be determined as previously described.¹⁸ All death assays can be performed in triplicate and data can be acquired using a BD Biosciences BD-LSR I Analytic Flow Cytometer and analyzed with CellQuest software (BD Biosciences). The percentage of cell death of T cell lines can be determined by labeling with annexin V⁻ and PI. In summary, this study is a possible extension of the chapter 4

and it will further give us better understanding of how HMOs play role in galectins' immunoregulation. Thus, it may justify the interactions of HMOs with galectins in human.

5.3 References

- (1) Kuwabara, N.; Hu, D.; Tateno, H.; Makyio, H.; Hirabayashi, J.; Kato, R. *FEBS Lett.* **2013**, *587*, 3620-3625.
- (2) Tateno, H.; Winter, H. C.; Goldstein, I. J. *Biochem J.* **2004**, *382*, 667-675.
- (3) Yu, Y.; Lasanajak, Y.; Song, X.; Hu, L.; Ramani, S.; Mickum, M. L.; Ashline, D. J.; Prasad, B. V.; Estes, M. K.; Reinhold, V. N. *Mol. Cell. Proteom.* **2014**, *13*, 2944-2960.
- (4) Jantscher-Krenn, E.; Lauwaet, T.; Bliss, L. A.; Reed, S. L.; Gillin, F. D.; Bode, L. *Brit J. Nutr.* **2012**, *108*, 1839-1846.
- (5) Kunz, C.; Rudloff, S.; Baier, W.; Klein, N.; Strobel, S. *Annu. Rev. Nutr.* **2000**, *20*, 699-722.
- (6) Rabinovich, G. A.; Baum, L. G.; Tinari, N.; Paganelli, R.; Natoli, C.; Liu, F.-T.; Iacobelli, S. *Trends Immunol.* **2002**, *23*, 313-320.
- (7) Hughes, R. C. *Biochimie* **2001**, *83*, 667-676.
- (8) Kasai, K.; Hirabayashi, J. *J. Biochem.* **1996**, *119*, 1-8.
- (9) Carlsson, S.; Carlsson, M. C.; Leffler, H. *Glycobiology* **2007**, *17*, 906-912.
- (10) Arthur, C. M.; Baruffi, M. D.; Cummings, R. D.; Stowell, S. R. In *Galectins: Methods and Protocols*, Stowell, R. S.; Cummings, D. R., Eds.; Springer New York: New York, NY, 2015, pp 1-35.
- (11) Bode, L. *Nutr. Rev.* **2009**, *67*, S183-S191.

- (12) Hirabayashi, J.; Hashidate, T.; Arata, Y.; Nishi, N.; Nakamura, T.; Hirashima, M.; Urashima, T.; Oka, T.; Futai, M.; Muller, W. E. *BBA-Gen. Subjects* **2002**, *1572*, 232-254.
- (13) Salomonsson, E.; Carlsson, M. C.; Osla, V.; Hendus-Altenburger, R.; Kahl-Knutson, B.; Öberg, C. T.; Sundin, A.; Nilsson, R.; Nordberg-Karlsson, E.; Nilsson, U. J. *J. Biol. Chem.* **2010**, *285*, 35079-35091.
- (14) Stillman, B. N.; Hsu, D. K.; Pang, M.; Brewer, C. F.; Johnson, P.; Liu, F.-T.; Baum, L. G. *J. Immunol.* **2006**, *176*, 778-789.
- (15) Lu, L.-H.; Nakagawa, R.; Kashio, Y.; Ito, A.; Shoji, H.; Nishi, N.; Hirashima, M.; Yamauchi, A.; Nakamura, T. *J. Biochem.* **2007**, *141*, 157-172.
- (16) Amano, M.; Galvan, M.; He, J.; Baum, L. G. *J. Biol. Chem.* **2003**, *278*, 7469-7475.
- (17) Opferman, J. T.; Korsmeyer, S. J. *Nat. Immunol.* **2003**, *4*, 410-415.
- (18) Pace, K. E.; Hahn, H. P.; Baum, L. G. *Methods Enzymol.* **2003**, *363*, 499.

Bibliography

Chapter 1

- (1) Holgersson, J.; Gustafsson, A.; Breimer, M. E. *Immunol. Cell Biol.* **2005**, *83*, 694-708.
- (2) Varki, A. C.; Cummings, R. D.; Esko, J. D.; Freeze, H. H.; Stanley, P.; Bertozzi, C. R.; Hart, G. W.; Etzler, M. E. *Essentials of Glycobiology*; Cold Spring Harbor Laboratory Press: Cold Spring Harbor, NY, 2009.
- (3) Ghazarian, H.; Idoni, B.; Oppenheimer, S. B. *Acta Histochem.* **2011**, *113*, 236-247.
- (4) Ohtsubo, K.; Marth, J. D. *Cell* **2006**, *126*, 855-867.
- (5) Bode, L. *Nutr. Rev.* **2009**, *67*, S183-S191.
- (6) Sharon, N.; Lis, H. *Science* **1989**, *246*, 227-234.
- (7) Ofek, I.; Hasty, D. L.; Sharon, N. *FEMS Immunol. Med. Mic.* **2003**, *38*, 181-191.
- (8) Lis, N. S. a. H. *Sci. Am.* **1993**, *268*, 82-89.
- (9) Opdenakker, G.; Rudd, P. M.; Ponting, C. P.; Dwek, R. A. *FASEB J.* **1993**, *7*, 1330-1337.
- (10) Mody, R.; Joshi, S. H. a.; Chaney, W. *J. Pharmacol. Toxicol.* **1995**, *33*, 1-10.
- (11) Disney, M. D.; Seeberger, P. H. *Chem. Biol.* **2004**, *11*, 1701-1707.
- (12) Blomme, B.; Van Steenkiste, C.; Callewaert, N.; Van Vlierberghe, H. *J. Hepatol.* **2009**, *50*, 592-603.
- (13) El-Hawiet, A.; Kitova, E. N.; Klassen, J. S. *Glycobiology* **2015**, *25*, 845-854.
- (14) Feizi, T.; Mulloy, B. *Curr. Opin. Struc. Biol.* **2003**, *13*, 602-604.
- (15) Wormald, M. R.; Sharon, N. *Curr. Opin. Struc. Biol.* **2004**, *14*, 591-592.

- (16) Oppenheimer, S. B.; Alvarez, M.; Nnoli, J. *Acta Histochem.* **2008**, *110*, 6-13.
- (17) Schwartz-Albiez, R.; Laban, S.; Eichmüller, S.; Kirschfink, M. *Autoimmunity Rev.* **2008**, *7*, 491-495.
- (18) Goetz, J. A.; Mechref, Y.; Kang, P.; Jeng, M. H.; Novotny, M. V. *Glycoconjugate J.* **2009**, *26*, 117-131.
- (19) Patsos, G.; Hebbe-Viton, V.; Robbe-Masselot, C.; Masselot, D.; Martin, R. S.; Greenwood, R.; Paraskeva, C.; Klein, A.; Graessmann, M.; Michalski, J. C.; Gallagher, T.; Corfield, A. *Glycobiology* **2009**, *19*, 382-398.
- (20) Powlesland, A. S.; Hitchen, P. G.; Parry, S.; Graham, S. A.; Barrio, M. M.; Elola, M. T.; Mordoh, J.; Dell, A.; Drickamer, K.; Taylor, M. E. *Glycobiology* **2009**, *19*, 899-909.
- (21) Rek, A.; Krenn, E.; Kungl, A. J. *Brit. J. Pharmacol.* **2009**, *157*, 686-694.
- (22) Shida, K.; Misonou, Y.; Korekane, H.; Seki, Y.; Noura, S.; Ohue, M.; Honke, K.; Miyamoto, Y. *Glycobiology* **2009**, *19*, 1018-1033.
- (23) Mammen, M.; Choi, S.-K.; Whitesides, G. M. *Angew. Chem. Int. Edit.* **1998**, *37*, 2754-2794.
- (24) Klemm, J. D.; Schreiber, S. L.; Crabtree, G. R. *Annu. Rev. Immunol.* **1998**, *16*, 569-592.
- (25) Sacchettini, J. C.; Baum, L. G.; Brewer, C. F. *Biochemistry* **2001**, *40*, 3009-3015.
- (26) Drickamer, K.; Taylor, M. E. *Annu. Rev. Cell Biol.* **1993**, *9*, 237-264.
- (27) Liu, F.-T. *Clin. Immunol.* **2000**, *97*, 79-88.
- (28) Bundle, D. R.; Young, N. M. *Curr. Opin. Struc. Biol.* **1992**, *2*, 666-673.
- (29) García-Hernández, E.; Hernández-Arana, A. *Protein Sci.* **1999**, *8*, 1075-1086.

- (30) Dam, T. K.; Brewer, C. F. *Chem. Rev.* **2002**, *102*, 387-430.
- (31) García-Hernández, E.; Zubillaga, R. A.; Rojo-Domínguez, A.; Rodríguez-Romero, A.; Hernández-Arana, A. *Proteins* **1997**, *29*, 467-477.
- (32) Toone, E. J. *Curr. Opin. Struc. Biol.* **1994**, *4*, 719-728.
- (33) García-Hernández, E.; Zubillaga, R. A.; Rodríguez-Romero, A.; Hernández-Arana, A. *Glycobiology* **2000**, *10*, 993-1000.
- (34) Lemieux, R. U. *Accounts Chem. Res.* **1996**, *29*, 373-380.
- (35) Rand, R. P.; Fuller, N. L.; Butko, P.; Francis, G.; Nicholls, P. *Biochemistry* **1993**, *32*, 5925-5929.
- (36) Swaminathan, C. P.; Surolia, N.; Surolia, A. *J. Am. Chem. Soc.* **1998**, *120*, 5153-5159.
- (37) Schlichting, I. *Method Mol. Biol.* **2005**, 155-165.
- (38) Palmer, R.; Niwa, H. *Biochem. Soc. Trans.* **2003**, *31*, 973-979.
- (39) Staunton, D.; Owen, J.; Campbell, I. D. *Accounts Chem. Res.* **2003**, *36*, 207-214.
- (40) Karlsson, R. *J. Mol. Recognit.* **2004**, *17*, 151-161.
- (41) De Crescenzo, G.; Boucher, C.; Durocher, Y.; Jolicoeur, M. *Cel. Mol. Bioeng.* **2008**, *1*, 204-215.
- (42) Daghestani, H. N.; Day, B. W. *Sensors* **2010**, *10*, 9630-9646.
- (43) Schuck, P. *Annu. Rev. Bioph. Biom.* **1997**, *26*, 541-566.
- (44) Larsen, K.; Thygesen, M. B.; Guillaumie, F.; Willats, W. G. T.; Jensen, K. J. *Carbohydr. Res.* **2006**, *341*, 1209-1234.
- (45) Rillahan, C. D.; Paulson, J. C. *Annu. Rev. Biochem.* **2011**, *80*, 797-823.
- (46) Alvarez, R. A.; Blixt, O. *Method. Enzymol.* **2006**, *415*, 292-310.

- (47) Blixt, O.; Head, S.; Mondala, T.; Scanlan, C.; Huflejt, M. E.; Alvarez, R.; Bryan, M. C.; Fazio, F.; Calarese, D.; Stevens, J.; Razi, N.; Stevens, D. J.; Skehel, J. J.; van Die, I.; Burton, D. R.; Wilson, I. A.; Cummings, R.; Bovin, N.; Wong, C.-H.; Paulson, J. C. *P. Natl. Acad. Sci. USA* **2004**, *101*, 17033-17038.
- (48) Smith, D. F.; Song, X.; Cummings, R. D. *Method. Enzymol.* **2010**, *480*, 417-444.
- (49) Liu, Y.; Palma, A. S.; Feizi, T. *Biol. Chem.* **2009**, *390*, 647-656.
- (50) Park, S.; Gildersleeve, J. C.; Blixt, O.; Shin, I. *Chem. Soc. Rev.* **2013**, *42*, 4310-4326.
- (51) Grant, O. C.; Smith, H. M.; Firsova, D.; Fadda, E.; Woods, R. J. *Glycobiology* **2013**, cwt083.
- (52) Sridharan, R.; Zuber, J.; Connelly, S. M.; Mathew, E.; Dumont, M. E. *BBA-Biomembranes* **2014**, *1838*, 15-33.
- (53) Wishart, D. *Curr. Pharm. Biotechnol.* **2005**, *6*, 105-120.
- (54) Zuiderweg, E. R. *Biochemistry* **2002**, *41*, 1-7.
- (55) Meyer, B.; Peters, T. *Angew. Chem. Int. Edit.* **2003**, *42*, 864-890.
- (56) Ganem, B.; Li, Y. T.; Henion, J. D. *J. Am. Chem. Soc.* **1991**, *113*, 6294-6296.
- (57) Drummond, J. T.; Loo, R. R. O.; Matthews, R. G. *Biochemistry* **1993**, *32*, 9282-9289.
- (58) Drake, R. R.; Schwegler, E. E.; Malik, G.; Diaz, J.; Block, T.; Mehta, A.; Semmes, O. J. *Mol. Cell. Proteom.* **2006**, *5*, 1957-1967.
- (59) Deroo, S.; Hyung, S.-J.; Marcoux, J.; Gordiyenko, Y.; Koripella, R. K.; Sanyal, S.; Robinson, C. V. *ACS Chem. Biol.* **2012**, *7*, 1120-1127.

- (60) Rosu, F.; Gabelica, V.; Shin-ya, K.; De Pauw, E. *Chem. Commun.* **2003**, 2702-2703.
- (61) Gabelica, V.; Rosu, F.; De Pauw, E. *Anal. Chem.* **2009**, *81*, 6708-6715.
- (62) Kebarle, P.; Peschke, M. *Anal. Chim. Acta* **2000**, *406*, 11.
- (63) Kebarle, P.; Tang, L. *Anal. Chem.* **1993**, *65*, 972A-986A.
- (64) Taylor, G.; McEwan, A. *J. Fluid Mech.* **1965**, *22*, 1-15.
- (65) Iribarne, J. V.; Thomson, B. A. *J. Chem. Phys.* **1976**, *64*, 2287.
- (66) Thomson, B. A.; Iribarne, J. V. *J. Chem. Phys.* **1979**, *71*, 4451.
- (67) Dole, M.; Mack, L. L.; Hines, R. L.; Mobley, R. C.; Ferguson, L. D.; Alice, M. B. *J. Chem. Phys.* **1968**, *49*, 2240.
- (68) Kebarle, P.; Verkerk, U. H. *Mass Spectrom. Rev.* **2009**, *28*, 898-917.
- (69) Iavarone, A. T.; Williams, E. R. *J. Am. Chem. Soc.* **2003**, *125*, 2319.
- (70) Konermann, L.; Ahadi, E.; Rodriguez, A. D.; Vahidi, S. *Anal. Chem.* **2012**, *85*, 2-9.
- (71) Ahadi, E.; Konermann, L. *J. Phys. Chem. B* **2011**, *116*, 104-112.
- (72) Konermann, L.; Rodriguez, A. D.; Liu, J. *Anal. Chem.* **2012**, *84*, 6798-6804.
- (73) Marshall, A. G.; Hendrickson, C. L.; Jackson, G. S. *Mass Spectrom. Rev.* **1998**, *17*, 1-35.
- (74) Marshall, A. G.; Hendrickson, C. L. *Int. J. Mass Spectrom.* **2002**, *215*, 59-75.
- (75) Xian, F.; Hendrickson, C. L.; Marshall, A. G. *Anal. Chem.* **2012**, *84*, 708-719.
- (76) Hoffmann, E. D.; Charette, J.; Stroobant, V.; Brodbelt, J. *J. Am. Soc. Mass Spectrom.* **1997**, *8*, 1193-1194.
- (77) Guilhaus, M.; Selby, D.; Mlynski, V. *Mass Spectrom. Rev.* **2000**, *19*, 65-107.

- (78) Takats, Z.; Wiseman, J. M.; Gologan, B.; Cooks, R. G. *Science* **2004**, *306*, 471-473.
- (79) Badu-Tawiah, A.; Bland, C.; Campbell, D. I.; Cooks, R. G. *J. Am. Soc. Mass Spectrom.* **2010**, *21*, 572-579.
- (80) Ifa, D. R.; Wu, C.; Ouyang, Z.; Cooks, R. G. *The Analyst* **2010**, *135*, 669-681.
- (81) Takats, Z.; Wiseman, J. M.; Cooks, R. G. *J. Mass Spectrom.* **2005**, *40*, 1261-1275.
- (82) Green, F.; Salter, T.; Gilmore, I.; Stokes, P.; O'Connor, G. *The Analyst* **2010**, *135*, 731-737.
- (83) Olumee, Z.; Callahan, J. H.; Vertes, A. *J. Phys. Chem. A* **1998**, *102*, 9154-9160.
- (84) Venter, A.; Sojka, P. E.; Cooks, R. G. *Anal. Chem.* **2006**, *78*, 8549-8555.
- (85) Zivolic, F.; Zancanaro, F.; Favretto, D.; Ferrara, S. D.; Seraglia, R.; Traldi, P. *J. Mass Spectrom.* **2010**, *45*, 411-420.
- (86) Douglass, K. A.; Venter, A. R. *J. Mass Spectrom.* **2013**, *48*, 553-560.
- (87) Costa, A. B.; Cooks, R. G. *Chem. Commun.* **2007**, 3915-3917.
- (88) Thomson, B.; Iribarne, J. *J. Chem. Phys.* **1979**, *71*, 4451-4463.
- (89) Mack, L. L.; Kralik, P.; Rheude, A.; Dole, M. *J. Chem. Phys.* **1970**, *52*, 4977-4986.
- (90) Shin, Y.-S.; Drolet, B.; Mayer, R.; Dolence, K.; Basile, F. *Anal. Chem.* **2007**, *79*, 3514-3518.
- (91) Heaton, K.; Solazzo, C.; Collins, M. J.; Thomas-Oates, J.; Bergström, E. T. *J. Archaeol. Sci.* **2009**, *36*, 2145-2154.
- (92) Myung, S.; Wiseman, J. M.; Valentine, S. J.; Takats, Z.; Cooks, R. G.; Clemmer, D. E. *J. Phys. Chem. B* **2006**, *110*, 5045-5051.

- (93) Ferguson, C. N.; Benchaar, S. A.; Miao, Z.; Loo, J. A.; Chen, H. *Anal. Chem.* **2011**, *83*, 6468-6473.
- (94) Banerjee, S.; Mazumdar, S. *Int. J. Anal. Chem.* **2012**, 2012, 282574.
- (95) Tjernberg, A.; Carno, S.; Oliv, F.; Benkestock, K.; Edlund, P. O.; Griffiths, W. J.; Hallen, D. *Anal. Chem.* **2004**, *76*, 4325-4331.
- (96) Kitova, E. N.; El-Hawiet, A.; Schnier, P. D.; Klassen, J. S. *J. Am. Soc. Mass Spectrom.* **2012**, *23*, 431-441.
- (97) El-Hawiet, A.; Kitova, E. N.; Arutyunov, D.; Simpson, D. J.; Szymanski, C. M.; Klassen, J. S. *Anal. Chem.* **2012**, *84*, 3867-3870.
- (98) Wortmann, A.; Rossi, F.; Lelais, G.; Zenobi, R. *J. Mass Spectrom.* **2005**, *40*, 777-784.
- (99) Wortmann, A.; Jecklin, M. C.; Touboul, D.; Badertscher, M.; Zenobi, R. *J. Mass Spectrom.* **2008**, *43*, 600-608.
- (100) Soya, N.; Shoemaker, G. K.; Palcic, M. M.; Klassen, J. S. *Glycobiology* **2009**, *19*, 1224-1234.
- (101) Kitova, E. N.; Kitov, P. I.; Paszkiewicz, E.; Kim, J.; Mulvey, G. L.; Armstrong, G. D.; Bundle, D. R.; Klassen, J. S. *Glycobiology* **2007**, *17*, 1127-1137.
- (102) El-Hawiet, A.; Kitova, E. N.; Kitov, P. I.; Eugenio, L.; Ng, K. K. S.; Mulvey, G. L.; Dingle, T. C.; Szpacenko, A.; Armstrong, G. D.; Klassen, J. S. *Glycobiology* **2011**, *21*, 1217-1227.
- (103) Yanes, O.; Villanueva, J.; Querol, E.; Aviles, F. X. *Nat. Prot.* **2007**, *2*, 119-130.
- (104) Jecklin, M. C.; Touboul, D.; Jain, R.; Toole, E. N.; Tallarico, J.; Drueckes, P.; Ramage, P.; Zenobi, R. *Anal. Chem.* **2008**, *81*, 408-419.

- (105) Yanes, O.; Villanueva, J.; Querol, E.; Aviles, F. X. *Mol. Cell. Proteom.* **2005**, *4*, 1602-1613.
- (106) Wilcox, D. E. *Inorg. Chim. Acta* **2008**, *361*, 857-867.
- (107) Chitta, R. K.; Rempel, D. L.; Gross, M. L. *J. Am. Soc. Mass Spectrom.* **2005**, *16*, 1031-1038.
- (108) Gabelica, V.; Galic, N.; Rosu, F.; Houssier, C.; De Pauw, E. *J. Mass Spectrom.* **2003**, *38*, 491-501.
- (109) Mathur, S.; Badertscher, M.; Scott, M.; Zenobi, R. *Phys. Chem. Chem. Phys.* **2007**, *9*, 6187-6198.
- (110) Wang, W. J.; Kitova, E. N.; Klassen, J. S. *Anal. Chem.* **2005**, *77*, 3060-3071.
- (111) Sun, J. X.; Kitova, E. N.; Wang, W. J.; Klassen, J. S. *Anal. Chem.* **2006**, *78*, 3010-3018.
- (112) Kitova, E. N.; Soya, N.; Klassen, J. S. *Anal. Chem.* **2011**, *83*, 5160-5167.
- (113) Sun, J.; Kitova, E. N.; Sun, N.; Klassen, J. S. *Anal. Chem.* **2007**, *79*, 8301-8311.
- (114) Deng, L.; Sun, N.; Kitova, E. N.; Klassen, J. S. *Anal. Chem.* **2010**, *82*, 2170-2174.
- (115) El-Hawiet, A.; Kitova, E. N.; Liu, L.; Klassen, J. S. *J. Am. Soc. Mass Spectrom.* **2010**, *21*, 1893-1899.
- (116) Sun, J.; Kitova, E. N.; Klassen, J. S. *Anal. Chem.* **2007**, *79*, 416-425.
- (117) Zhang, H.; Lu, H.; Chingin, K.; Chen, H. *Anal. Chem.* **2015**, *87*, 7433-7438.
- (118) Bagal, D.; Kitova, E. N.; Liu, L.; El-Hawiet, A.; Schnier, P. D.; Klassen, J. S. *Anal. Chem.* **2009**, *81*, 7801-7806.
- (119) DeMuth, J. C.; Bu, J.; McLuckey, S. A. *Rapid Commun. Mass Spectrom.* **2015**, *29*, 973-981.

- (120) Clark, S. M.; Konermann, L. *Anal. Chem.* **2004**, *76*, 7077-7083.
- (121) Liu, L.; Kitova, E. N.; Klassen, J. S. *J. Am. Soc. Mass Spectrom.* **2011**, *22*, 310-318.
- (122) Oyelaran, O.; Gildersleeve, J. C. *Curr. Opin. Chem. Biol.* **2009**, *13*, 406-413.
- (123) Nimrichter, L.; Gargir, A.; Gortler, M.; Altstock, R. T.; Shtevi, A.; Weisshaus, O.; Fire, E.; Dotan, N.; Schnaar, R. L. *Glycobiology* **2004**, *14*, 197-203.
- (124) Dickinson, L. E.; Ho, C. C.; Wang, G. M.; Stebe, K. J.; Gerecht, S. *Biomaterials* **2010**, *31*, 5472-5478.
- (125) Šardžik, R.; Sharma, R.; Kaloo, S.; Voglmeir, J.; Crocker, P. R.; Flitsch, S. L. *Chem. Commun.* **2011**, *47*, 5425-5427.
- (126) Song, X.; Lasanajak, Y.; Xia, B.; Heimbürg-Molinaro, J.; Rhea, J. M.; Ju, H.; Zhao, C.; Molinaro, R. J.; Cummings, R. D.; Smith, D. F. *Nat. Methods* **2011**, *8*, 85-90.
- (127) Arndt, N. X.; Tiralongo, J.; Madge, P. D.; von Itzstein, M.; Day, C. J. *J. Cell. Biochem.* **2011**, *112*, 2230-2240.
- (128) Liang, P.-H.; Wu, C.-Y.; Greenberg, W. A.; Wong, C.-H. *Curr. Opin. Chem. Biol.* **2008**, *12*, 86-92.
- (129) Heimbürg-Molinaro, J.; Song, X.; Smith, D. F.; Cummings, R. D. *Curr. Protoc. Prot. Sci.* **2011**, 12.10. 11-12.10. 29.
- (130) Arthur, C. M.; Rodrigues, L. C.; Baruffi, M. D.; Sullivan, H. C.; Heimbürg-Molinaro, J.; Smith, D. F.; Cummings, R. D.; Stowell, S. R. *Galectins: Methods and Protocols* **2015**, 115-131.

- (131) Raman, R.; Raguram, S.; Venkataraman, G.; Paulson, J. C.; Sasisekharan, R. *Nat. Methods* **2005**, *2*, 817-824.
- (132) Liang, C.-H.; Wu, C.-Y. *Expert Rev Proteom.* **2009**, *6*, 631-645.
- (133) Drickamer, K.; Taylor, M. E. *Genome Biol.* **2002**, *3*, 1034.
- (134) Kilcoyne, M.; Gerlach, J. Q.; Kane, M.; Joshi, L. *Anal. Methods* **2012**, *4*, 2721-2728.
- (135) Grant, O. C.; Smith, H. M.; Firsova, D.; Fadda, E.; Woods, R. J. *Glycobiology* **2014**, *24*, 17-25.
- (136) Paulson, J. C.; Blixt, O.; Collins, B. E. *Nat. Chem. Biol.* **2006**, *2*, 238-248.

Chapter 2

- (1) Bewley, C. A., *Protein-carbohydrate Interactions in Infectious Diseases*. RSC Publishing: Cambridge, UK; **2006**.
- (2) Disney, M. D.; Seeberger, P.H., *Chem. Biol.* **2004**, *11*, 1701-1707.
- (3) Leavitt, S.; Freire, E., *Curr. Opin. Struct. Biol.* **2001**, *11*, 560-566.
- (4) Frostell, Å.; Vinterbäck, L.; Sjöbom, H., *Methods Mol. Biol.* **2013**, *1008*, 139-165.
- (5) Zech, S. G.; Olejniczak, E.; Hajduk, P.; Mack, J.; McDermott, A. E., *J. Am. Soc. Mass Spectrom.* **2004** *126*, 13948-13953.
- (6) Orosz, F.; Ovadi, J., *J. Immunol. Methods.* **2002**, *270*, 155-162.
- (7) El-Hawiet, A.; Kitova, E. N.; Klassen, J. S. *Anal. Chem.* **2013**, *85*, 7637-7644.
- (8) Lin, H.; Kitova, E. N.; Klassen, J. S. *J. Am. Soc. Mass Spectrom.* **2014**, *25*, 104-110.

- (9) Han, L.; Kitov, P. I.; Kitova, E. N.; Tan, M.; Wang, L.; Xia, M.; Jiang, X.; Klassen, J.S. *Glycobiology*. **2013**, *23*, 276-285.
- (10) El-Hawiet, A.; Kitova, E. N.; Arutyunov, D.; Szymanski, C. M.; Klassen, J. S. *Anal. Chem.* **2012**, *84*, 3867–3870.
- (11) El-Hawiet, A.; Kitova, E. N.; Klassen, J. S. *Biochemistry*, **2012**, *51*, 4244-4253.
- (12) Daniel, J. M.; Friess, S. D.; Rajagopalan, S.; Wendt, S.; Zenobi, R. *Int. J. Mass Spectrom.* **2002**, *216*, 1-27.
- (13) Kitova, E. N.; El-Hawiet, A.; Schnier, P. D.; Klassen, J. S. *J. Am. Soc. Mass Spectrom.* **2012**, *23*, 431-441.
- (14) El-Hawiet, A.; Kitova, E. N.; Liu, L.; Klassen, J. S. *J. Am. Soc. Mass Spectrom.* **2010**, *21*, 1893-1899.
- (15) Deng, L.; Sun N; Kitova, E. N.; Klassen, J. S. *Anal. Chem.* **2010**, *82*, 2170-2174.
- (16) El-Hawiet, A., Shoemaker, G. K., Daneshfar, R., Kitova, E. N., Klassen, J. S. *Anal. Chem.* **2011**, *84*, 50-58.
- (17) Loo, J. A. *Mass Spectrom. Rev.* **1997**, *16*, 1-23.
- (18) Wang, W.; Kitova, E. N.; Klassen, J. S. *Anal. Chem.* **2003**, *75*, 4945-4955.
- (19) Kebarle, P. *J. Mass Spectrom.* **2000**, *35*, 804-817.
- (20) Banerjee, S.; Mazumdar, S. *Int. J. Anal. Chem.* **2012**, *2012*, 282574.
- (21) Sterling, H., Batchelor, J., Wemmer, D., Williams, E. *J. Am. Soc. Mass Spectrom.* **2010**, *21*, 1045-1049.
- (22) Yang P.; Cooks R. G.; Ouyang Z. *Anal. Chem.* **2005**, *77*, 6174-6183.
- (23) Takáts, Z.; Wiseman, J. M.; Gologan, B.; Cooks, R. G. *Science* **2004**, *306*, 471-473.

- (24) Shin, Y.-S.; Drolet, B.; Mayer, R.; Dolence, K.; Basile, F. *Anal. Chem.* **2007**, *79*, 3514-3518.
- (25) Lu, X.; Ning, B.; He, D.; Huang, L.; Yue, X.; Zhang, Q.; Huang, H.; Liu, Y.; He, L.; Ouyang, J. *J. Am. Soc. Mass Spectrom.* **2014**, *25*, 454-463.
- (26) Miao, Z.; Chen, H. *J. Am. Soc. Mass Spectrom.* **2009**, *20*, 10-19.
- (27) Liu, P.; Zhang, J.; Ferguson, C. N.; Chen, H.; Loo, J. A. *Anal. Chem.* **2013**, *85*, 11966-11972.
- (28) Ferguson, C. N.; Benchaar, S. A.; Miao, Z.; Loo, J. A.; Chen, H. *Anal. Chem.* **2011**, *83*, 6468-6473.
- (29) Moore, B. N.; Hamdy, O.; Julian, R. R. *Int. J. Mass Spectrom.* **2012**, 330–332, 220-225.
- (30) Takáts, Z.; Wiseman, J. M.; Cooks, R. G. *J. Mass Spectrom.* **2005**, *40*, 1261-1275.
- (31) Veros, C. T.; Oldham, N. J. *Rapid Commun. Mass Spectrom.* **2007**, *21*, 3505-3510.
- (32) Sun, N.; Soya, N.; Kitova, E.; Klassen, J. *J. Am. Soc. Mass Spectrom.* **2010**, *21*, 472-481.
- (33) Jecklin, M.; Touboul, D.; Bovet, C.; Wortmann, A.; Zenobi, R. *J. Am. Soc. Mass Spectrom.* **2008**, *19*, 332-343.
- (34) Zdanov, A.; Li, Y.; Bundle, D. R.; Deng, S. J.; MacKenzie, C. R.; Narang, S. A.; Young, N. M.; Cygler, M. *Proc. Natl. Acad. Sci.* **1994**, *91*, 6423-6427.
- (35) Rademacher, C.; Shoemaker, G. K.; Kim, H.-S.; Zheng, R. B.; Taha, H.; Liu, C.; Nacario, R. C.; Schriemer, D. C.; Klassen, J. S.; Peters, T.; Lowary, T. L. *J. Am. Chem. Soc.* **2007**, *129*, 10489-10502.

- (36) Wang, W.; Kitova, E. N.; Klassen, J. S. *Anal. Chem.* **2005**, *77*, 3060-3071.
- (37) Sun, J.; Kitova, E. N.; Wang, W.; Klassen, J. S. *Anal. Chem.* **2006**, *78*, 3010-3018.
- (38) Daneshfar, R.; Kitova, E. N.; Klassen, J. S. *J. Am. Chem. Soc.* **2004**, *126*, 4786-4787.
- (39) Kitova, E. N.; El-Hawiet, A.; Klassen, J. S. *J. Am. Soc. Mass Spectrom.* **2014**, *25*(11), 1908-1916.
- (40) Schindler, M.; Assaf, Y.; Sharon, N.; Chipman, D. M. *Biochemistry* **1977**, *16*, 423-431.
- (41) Hunter, E. P.; Lias, S. G. *J. Phys. Chem. Ref. Data* **1998**, *27*, 413-656.
- (42) Venter, A.; Sojka, P. E.; Cooks, R. G. *Anal. Chem.* **2006**, *78*, 8549-8555.
- (43) Miao, Z.; Wu, S.; Chen, H. *J. Am. Soc. Mass Spectrom.* **2010**, *21*, 1730-1736.
- (44) Hopper, J. T. S.; Sokratous, K.; Oldham, N.J. *Anal. Biochem.* **2012**, *421*, 788-790.
- (45) Hopper, J. T. S., Oldham, N. J. *Anal. Chem.* **2011**, *83*, 7472-7479.

Chapter 3

- (1) Ohtsubo, K.; Marth, J. D. *Cell* **2006**, *126*, 855-867.
- (2) Hakomori, S. *Curr. Opin. Hematol.* **2003**, *10*, 16-24.
- (3) Sharon, N.; Lis, H. *Sci. Am.* **1993**, *268*, 82-89.
- (4) Varki, A., Sharon, N. In *Essentials of Glycobiology, 2nd edition*; Varki, A., Cummings, R. D., Esko, J. D., Freeze, H. H., Stanley, P., Bertozzi, C. R., Hart, G. W., Etzler, M. E., Eds; Cold Spring Harbor (NY): Cold Spring Harbor Laboratory Press; **2009**, Part 1.

- (5) Dwek, R. A. *Chem. Rev.* **1996**, 96, 683-720.
- (6) Schulze, H.; Sandhoff, K. *BBA-Mol. Cell. Biol. L.* **2014**, 1841, 799-810.
- (7) Meyer, S.; van Liempt, E.; Imberty, A.; van Kooyk, Y.; Geyer, H.; Geyer, R.; van Die, I. *J. Biol. Chem.* **2005**, 280, 37349-37359.
- (8) Janes, P. W.; Ley, S. C.; Magee, A. I.; Kabouridis, P. S. *Semin. Immunol.* **2000**, 12, 23-34.
- (9) Lis, H.; Sharon, N. *Chem. Rev.* **1998**, 98, 637-674.
- (10) Lee, Y. C.; Lee, R. T. *Accounts Chem. Res.* **1995**, 28, 321-327.
- (11) Cohen, M. *Biomolecules* **2015**, 5, 2056-2072.
- (12) Bode, L. *Nutr. Rev.* **2009**, 67, S183-S191.
- (13) Hickey, R. M. *Int. Dairy J.* **2012**, 22, 141-146.
- (14) Newburg, D. S.; Ruiz-Palacios, G. M.; Morrow, A. L. *Annu. Rev. Nutr.* **2005**, 25, 37-58.
- (15) Bode, L.; Jantscher-Krenn, E. *Adv. Nutr.* **2012**, 3, 383S-391S.
- (16) Ruiz-Palacios, G. M.; Cervantes, L. E.; Ramos, P.; Chavez-Munguia, B.; Newburg, D. S. *J. Biol. Chem.* **2003**, 278, 14112-14120.
- (17) Ernst, B.; Magnani, J. L. *Nat. Rev. Drug Discov.* **2009**, 8, 661-677.
- (18) Magnani, J. L. *Glycoscience: Biology and Medicine* **2015**, 1517-1522.
- (19) Cooper, M. A. *Nat. Rev. Drug Discov.* **2002**, 1, 515-528.
- (20) de Azevedo, J.; Walter, F.; Dias, R. *Curr. Drug Targets* **2008**, 9, 1071-1076.
- (21) Slon-Usakiewicz, J. J.; Ng, W.; Dai, J.-R.; Pasternak, A.; Redden, P. R. *Drug Discov. Today* **2005**, 10, 409-416.
- (22) Meyer, B.; Peters, T. *Angew. Chem. Int. Edit.* **2003**, 42, 864-890.

- (23) Smith, E. A.; Thomas, W. D.; Kiessling, L. L.; Corn, R. M. *J. Am. Chem. Soc.* **2003**, 125, 6140-6148.
- (24) Rossi, A. M.; Taylor, C. W. *Nat. Protoc.* **2011**, 6, 365-387.
- (25) Myszka, D. G. *Curr. Opin. Biotech.* **1997**, 8, 50-57.
- (26) Boer, A. R.; Hokke, C. H.; Deelder, A. M.; Wuhrer, M. *Glycoconjugate J.* **2008**, 25, 75-84.
- (27) Mehta-D'souza, P. In *Galectins: Methods and Protocols*, Stowell, R. S.; Cummings, D. R., Eds.; Springer New York: New York, NY, **2015**, 105-114.
- (28) del Carmen Fernández-Alonso, M.; Díaz, D.; Alvaro Berbis, M.; Marcelo, F.; Jimenez-Barbero, J. *Curr. Protein Pept. Sci.* **2012**, 13, 816-830.
- (29) Rillahan, C. D.; Brown, S. J.; Register, A. C.; Rosen, H.; Paulson, J. C. *Angew. Chem. Int. Edit.* **2011**, 50, 12534-12537.
- (30) Ng, E. S. M.; Yang, F.; Kameyama, A.; Palcic, M. M.; Hindsgaul, O.; Schriemer, D. C. *Anal. Chem.* **2005**, 77, 6125-6133.
- (31) Oyelaran, O.; Gildersleeve, J. C. *Curr. Opin. Chem. Biol.* **2009**, 13, 406-413.
- (32) Nimrichter, L.; Gargir, A.; Gortler, M.; Altstock, R. T.; Shtevi, A.; Weisshaus, O.; Fire, E.; Dotan, N.; Schnaar, R. L. *Glycobiology* **2004**, 14, 197-203.
- (33) Dickinson, L. E.; Ho, C. C.; Wang, G. M.; Stebe, K. J.; Gerecht, S. *Biomaterials* **2010**, 31, 5472-5478.
- (34) Šardžik, R.; Sharma, R.; Kaloo, S.; Voglmeir, J.; Crocker, P. R.; Flitsch, S. L. *Chem. Commun.* **2011**, 47, 5425-5427.

- (35) Song, X.; Lasanajak, Y.; Xia, B.; Heimburg-Molinaro, J.; Rhea, J. M.; Ju, H.; Zhao, C.; Molinaro, R. J.; Cummings, R. D.; Smith, D. F. *Nat. Methods* **2011**, *8*, 85-90.
- (36) Arndt, N. X.; Tiralongo, J.; Madge, P. D.; von Itzstein, M.; Day, C. J. *J. Cell. Biochem.* **2011**, *112*, 2230-2240.
- (37) Liang, P.-H.; Wu, C.-Y.; Greenberg, W. A.; Wong, C.-H. *Curr. Opin. Chem. Biol.* **2008**, *12*, 86-92.
- (38) Heimburg-Molinaro, J.; Song, X.; Smith, D. F.; Cummings, R. D. *Curr. Protoc. Protein Sci.* **2011**, *64*: 12.10. 11-12.10. 29.
- (39) Arthur, C. M.; Rodrigues, L. C.; Baruffi, M. D.; Sullivan, H. C.; Heimburg-Molinaro, J.; Smith, D. F.; Cummings, R. D.; Stowell, S. R. In *Galectins: Methods and Protocols*, Stowell, R. S.; Cummings, D. R., Eds.; Springer New York: New York, NY, **2015**, 115-131.
- (40) Raman, R.; Raguram, S.; Venkataraman, G.; Paulson, J. C.; Sasisekharan, R. *Nat. Methods* **2005**, *2*, 817-824.
- (41) Liang, C.-H.; Wu, C.-Y. *Expert Rev. Proteom.* **2009**, *6*, 631-645.
- (42) Rillahan, C. D.; Paulson, J. C. *Annu. Rev. Biochem.* **2011**, *80*, 797-823.
- (43) Drickamer, K.; Taylor, M. E. *Genome Biol.* **2002**, *3*, 1034.
- (44) Kilcoyne, M.; Gerlach, J. Q.; Kane, M.; Joshi, L. *Anal. Methods* **2012**, *4*, 2721-2728.
- (45) Grant, O. C.; Smith, H. M.; Firsova, D.; Fadda, E.; Woods, R. J. *Glycobiology* **2014**, *24*, 17-25.
- (46) Paulson, J. C.; Blixt, O.; Collins, B. E. *Nat. Chem. Biol.* **2006**, *2*, 238-248.

- (47) Smith, D. F.; Song, X.; Cummings, R. D. *Method Enzymol.* **2010**, 480, 417-444.
- (48) Daniel, J. M.; Friess, S. D.; Rajagopalan, S.; Wendt, S.; Zenobi, R. *Int. J. Mass Spectrom.* **2002**, 216, 1-27.
- (49) Schug, K. A. *Com. Chem. High T. Scr.* **2007**, 10, 301-316.
- (50) Heck, A. J.; van den Heuvel, R. H. *Mass Spectrom. Rev.* **2004**, 23, 368-389.
- (51) El-Hawiet, A.; Kitova, E. N.; Liu, L.; Klassen, J. S. *J. Am. Soc. Mass Spectrom.* **2010**, 21, 1893-1899.
- (52) Lin, H.; Kitova, E. N.; Klassen, J. S. *J. Am. Soc. Mass Spectrom.* **2014**, 25, 104-110.
- (53) Liu, L.; Kitova, E. N.; Klassen, J. S. *J. Am. Soc. Mass Spectrom.* **2011**, 22, 310-318.
- (54) Kitova, E. N.; El-Hawiet, A.; Klassen, J. S. *J. Am. Soc. Mass Spectrom.* **2014**, 25, 1908-1916.
- (55) El-Hawiet, A.; Shoemaker, G. K.; Daneshfar, R.; Kitova, E. N.; Klassen, J. S. *Anal. Chem.* **2012**, 84, 50-58.
- (56) Leney, A. C.; Fan, X.; Kitova, E. N.; Klassen, J. S. *Anal. Chem.* **2014**, 86, 5271-5277.
- (57) El-Hawiet, A.; Kitova, E. N.; Arutyunov, D.; Simpson, D. J.; Szymanski, C. M.; Klassen, J. S. *Anal. Chem.* **2012**, 84, 3867-3870.
- (58) El-Hawiet, A.; Kitova, E. N.; Klassen, J. S. *Anal. Chem.* **2013**, 85, 7637-7644.
- (59) Zhang, Y. X.; Liu, L.; Daneshfar, R.; Kitova, E. N.; Li, C. S.; Jia, F.; Cairo, C. W.; Klassen, J. S. *Anal. Chem.* **2012**, 84, 7618-7621.

- (60) Han, L.; Kitova, E. N.; Tan, M.; Jiang, X.; Klassen, J. S. *J. Am. Soc. Mass Spectrom.* **2014**, *25*, 111-119.
- (61) Han, L.; Tan, M.; Xia, M.; Kitova, E. N.; Jiang, X.; Klassen, J. S. *J. Am. Chem. Soc.* **2014**, *136*, 12631-12637.
- (62) Han, L.; Kitova, E. N.; Tan, M.; Jiang, X.; Pluinage, B.; Boraston, A. B.; Klassen, J. S. *Glycobiology* **2015**, *25*, 170-180.
- (63) Diehl, C.; Genheden, S.; Modig, K.; Ryde, U.; Akke, M. *J. Biomol. NMR* **2009**, *45*, 157-169.
- (64) Higgins, M. A.; Ficko-Blean, E.; Meloncelli, P. J.; Lowary, T. L.; Boraston, A. B. *J. Mol. Biol.* **2011**, *411*, 1017-1036.
- (65) Arnaud, J.; Tröndle, K.; Claudinon, J.; Audfray, A.; Varrot, A.; Römer, W.; Imberty, A. *Angew. Chem. Int. Edit.* **2014**, *53*, 9267-9270.
- (66) Zdanov, A.; Li, Y.; Bundle, D. R.; Deng, S.-J.; MacKenzie, C. R.; Narang, S. A.; Young, N. M.; Cygler, M. *P. Natl. Acad. Sci. USA* **1994**, *91*, 6423-6427.
- (67) Sun, J. X.; Kitova, E. N.; Wang, W. J.; Klassen, J. S. *Anal. Chem.* **2006**, *78*, 3010-3018.
- (68) Meloncelli, P. J.; Lowary, T. L. *Aust. J. Chem.* **2009**, *62*, 558-574.
- (69) Meloncelli, P. J.; Lowary, T. L. *Carbohydr. Res.* **2010**, *345*, 2305-2322.
- (70) Meloncelli, P. J.; West, L. J.; Lowary, T. L. *Carbohydr. Res.* **2011**, *346*, 1406-1426.
- (71) Kostlánová, N.; Mitchell, E. P.; Lortat-Jacob, H.; Oscarson, S.; Lahmann, M.; Gilboa-Garber, N.; Chambat, G.; Wimmerová, M.; Imberty, A. *J. Biol. Chem.* **2005**, *280*, 27839-27849.

- (72) Tan, M.; Hegde, R. S.; Jiang, X. *J. Virol.* **2004**, *78*, 6233-6242.
- (73) Tan, M.; Jiang, X. *J. Virol.* **2005**, *79*, 14017-14030.
- (74) Han, L.; Kitov, P. I.; Kitova, E. N.; Tan, M.; Wang, L.; Xia, M.; Jiang, X.; Klassen, J. S. *Glycobiology* **2013**, *23*, 276-285.
- (75) Urashima, T.; Asakuma, S.; Leo, F.; Fukuda, K.; Messer, M.; Oftedal, O. T. *Adv. Nutr.* **2012**, *3*, 473S-482S.
- (76) Arthur, C. M.; Baruffi, M. D.; Cummings, R. D.; Stowell, S. R. In *Galectins: Methods and Protocols*, Stowell, R. S.; Cummings, D. R., Eds.; Springer New York: New York, NY, **2015**, 1-35.

Chapter 4

- (1) Lara-Villoslada, F.; Olivares, M.; Sierra, S.; Rodríguez, J. M.; Boza, J.; Xaus, J. *Brit. J. Nutr.* **2007**, *98*, S96-S100.
- (2) Martín, R.; Langa, S.; Reviriego, C.; Jiménez, E.; Marín, M. L.; Xaus, J.; Fernández, L.; Rodríguez, J. M. *J. Pediatr.* **2003**, *143*, 754-758.
- (3) Wu, S.; Tao, N.; German, J. B.; Grimm, R.; Lebrilla, C. B. *J. Proteom. Res.* **2010**, *9*, 4138-4151.
- (4) Chichlowski, M.; German, J. B.; Lebrilla, C. B.; Mills, D. A. *Annu. Rev. Food Sci.* **2011**, *2*, 331-351.
- (5) Bode, L. *J. Nutr.* **2006**, *136*, 2127-2130.
- (6) Bode, L.; Jantscher-Krenn, E. *Adv. Nutr.* **2012**, *3*, 383S-391S.
- (7) Bode, L. *Glycobiology* **2012**, *22*, 1147-1162.

- (8) Bhargava, P.; Li, C.; Stanya, K. J.; Jacobi, D.; Dai, L.; Liu, S.; Gangl, M. R.; Harn, D. A.; Lee, C.-H. *Nat. Med.* **2012**, *18*, 1665-1672.
- (9) Gnoth, M. J.; Rudloff, S.; Kunz, C.; Kinne, R. K. *J. Biol. Chem.* **2001**, *276*, 34363-34370.
- (10) Goehring, K. C.; Kennedy, A. D.; Prieto, P. A.; Buck, R. H. *PloS One* **2014**, *9*, e101692.
- (11) Newburg, D. S.; Ruiz-Palacios, G. M.; Morrow, A. L. *Annu. Rev. Nutr.* **2005**, *25*, 37-58.
- (12) Rudloff, S.; Pohlentz, G.; Diekmann, L.; Egge, H.; Kunz, C. *Acta Paediatr.* **1996**, *85*, 598-603.
- (13) Obermeier, S.; Rudloff, S.; Pohlentz, G.; Lentze, M.; Kunz, C. *Isot. Environ. Healt. S.* **1999**, *35*, 119-125.
- (14) El-Hawiet, A.; Kitova, E. N.; Klassen, J. S. *Glycobiology* **2015**, *25*, 845-854.
- (15) Eiwegger, T.; Stahl, B.; Haidl, P.; Schmitt, J.; Boehm, G.; Dehlink, E.; Urbanek, R.; Szépfalusi, Z. *Pediat. Aller. Immunol.* **2010**, *21*, 1179-1188.
- (16) de Kivit, S.; Kraneveld, A. D.; Garssen, J.; Willemsen, L. E. *Eur. J. Phar.* **2011**, *668*, S124-S132.
- (17) Rabinovich, G. A.; Baum, L. G.; Tinari, N.; Paganelli, R.; Natoli, C.; Liu, F.-T.; Iacobelli, S. *Trend. Immunol.* **2002**, *23*, 313-320.
- (18) Hughes, R. C. *Biochimie* **2001**, *83*, 667-676.
- (19) Vasta, G. R. *Nat. Rev. Microbiol.* **2009**, *7*, 424-438.
- (20) Astorgues-Xerri, L.; Riveiro, M. E.; Tijeras-Raballand, A.; Serova, M.; Neuzillet, C.; Albert, S.; Raymond, E.; Faivre, S. *Cancer Treat. Rev.* **2014**, *40*, 307-319.

- (21) Song, L.; Tang, J.-w.; Owusu, L.; Sun, M.-Z.; Wu, J.; Zhang, J. *Clin. Chim. Acta* **2014**, *431*, 185-191.
- (22) Vladoiu, M. C.; Labrie, M.; St-Pierre, Y. *Int. J. Oncol.* **2014**, *44*, 1001-1014.
- (23) Rubinstein, N.; Alvarez, M.; Zwirner, N. W.; Toscano, M. A.; Ilarregui, J. M.; Bravo, A.; Mordoh, J.; Fainboim, L.; Podhajcer, O. L.; Rabinovich, G. A. *Cancer Cell* **2004**, *5*, 241-251.
- (24) Cerliani, J. P.; Stowell, S. R.; Mascanfroni, I. D.; Arthur, C. M.; Cummings, R. D.; Rabinovich, G. A. *J. Clin. Immunol.* **2011**, *31*, 10-21.
- (25) Di Lella, S.; Sundblad, V.; Cerliani, J. P.; Guardia, C. M.; Estrin, D. A.; Vasta, G. R.; Rabinovich, G. A. *Biochemistry* **2011**, *50*, 7842-7857.
- (26) Matsushita, N.; Nishi, N.; Seki, M.; Matsumoto, R.; Kuwabara, I.; Liu, F.-T.; Hata, Y.; Nakamura, T.; Hirashima, M. *J. Biol. Chem.* **2000**, *275*, 8355-8360.
- (27) Paclik, D.; Danese, S.; Berndt, U.; Wiedenmann, B.; Dignass, A.; Sturm, A. *PLoS One* **2008**, *3*, e2629.
- (28) Stowell, S. R.; Qian, Y.; Karmakar, S.; Koyama, N. S.; Dias-Baruffi, M.; Leffler, H.; McEver, R. P.; Cummings, R. D. *J. Immunol.* **2008**, *180*, 3091-3102.
- (29) Camby, I.; Le Mercier, M.; Lefranc, F.; Kiss, R. *Glycobiology* **2006**, *16*, 137R-157R.
- (30) Ilarregui, J.; Bianco, G.; Toscano, M.; Rabinovich, G. *Ann. Rheum. Dis.* **2005**, *64*, iv96-iv103.
- (31) López-Lucendo, M. F.; Solís, D.; André, S.; Hirabayashi, J.; Kasai, K.; Kaltner, H.; Gabius, H.-J.; Romero, A. *J. Mol. Biol.* **2004**, *343*, 957-970.

- (32) Yoshida, H.; Teraoka, M.; Nishi, N.; Nakakita, S.-i.; Nakamura, T.; Hirashima, M.; Kamitori, S. *J. Biol. Chem.* **2010**, *285*, 36969-36976.
- (33) Collins, P. M.; Bum-Erdene, K.; Yu, X.; Blanchard, H. *J. Mol. Biol.* **2014**, *426*, 1439-1451.
- (34) Hirabayashi, J.; Hashidate, T.; Arata, Y.; Nishi, N.; Nakamura, T.; Hirashima, M.; Urashima, T.; Oka, T.; Futai, M.; Muller, W. E. *BBA-Gen. Subjects* **2002**, *1572*, 232-254.
- (35) Bachhawat-Sikder, K.; Thomas, C. J.; Surolia, A. *FEBS Lett.* **2001**, *500*, 75-79.
- (36) Carlsson, S.; Carlsson, M. C.; Leffler, H. *Glycobiology* **2007**, *17*, 906-912.
- (37) Ideo, H.; Seko, A.; Ohkura, T.; Matta, K. L.; Yamashita, K. *Glycobiology* **2002**, *12*, 199-208.
- (38) Sparrow, C.; Leffler, H.; Barondes, S. *J. Biol. Chem.* **1987**, *262*, 7383-7390.
- (39) Noll, A. J.; Gourdine, J. P.; Yu, Y.; Lasanajak, Y.; Smith, D. F.; Cummings, R. D. *Glycobiology* **2016**, cww002.
- (40) Yu, Y.; Lasanajak, Y.; Song, X.; Hu, L.; Ramani, S.; Mickum, M. L.; Ashline, D. J.; Prasad, B. V.; Estes, M. K.; Reinhold, V. N. *Mol. Cell. Proteom.* **2014**, *13*, 2944-2960.
- (41) Ashline, D. J.; Yu, Y.; Lasanajak, Y.; Song, X.; Hu, L.; Ramani, S.; Prasad, V.; Estes, M. K.; Cummings, R. D.; Smith, D. F. *Mol. Cell. Proteom.* **2014**, *13*, 2961-2974.
- (42) Agravat, S. B.; Song, X.; Rojsajakul, T.; Cummings, R. D.; Smith, D. F. *Bioinformatics* **2016**, *32*(10), 1471-1478.

- (43) Urashima, T.; Asakuma, S.; Leo, F.; Fukuda, K.; Messer, M.; Oftedal, O. T. *Adv. Nutr.* **2012**, *3*, 473S-482S.
- (44) Tao, N.; Wu, S.; Kim, J.; An, H. J.; Hinde, K.; Power, M. L.; Gagneux, P.; German, J. B.; Lebrilla, C. B. *J. Proteom. Res.* **2011**, *10*, 1548-1557.
- (45) Urashima, T.; Kitaoka, M.; Asakuma, S.; Messer, M. In *Adv. Dairy Chem.*; Springer, **2009**, 295-349.
- (46) Arthur, C. M.; Rodrigues, L. C.; Baruffi, M. D.; Sullivan, H. C.; Heimbürg-Molinaro, J.; Smith, D. F.; Cummings, R. D.; Stowell, S. R. *Galectins: Methods and Protocols* **2015**, 115-131.
- (47) Heimbürg-Molinaro, J.; Song, X.; Smith, D. F.; Cummings, R. D. *Curr. Prot. Protein Sci.* **2011**, 12.10. 11-12.10. 29.
- (48) Rillahan, C. D.; Paulson, J. C. *Annu. Rev. Biochem.* **2011**, *80*, 797-823.
- (49) Kilcoyne, M.; Gerlach, J. Q.; Kane, M.; Joshi, L. *Anal. Methods* **2012**, *4*, 2721-2728.
- (50) Paulson, J. C.; Blixt, O.; Collins, B. E. *Nat. Chem. Biol.* **2006**, *2*, 238-248.
- (51) Smith, D. F.; Song, X.; Cummings, R. D. *Methods Enzymol.* **2010**, *480*, 417-444.
- (52) Grant, O. C.; Smith, H. M.; Firsova, D.; Fadda, E.; Woods, R. J. *Glycobiology* **2014**, *24*, 17-25.
- (53) Wang, W. J.; Kitova, E. N.; Klassen, J. S. *Methods Enzymol.* **2003**, *362*, 376-397.
- (54) El-Hawiet, A.; Kitova, E. N.; Liu, L.; Klassen, J. S. *J. Am. Soc. Mass Spectrom.* **2010**, *21*, 1893-1899.

- (55) El-Hawiet, A.; Kitova, E. N.; Kitov, P. I.; Eugenio, L.; Ng, K. K. S.; Mulvey, G. L.; Dingle, T. C.; Szpacenko, A.; Armstrong, G. D.; Klassen, J. S. *Glycobiology* **2011**, *21*, 1217-1227.
- (56) Ouellet, M.; Mercier, S.; Pelletier, I.; Bounou, S.; Roy, J.; Hirabayashi, J.; Sato, S.; Tremblay, M. J. *J. Immunol.* **2005**, *174*, 4120-4126.
- (57) Hirabayashi, J.; Kasai, K. *J. Biol. Chem.* **1991**, *266*, 23648-23653.
- (58) Diehl, C.; Genheden, S.; Modig, K.; Ryde, U.; Akke, M. *J. Biomol. NMR* **2009**, *45*, 157-169.
- (59) Nagae, M.; Nishi, N.; Murata, T.; Usui, T.; Nakamura, T.; Wakatsuki, S.; Kato, R. *Glycobiology* **2009**, *19*, 112-117.
- (60) Kitova, E. N.; El-Hawiet, A.; Schnier, P. D.; Klassen, J. S. *J. Am. Soc. Mass Spectrom.* **2012**, *23*, 431-441.
- (61) El-Hawiet, A.; Kitova, E. N.; Klassen, J. S. *Biochemistry* **2012**, *51*, 4244-4253.
- (62) Cho, M.; Cummings, R. D. *Biochemistry* **1996**, *35*, 13081-13088.
- (63) Stowell, S. R.; Karmakar, S.; Arthur, C. M.; Ju, T.; Rodrigues, L. C.; Riul, T. B.; Dias-Baruffi, M.; Miner, J.; McEver, R. P.; Cummings, R. D. *Mol. Biol. Cell* **2009**, *20*, 1408-1418.
- (64) Leppänen, A.; Stowell, S.; Blixt, O.; Cummings, R. D. *J. Biol. Chem.* **2005**, *280*, 5549-5562.
- (65) Sun, J. X.; Kitova, E. N.; Wang, W. J.; Klassen, J. S. *Anal. Chem.* **2006**, *78*, 3010-3018.

- (66) Salomonsson, E.; Carlsson, M. C.; Osla, V.; Hendus-Altenburger, R.; Kahl-Knutson, B.; Öberg, C. T.; Sundin, A.; Nilsson, R.; Nordberg-Karlsson, E.; Nilsson, U. J. *J. Biol. Chem.* **2010**, *285*, 35079-35091.
- (67) Ben, X. M.; Li, J.; Feng, Z. T.; Shi, S. Y.; Lu, Y. D.; Chen, R.; Zhou, X. Y. *World J. Gastroenterol.* **2008**, *14*, 6564-6568.
- (68) Ben, X. M.; Zhou, X. Y.; Zhao, W. H.; Yu, W. L.; Pan, W.; Zhang, W. L.; Wu, S. M.; Van Beusekom, C. M.; Schaafsma, A. *Chinese Med. J-Peking* **2004**, *117*, 927-931.
- (69) Fanaro, S.; Marten, B.; Bagna, R.; Vigi, V.; Fabris, C.; Peña-Quintana, L.; Argüelles, F.; Scholz-Ahrens, K. E.; Sawatzki, G.; Zelenka, R. *J. Pediatr. Gastroenterol. Nutr.* **2009**, *48*, 82-88.
- (70) Arslanoglu, S.; Moro, G. E.; Schmitt, J.; Tandoi, L.; Rizzardi, S.; Boehm, G. *J. Nutr.* **2008**, *138*, 1091-1095.
- (71) Bruzzese, E.; Volpicelli, M.; Squeglia, V.; Bruzzese, D.; Salvini, F.; Bisceglia, M.; Lionetti, P.; Cinquetti, M.; Iacono, G.; Amarri, S. *Clin. Nutr.* **2009**, *28*, 156-161.
- (72) Shoaf, K.; Mulvey, G. L.; Armstrong, G. D.; Hutkins, R. W. *Infect. Immun.* **2006**, *74*, 6920-6928.
- (73) Sinclair, H. R.; de Slegte, J.; Gibson, G. R.; Rastall, R. A. *J. Agric. Food Chem.* **2009**, *57*, 3113-3119.
- (74) Costalos, C.; Kapiki, A.; Apostolou, M.; Papathoma, E. *Early Hum. Dev.* **2008**, *84*, 45-49.

- (75) Fanaro, S.; Boehm, G.; Garssen, J.; Knol, J.; Mosca, F.; Stahl, B.; Vigi, V. *Acta Paediatr.* **2005**, *94*, 22-26.
- (76) Schmelzle, H.; Wirth, S.; Skopnik, H.; Radke, M.; Knol, J.; Böckler, H.-M.; Brönstrup, A.; Wells, J.; Fusch, C. *J. Pediatric Gastroenterol. Nutr.* **2003**, *36*, 343-351.
- (77) Veereman-Wauters, G. *Brit. J. Nutr.* **2005**, *93*, S57-S60.
- (78) Chonan, O.; Watanuki, M. *J. Nutr. Sci. Vitam.* **1995**, *41*, 95-104.
- (79) Chonan, O.; Watanuki, M. *Int. J. Vit. Nutr. Res.* **1995**, *66*, 244-249.
- (80) van den Heuvel, E. G.; Schoterman, M. H.; Muijs, T. *J. Nutr.* **2000**, *130*, 2938-2942.
- (81) Weaver, C. M.; Martin, B. R.; Nakatsu, C. H.; Armstrong, A. P.; Clavijo, A.; McCabe, L. D.; McCabe, G. P.; Duignan, S.; Schoterman, M. H.; van den Heuvel, E. G. *J. Agr. Food Chem.* **2011**, *59*, 6501-6510.
- (82) Whisner, C. M.; Martin, B. R.; Schoterman, M. H.; Nakatsu, C. H.; McCabe, L. D.; McCabe, G. P.; Wastney, M. E.; van den Heuvel, E. G.; Weaver, C. M. *Brit. J. Nutr.* **2013**, *110*, 1292-1303.
- (83) Sabater-Molina, M.; Larqué, E.; Torrella, F.; Zamora, S. *J. Phys. Biochem.* **2009**, *65*, 315-328.
- (84) Oozeer, R.; van Limpt, K.; Ludwig, T.; Amor, K. B.; Martin, R.; Wind, R. D.; Boehm, G.; Knol, J. *Am. J. Clin. Nutr.* **2013**, *98*, 561S-571S.

Chapter 5

- (1) Kuwabara, N.; Hu, D.; Tateno, H.; Makyio, H.; Hirabayashi, J.; Kato, R. *FEBS Lett.* **2013**, *587*, 3620-3625.
- (2) Tateno, H.; Winter, H. C.; Goldstein, I. J. *Biochem J.* **2004**, *382*, 667-675.
- (3) Yu, Y.; Lasanajak, Y.; Song, X.; Hu, L.; Ramani, S.; Mickum, M. L.; Ashline, D. J.; Prasad, B. V.; Estes, M. K.; Reinhold, V. N. *Mol. Cell. Proteom.* **2014**, *13*, 2944-2960.
- (4) Jantscher-Krenn, E.; Lauwaet, T.; Bliss, L. A.; Reed, S. L.; Gillin, F. D.; Bode, L. *Brit J. Nutr.* **2012**, *108*, 1839-1846.
- (5) Kunz, C.; Rudloff, S.; Baier, W.; Klein, N.; Strobel, S. *Annu. Rev. Nutr.* **2000**, *20*, 699-722.
- (6) Rabinovich, G. A.; Baum, L. G.; Tinari, N.; Paganelli, R.; Natoli, C.; Liu, F.-T.; Iacobelli, S. *Trends Immunol.* **2002**, *23*, 313-320.
- (7) Hughes, R. C. *Biochimie* **2001**, *83*, 667-676.
- (8) Kasai, K.; Hirabayashi, J. *J. Biochem.* **1996**, *119*, 1-8.
- (9) Carlsson, S.; Carlsson, M. C.; Leffler, H. *Glycobiology* **2007**, *17*, 906-912.
- (10) Arthur, C. M.; Baruffi, M. D.; Cummings, R. D.; Stowell, S. R. In *Galectins: Methods and Protocols*, Stowell, R. S.; Cummings, D. R., Eds.; Springer New York: New York, NY, 2015, pp 1-35.
- (11) Bode, L. *Nutr. Rev.* **2009**, *67*, S183-S191.
- (12) Hirabayashi, J.; Hashidate, T.; Arata, Y.; Nishi, N.; Nakamura, T.; Hirashima, M.; Urashima, T.; Oka, T.; Futai, M.; Muller, W. E. *BBA-Gen. Subjects* **2002**, *1572*, 232-254.

- (13) Salomonsson, E.; Carlsson, M. C.; Osla, V.; Hendus-Altenburger, R.; Kahl-Knutson, B.; Öberg, C. T.; Sundin, A.; Nilsson, R.; Nordberg-Karlsson, E.; Nilsson, U. J. *J. Biol. Chem.* **2010**, *285*, 35079-35091.
- (14) Stillman, B. N.; Hsu, D. K.; Pang, M.; Brewer, C. F.; Johnson, P.; Liu, F.-T.; Baum, L. G. *J. Immunol.* **2006**, *176*, 778-789.
- (15) Lu, L.-H.; Nakagawa, R.; Kashio, Y.; Ito, A.; Shoji, H.; Nishi, N.; Hirashima, M.; Yamauchi, A.; Nakamura, T. *J. Biochem.* **2007**, *141*, 157-172.
- (16) Amano, M.; Galvan, M.; He, J.; Baum, L. G. *J. Biol. Chem.* **2003**, *278*, 7469-7475.
- (17) Opferman, J. T.; Korsmeyer, S. J. *Nat. Immunol.* **2003**, *4*, 410-415.
- (18) Pace, K. E.; Hahn, H. P.; Baum, L. G. *Methods Enzymol.* **2003**, *363*, 499.